CONTROLLED OPHTHALMIC DRUG DELIVERY BY SURFACTANT-LADEN CONTACT LENSES

By

YASH KAPOOR

A DISSERTATION PRESENTED TO THE GRADUATE SCHOOL
OF THE UNIVERSITY OF FLORIDA IN PARTIAL FULFILLMENT
OF THE REQUIREMENTS FOR THE DEGREE OF
DOCTOR OF PHILOSOPHY

UNIVERSITY OF FLORIDA

2008

To my parents and my lovely wife, Ananya

ACKNOWLEDGMENTS

I thank my advisor, Dr. Anuj Chauhan for his excellent guidance and help during my research work. He has been an extraordinary mentor to me, never letting me down. He has also been a great friend and I have personally learnt more from him than anyone else I have had a chance to interact. He has been a constant motivational force behind me and this work would not have been possible if it was not for his continuous presence throughout my graduate life.

I would also like to thank Professor Vijay John and his student Dr. Grace Tan from Tulane University who helped me getting the Cryo SEM images for my samples. I am also thankful to Professor Dinesh Shah, Dr. Jason Butler, Dr. Sergey Vasenkov, Professor Christopher Batich, Dr. Yiider Tseng and Dr. Tanmay Lele from Chemical Engineering department at University of Florida for their insightful discussions regarding my research, progress and my future endeavors.

I have been extremely lucky to have had an excellent advisor and an amazing set of group members, who have been very understanding and friendly throughout my stay in the department. First and foremost I would like to thank Dr. Jinah Kim, whose mere presence in the lab made everybody jovial and energetic. She helped me designing some of my experiments and will always be a great friend. I have had some stimulating interactions with Dr. Heng Zhu and Dr. Chi-Chung Li in our group. They helped me in settling in our lab when I joined and were always there to help. I also thank Cheng Chun Peng and Hyun Jung Jung for their support in the lab. Chavvi Gupta has been an excellent friend to me and he has helped me with some of my lab work, especially through some difficult times. I will always remain indebted to him. Lastly, I would like to extend my thanks to Brett Howell with whom I have had a chance to work on the Liposome permeability assay for in vitro toxicity. He is and will always be an exceptional researcher. His dedication to his work and his zeal to learn and succeed are unparalleled. Chapter 6 in my thesis would not have been possible without his help.

I would also like to thank some wonderful undergraduate students whom I had a chance to work with. Justin Thomas, Anthony Conway, Andrew Cohen and Maung Zaw. All these undergraduate students were exceptional in their work and were excellent learners.

I would also like to acknowledge the technical help provided by James Hinnant and Dennis Vince. I would like to thank the staff members, specially, Shirley Kelly, Deborah Aldrich, Cynthia Sain, Deborah Sandoval and Janice Harris for their support and comfort during my stay in the Chemical Engineering Department. Help provided by Sean Poole for computer support is also greatly appreciated.

Finally, I would like to thank my mother and father, Meena Rani Kapoor and Kailash Kapoor, for their continuous support in all my endeavors, I am here because of them and hope that I can extend the same love, care and support to them as they have bestowed on me. I love them and they will always be my heroes. I thank my wife, Ananya, from the bottom of my heart. She is one of the most understanding and caring persons I have ever met. Her sacrifices during my extended work hours in the lab cannot be evaluated. I just know that she is the most precious thing in my life and I cannot thank her enough for being there to support me.

TABLE OF CONTENTS

page

LIST OF TABLES

LIST OF FIGURES

LIST OF ABBREVIATIONS

BKC	Benzalkonium Chloride
Brij 56	Poly Oxy Ethylene (10) Cetyl Ether
Brij 58	Poly Oxy Ethylene (20) Cetyl Ether
Brij 76	Poly Oxy Ethylene (10) Stearyl Ether
Brij 78	Poly Oxy Ethylene (20) Stearyl Ether
Brij 700	Poly Oxy Ethylene (100) Stearyl Ether
Brij 97	Poly Oxy Ethylene (10) Oleyl Ether
Brij 98	Poly Oxy Ethylene (20) Oleyl Ether
C*	Critical Aggregation Concentration
CH	Cholestrol
CMC	Critical Micelle Concentration
CPB	Cetyl Pyridinium Bromide
CPC	Cetyl Pyridinium Chloride
CTAB	Hexadecyl Trimethylammonium Bromide
CyA	Cyclosporine A
D	Diffusivity of the Drug
D_S	Diffusivity of Surfactant
DI	Deionized
DMPC	1,2 Dimyristyl-sn-Glycero 3 Phosphocholine
DMPG	1,2 Dimyristyl-sn-Glycero 3 Phospho-rac-glycerol
DMS	Dexamethasone
DMSA	Dexamethasone Acetate
DOPE	1,2 Dioleoyl-sn-Glycero 3 Phosphoethanolamine
DTAB	Dodecyl Trimethylammonium Bromide

EGDMA	Ethylene Glycol Dimethacrylate
EWC	Equilibrium Water Content
HEMA	Hydroxy Ethyl Methacrylate
HLB	Hydrophilic Lipophilic Balance
MTAB	Myristyl Trimethylammonium Bromide
OTAB	Octadecyl Trimethylammonium Bromide
PBS	Phosphate Buffered Saline
PLTF	Pre Lens Tear Film
POLTF	Post Lens Tear Film
SDS	Sodium Dodecyl Sulfate
Tween 20	Polyoxyethylene Sorbitan Monolaurate
Tween 40	Polyoxyethylene Sorbitan Monopalmitate
Tween 80	Polyoxyethylene Sorbitan Monooleate

Abstract of Dissertation Presented to the Graduate School
of the University of Florida in Partial Fulfillment of the
Requirements for the Degree of Doctor of Philosophy

CONTROLLED OPHTHALMIC DRUG DELIVERY BY SURFACTANT-LADEN CONTACT LENSES

By

Yash Kapoor

December 2008

Chair: Anuj Chauhan
Major: Chemical Engineering

Drug delivery via eye drops has been found to be inefficient due to low bioavailability of less than 5%, and bioavailability of these drugs can be substantially improved to about 50% by delivering it via contact lenses. Commercial contact lenses are not suitable for drug delivery as the drug diffuses from these gels within a few hours to a day. Also, they have limited loading of the drug due to limited solubility of the drug in the contact lens material. Surfactants are commonly incorporated into hydrogels to increases solute loading and attenuate the drug release rates.

Our study focused on development of nanostructured poly (2-hydroxyethyl methacrylate) (p-HEMA) hydrogels containing microemulsions of Brij 97 surfactant and micelles of Brij 97, 78, 98 and 700 surfactants for extended delivery of ophthalmic drugs, specifically Cyclosporine A (CyA). Also, the effect of loading drug nanoparticles inside the hydrogels is explored. The release of CyA from these nanostructured hydrogels was performed *in vitro* and the effects of surfactant concentration, processing conditions, shelf life stability and gel thickness on the release of CyA was studied. We focus on various Brij surfactants to investigate the effects of chain length and presence of an unsaturated group on the drug release dynamics and partitioning

inside the surfactant domains inside the gel. The release of drug and surfactant from the hydrogels is found to be diffusion controlled and the duration of drug release increases with increasing surfactant loading and is relatively similar for both surfactant and microemulsion-laden gels. We also focus on understanding and modeling the mechanisms of both surfactant and drug transport in hydrogels. These models can aid in tuning the drug release rates from hydrogels by controlling the surfactant concentration. These studies also show that these hydrogels retain their effectiveness as drug delivery vehicles even after exposure to the relevant processing conditions needed in contact lens manufacturing including unreacted monomer extraction, autoclaving and packaging. The gels were imaged by Cryogenic Scanning Electron Microscopy (Cryo-SEM) to obtain direct evidence of the presence of surfactant-aggregates in the gel and to investigate the detailed microstructure for different surfactants. The images show a distribution of nano pores inside the surfactant laden hydrogels that we speculate are regions of surfactant aggregates, possibly vesicles that have a high affinity for the hydrophobic drug molecule. The gels are further characterized by studying their mechanical and physical properties such as transparency, surface contact angle, and equilibrium water content to determine their suitability as extended wear contact lenses. Results show that Brij surfactant-laden p-HEMA gels provide extended release of CyA, and have suitable mechanical and optical properties for contact lens applications.

Surfactants can also cause potential toxicity if they diffuse from the contact lenses to the ocular surface. Hence, we also designed an *in vitro* liposomal study to predict ocular toxicity of the surfactants utilized in the study for which ocular toxicity data is currently unavailable.

CHAPTER 1
INTRODUCTION

Millions of people around the world suffer from various eye diseases and the effective treatment of these diseases has become a focus of researchers around the world. The most convenient way of instilling drugs to ocular tissues is through topical administration and approximately 90% of all ophthalmic drugs formulations used to treat these diseases are applied as eye-drops [1]. Drugs applied through topical administration can reach the ocular tissue by either penetrating through the cornea or penetrating through the conjunctiva. Penetration of the drug inside the cornea depends on two important factors that include permeability of the drug across corneal epithelium and the residence time of the drug on the corneal surface. Permeability of most ocular drugs is very small and there is small residence time of the drug is small when applied through eye drops [2-7]. Thus, the bioavailability of the drug when using eye drops is minimal and only about 1-5% of the drug applied via eye drops eventually reaches the target tissue while the remaining 95-99% enters the systemic circulation through conjunctival uptake or drainage into the nasal cavity [8]. The low bioavailability leads to drug wastage and, more importantly, the systemic uptake of ophthalmic drugs can lead to side effects.

One way of increasing residence times of the drug on the corneal surface is by increasing the viscosity of the applied solution. Various viscosity enhancers have been used to increase the viscosity of the applied drops to increase the resulting residence time and thus the bioavailability [9,10]. Apart from viscosity enhancers, shear thinning polymers have also been explored which conform under shear generated by blinking to reduce stress on the corneal surface and also increase the residence time of the drug. Also, mucoadhesive polymers have been explored in literature which leads to higher contact time of the drug containing solution due to its physical

binding with the mucin layer [11]. Major disadvantages of these polymer based delivery systems is blurring of vision and uncomfortable feeling due to the sticky nature of these polymers.

Several solid particle suspensions have also been explored for instilling various drugs. These systems mainly include liposomes, niosomes, microsperes, and microemulsion particles [12,13]. Major issues concerning these systems are the stability and sterilization for mass production making them quite ineffective for use. Various soluble, biodegradable, and non-soluble ocular inserts have also been explored in literature. These systems can lead to programmed delivery of the drug to the ocular surface, but the difficulty involved in handling these systems along with bad patient compliance has led to limited applications.

To avoid all these issues, contact lenses have been widely studied due to the high degree of comfort and biocompatibility. On insertion of a medicated contact lens in the eye, drug diffuses through the lens matrix into the thin tear film named post-lens tear film (POLTF) trapped between the lens and the cornea, and the drug has a residence time about 30 min in the eye [14,15]. An increase in the residence time leads to a significant increase in the bioavailability. Both mathematical models and clinical data suggest that the bioavailability for ophthalmic drug delivery using contact lenses can be as large as 50% [16].

This work addresses the issue of drug delivery using microemulsion and micelles laden contact lenses. An in-depth understanding of drug interaction with contact lens material followed by changes in drug interaction in the presence of microemulsions and micelles inside the contact lenses is presented by rigorous experiments and by proposing some new models to understand these interactions. The focus of this work was to tackle the most common ocular disease, dry eyes, by using the currently approved drug called Cyclosporin A (CyA). Chapter 1

focuses on drug release from contact lenses loaded with drug nanoparticles and key factors in polymer drug interactions are evaluated in this chapter.

Dry eye disease is mainly treated by instilling artificial tears into the eyes. Dry eyes syndrome, one of the most commonly occurring problems in the world, can be broadly classified into mild, moderate, and severe depending upon the intensity of the disease. Mild damages to cornea and conjunctiva can be treated readily using tear substitutes available in the market. More frequent instillation of artificial tears is needed in the case of moderate damage and this can again be treated readily by using commercial products. Severe dry eye syndrome on the other hand can lead to far greater damage to the ocular surface, both in the cornea and conjunctiva, and simple treatments like artificial tears and ointments can be of minimal use. Also, mimicking the complex composition of real tears has been a major challenge in the industry. Significant advances have been made to develop systems which resemble the real ocular physiology and current artificial tears available to the patients come with various additives which have specific roles such as providing comfort, improving retention time on the corneal epithelium and maintaining pH levels at physiological values. Natural tears include salts, proteins, lipids, and hydrocarbons and the tear film is made up of three layers: a mucin layer in contact with the ocular surface, an aqueous layer above this mucin layer with a lipid bi-layer in contact with the environment. Artificial tears cannot generate the three layer structure of tears which is necessary for its effective function [17-19].

Another proposed way of treating this disease is by blocking the lacrimal drainage route so that the residence time of tears on the ocular surface increases [20]. This treatment can lead to a build-up of inflamed tears on the ocular surface that can further enhance the severity of the condition by influencing the inflammation cascade [21]. Loss of corneal sensation has also been

reported as an associated problem with this technique [22]. Overall, significant problems associated with this method can lead to further discomfort on the patient's eye and may not be well accepted.

Elimination of tears from the ocular surface can also be controlled by controlling the evaporation rate of the tears from the ocular surface. This can be achieved by wearing goggles or by maintaining some humid environment around the eyes, but this can lead to minimal comfort as the evaporation rate cannot be altered significantly and thus cannot help in treating the disease. Increasing tear production by stimulating the lacrimal gland by drugs such as pilocarpine has also been studied [23]. Excessive production of inflamed tears from already suffering eyes can lead to enhanced severity because of increased inflammatory response of the immune system.

All the above listed methods can give relief to the patients during the disease and may cure the disease if it is not very severe, but none of them address treating the underlying cause of the disease. Though still under scrutiny, physicians believe that dry eyes is caused by an anti-inflammatory immune response of the body which itself leads to inflammation. Dry eye syndrome can be triggered by common reasons such as living in a very dry environment or due to some infection in the eye. This results in inflammation on the ocular surface causing an immune response of the body which activates the T-cells which in turn produce cytokines to fight the inflammation. The ensuing inflammation, of both the ocular surface and the lacrimal gland results in production of inflamed tears. Since the tears are not normal, the irritated eye is not properly nourished or lubricated, encouraging the cycle of inflammation to repeat. CyA prevents T-cell activation, breaking the inflammatory cycle and hence treating the cause of the disease.

CyA is a cyclic polypeptide consisting of 11 amino acids. It is the most commonly used immunosuppressant, and it is prescribed for a number of ophthalmic applications such as dry eyes [24], uveitis in children and adolescents [25], vernal keratoconjunctivitis [26], and peripheral ulcerative keratitis [27]. Due to its limited solubility in water, it is not useful to formulate an aqueous solution of CyA, and thus a variety of systems such as solutions of drug in castor oil [28] and olive oil [29] have been explored in literature for controlled topical delivery of this drug in eyes. Since CyA is a lipophilic compound, it seems reasonable to use the oils to instill the drug but these studies show that CyA does not penetrate the cornea and there is a small bioavailability of CyA at the corneal surface. Furthermore, these oils do not have a good compatibility with eyes and cause irritation, blurred vision and toxic effects. Some of the problems associated with oily solutions of drug can be eliminated by formulating drug loaded emulsions in water. Emulsions of castor oil have been investigated for delivery of CyA in albino rabbits and beagle dogs. These systems showed promising results but were only effective for a period of about 12 hours [30]. Other types of emulsions, particularly the positively charged emulsions such as triglyceride emulsion stabilized by β-tecopherol, which show extended interaction with negatively charged epithelial corneal cells, have also been extensively studied for ophthalmic delivery of CyA [31]. These systems seem to enhance the retention time of the drug but are not well tolerated in the eyes. Cyclodextrins, which have an internal lipophilic and outer hydrophilic region, can trap the hydrophobic drug in the internal core and also be dispersed in the aqueous tear fluid. The studies on loading of CyA in the hydrophobic core of the cyclodextrins increase the penetration by a factor of about 10 in comparison to the oil based systems [32]. The major problem with the CyA release by cyclodextrin is the lack of a continuous delivery which makes the drug delivery ineffective. Penetration enhancers like

benzalkonium chloride, dimethylsulfoxide and Cremophor-EL have been used to increase the permeation of CyA [33]. These substances increased the permeability of CyA across the cornea, but only marginally compared to pure CyA and the release were observed for only a few hours. Also, these enhancers are poorly tolerated by eyes and add to the toxicity level in blood. Nonionic surfactants such as polyoxyl 40 stearate have been used to form micelles and increase CyA solubility in aqueous medium. These suspension show a 60 fold increase in the corneal uptake compared to oil water emulsions and other oil based delivery systems [34]. However, the stability of micelles and their low shelf life is one major disadvantage of this system. Liposome particles formed by phospholipids namely phosphatidylcholine and phosphatidylserine, have been used as a vehicle to deliver CyA [35]. There is large upload efficiency in these particles but there short retention times make them of limited use. Nanoparticles such as chitosan particles have also been researched as potential delivery vehicles for CyA. They are of significant interest because of their good tolerance and higher corneal permeability [36]. These systems release drugs for as long as 48 hours, but a major part of the drug has been shown to diffuse in the initial hour making sustained delivery difficult [37]. Another major problem associated with chitosan is the lack of reproducibility in drug release, which occurs due to the heterogeneities in the structure of this naturally occurring polymer. Later studies of positively charged chitosan particles show only a slight improvement in bioavailability and retention time as compared to uncharged chitosan particles [38]. Collagen shields have been another popular vehicle to study CyA to enhance contact time and continuous delivery to ocular tissues [39]. These shields can be effective for a period of about eight hours but patient discomfort due to blurring of vision and difficulty in self administration by patients leads to a lack of acceptability. Disaggregating collagen matrix in the eyes during implant is another major concern. Lastly, prodrugs have been

studied to enhance penetration of CyA in eyes [40]. The only advantage of this system seems to be better tolerance in the system, but the retention time of the drug is low making the method less affective. A controlled way of delivering CyA for an extended period of time using vinylpyrrolidone and HEMA polymer has been discussed in the literature [41]. Authors looked into the affect of different copolymer compositions on drug release data but no further investigation is presented on the release rate dependency on different drug loading. They have also looked in to the in-vivo studies for a particular composition [42].

As discussed earlier, contact lenses can increase the bioavailability of the ocular drugs by increasing the residence time on the ocular surface. Also, easy availability and ease of application make them a suitable vehicle for drug delivery. Soft contact lenses as a drug delivery vehicle were first used in 1965 [43]. The major problem with commercial contact lenses is that most of the drug diffuses from these systems within a few hours [44]. Drugs like cromolyn sodium, ketotifen fumarate, ketorolac tromethamine, dexamethasone sodium phosphate [45], timolol [46], pilocarpine [47], and fluoroquinolones [48] have been studied for uptake and release by soft contact lenses. None of these drugs seem to release drugs for more than 6 h. A number of studies have been conducted for uptake of the drug by soaking the lens in concentrated drug solution followed by *in vitro* or *in vivo* release studies [49-57]. The major problem of loading drug by this method is that in most cases the loading capacity of the soaked contact lenses is inadequate. The drug loading capacity could be increased by 2-3 times by designing a molecularly imprinted soft contact lens [58,59]. Another commonly used method of entrapping drugs in gels is direct addition of drug in the polymerizing medium [60-62]. None of these methods seem to be effective in controlling the drug release and effectively designing a system which can be tweaked according to the patients needs.

This work represents a thorough overview of how microemulsion and micelles can be used to control delivery of CyA. Release kinetics from hydrogels is a strong function of hydrogel properties such as pore size and swelling of the hydrogels. Larger pore sizes can affect permeability of the drug or alternatively the diffusion of the drug from the hydrogels and both these properties can be significantly altered by incorporation of surfactants inside the gels. Thus, addition of surfactants inside conventional hydrogels can not only induce structural and rheological changes but also effect the drug release kinetics and drug interaction within the hydrogel, having considerable implications on drug delivery mechanisms. The drug, which was previously interacting with the polymer, can now associate with the surfactants inside the hydrogels through hydrogen bonding, electrostatic or hydrophobic interactions. To comprehend polymer-drug-surfactant interactions it is imperative to first clearly understand how surfactant-drug, drug-polymer and polymer-surfactant interact with each other and what factors govern these interactions.

Surfactants, which are amphiphillic molecules can self assemble inside a solution after a critical concentration referred to as the critical micelle concentration (CMC) is reached. Surfactants as drug delivery vehicles have been explored in the past mainly because of their property of self assembly. Surfactants can be used to a) enhance the permeability of drug through lipid bi-layers, b) control drug delivery, c) increase solubility of poorly soluble drugs, d) decrease toxicity inside the body due to excess dosage and e) increase drug bioavailability. Park et al explained how surfactants can enhance permeability of drugs across the lipid bi-layer on the skin and did a thorough study of hydrophilic chain length, hydrophobic chain length and hydrophilic-lipophilic balance (HLB) on permeation of ibuprofen through outer most layer of the skin, stratum corneum [63]. There have been numerous studies in the similar area [64-66] and

researches have also studied use of surfactants to enhance ocular bioavailability of certain hydrophobic and hydrophilic drugs [67-69]. It is believed that penetration enhancers increase permeability of hydrophilic drug more significantly than the hydrophilic drugs.

Polymeric micelles have been also shown to be effective as drug carriers and controlled delivery vehicles especially for delivery of drugs inside the body. Worm-like micelles prepared from degradable polymer (polyethylene oxide (PEO)-polylactic acid) and inert (PEO-polyethylethylene and PEO-polybutadiene) were studied for uptake of a hydrophobic drug Triameterene and release of two hydrophobic dyes, showing that these systems can be used for controlled delivery of hydrophobic molecules [70]. Authors further showed that the size of worm micelles was ideal to deliver drug into porous tissues by conducting permeation studies of the worm micelles through agarose gels whereas 100nm size vesicles were unable to permeate through the same gels making vesicles less effective than micelles to deliver drug inside the tissues. For *in vivo* applications, interaction of the micelles with the blood plasma and other lipids and proteins inside the body determines its stability and further usefulness as a drug carrier. Polymeric micelles are generally 10-100 nm in size, smaller than liposomes but larger in size than conventional surfactant micelles (<5 nm in size) making them more stable inside the blood plasma. Due to their larger size, polymeric micelles if injected intravenously have high residence time due to reduced elimination from the body. Major advantage of this drug delivery system is the reduced toxicity of the drug as they can be used to target specific organs inside the body. This not only increases drug bioavailability, but also reduces loss of drug activity due to drug interaction with other proteins and lipids inside the body [71].

Drug loading inside a micelle typically depends on a) its solubility in the continuous phase, b) initial drug loading, c) drug loading procedure (chemical conjugation, physical adsorption or

electrostatic interaction), d) drug affinity to the micellar interior and e) pH and temperature of the system. Drug loading has also been shown to be a strong function of the aggregation number of the surfactant inside the solution [72]. Larger the hydrophobic part of the surfactant, larger would be the hydrophobic interior of the micelle resulting in increased solubility of a hydrophobic drug. On the other hand, as the hydrophilic chain length is increased, CMC of surfactant increases resulting in lesser number of surfactant micelles for a given concentration of surfactant resulting in lesser drug solubilization. A review by Torchillin discussed the usefulness of micelles in pharmaceutical industry as drug carriers and other potential applications pertaining to properties and nature of surfactant-drug interactions [73]. The author has also discussed the possible mechanism for targeted drug delivery using micelles as drug delivery vehicles [74].

Polymer-surfactant interaction can be classified into three categories: ionic, hydrophobic, and through hydrogen bonding. For non-ionic surfactants the interaction is predominantly hydrophobic in nature whereas in the presence of anionic and cationic surfactants the electrostatic interaction dominates. These interactions can be significantly altered by changes in pH, ionic strength of the solution, presence of solutes and physiological changes such as temperature. Strong interactions between polymer and surfactant once mixed together can significantly affect the polymerization process, affecting the microstructure of chemical hydrogel during polymerization. Vlachou et. al. demonstrated that incorporation of surfactants inside polymeric tablets increases wettability and water content on incorporation of non-ionic surfactant Tegobatain, though a clear understanding of polymer surfactant interaction was not presented [75]. Surfactants can alter the swelling properties of chemical hydrogels which can be directly correlated to the pore size change inside the hydrogel. In some cases, the presence of oppositely charged surfactant in a polymeric matrix can also lead to collapse of the gel so that the water

content inside the gel decreases due to ion pairing between the gel and the surfactant [76]. A more detailed study of interactions between charged and uncharged polymers with cationic (Cetylpyrridium chloride) and anionic (sodium dodecylbenzene sulfonate) surfactants has been shown by Philippova et al [77]. They showed that a charged gel collapses in presence of cationic and anionic surfactants due to electrostatic and hydrophobic interactions respectively. They also discussed the charge specific interaction of uncharged polymer with cationic and anionic surfactants showing that polyacrylic acid (PAA) gels and hydrophobically modified PAA gels swelled in presence of anionic surfactant while they collapsed in presence of cationic surfactants.

Surfactants have been shown to have significant effect on viscosity of the polymer mixtures especially at concentration above their critical aggregation concentration (CAC) as they start associating with the hydrophobic polymer chains. Furthermore, mixed micelles seem to interact more with polymers consisting of hydrophobic units than single surfactants since change in viscosity is more pronounced in case of mixed micelles [78]. A significant effect of ions on surfactant interaction with polymer matrix has also been observed. Researchers have observed that carbopol gels interact differently with ionic and non-ionic surfactants in water, 0.9% NaCl solution, and lacrimal fluid [79]. So, interaction between surfactant-polymer changes not only due to presence of salt but also due to nature of ions. Many drugs also have amphiphillic character, interacting with polymers in similar way as does a surfactant molecule.

Using hydrogels to control drug release has been explored extensively in literature [80]. The rate of release strongly depends on the interaction of the solutes such as drugs with the hydrogels. Various rheological and structural changes can be introduced in hydrogels by changing physiological conditions such as pH [81] and temperature [82] or providing some stimuli like magnetic field [83] and ultrasound [84]. Even presence of ions or specific chemicals

can bring significant changes in the gels [85]. All these parameters or conditions can then be controlled to deliver drugs at specific location in the body. If some lipophilic modifications are done to the polymer, they can further lower the release rates of the drug molecule [86]. Drug, which can be bound to the polymer due to hydrophobic attraction, hydrogen bonding or ionic pairing, can either diffuse along the polymer, i.e., by surface diffusion or by dissolving in the solution surrounding the polymer. Mathematical models to describe diffusion from non-swellable polymeric slab have been explored previously [87]. Many theoretical mechanisms have been proposed to describe the diffusion of solutes from hydrogels and these can be divided into three basic theories: a) Free volume theory, b) Obstruction theory and c) hydrodynamic theory [88]. These theories predict the diffusion coefficient of the solute when incorporated in various gels depending on various parameters such as volume fraction of polymer in gel, area of solute, radius of solute, length of polymer chain, molecular weight of the polymer, hydraulic permeability of the medium etc. These models and experiments are limited to a low solute and polymer concentration inside the hydrogel. Drug loaded above a critical concentration can precipitate and form aggregates inside the hydrogels. Overall diffusion of drug molecules will then governed by diffusion of free drug molecules and dissolution of drug aggregates. The earliest model describing drug release from a medium in which dug concentration is above the solubility limit was done by Higuchi [89].

Properties of polymers and surfactants and their interaction with the drug molecules can be combined to affect the drug release mechanism and rates. Incorporation of surfactants inside the gel matrix can enhance gel properties and further enhance the drug loading capacity of hydrogels, especially if the concentration of surfactant is above CAC inside the hydrogel. Hydrophobic drugs can partition into these aggregates leading to enhanced loading, and the drug-

laden micelles can act as depots of drug leading to extended drug release. Also, surfactants present in the release medium can enhance drug diffusion from polymeric gels to the release medium by a) increasing the solubility of the drug in the outer fluid and b) by lowering the interfacial tension between the gel and the release medium. In the gel matrix, surfactants can exist in three forms: a) free form, not interacting with other surfactants or the polymer b) as micellar aggregates or c) interacting with the polymer matrix. Similarly, drug also exists in three different forms: a) free form, b) inside micellar aggregates, c) adsorbed on the polymer. In most cases, drug interacting with surfactant aggregates controls the drug release rates from the gel matrix. If drug has substantial affinity for the micellar aggregates inside the hydrogel, i.e., it has a very high partition coefficient favoring its adsorption inside the micelles, then the free drug concentration would be less and the lower free drug concentration may lead to slower drug release rates and longer duration of release.

Paulsson and Edsman explored diffusion of hydrophobic drugs in carbopol gels loaded with Brij 58 and sodium dodecyl sulfate (SDS) and showed that as the hydrophobic nature of the drugs was increased, there was a significant decrease in the diffusion rates [90]. They concluded that the reduction in diffusion rate can be attributed to the lipophilic interactions between the drug and the surfactant micelles. They also showed that the interactions between charged drug and oppositely charged surfactant can further decrease the diffusion of the drug [91,92]. The polymer content in all their formulations was less than 2%. Lin et al also explored carbopol gels and showed that pluronic F-127 surfactant can be used to control the release of the drug especially if the gel and surfactant are mixed in a particular ratio [93]. Liu et al used a cationic surfactant (dodecyl trimethyl ammonium bromide) and an anionic surfactant (SDS) to solubilize a hydrophobic drug Camtothecin (CPT), and the surfactant-drug mixture was loaded in agarose

gels [94,95], They showed that the release of CPT was slowed down with increasing concentration of surfactant. In a later study, authors reported that if a mixture of a cationic surfactant (cetyltrimethylammonium bromide) and an anionic hydrophilic polysaccharide (k-carrageenan) were introduced in agarose gels, they further affected the release of the drug [96]. Concheiro et al explored the changes in microviscosity of mixtures due to presence of surfactants and suggested that these systems could be used in ophthalmic applications to increase the retention time of eye drops and thus prolong the release of the drug to the ocular tissues [97]. The gel-surfactant-drug interactions and the consequences on the drug release rates have also been reviewed in detail by Alvarez-Lorenzo and Concheiro [98]. Wu et al did a study on interaction of the drug, lidocaine hydrochloride with silica based xerogels in presence of a non-ionic surfactant Igepal CO 720 [99]. They found that drug release was slowed down due to hydrophobic interactions with surfactant micelles but more interestingly, surfactant release increased as drug concentration was increased inside the xerogel due to reduced interaction of the surfactant with the gel. Thermosensitive polymers as controlled delivery vehicles have also been explored. Above a certain temperature, called the cloud point, the polymer is insoluble in a solution thereby not releasing any drug. Whereas below the cloud point, polymer starts dissolving, gradually eluding the drug molecules. This phenomenon can be used to design systems with polymers having a cloud point less than the physiological temperature of 37 ^{o}C. Cloud point of polymers can be increased by incorporating surfactants inside the polymer matrix and delay in drug release can be controlled by changing surfactant concentration inside the polymers [100].

Despite a significant focus on incorporating surfactants in hydrogels for impeding drug release rates, there has been very less work on drug interaction with surfactant containing

chemical hydrogels where polymer content is considerably higher, for example, hydrogel contact lenses which have 60% polymer w/w when swollen. In such systems, there is a competing affect of drug interaction with the polymer matrix and the surfactant micelles. It is thus essential that for the surfactants to retard drug transport in these systems, the surfactant aggregates must have a very high partitioning for the drug compared to the hydrogel. Incorporation of microemulsions inside polyhydroxy ethyl methacrylate was studied to deliver lidocaine at therapeutic dosages to the ocular surface [101]. It was reported that the drug release from these gels was combination of diffusion from the hydrogel and from the microemulsion particle. In chapter 3 we try to use microemulsions to impede CyA release from the gels. It is shown in this chapter that microemulsion laden gels and surfactant laden gels, utilizing same surfactant, behave similarly and that oil phase has minimal role in impeding drug release. A thorough investigation of surfactant loading, storage conditions and processing conditions are studied in this chapter.

Chapter 4 focuses on modeling surfactant and drug release from these hydrogels. Drug release model can be used to predict the partition coefficient of the drug and it is shown that we can control specific parameters during formulation to control drug release from the hydrogels. Experimental data agrees well with the proposed model and already published data from other authors is also shown to agree well with the model.

In Chapter 5 we extend our understanding of these systems by studying various surfactants and elucidate factors governing the drug release rates based on surfactant structure. In this chapter we also evaluate physical and mechanical properties of surfactant laden gels to determine the suitability of these surfactant laden systems as contact lenses. It is shown that presence of surfactants enhances water uptake and surface properties of the hydrogels whereas there is no effect on the mechanical properties and transparency of the gels. We also propose a model for

viscoelastic response of the gels in this chapter. Also, a thorough understanding of microstructure change inside the hydrogels is investigated in this chapter by performing Cryo SEM imaging on the surfactant laden gels. Introduction of surfactants can change the microstructure of the gels though not compromising the mechanical properties.

After application of these hydrogels on the ocular surface, surfactants can diffuse out and they can cause potential toxicity. Surfactants used in this study are non-ionic surfactants which are expected to cause minimal toxicity on the ocular surface. Since literature had scarce data on the ocular toxicity of the surfactants used in this study, we used an in vitro assay to evaluate their toxicity in chapter 6. The popular method to evaluate toxicity of substances is by performing a Draize eye test. The Draize eye test has been criticized in the past for its lack of reproducibility and the cruelty associated with harsh testing conditions for animals [102,103]. Alternatives to this test have been proposed, but a widely accepted model to assess toxicity in vivo has not yet been found. Varied levels of success have been obtained by each newly proposed method, with some researchers showing excellent correlations to in vivo data and others showing insufficient ones, sometimes even with the same method. Vian et al. showed relatively poor correlations for neutral red uptake (NRU), the MTT tetrazolium salt assay, and cell proliferation via total protein content measurements [104]. Matsukawa et al. reported mixed results for the EYTEX™ test, clearly showing several weaknesses of the test [105]. The use of red blood cells to measure ocular toxicity has been touted as quick, inexpensive, and effective [106]. The correlation between this test and the Draize eye score has been found to be poor, though the authors have claimed that it could effectively verify the toxicity of chemicals with Draize scores greater than 50 [107]. Okahata and Ebato used a lipid-coated quartz microbalance to correlate partition coefficients of surfactants between lipid bilayers and distilled water with Draize scores and

found excellent correlations [108]. Perhaps the most successful type of test developed thus far has been those utilizing cell cultures to assess the cell permeability of the compounds in question. Cottin and Zanvit reported successful correlation results from such a test [109]. The fact remains, however, that no test has been proven robust enough to completely replace in vivo testing [110].

One in vitro method of assessing ocular toxicity is the utilization of liposomes to mimic cell permeation by the test substance. The advantages of using liposome leakage to assess ocular toxicity include low cost and the ability to assess many compounds rapidly. Additionally, the test is quantitative and so it lacks the unpredictability that can be associated with using live cells and requires no specialized equipment or expertise to conduct. This test is based on the idea that the permeation of a test substance through lipid bilayers is the root cause of inducing ocular toxicity, with toxicity being caused due to leakage of cellular components which increases substantially after binding of the test substance to the bilayer. The liposome based assay is designed so that the lipid composition of the bilayers imitates the composition of corneal epithelial cells. The test measures the leakage of fluorescent dye from the liposome core upon interaction with a test substance. The maximum score of the Draize eye test is 110, with 80 out of 110 coming from the cornea alone, suggesting that the assessment of corneal toxicity should be the main focus of an in vitro alternative. This fact first inspired researchers to test liposomes as a possible means of assessing the ocular toxicity of surfactants [111,112]. Since that time, a few others have examined liposome leakage as well [108,113]. Good correlations to in vivo data were obtained in some cases for some surfactants, with gross outliers sometimes present. We show that the lack of good correlation in some studies between the liposome based assay and the

Draize test was due to neglect of mechanistic issues, and that a better correlation can be obtained by designing the liposome assay after mechanistic considerations.

CHAPTER 2
CYCLOSPORINE A RELEASE FROM POLY(HYDOXYETHYL METHACRYLATE) HYDROGELS

2.1 Introduction

In this Chapter we investigate the uptake and release of CyA from p-HEMA gels focusing on the drug polymer interaction and the dynamics of drug transport both below and above the solubility limit of the drug in the p-HEMA matrix. This is a first attempt to show that contact lenses loaded with drug above the solubility limit as drug-nanoparticles can be potentially used to deliver drugs like CyA at therapeutic dosages for extended periods.

2.2 Materials and Methods

2.2.1 Materials

2-Hydroxyethyl methacrylate (HEMA) monomer, ethylene glycol dimethacrylate (EGDMA), Dulbecco's phosphate buffered saline (PBS) acetonitrile and HPLC grade water were purchased from Sigma-Aldrich Chemicals (St Louis, MO). 2,4,6-trimethylbenzoyl-diphenyl-phophineoxide (TPO) was kindly provided by Ciba (Tarrytown, NY). CyA was purchased from LC Laboratories (Woburg, MA). All the chemicals were reagent grade. Acetonitrile was filtered before use and all the other chemicals were used without further purification.

2.2.2 Methods

2.2.2.1 Synthesis of drug laden and pure p-HEMA gels

p-HEMA hydrogels were synthesized by free radical solution polymerization of the monomer with chemical initiation. Drug was loaded in the p-HEMA gels by dissolving the drug in the monomer mixture before polymerization and the drug concentration was varied from 0.125 % to 5.25 % (w/dry gel w) for all the experiments. Briefly, 2.7 ml of drug loaded HEMA monomer was mixed with 15 μl of the crosslinker (EGDMA) and 2ml of deionized (DI) water. The solution was then degassed by bubbling nitrogen for 10 minutes. Next, 6 mg of the initiator

(TPO) was added, and the solution was stirred at 300 rpm for 10 minutes to ensure complete solubililization of the initiator. The solution was then poured into a mold comprising two glass plates separated by a polyester spacer having a thickness of 200 μm. The mold was then placed on Ultraviolet transilluminiator UVB-10 (Ultra Lum, Inc.) and the gel was cured by irradiating UVB light (305 nm) for 40 min. After polymerization, each gel was removed from the glass mold and was cut into smaller square pieces weighing about 40 mg and these gels were dried at room temperature for two days before drug release was initiated. p-HEMA gels without any drug were synthesized in a similar manner as described above except that the drug was not mixed in the monomer solution before polymerization.

2.2.2.2 Drug detection: HPLC assay

CyA concentration was measured using a HPLC (Waters, Alliance System) equipped with a C18 reverse phase column and a UV detector [114]. The mobile phase composition was 70% acetonitrile and 30% DI water, and the column was maintained at 60°C. The flow rate was fixed at 1.2 ml/min and the detection wavelength was set at 210 nm. The retention time for CyA under these conditions was 4.55 minutes, and the calibration curve for area under the peak vs. concentration was linear ($R^2 = 0.995$).

2.2.2.3 Drug release: Equilibrium experiments

The interaction of the p-HEMA matrix with the drug can be characterized by the equilibrium partition coefficient, which is the ratio of the drug concentration in the gel and that in PBS at equilibrium. The partition coefficient was obtained by soaking the square gel pieces about 40 mg in weight with known drug amounts in 3.5 ml PBS and measuring dynamic drug concentrations. The drug concentrations after equilibrium were used to obtain the partition coefficient. In another set of experiments, the square gel pieces without drug were soaked in 3.5 ml drug solutions, and the dynamic drug concentrations in the loading solutions were measured.

Again, the concentration after equilibrium was used to obtain the partition coefficient. Again, dynamic uptake was recorded for these systems till there was no further uptake of the drug by the gel. The injection volume in HPLC was set as 20 μl which was significantly lower than the total fluid volume (3.5 ml) to ensure negligible volume changes during the equilibrium experiments.

2.2.2.4 Drug release: PBS change experiments

Drug release experiments were also conducted under perfect sink conditions by periodic replacement of the PBS. As before, square gel pieces about 1.5X1.5 cm in size and 40 mg in weight were utilized for drug release in PBS change experiments. Drug release kinetics was measured by soaking the gel in 3.5 ml PBS buffer which was replaced every 24 hours. The volume of the release medium was chosen to be 3.5 ml to approximately match the in vivo conditions of tear turnover. These experiments were conducted till a majority of the drug diffused from the gel matrix.

2.2.2.5 Transmittance measurements

Transparency of drug containing hydrogels was quantified by measuring the transmittance of 200 μm thick hydrated gels at 600 nm using a UV-VIS spectrophotometer (Thermospectronic Genesys 10 UV). Gels were soaked in 3 ml of PBS for a day before the transmittance measurements were made.

2.2.2.6 Statistical analysis

Linear regression analysis to determine slopes, correlation coefficients and confidence intervals was done in JMP which was developed by SAS (Cary, North Carolina). Slopes were compared by determining the confidence interval for the respective systems.

2.3 Results and Discussion

2.3.1 Drug Release: Equilibrium Experiments

Figure 2-1 shows the drug release profiles from gels loaded with varying drug amounts through direct drug addition to the polymerizing mixture. In the same figure, uptake studies are also plotted for different initial drug PBS solutions. In these profiles, the percentage of drug absorbed (for loading studies) or released (for release studies) is plotted as a function of time. The results show that all the uptake profiles overlap within 95% confidence interval (CI) and the percentage drug release profiles also overlap within 95% CI if the initial drug loading is less than or equal to 0.4% w/w in the dry gel. The release profiles begin to differ if the drug loading is beyond 0.4% with the total percentage release decreasing with increased initial loading. This effect likely arises due to the fact that at high drug loadings the drug precipitates inside the gel, and so even after equilibrium is established a fraction of the drug is present in the gel as drug particles. This issue is further explored by calculating the partition coefficients.

The partition coefficient is defined as the ratio of the concentration in the gel and the concentration in the aqueous phase at equilibrium,

$$K = \frac{C_g}{C_w} \tag{2-1}$$

The amount of CyA in the gel phase was calculated by subtracting the content of CyA in PBS phase from the initial loaded content of the drug in the gel matrix at equilibrium. Similarly, for experiments in which uptake of the drug was measured, the amount of CyA inside the gel phase was calculated by subtracting the amount left in the solution from the initial drug dissolved. Figure 2-2 shows the dependence of partition coefficient on the equilibrium drug concentration in the release medium. Since the partition coefficient of the drug is very large in all the cases, it can be safely concluded that there is significant binding of the drug to the p-

HEMA matrix. The partition coefficient of the drug between the poly-HEMA matrix and the PBS solution is relatively constant at about 148±24.16 till a critical concentration C_{cr} of about 0.02 mM, which equals 24.05 μg/ml. Beyond this critical concentration, the partition coefficient increases very sharply. The critical value of 24.05 μg/ml is close to the solubility limit of CyA in water at room temperature, which has been reported to be about 27.67 μg/ml [115]. We propose that the sharp increase in the partition coefficient is evidence of the fact that for gels with sufficiently large initial drug loading even after equilibrium is reached, a fraction of the drug inside the gel is present as particles. In these systems, the drug concentration of the unaggregated form is fixed by equilibrium to be $K(C_r)C_r$, and the remaining amount is present as precipitates. Thus the rapid increase in the partition coefficient is only an artifact of the presence of the aggregates in the gel. In these systems, the drug in the gel is present in three possible forms: free drug dissolved in the aqueous phase in the gel, drug bound to the polymer, and the drug particles. At equilibrium the chemical potential of the drug molecules in the aqueous phase in the gel must equal the chemical potential of the drug molecules in the release medium. If the drug molecules in the aqueous phase in the gel are unaffected by the constraining effects of the gel, one may expect that the equilibrium concentration of the drug in the aqueous phase of the gel will equal the concentration in the release medium. At sufficiently high drug loadings in the gel, the concentration of the drug in the release medium is close to the solubility limit, and this suggests that the concentration of the drug in the aqueous phase in the gel is indeed equal to the concentration in the release medium, and the high value of the partition coefficient is due to the drug bound to the p-HEMA polymer.

2.3.2 Model for Drug Release

Below the solubility limit of the drug in the gel, the drug release under perfect sink conditions at short times is given by [87],

$$\%\text{Drug Release} = \sqrt{\frac{4Dt}{\pi h^2}} \times 100 \tag{2-2}$$

Here D is the effective diffusivity of the drug that includes contribution from both bulk and surface diffusion of the drug, 'h' is the half-thickness of the gel and 't' is the time of release. A detailed model for evaluating diffusivity of CyA from p-HEMA gels has been discussed in Section 4.3.1 in chapter 4, and the value of diffusivity determined by fitting the release data to the above equation is 1.44×10^{-14} m^2/s.

The drug release profiles cannot be described by the above equation if the drug loading in the gel is increased above a threshold corresponding to the solubility limit inside the gel matrix. In such situations, as mentioned earlier and illustrated in Figure 2-3, the drug is present in three different forms: free form dissolved in the aqueous phase, bound to the polymer, and particles. When the drug concentration is below a threshold limit inside the gel matrix, most of the drug is bind to the polymer (Figure 2-3A). As the polymer matrix reaches saturation, drug aggregates start forming inside the hydrogel (Figure 2-3B) and after further loading of the drug, the concentration of drug present as aggregates far exceeds the drug concentration bound to the polymer matrix (Figure 2-3C). On soaking of this gel in PBS solution, free drug and the adsorbed drug would diffuse out from the gel into the release medium. This transport would then reduce the free drug concentration in the gel matrix leading to breakup of the drug aggregates to compensate for the drug loss. This mechanism results in creation of a depletion zone near the surface which does not contain drug aggregates because these are already dissolved, and the thickness of this zone (δ) increases with time. The free concentration of the

drug in the zone that still contains the aggregates must be equal to the solubility concentration (C_S), and the drug contained in the aggregates should be at concentration $C_A = C_{TOTAL} - C_S$, where C_{TOTAL} is the initial drug concentration. Thus, we get the following model to describe drug transport from gel systems when the loading is above the solubility limit of the drug in the gel matrix,

$$\frac{\partial C}{\partial t} = D\frac{\partial^2 C}{\partial y^2} \quad \text{from} \quad 0 < y < \delta(t) \tag{2-3}$$

$$C = C_S \quad \text{from} \quad \delta(t) \le y < h \tag{2-4}$$

With the following initial and boundary conditions,

$$C(t, y = 0) = 0 \tag{2-5}$$

$$\mathrm{C(t, y = \delta) = C_S} \tag{2-6}$$

$$\mathrm{D}\frac{\partial C}{\partial y} = \mathrm{C_A}\frac{\partial \delta}{\partial \mathrm{t}} \quad \text{for} \quad \mathrm{y = \delta} \tag{2-7}$$

$$\delta(t = 0, y) = 0 \tag{2-8}$$

In the above equations C is the concentration of the un-aggregated drug molecules, which includes both free and polymer bound drug. The first boundary condition (Equation 2-5) assumes perfect sink conditions, the second boundary condition (Equation 2-6) arises from continuity of concentration and the third condition (Equation 2-7) states that the drug flux at the intersection of the zone with drug aggregates and the one without drug aggregates is equal to the amount released by the dissolution of the aggregates. The above model is only valid till δ is less than h, and after that the transport is purely diffusive.

A similar model is solved for surfactant diffusion from p-HEMA hydrogels in Chapter 4, Section 4.3.2. The amount of drug release under the limit $\frac{C_A}{C_S} >> 1$ is given by

$$N = 2A\sqrt{2DtC_S C_A} \tag{2-9}$$

Where 'A' is the surface area of the polymer gel and t is the time of release. If the above limit is satisfied, the value of C_A would be equal to the total drug concentration initially loaded into the gel (C_{TOTAL}). Thus, the percentage drug release (%) from the system can than be given by,

$$\%\text{Drug Release} = \frac{\sqrt{2DC_S}}{h}\sqrt{\frac{t}{C_{TOTAL}}} \times 100 \tag{2-10}$$

Based on the above equation, the plots of percentage drug release for systems with various C_{TOTAL} vs. $\sqrt{\frac{t}{C_{TOTAL}}}$ should be a straight lines with the same slope of $\frac{\sqrt{2DC^*}}{h} \times 100$, as long as the drug concentration inside the hydrogel is above the solubility limit. This result is identical to an earlier proposed equation by Higuchi for describing a drug release from ointments that contain drug as suspension [89]. We conducted release experiments under perfect sink conditions from gels with various drug loadings to explore the validity of the model proposed above, which are described below.

2.3.3 Drug Release: PBS Replacement

To validate the model developed above, it was decided to explore the effect of initial drug loading on release rates of the drug from the p-HEMA gels. The release experiments were conducted in 3.5 ml PBS with PBS replaced every day, and the drug loading was varied from 0.125% to 5% inside the gel matrix. The thickness of the gel was kept constant at 200 μm. The data from all the experiments is plotted in Figure 2-4 as percentage release vs. time. As expected the percentage release profiles do not overlap, as would be the case for gels with initial drug loadings below the solubility limit. In Figure 2-5, the percentage release is plotted vs. $\gamma \equiv \sqrt{\frac{t}{C_{TOTAL}}}$. The release curves overlap for initial drug loadings larger than or equal to 0.77%

but the profile for 0.125% is clearly different. This suggests that the solubility limit in the gels is above 0.125%. The slope from the data with higher drug loadings represents $\frac{\sqrt{2DC_S}\times 100}{h}$ and has a value of 17.68±0.47. Utilizing the value of diffusivity of the drug evaluated from the p-HEMA matrix ($1.44\text{x}10^{-14}$ m^2/s), we can determine the solubility, C_S, of the drug in the p-HEMA matrix to be 3mM, which equals 0.37% w/w in the dry gel.

The results shown above prove the validity of the developed model. Also, the release duration of the drug can be significantly altered once the drug forms aggregates inside the hydrogel as can be seen in Figure 2-5. Thus, the desired release rates of the drug can be achieved by loading varying amount of drug inside hydrogels, e.g., contact lenses.

2.3.4 Theoretical Model

Brinkman combined Darcy's law and Navier-Stokes equation to describe diffusion of solutes through a porous medium such as a hydrogel [143]. Phillips et al. confirmed the validity of using Brinkman's equation for solute diffusion through a porous medium by both experiments and Stokesian dynamics [144]. The following equation can then be used for evaluating diffusivity of a molecule from a hydrogel,

$$D_{TH} = \frac{k_B T}{6\pi\mu r}\left(1+\left(r^2/k\right)^{1/2}+\frac{1}{3}\left(r^2/k\right)\right)^{-1} \qquad (2\text{-}11)$$

Where, D_{TH} is the theoretically determined diffusivity of the molecule, 'r' is the solute radius, 'k' is the hydraulic permeability of the medium, 'μ' is the viscosity of water, 'T' is the temperature and k_B is the Boltzmann's constant. Later it was suggested that Equation 2-11 is valid only if there is a pressure driven flow and in its absence, the coefficient of r^2/k should be 1/9 instead of 1/3 [145]. Due to lack of pressure driven flow in our systems, we use a modified Equation 2-11 with 1/3 replaced by 1/9. The values of various parameters needed for evaluating

the theoretical diffusivity are listed in Table 2-1 and the value of the diffusivity for CyA is determined to be, 5.6×10^{-12} m^2/s. This value is significantly different from the experimentally determined value of 1.44×10^{-14} m^2/s. To reconcile this difference, we reiterative that below the solubility limit, the drug molecules in the gel are present both in free and polymer-bound form. The effective diffusivity obtained from the macroscopic transport model is a combination of both surface and bulk diffusion and can be defined as,

$$D = \frac{fD_f + D_{SU}(K - f)}{K} \tag{2-12}$$

Where, D_f and D_{SU} are the diffusivities of the free and the bound drug, respectively, 'f' is the fraction of water in the gel which is 0.4 for p-HEMA gels, and K is the partition coefficient determined in section 2.3.1 as 148. It is implicitly assumed in the above equation that the free and the bound form are always in equilibrium, i,e., the binding-unbinding events occur on a time scale much faster than diffusion. The surface diffusion is expected to be smaller than the bulk diffusion due to friction with the polymer and so as an extreme case we assume D_{SU} to be 0, and evaluate D_f from Equation 2-12 to be 5.33×10^{-12} m^2/s. This value is similar to that evaluated from the Brinkman model for solute diffusivity in porous medium suggesting that hydrodynamic interactions of the polymer matrix with the drug molecule have a significant contribution in molecular transport from p-HEMA gels. This also suggests that surface diffusivity for CyA inside the gel matrix is negligible.

2.3.5 Effect of Drug Concentration on Transparency

The presence of drug aggregates at loadings beyond the solubility limit could potentially cause scattering leading to a loss of transparency, which is a critical requirement for contact lenses. To explore this issue, the transmittance of the gels was measured, and these are reported in Figure 2-6. The gels are transparent with transmittance >99% for drug loadings below 0.3%.

On increasing the drug loading transparency decreases, the gels become hazy, and at loadings beyond 5.25%, the gels are almost opaque. Thus the transition point for loss of transparency coincides with the solubility limit that was determined to be 3mM (0.37%). This suggests that while gels with drug particles may not be suitable for contact lens applications. It is however noted that the size of the drug particles will likely depend on the polymerization dynamics and if conditions are found in which the particle aggregates are nanosized, the gels may retain transparency even above the solubility limit.

2.4 Conclusion

The drug CyA can be released from the 200 μm thick pHEMA gels for about a week, which is consistent with prior reports from VP-HEMA copolymer gels [41]. Here the authors did not mention the volume of the container in which drug release was conducted and so a direct comparison of their results with our results is not possible. Since the drug transport is diffusion controlled, 100 μm thick gels will release drug only for about 1.5 days. The drug CyA exhibits strong interaction with the p-HEMA matrix as evident by the high and concentration independent partition coefficient of 148±24.16. The release duration of the drug from the gel can be increased by loading drug above the solubility limit. This however leads to a reduction of transparency which is undesirable for contact lens applications. The release of drug from systems with drug particles can be described by the same model as proposed earlier for release from drug suspension in ointments. The diffusive transport of the drug mainly occurs due to diffusion of the free drug. The polymer bound drug does not diffuse along the polymer chains, but it always in equilibrium with the free drug, and thus surface bound drug can desorb and then diffuse. The diffusivity of the drug CyA in the p-HEMA gels can be described by the Brinkman model with some modifications to account for the absence of pressure driven flow.

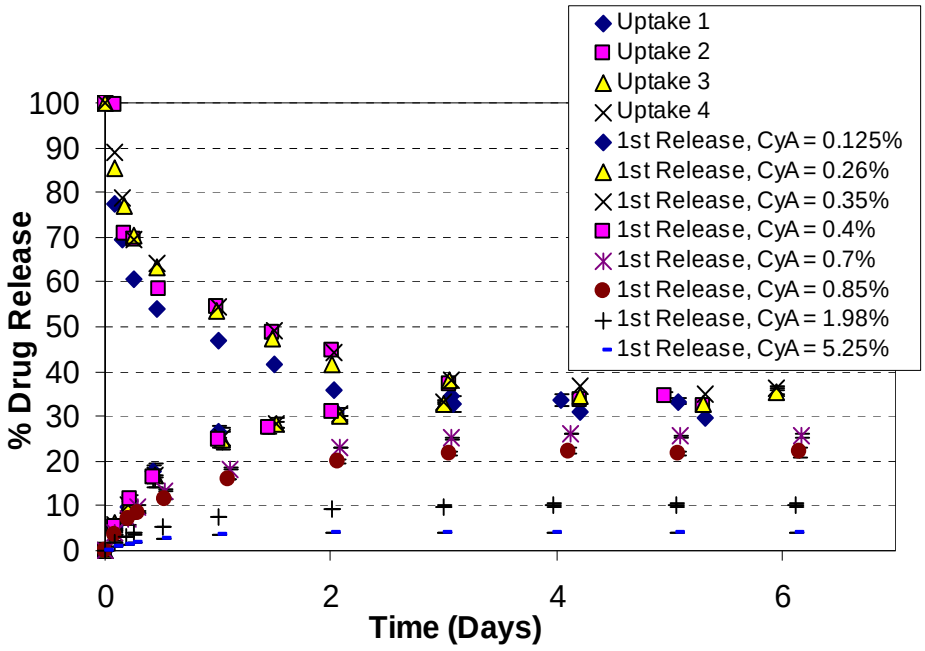

Figure 2-1. Percentage drug release from 200 μm thick p-HEMA hydrogel. Amount of drug loaded in the hydrogel is indicated. Uptake experiments were conducted from a drug solution where starting concentration of CyA in PBS was 11 μg/ml for Uptake 1 & Uptake 2 and it was 14 μg/ml for Uptake 3 &Uptake 4.

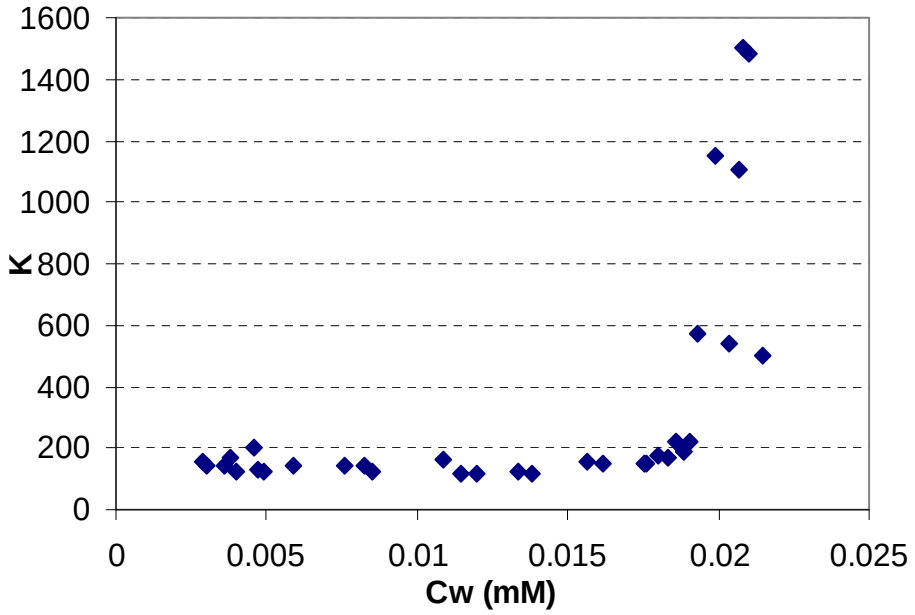

Figure 2-2. Partition coefficient plotted against concentration of drug in the PBS at equilibrium. There is a significant jump in the partition coefficient around 0.02 mM which is the solubility limit of CyA in the PBS buffer.

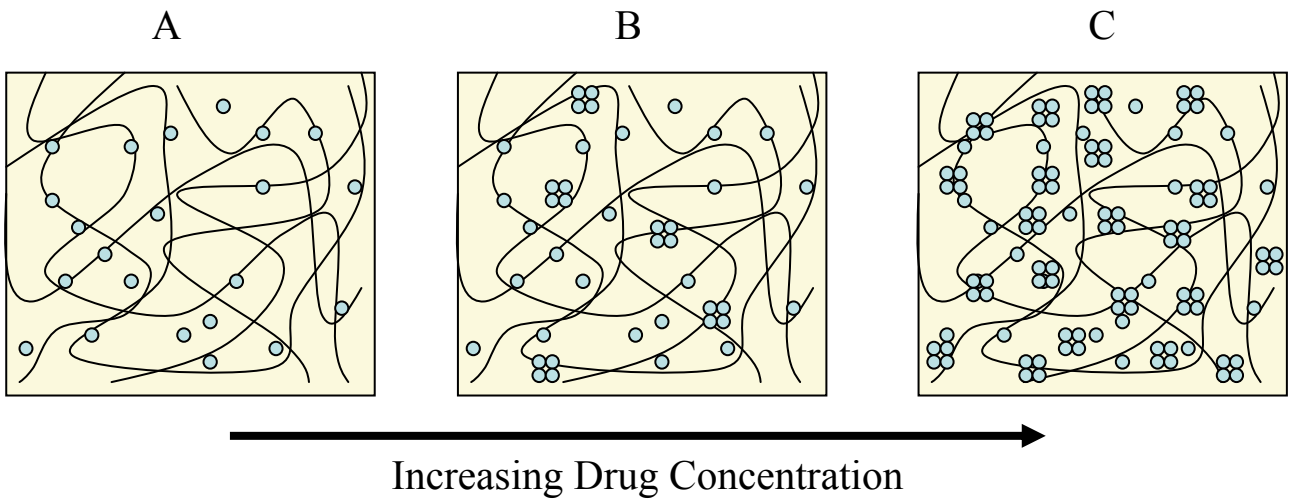

Figure 2-3. A schematic of drug interaction with the p-HEMA matrix as drug loading is increased. A) Drug loading is below the solubility limit and most of the drug is adsorbed on the polymer matrix. B) As the drug loading is increased beyond the solubility limit of the drug in the hydrogel matrix, drug starts to precipitates and forms aggregates inside the hydrogel. C) At a very high drug loading, concentration of drug aggregates is much higher than the concentration of polymer bound drug.

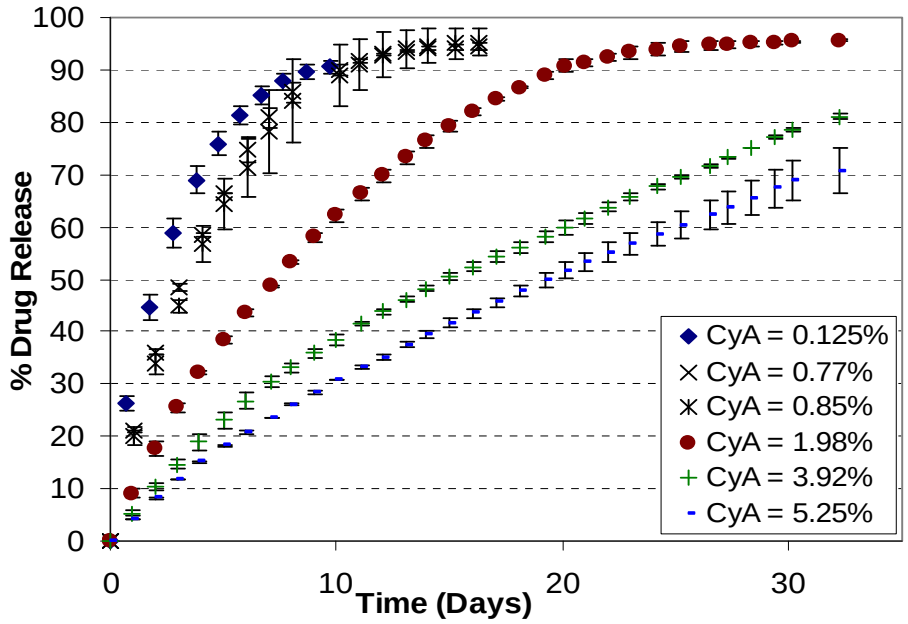

Figure 2-4. Effect of drug loading on cumulative drug release from 200 μm thick gels in PBS change experiments

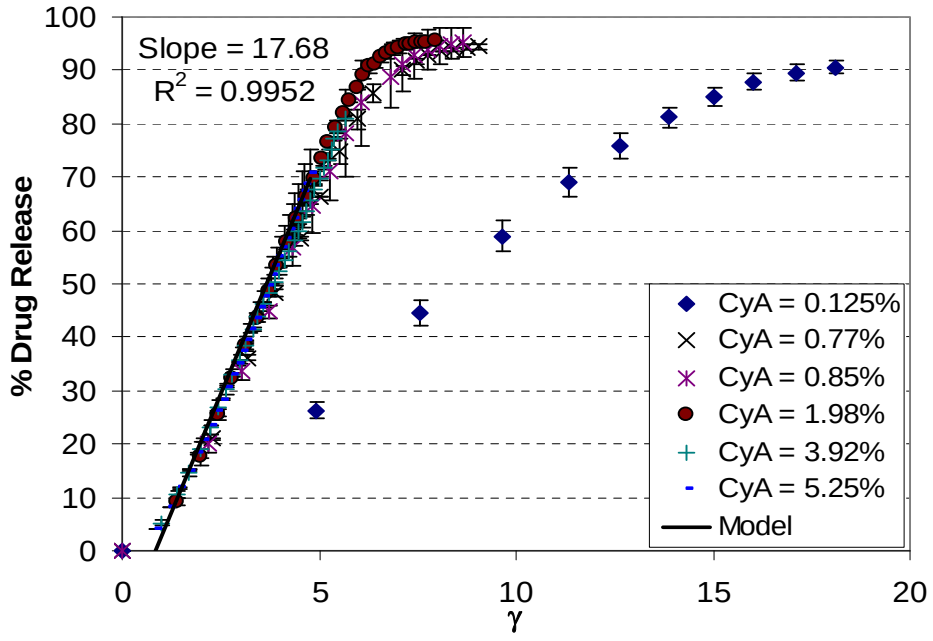

Figure 2-5. Cumulative percentage release of drug from 200 μm thick surfactant-laden gels in PBS change experiments after rescaling the time. γ represents $\sqrt{t}/C_{TOTAL}$ where t is time (h) and C_{TOTAL} (mM) is the total concentration of drug present inside the gel matrix.

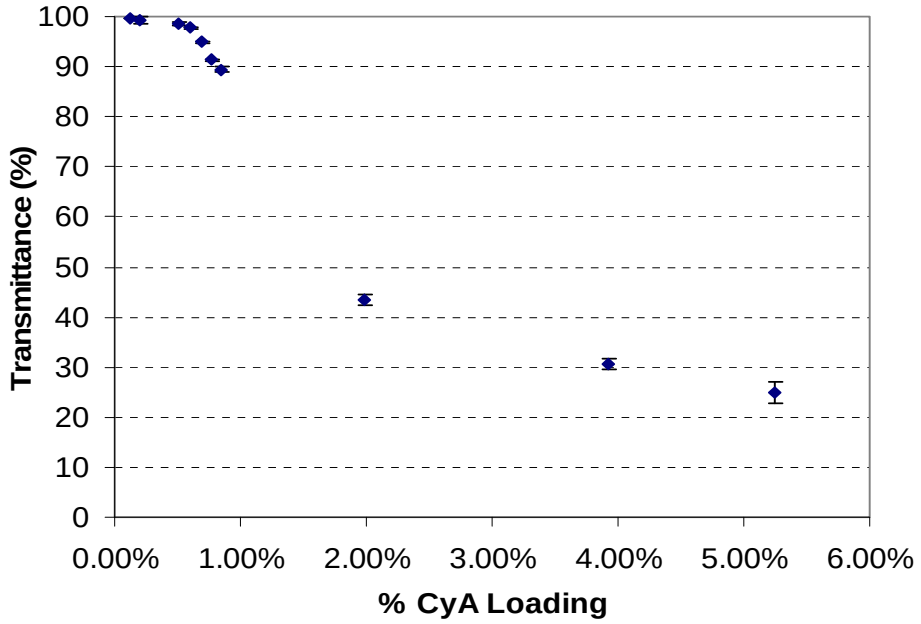

Figure 2-6. Transmittance of the gel with increasing drug concentrations. Transmittance values start to go down as the drug loading inside the hydrogel reaches the solubility limit.

Table 2-1. Physical properties of CyA at room temperature

Properties of CyA	Values
Diffusivity	1.44×10^{-14} m^2/s
Solubility in p-HEMA matrix	3 mM
Solubility in PBS	0.02 mM
Solubility un Water	0.023 mM

CHAPTER 3
CYCLOSPORINE A RELEASE FROM BRIJ 97 MICROEMULSION AND SURFACTANT LADEN HYDROGELS

3.1 Introduction

In this chapter we show that contact lenses made from microemulsion and surfactant-laden hydrogels can be used for extended delivery of Cyclosporine A (CyA) at therapeutic dosages. Also, we show that surfactant-laden hydrogels can go through all the processing steps that a typical contact lens goes through including monomer extraction, autoclaving and packaging, and still provide extended drug release at therapeutic dosages. The results of this study provide strong evidence that microemulsion and/or surfactant-laden contact lenses can be used for extended delivery of various ophthalmic drugs including CyA.

3.2 Materials and Methods

3.2.1 Materials

2-Hydroxyethyl methacrylate (HEMA) monomer, ethylene glycol dimethacrylate (EGDMA), ethyl butyrate, Dulbecco's phosphate buffered saline (PBS), acetonitrile and polyoxyethylene (10) oleyl ether (Brij 97) were purchased from Sigma-Aldrich Chemicals (St Louis, MO). 2,4,6-trimethylbenzoyl-diphenyl-phophineoxide (TPO) was kindly provided by Ciba (Tarrytown, NY). CyA was purchased from LC Laboratories (Woburg, MA). All the chemicals were reagent grade. Acetonitrile was filtered before use and all the other chemicals were used without further purification.

3.2.2 Microemulsion Formulation

The surfactant solution was prepared by adding the Brij 97 surfactant to de-ionized (DI) water in the required ratio and then stirring the mixture at 600 rpm and at room temperature for a period of about 10 hours. Specifically, 1, 1.5, and 2 g of Brij 97 was dissolved in 10 ml DI water to prepare three different surfactant solutions (named M1, M2, M3, respectively). Separately,

0.4 g of CyA was dissolved in 5 ml of ethyl butyrate to prepare the drug loaded oil phase. Next, 100 µl of the drug loaded oil was added to 5 ml of the surfactant solution, and the mixture was then stirred at 600 rpm (70^{o}C) for 20 minutes. The solution was then cooled to room temperature, resulting in formation of a clear microemulsion. Microemulsions without the drug were synthesized by eliminating CyA in the formulation described above.

3.2.3 Particle Size Analysis

The particle sizes for microemulsions were measured using a Precision Detectors PDDLS/CoolBatch+90T instrument. The data was analyzed with the Precision Deconvolve32 Program. The measurements were obtained at 20°C and 90° scattering angle, using a 683 nm laser source.

3.2.4 Preparation of Microemulsion Laden Gels

The microemulsion-laden p-HEMA hydrogels were prepared by free radical solution polymerization with UV initiation. Specifically, 2.7 ml of HEMA monomer was mixed with 15 µl of the crosslinker (EGDMA) and 2ml of the CyA containing microemulsion. The solution was then degassed by bubbling nitrogen for 10 minutes. Next, 6 mg of the initiator (TPO) was added, and the solution was stirred at 300 rpm for 10 minutes to ensure complete solubililization of the initiator. The solution was then poured in a mold that comprised two glass plates separated by a 200 µm (thick gels) or 100 µm (thin gels) thick spacer. The mold was placed on Ultraviolet transilluminiator UVB-10 (Ultra Lum, Inc.) and the gel was cured by irradiating UVB light (305 nm) for 40 min. The gels loaded with microemulsions M1, M2 and M3 were named M1, M2 and M3 gels, respectively. Microemulsions without any drug were incorporated in the polymerizing mixture for synthesizing gels with no drug and the synthesis protocol was same as described above.

3.2.5 Preparation of Surfactant Laden Gels

The surfactant solution was prepared as described earlier. Specifically, 0.2, 0.6, 1.5 g of Brij 97 surfactant was dissolved in 10 ml DI water to make three different surfactant solutions (named S1, S2, S3, respectively). Separately, 3.5 mg of CyA was dissolved in 2.7 ml of HEMA monomer and stirred at 600 rpm for a period of 5 hours. Next 15 µl of the crosslinker and 2ml of surfactant solution were added to the 2.7 ml of drug loaded monomer. The hydrogels were then prepared by adding the mixture to the molds followed by UV curing, as described above. Control, drug loaded p-HEMA gels without surfactants (D1) were prepared by following procedures identical to those described above except that the 2 ml surfactant solution was replaced by 2 ml DI water. Also, surfactant laden gels without any drug were synthesized in a similar manner as above by not incorporating drug in the monomer mixture.

3.2.6 CyA Detection by HPLC

CyA concentration was measured using a HPLC (Waters, Alliance System) equipped with a C_{18} reverse phase column and a UV detector [114]. The mobile phase composition was 70% acetonitrile and 30% DI water, and the column was maintained at 60°C. The flow rate was fixed at 1.2 ml/min and the detection wavelength was set at 210 nm. The retention time for CyA under these conditions was 4.55 minutes, and the calibration curve for area under the peak vs. concentration was linear ($R^2 = 0.995$).

3.2.7 Drug Release Kinetics from Gels Loaded with CyA by Drug Addition to the Monomer

After polymerization, each gel was removed from the glass mold and was cut into smaller pieces that were about 1.5X1.5 cm (for thick gels) and 1.5X3 cm (for thin gels) in size and about 40 mg in weight. Drug release kinetics was measured by soaking the gel in 3.5 ml PBS buffer which was replaced every 24 hours and all the measurements were done at room temperature. The volume of the release medium was chosen to be 3.5 ml to approximately match the in vivo

conditions of tear turnover. Additionally, some experiments were conducted without PBS replacement till the gel and the release medium equilibrated. These experiments were conducted to explore the rate limiting step in the drug transport by conducting drug release from gels with two different thicknesses. The dynamic drug concentrations in the release medium were measured for both sets of the drug release experiments by the HPLC method described above. The injection volume in HPLC was set as 20 μl which was significantly lower than the total fluid volume (3.5 ml) to ensure negligible volume changes during the equilibrium experiments.

3.2.8 Drug Uptake and Release Kinetics from Gels Loaded with CyA after Polymerization

In the release protocol described above, CyA was loaded in the hydrogels by dissolving it into the oil phase of the microemulsion. It is conceivable that the process of gel formation may lead to partial loss of drug activity and some irreversible entrapment of the drug. To eliminate the possible loss of activity due to the polymerization process, it was decided to conduct experiments in which the microemulsions (without drug) were entrapped in the gel, and the drug was loaded by soaking the gels into aqueous drug solutions. Specifically, drug was loaded by soaking the gels, about 40 mg in weight, in 4 ml of 11.5 μg/ml drug solution. To determine the time needed for uptake of drug by the microemulsion-laden gels, the duration of soaking period was varied between 5 and 15 days. The release kinetics was subsequently measured by following the same protocols as described in the previous section and these results are discussed in section 3.3.2.

3.2.9 Packaging Solution for Drug Release

To explore the effect of packaging solution on drug release from hydrogels containing drug incorporated inside the microemulsions, it was decided to soak the drug containing microemulsion laden gels (M2) in 1.5 ml of a packaging medium for specific durations and then

measure drug release kinetics from these gels. The duration of soaking in packaging solutions was varied from 10 – 100 days to evaluate the effect of storage on these hydrogels. Also, three different compositions of packaging solutions were explored. The first packaging medium was simply DI water, and the second and the third were 0.85% and 4.25% w/w salt solutions, respectively. The salt concentration of 0.85% (0.14 M) was chosen to match the typical concentration in commercial packaging solution [116], and higher (4.25%) and lower (DI water) salt concentration was used to observe the effect of salt on equilibrium amount of CyA released in the packaging solution. Drug release from these gels after packaging period were carried out in 3.5 ml of PBS with daily PBS replacement as described earlier, and release kinetics from gels used for packaging studies are discussed in section 3.3.3.

3.2.10 Processing Conditions in Contact Lens Manufacturing

To evaluate the suitability of the Brij 97 microemulsion and surfactant laden gels as contact lenses, it was decided to subject these gels through processing conditions similar to those used in contact lens manufacturing. The gels were first subjected to an extraction stage in which the un-reacted monomer was extracted from the gels by soaking gels in 10 ml of DI water at 50^{o}C. The DI water was replaced every 5 minutes, and this step was repeated 5 times. After extraction, each gel was soaked in 4 ml of CyA-water (12 μg/ml) for a period of 12 days. Each gel was then soaked in 1.5 ml of DI water and autoclaved for 15 min at 121^{o}C followed by storage at room temperature for a period of 10 days. In the final step, each gel was submerged in 3.5 ml of PBS, which was replaced every 24 hours, and the concentration of the drug was measured to determine the release kinetics. The results from this study are discussed in section 3.3.6.

3.2.11 Surfactant Release

To measure the surfactant release from the gels, surfactant laden gel samples were soaked in 3.5 ml of DI water. The DI water was replaced after regular intervals and the surface tension of the solution was measured by the Wilhelmy plate method to determine the concentration of Brij 97. We used a sand blasted platinum plate attached to a Scaime France Microbalance which was further connected to a Stathan Universal transducer (SC001). The transducer was calibrated by using DI water (σ = 72 mN/m) and acetone (σ = 23 mN/m) as standards. To ensure complete removal of impurities, the platinum plate was rinsed with DI water and acetone, followed by annealing till red hot using a propane burner before each measurement. For each measurement, the solution was kept still for a period of 1 hour to ensure an equilibrium surface coverage of surfactant at the air-liquid interface.

3.2.12 Statistical Analysis

Linear regression analysis to determine slopes, correlation coefficients and confidence intervals was performed in JMP developed by SAS (Cary, North Carolina). The 95% confidence intervals (CI) were obtained to compare release kinetics.

3.3 Results and Discussion

3.3.1 Particle Size Analysis of Microemulsions and Drug Release from Microemulsion-Laden Gels

Figure 3-1 plots the particle size distributions for the three microemulsions that were explored in this study. These microemulsions have mean particle sizes ranging from 10-13 nm, which is typical for microemulsions. The mean particle size increased with a reduction in surfactant loading, which was expected. The drug release profiles (with PBS change every 24 hours) from a control p-HEMA gels and gels loaded with microemulsions are compared in Figure 3-2. The amount of surfactant in the three systems was 5.6%, 8% and 9.4% w/dry gel w

for M1, M2 and M3, respectively. The CyA release from p-HEMA gels last only about 6-7 days but the microemulsion-laden gels release drug for about 20 days. The results in Figure 2 clearly demonstrate a significant reduction in delivery rate and a concurrent increase in the duration of release on addition of microemulsions to the gels. We speculate that since CyA is a hydrophobic molecule, it preferentially partitions into the oil phase of the microemulsions, leading to a reduction in the free drug concentration, and thus a reduction in the drug flux. It is also possible that during the gel preparation and subsequent hydration, some surfactant molecules desorb from the oil drops and then aggregate in the gel pores to form micelles. The presence of micelles is also expected to retard drug transport from the hydrogels.

The short time release from a hydrogel can be described by the following equation [87],

$$\%\text{Drug Release} = 4\sqrt{\frac{Dt}{\pi h^2}} \times 100 \tag{3-1}$$

Equation 3-1 is valid for short time scales when the released drug percentage is less than 60%. In Equation 3-1, 'D' is the effective diffusivity of the drug, 'h' is the thickness of the gel, and 't' is the release time. The release data shown in Figure 3-2 were fitted to the above equation to determine the effective diffusivity of the drug for the control p-HEMA gel and the microemulsion-laden gels. Based on Equation 3-1, a plot of cumulative release vs. $\sqrt{t}$ must be a straight line. The fit between the data and the model is shown in Figure 3-3, and the values of the slopes along with the 95% CI are listed in Table 3-1. For clarity, only average values for each system are plotted while the fitted line is evaluated by using all the data points for each system. The slopes were then utilized to determine the effective diffusivities, which are also listed in Table 3-1. We observe that the drug release from the microemulsion laden systems depends on surfactant loading, and effective diffusivity decreases with increasing surfactant loading. It is noted that the cumulative release profiles for the microemulsion-laden gels are

linear at short times but they intercept the x-axis at about $\sqrt{t} = 2.9$, implying $t \sim 8.4$ h. This suggests that at very short times the drug transport rates are much smaller than those predicted by diffusion mechanism, leading to a delay in release. The delay in drug release could potentially be caused due to the time needed to hydrate the interfacial region of the microemulsions. A similar phenomenon is observed with surfactant-laden gels (see section 3.3.4) which supports the hypothesis of delay caused by hydration of micelles or microemulsion interface.

3.3.2 Release of Drug after Soaking Microemulsion-Laden Gels in Drug Solution

As explained in section 3.2.8, in some experiments, drug was loaded into the gels after polymerization by soaking them in drug solution. After the soaking phase, the gels were withdrawn and the concentration of drug in the aqueous phase was measured. The mass of drug taken up by the gels was determined by subtracting the mass of drug left in the solution from the initial mass of drug in the soaking solution. The systems explored here had 8% surfactant in the dry gel (w/dry gel w), and Table 3-2 lists the amounts of drug that were taken up by these gels for the different soaking durations. The results in Table 3-2 show that the mass of the drug taken up by the gels is relatively similar for all the gels. This shows that 5 days of soaking time is sufficient to establish equilibrium. The drug release profiles shown in Figure 3-4 are within 95% CI of each other (CI not shown in the plot), which is expected because each gel absorbed similar amount of drug. These results also show that the duration of drug release for the systems in which the drug is loaded by soaking in the drug solution is similar to the systems in which the drug is entrapped in the microemulsions before polymerization, which suggests that the surfactant loss during the drug loading step was negligible.

3.3.3 Effect of Packaging Conditions on Drug Release

At the end of the packaging phase described in section 3.2.9, the gels were withdrawn and the concentration of drug in the liquid was measured to determine the amount of drug that

diffused out during this step (Table 3-3). The amount of drug that diffuses out of the gel during storage is less in salt solutions because CyA is a hydrophobic drug and so increasing ionic strength reduces drug solubility. Also, the amount of drug released into the packaging solution is largest for the 100 day soak which shows that the equilibration time for drug release from these gels is at least more than 30 days.

After the end of the storage phase, the gels were withdrawn and drug release experiments were conducted as described earlier. At short times, all the drug release profiles in Figure 3-5 are within 95% CI except the 100 day soak in 0.85% salt solution. Also the release duration from these systems is comparable to that from gels that were not subjected to packaging (Figure 3-4). These results demonstrate that the drug release profiles are relatively unaffected by soaking in packaging solution, and also by the composition of the packaging solution.

These results are encouraging but the microemulsion-laden gels also have several drawbacks. Firstly, preparation of microemulsion-laden gels is a two step process, which renders it cumbersome. Secondly, although the oil phase of the microemulsion is only slightly soluble in tears, it will likely elude at a slow rate, and thus could potentially cause ocular toxicity. Ethyl butyrate is food grade oil suitable for in vivo applications [117,118], but to our knowledge ocular toxicity of ethyl butyrate has not been investigated. To avoid potential ocular toxicity due to oil and to simplify the gel preparation, it is desirable to replace the microemulsions with micelles which may also impede drug release leading to extended drug delivery. To test this hypothesis, surfactant laden gels were fabricated, and drug release studies from these systems are described in section 3.3.4.

3.3.4 Drug Release from Micelle Laden Hydrogels

Figure 3-6 shows the drug release profile for S3 gels, i.e., gels loaded with 8% surfactant (w/dry gel w) with daily PBS change. The drug release profiles from microemulsion-laden gels

(M2) with similar surfactant loading are included in the figure for comparison. The results show that surfactant-laden gels also provide extended drug release lasting more than 20 days. The release rates of the microemulsion-laden gels are less than that for the surfactant-laden gels with 8% surfactant loading suggesting that the presence of oil further slows down drug transport. The effective diffusivity of the drug from the S3 gels was obtained by fitting the short time data to Equation 3-1 (Figure 3-7). The fitted diffusivity is 4.34×10^{-15} m^2/s, which is more than that for the M2 gels within 95% CI. We speculate that the surfactant-laden gels contain micelles and the drug preferentially partitions into the hydrophobic core of these micelles. The reported values of the critical micelle concentration (CMC) of Brij 97 range from 0.217 mM [119] to 0.94 mM [120]. The hydrated p-HEMA gels absorb about 39% water w/w. Based on these values, if the surfactant loading in a gel exceeds 0.061% - 0.27% (w/dry gel w), its concentration in the hydrated state is expected to be above the CMC. It is noted that this estimation neglects binding of surfactant to the gel, which is likely because the gel has some hydrophobic sites to which the surfactants are expected to adsorb. Also, the shapes of these micellar aggregates may be complex due to the confining effects of the gel. The cumulative release profile for surfactant system intercepts the x-axis at $\sqrt{t}= 2.5$, which lies within 95% CI of the intercepts for the microemulsion-laden gels (2.9±0.6), supporting the hypothesis that the initial delay in the drug release is caused due to hydration of surfactant aggregates.

3.3.5 Mechanism of Drug Release

The drug release from the surfactant-laden gels could be controlled by two potential mechanisms: transport of the drug from inside the micelles trapped in the gel to the bulk gel, or diffusion through the gel. The linear relationship between cumulative release and $\sqrt{t}$ suggested that the transport is controlled by diffusion through the gel. If the release is controlled by

diffusion, the release time scales as (thickness)^2, and if the release is controlled by transport from inside the micelles to outside, the release time should be independent of thickness.

To determine the rate limiting step, drug release profiles from 100 μm thick gels were compared with those from the 200 μm thick gels. These were equilibrium studies in which PBS was not replaced and the system was allowed to equilibrate. It is noted that the weights of both the thick and thin gels were about same because the cross sectional area of the thin gel was double that of the thick gel. The results from these studies are shown in Figure 3-8, where the percentage release of drug is plotted as a function of scaled time, where

$$\text{Scaled Time} = \text{Time} \times \left(\frac{100}{\text{h (in microns)}} \right)^2 \qquad (3\text{-}2)$$

In Equation 3-2, 'h' represents the thickness of the hydrogel. To compare the profiles shown in Figure 3-8, we computed the relative error defined as the ratio of the difference in cumulative percentage release between the thin and the thick gels and the cumulative release for the thick gels. We observe that the percentage release vs. scaled time profiles for the thin and the thick pure p-HEMA gels and also for the thick and the thin S3 gels are similar with root mean square of the relative error being 13.5% and 5.7% for the p-HEMA and the S3 gels, proving that the diffusion through the gel matrix is the rate controlling step.

3.3.6 Processing Conditions

S1, S2, S3, M2 and D1 gels were prepared by following procedures described earlier, and the drug was not loaded in these gels. These gels were about 100 μm thick and weighed about 40 mg. After monomer extraction described earlier, drug was loaded in these gels by soaking in drug solution and the amount of drug loaded into the gel was determined by calculating the

difference between the initial and the final concentrations in the drug solution. The results for the amount of drug loaded into these gels are shown in Table 3-4.

After autoclaving and 10 day storage in 1.5 ml DI water, the concentration in the aqueous phase was measured to determine the amount of drug that was released from the gel during the autoclaving and storage period. By subtracting this amount from the amount of drug taken up by the gel, amount of drug retained by the gel was determined. These results are also shown in Table 3-4. Each gel released about 25% of the entrapped drug into the solution during autoclaving and packaging.

The drug release profiles for the cumulative release as a function of time are shown in Figure 3-9 and the drug amounts released are shown in Table 3-4. We observe that each gel releases almost 100% of the entrapped drug. A 100% release along with the fact that the elusion spectra of the drug from the HPLC column (absorbance vs. time) is not altered by autoclaving suggests that the drug does not degrade during processing. The duration of drug release from the surfactant and microemulsion-laden gels is much longer than that for the pure p-HEMA gels, which shows that the processing steps, particularly autoclaving do not cause significant changes in the gel structure. We also believe that a significant amount of surfactant diffused out from these systems during processing and hence the release duration decreases due to processing conditions. Nevertheless, the systems with the higher surfactant loading release drug at the slower rate compared to p-HEMA gels, which suggests that even after processing steps there is enough surfactant in these systems to attenuate the drug release rates.

3.3.7 Brij 97 Release from p-HEMA Hydrogels

Surfactant is likely to diffuse into the tear film after a surfactant-laden contact lens is placed on the eye. It was thus important to measure the rate of surfactant release from the gels. The rate of surfactant released was measured from surfactant laden gels which contained 8%

surfactant by weight in dry gel (S3). By performing control experiments, it was verified that other components in the gels were not surface active. During the surface tension measurement, the surface area created was small and so the change in bulk concentration due to surfactant adsorption at the surface was negligible. Firstly, relationship between the surface tension and the bulk concentration of Brij 97 was measured, and this was used as a calibration curve to later relate the measured surface tension to the bulk concentration of the surfactant in the release experiments (Figure 3-10). To maximize the sensitivity of the measurements, the 3.5 ml solution was diluted by trial and error to surface tensions above 40 mN/m at which the surface tension is most sensitive to concentration. The percentage releases of the surfactant from both thick and thin gels are plotted against $\theta \equiv \sqrt{t\frac{100^2}{h^2}}$ in Figure 3-11 where 'h' is the thickness of the hydrogel and 't' is time in hours. These curves when fitted with a straight line had a slope of 1.47±0.08 ($R^2 = 0.99$) for the thick gels and 1.4±0.23 ($R^2 = 0.98$) for thin gels, matching within a 95% CI. The thin gels, which were about the same thickness as typical contact lenses, released about 48% of the surfactant in a period of 65 days. This corresponds to around 1500 μg of surfactant released in 65 days, or equivalently an average of 25 μg/day. Brij 97 surfactant has been previously explored as oral delivery vehicle but ocular toxicity of this surfactant has not been evaluated in literature [117,121,122]. However, similar surfactants from the series of Brij surfactants (Brij 35, Brij 78, Brij 98) have been shown to be non-toxic at high concentrations on the corneal surface and have also been shown to be useful as cornea permeability enhancers [67,68,123]. Thus a slow release of surfactants from the lens could have the beneficial effect of increase in corneal permeability of the drug leading to increased bioavailability.

3.4 Conclusion

This chapter focused on exploring microemulsion and surfactant-laden hydrogels for extended delivery of CyA. It was shown that by using Brij 97 surfactant, both surfactant and microemulsion-laden gels exhibit slow and extended drug release lasting for about 20 days. This is a significant improvement compared to the control (pure p-HEMA gels), which releases drug for less than 5 days. The duration of drug release depends on the surfactant loading, and the rates of drug release are slightly smaller for microemulsion-laden gels compared to surfactant-laden gels with same surfactant loading.

The transport of CyA in the surfactant-laden gels is controlled by diffusion. The hydrated gels are expected to contain surfactant aggregates and CyA, which is a hydrophobic drug, partitions into the hydrophobic domains of these aggregates leading to an increase in partition coefficient leading to a slow down in transport rates from the gel.

The drug release profiles are unaffected by the method of drug loading. The gels which had CyA loaded by soaking in solutions had similar results compared to those gels in which the drug was added before polymerization. The duration of drug release was longest for highest surfactant containing gels after processing conditions which included autoclaving and packaging. These results are very encouraging and it seems that surfactant or microemulsion-laden gels may be suitable for delivering CyA to eyes. In addition to treating ocular disorders, CyA has also shown promise in treating contact lens mediated dry eyes, and so these systems could also be very useful for a large population that is unable to wear contact lenses due to discomfort [124]. Furthermore, the surfactant-laden gels are expected to have better wettability that could also lead to improved comfort.

While these systems are promising, it is noted that p-HEMA lenses cannot be used for extended wear because of low oxygen permeability. Thus the surfactant-laden p-HEMA contact

lenses will need to be taken off at night and cleaned to remove the protein and lipid deposits. The impact of these steps on CyA release needs to be assessed.

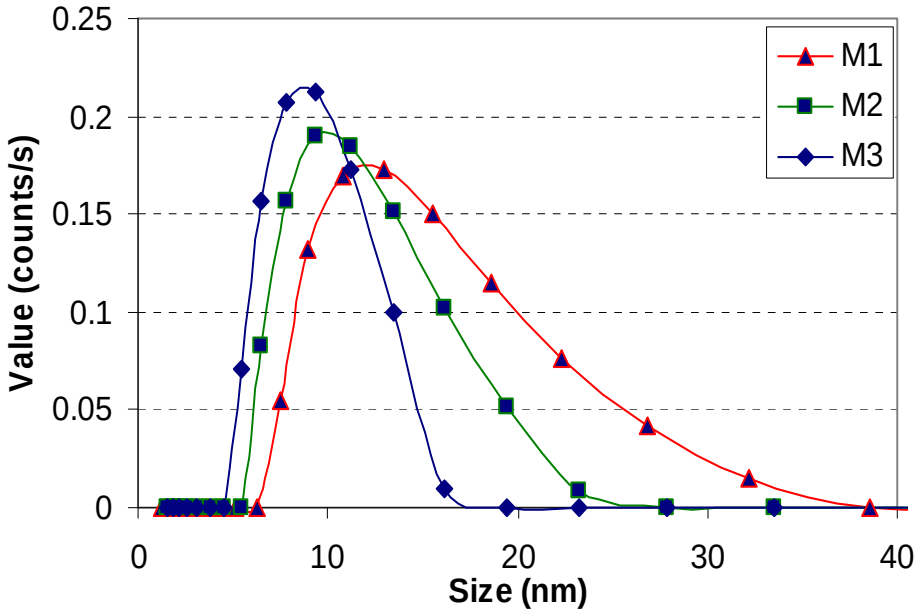

Figure 3-1. Size distribution of microemulsions with three different surfactant loadings

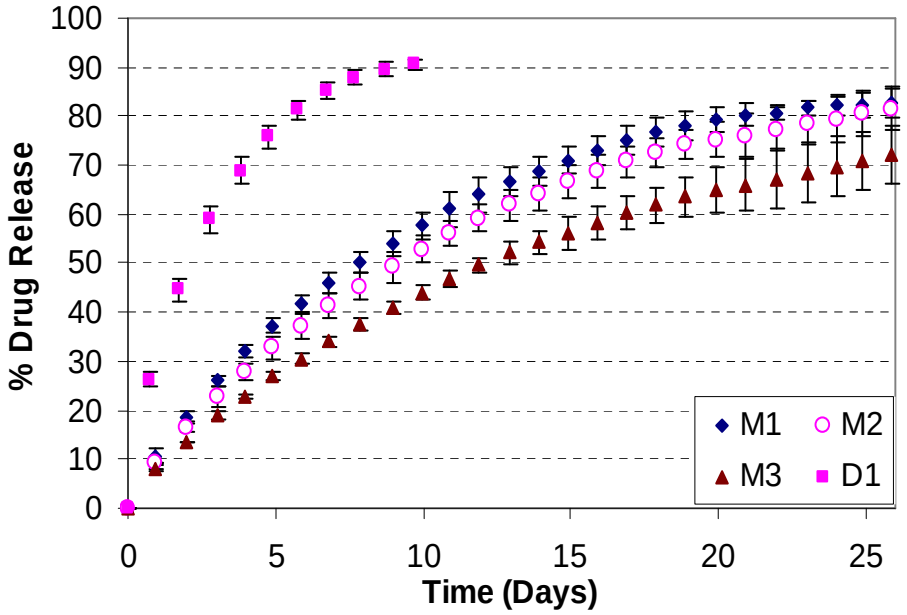

Figure 3-2. Cumulative percentage release of drug from microemulsion laden gels with varying surfactant loading and pure p-HEMA gels. All the gels were 200 μm thick in dry state and gels M1, M2, M3 and D1 contained 48.5, 52.2, 53.4 and 53.3 μg of drug, respectively. Data are plotted as mean SD for M2, D1 gels (n = 3). The error bars for M1 and M3 systems represent half the difference between the data from two repeat runs.

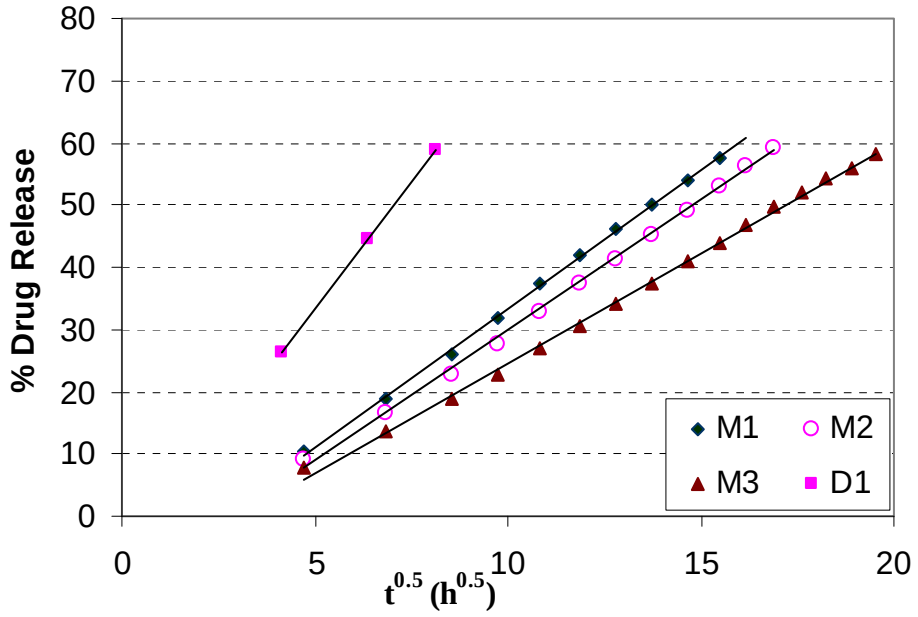

Figure 3-3. Linear fits for the short time release data to obtain the effective diffusivity for microemulsion and pure p-HEMA gels

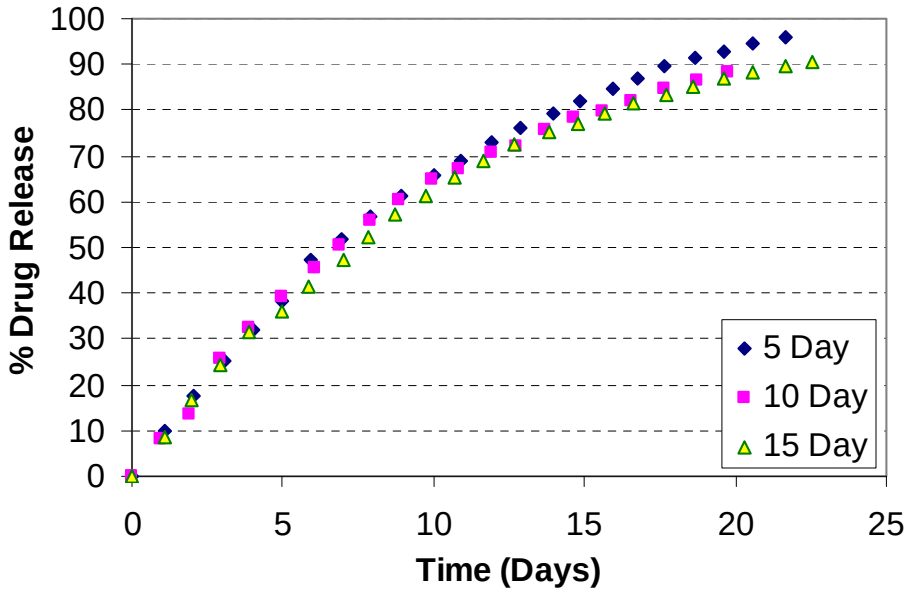

Figure 3-4. Cumulative percentage release of drug from microemulsion gels after loading the drug into gels by soaking in a drug solution for 5, 10 and 15 days

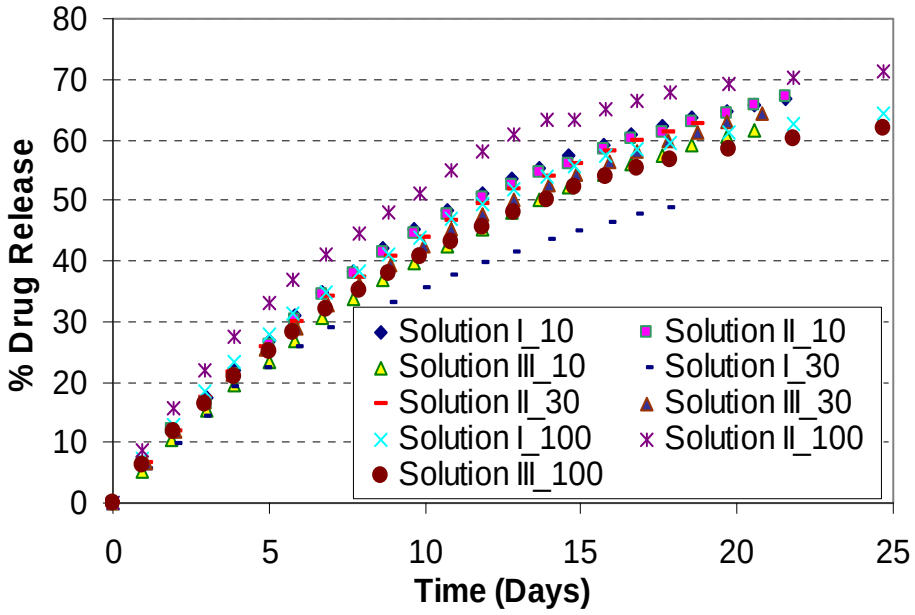

Figure 3-5. Cumulative percentage release of drug from microemulsion laden gels after packaging in three different salt solutions for different durations of time. Solution 1 ≡ DI water; Solution II ≡ 0.85% salt solution; Solution III ≡ 4.25% slat solution. All the gels were 200 μm thick in dry state.

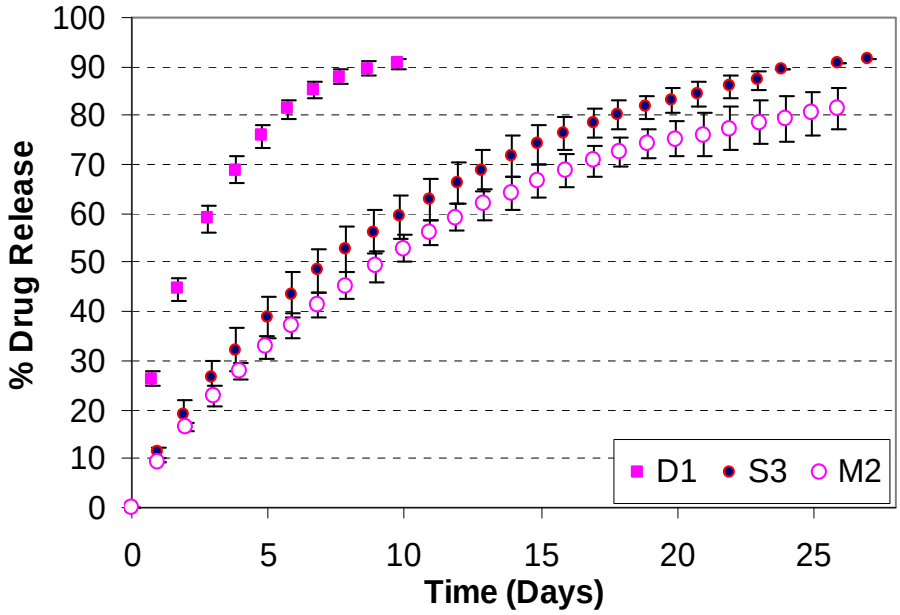

Figure 3-6. Cumulative percentage release of drug from Brij 97 surfactant laden, microemulsion laden and pure p-HEMA gels. All the gels were 200 μm thick in dry state and gels S3, M2 and D1 contained 49.2, 52.2 and 53.3 μg of drug, respectively. Data are plotted as mean SD (n = 3).

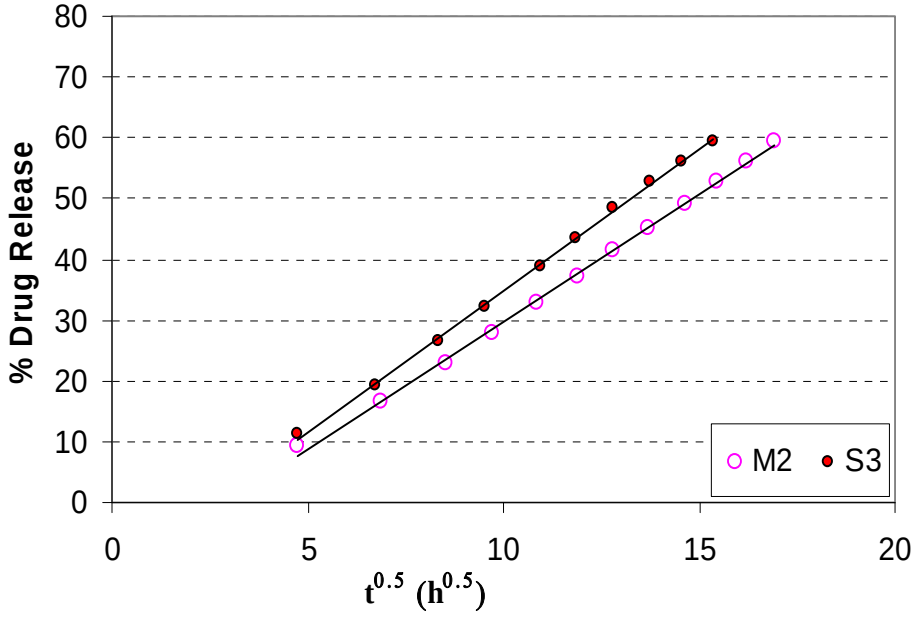

Figure 3-7. Linear fits for the short time release data to obtain the effective diffusivity for surfactant laden gels

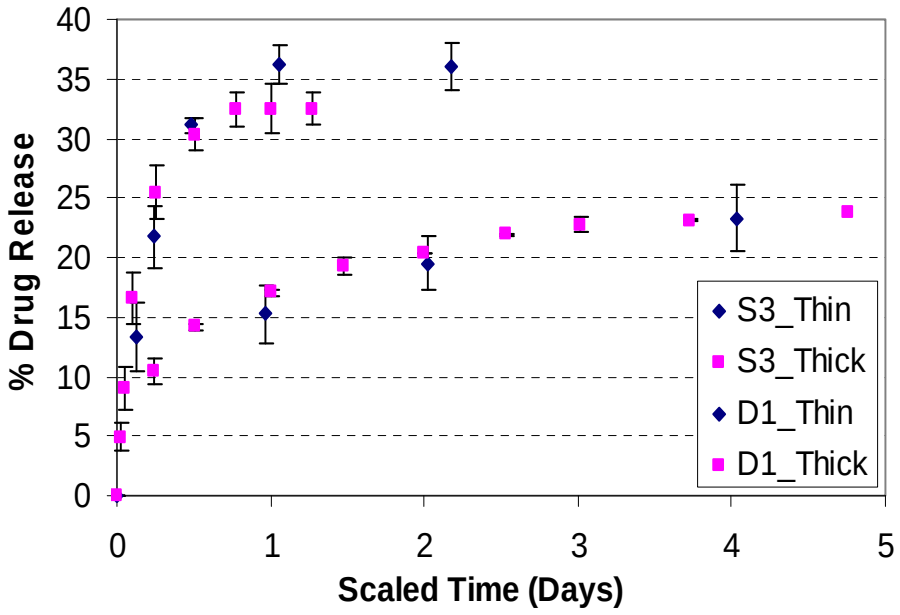

Figure 3-8. Effect of thickness on percentage release for p-HEMA gels and surfactant laden gels for equilibrium experiments. S3_Thin, S3_Thick, D1_Thin and D1_Thick contained 49.2, 52.4, 56.2 and 57.7 μg of drug, respectively. Data are plotted as mean SD (n = 3).

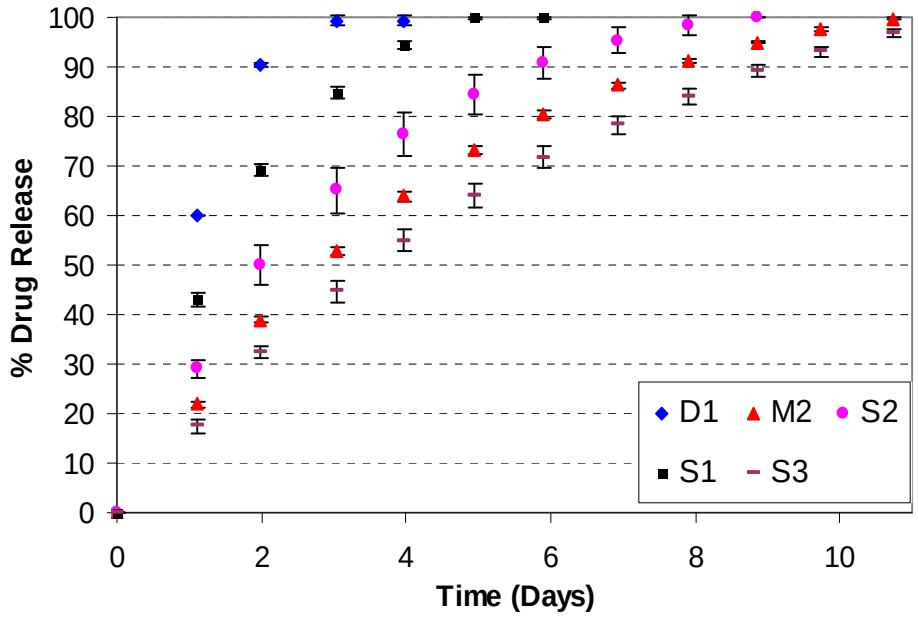

Figure 3-9. Effect of surfactant loading and processing conditions on cumulative percentage release from pure p-HEMA, the microemulsion laden and surfactant laden gels. All the gels were 100 μm in thickness. The error bars represent half the difference between the data from two repeat runs.

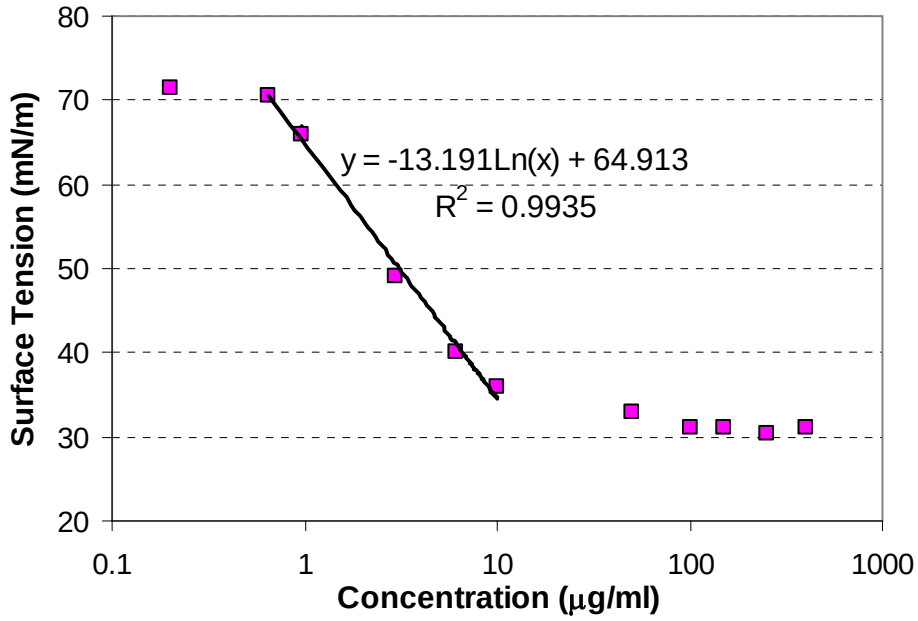

Figure 3-10. Dependence of surface tension on the bulk surfactant concentration. for Brij 97 surfactant

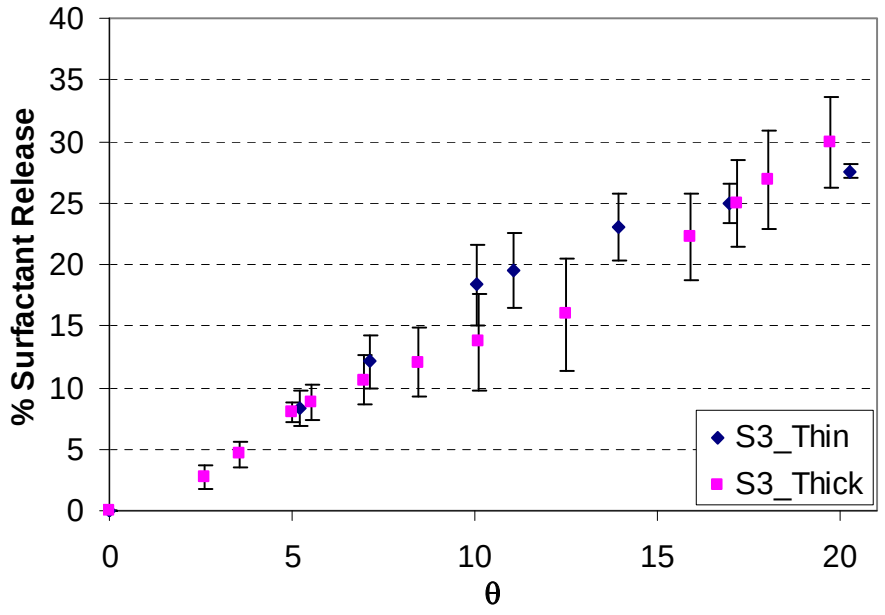

Figure 3-11. Cumulative percentage release of surfactant from surfactant laden gels. Thin gels contained 3245 µg of surfactant and thick gels contained 3344 µg of surfactant. Data are plotted as mean SD (n = 3).

Table 3-1. Diffusion coefficients of the drug for the microemulsion laden systems

System	Slope	95% CI for slope	$Dx10^{15}$ m^2/s	R^2
M1	4.47	(4.30, 4.64)	4.36	0.99
M2	4.12	(3.98, 4.26)	3.70	0.98
M3	3.52	(3.41, 3.62)	2.70	0.99
D1	8.12	(7.46, 8.78)	14.4	1.00

Table 3-2. Drug uptake by microemulsion laden gel M2 after soaking in drug solution

X Days	Amount of CyA initially in solution (μg)	Amount of CyA left in solution after X Days(μg)	Amount of CyA loaded in the gel (μg)
5	46	16.2	29.8
10	46	15.1	30.9
15	46	15.2	30.8

Table 3-3. Drug released in the packaging medium from microemulsion-laden gels M2

	X Days	Drug inside the gel before packaging (μg)	Drug released in packaging (μg)	Drug left in the gel after packaging (μg)
Solution I	10	44.2	7.1	37.1
(DI Water)	30	49.8	9.7	40.1
	100	46.9	17.6	29.3
Solution II	10	49.8	6.7	43.1
(0.85% w/w Salt Solution)	30	47.7	10.3	37.4
	100	47.9	16.6	31.3
Solution III	10	52.3	3.3	48.0
(4.25% w/w Salt Solution)	30	47.9	5.6	42.3
	100	52.6	9.6	43.0

Table 3-4. Drug loading and release from surfactant-laden and microemulsion-laden gels subjected to processing conditions. The error bars represent half the difference between the data from two repeat runs.

System	Drug in solution initially (μg)	Drug remaining in the solution after 12 days of soaking (μg)	Amount of drug inside the gel (μg)	Amount of drug released during storage (μg)	Amount of drug retained in the gel (μg)	Amount of drug released during experiments (μg)
S3	48	18.2 ± 1.1	29.8 ± 1.1	5.5 ± 0.4	24.4 ± 1.5	22.1 ± 0.0
S2	48	25.0 ± 2.9	23.0 ± 2.9	4.5 ± 0.1	18.6 ± 2.9	20.0 ± 1.1
S1	48	23.2 ± 0.6	24.9 ± 0.6	6.9 ± 0.1	17.9 ± 0.6	14.6 ± 1.0
M2	48	22.5 ± 0.6	25.6 ± 0.6	6.5 ± 0.1	19.1 ± 0.5	19.5 ± 0.1

CHAPTER 4
MODEL FOR SURFACTANT AND DRUG TRANSPORT FROM P-HEMA HYDROGEL

4.1 Introduction

Goals of this chapter are to understand and model the transport of both surfactant and drug from the hydrogels. In this chapter we specifically focus on p-HEMA hydrogels that are loaded with Brij 98 surfactant and drug CyA. Experiments are done to validate the model and data from publications of other authors are also shown to approve with the developed model. While this work focuses on a specific set of drug, surfactant and polymer, the model developed here is expected to be valid for a wide variety of systems.

4.2 Materials and Methods

4.2.1 Materials

HEMA monomer, ethylene glycol dimethacrylate (EGDMA), Dulbecco's phosphate buffered saline (PBS), Acetonitrile, HPLC grade water and Brij 98 were purchased from Sigma-Aldrich Chemicals (St Louis, MO). Darocur TPO was kindly provided by Ciba (Tarrytown, NY). CyA was purchased from LC Laboratories (Woburg, MA). All the chemicals were reagent grade. Acetonitrile was filtered before use and all the other chemicals were used without further purification.

4.2.2 Synthesis of Surfactant Laden Gels

Surfactant solutions of three different concentrations were prepared by adding 0.25, 0.6, 1.5 g of the surfactant to 10 ml water and then stirring the mixture at 600 rpm and at room temperature for a period of about 10 hours. Separately, 3.8 mg of CyA was dissolved in 2.7 ml of HEMA monomer and stirred at 600 rpm for a period of 5 hours. 15 µl of the crosslinker (EGDMA) and 2ml of surfactant solution were added to the 2.7 ml of drug-HEMA mixture. The solution was then degassed by bubbling nitrogen for 10 minutes. Next, 6 mg of the initiator

(TPO) was added and the solution was stirred at 300 rpm for 10 minutes to completely solubilize the initiator. The solution was then poured in between two glass plates that were separated either by a 200 μm (thick gels) or 100 μm (thin gels) thick spacer. The mold was then placed on Ultraviolet transilluminiator UVB-10 (Ultra Lum, Inc.) and the gel was cured by irradiating UVB light (305 nm) for 40 min. To synthesize HEMA gels without surfactants, 2 ml of the surfactant solution was replaced by 2 ml DI water. These gels are referred to as pure gels in the following sections.

4.2.3 Drug Release Experiments

After polymerization, each gel was removed from the glass mold and was cut into smaller pieces that were about 1.5 cm X 1.5 cm X 200 μm for the thick gels and 1.5 cm X 3 cm X 100 μm for the thin gels, with each gel weighed nearly 40 mg. Two sets of experiments were performed for the drug release studies. In the first set of experiments, gel was soaked in 3.5 ml of PBS and the drug concentrations in the release medium were measured periodically until the drug flux approached zero. In the second set of experiments, we attempted to create perfect sink conditions in the release medium of 3.5 ml PBS by replacing the medium every 24 hours. CyA concentration was measured using an HPLC (Waters, Alliance System) equipped with a C_{18} reverse phase column and a UV detector. The mobile phase composition was 70% acetonitrile and 30% DI water, and the column was maintained at 60°C. The flow rate was fixed at 1.2 ml/min and the detection wavelength was set at 210 nm [114]. The retention time for CyA under these conditions was 5.3 minutes, and the calibration curve for area under the peak vs. concentration was linear ($R^2 = 0.98$).

4.2.4 Surfactant Release

The rates of surfactant release from the gels were measured by soaking them in 3.5 ml DI water and replacing the release medium at regular intervals. The surfactant concentration in the release medium was determined by measuring surface tensions (σ), which was then related to the concentration through a $\sigma(C)$ calibration curve. The surface tension was measured by using a Wilhelmy plate (sand blasted platinum plate) attached to a Scaime France Microbalance which was further connected to a Stathan Universal transducer (SC001). The transducer was calibrated by using DI water (σ = 72 mN/m) and acetone (σ = 23 mN/m) as standards. The Wilhelmy plate was rinsed with DI water and acetone followed by annealing till red hot using a propane burner. The annealing process was done to remove impurities which rinsing was not able take away from the platinum surface. This process was repeated before every measurement and the plate was left to cool for one minute before taking the measurement. The solution was allowed to equilibrate for an hour prior to the measurement to ensure that the surface coverage was in equilibrium with the bulk concentration. It was also ensured that the surface area to volume ratio was sufficiently small to cause a negligible change in bulk concentration due to adsorption of the surfactant on the surface.

4.3 Results and Discussion

4.3.1 Drug Release from Pure p-HEMA Gels with Daily PBS Replacement

The drug loaded into pure p-HEMA gels is present either as free drug in the water phase (C) inside the gel or as drug bound to the polymer (Γ). The mean drug concentration in the gel (Cg), which is essentially the sum of the bound and the free drug concentration, is given by $(S/V)_{gel}\Gamma + fC$, where $(S/V)_{gel}$ is the surface area per volume of the gel available for the drug to adsorb and 'f' is the volume fraction of water in hydrated gel (Figure 4-1). The value of 'f' for

p-HEMA gels was determined to be 0.39 from the swelling experiments. The free and the bound drug are expected to be in equilibrium and so the total gel concentration and the free drug concentration can be related through a partition coefficient $K_d = C_g/C$, which is assumed to be concentration independent. The transport of the drug in the hydrogel is expected to occur by a combination of bulk and surface diffusion, and thus it can be described by the modified diffusion equation, i.e.,

$$\frac{\partial C_g}{\partial t} = fD_f \frac{\partial^2 C}{\partial y^2} + D_{SU}\left(\frac{P}{A}\right)\frac{\partial^2 \Gamma}{\partial y^2} \tag{4-1}$$

where D_f and D_{SU} are the diffusivities of the drug in solution and on the surface, respectively, and (P/A) is the perimeter of the gel fibers per unit cross-sectional area, which can be approximated as (S/V). For a number of drugs including CyA, the partition coefficient K_d is much larger than 1, and so most of the drug can be safely assumed to be bound to the polymer matrix. Utilizing the definition of partition coefficient in the above equation gives

$$\frac{\partial C}{\partial t} = \frac{\left(fD_f + D_{SU}(K_d - f)\right)}{K_d}\frac{\partial^2 C}{\partial y^2} = D\frac{\partial^2 C}{\partial y^2} \tag{4.2}$$

In Equation 4-2, $D \equiv \dfrac{\left(fD_f + D_{SU}(K_d - f)\right)}{K_d}$ is the effective diffusivity of drug in the gel.

Equation 4-2 is subjected to the following boundary conditions,

$$\frac{\partial C}{\partial y}(t, y = 0) = 0 \tag{4-3}$$

$$C(t, y = h) = 0 \tag{4-4}$$

where 'h' is the half-thickness of the gel. The first boundary condition (Equation 4-3) assumes symmetry at the center of the gel and the second boundary condition (Equation 4-4) assumes

infinite sink conditions in the release medium. The initial condition for the drug release experiments is:

$$C(y, t = 0) = C_i \tag{4-5}$$

Where, C_i is the initial concentration of drug inside the hydrogel.

Equations 4-2 to 4-5 can be solved to give

$$C = \sum_{n=0}^{\infty} \frac{(-1)^n 4C_i}{(2n+1)\pi} \cos\left(\frac{(2n+1)\pi}{2h} y\right) e^{-\frac{(2n+1)^2 \pi^2}{4h^2} Dt} \tag{4-6}$$

The fraction released can be computed from Equation 4-6 to give

$$R_D(\%) = \frac{8}{\pi^2} \sum_{n=0}^{\infty} \frac{1}{(2n+1)^2} \left(1 - e^{-\frac{(2n+1)^2 \pi^2}{4h^2} Dt}\right) \times 100 \tag{4-7}$$

In the short time limit, Equation 4-7 simplifies to the following form [87],

$$R_D(\%) = \sqrt{\frac{4Dt}{\pi h^2}} \times 100 \tag{4-8}$$

Figure 4-2 plots the percentage release of CyA from pure p-HEMA gels vs.√t and the slope of the plot is used to obtain D, which has a value of 1.44×10^{-14} m^2/s. This value is much lower than the free solution diffusivity of CyA due to the small pore size of the p-HEMA gels.

4.3.2 Surfactant Release from the Hydrogels

4.3.2.1 Model

The hydrated surfactant laden hydrogels are expected to contain the surfactant in three different forms: free surfactant, surfactant adsorbed on the polymer and surfactant present in aggregates. On soaking of this gel in aqueous solution, free surfactant and the adsorbed surfactant diffuse and elude from the gel into the release medium. This transport reduces the free concentration of the surfactant below the critical aggregation concentration (CAC) leading to breakup of the aggregates. This mechanism results in creation of a depletion zone near the

surface which does not contain aggregate particles because these are already dissolved, and the thickness of this zone (δ) increases with time (Figure 4-3). The free concentration of surfactant in the zone that still contains the aggregates must be equal to the CAC (C*), and the surfactant contained in the aggregates should be at concentration $C_p = C_{iS} - C^*$, where C_{iS} is the initial surfactant concentration. Thus, we get the following model to describe surfactant transport from gel systems,

$$\frac{\partial C_S}{\partial t} = D_S \frac{\partial^2 C_S}{\partial y^2} \quad \text{for} \quad 0 < y < \delta(t) \tag{4-9}$$

$$C_S = C^* \qquad \text{for} \quad \delta(t) \le y < h \tag{4-10}$$

With the following initial and boundary conditions,

$$C_S(t, y = 0) = 0 \tag{4-11}$$

$$C_S(t, y = \delta) = C^* \tag{4-12}$$

$$D_S \frac{\partial C_S}{\partial y} = C_p \frac{\partial \delta}{\partial t} \quad \text{for} \quad y = \delta \tag{4-13}$$

$$\delta(t = 0, y) = 0 \tag{4-14}$$

Where, 'h' is the half thickness of the gel, and C_S is the concentration of the un-aggregated surfactant, which includes both free and polymer bound surfactants. Also D_S is the average surfactant diffusivity that includes contributions from both free and surface diffusion of the surfactant. The first boundary condition (Equation 4-11) assumes perfect sink conditions, the second boundary condition (Equation 4-12) arises from continuity of concentration and the third condition (Equation 4-13) states that the surfactant flux at the intersection of the zone with aggregates and the one without aggregates is equal to the amount released by the dissolution of the aggregates. The above model is only valid till δ is less than h, and after that the transport is

purely diffusive. It is noted that the above model is very simplistic because it neglects drug-surfactant interaction.

The above partial differential equation admits a similarity solution of the form $C_S(y,t) = C_S(\eta)$, where $\eta = y/\sqrt{4D_S t}$ and $\delta = \alpha\sqrt{4D_S t}$. With these substitutions, the equations and the boundary conditions reduce to the following form:

$$2\eta \frac{dC_S}{d\eta} + \frac{d^2 C_S}{d\eta^2} = 0 \tag{4-15}$$

$$C_S(\eta = 0) = 0 \tag{4-16}$$

$$C_S(\eta = \alpha) = C^* \tag{4-17}$$

$$\left(\frac{dC_S}{d\eta}\right)_{\eta=\alpha} = 2\alpha C_p \tag{4-18}$$

Equation 4-15 is a ordinary differential equation and it can be solved to yield the concentration profile

$$C_S = C^* \frac{\int_0^\eta e^{-\xi^2} d\xi}{\int_0^\alpha e^{-\xi^2} d\xi} \tag{4-19}$$

Where α can be obtained by solving the following implicit equation:

$$2\alpha \frac{C_p}{C^*} = \frac{e^{-\alpha^2}}{\int_0^\alpha e^{-\xi^2} d\xi} \tag{4-20}$$

For case of , $\frac{C_p}{C^*} >> 1$, Equation 4-20 can be simplified to yield

$$\alpha = \sqrt{\frac{C^*}{2C_p}} \tag{4-21}$$

The flux from the gel to the outside fluid medium can be calculated as

$$j = \left(D_S \frac{\partial C_S}{\partial y} \right)_{y=0} = \sqrt{\frac{D_S}{4t}} \frac{C^*}{\int_0^{\alpha} e^{-\xi^2} d\xi} \tag{4-22}$$

The total amount of surfactant released from a gel can then be calculated by integrating the flux in time and then multiplying by the surface area 2A to give

$$N_S = 2A\sqrt{D_S t} \frac{C^*}{\int_0^{\alpha} e^{-\xi^2} d\xi} \tag{4-23}$$

Again in the limit $\frac{C_p}{C^*} >> 1$ the above expression can be simplified to yield

$$N_S = 2A\sqrt{2D_S t C^* C_p} \tag{4-24}$$

Physically, the limit $C_P >> C^*$ represents the pseudo-steady solution to the above equations as in this limit the time scale of changes in δ due to micellar breakup far exceed the diffusive time scales in region I and so the concentration profile of the surfactant in region I is linear. Furthermore, in this limit, the values of C_p are close to the total surfactant concentration initially loaded into the gel (C_{iS}). The amount of drug initially loaded into the gel can be approximated as $2AhC_p$, and thus the percentage surfactant release $R_S(\%)$ from the system is given by

$$R_S(\%) = \sqrt{2D_S C^*} \sqrt{\frac{t}{C_p h^2}} \times 100 \tag{4-25}$$

Thus plots of percentage release vs. $\sqrt{\frac{t}{C_p h^2}}$ should be a straight line with slope $\sqrt{2D_S C^*} \times 100$. It is noted that this result sharply contrasts with the result for pure Fickian

diffusion without any aggregate formation for which case the release rates scale linearly with loading and so the percentage release is independent of the initial surfactant loading. A similar equation has been proposed in the past for drug diffusion from suspension inside an ointment [89]. So it seems that both the systems are similar, though this method is more rigorous and helps in understanding of the structural details due to incorporation of surfactants inside the hydrogels. Our model can be solved numerically to determine the complete release profiles of surfactants whereas Higuchi model was solved assuming pseudo steady state and is valid for a small time of release.

4.3.2.2 Experimental results

The concentration of the surfactant in the release medium was determined by measuring the surface tension of the fluid and relating it to the surfactant concentration through the measured $\sigma(C)$ relationship shown in Figure 4-4. It should be noted that during these studies, 3.5 ml of water was used as the release medium. To maximize the sensitivity of the measurements, the 3.5 ml solution was diluted by trial and error to surfactant concentrations below its critical micelle concentration (CMC) at which the surface tension is most sensitive to concentration. We also performed control experiments to check for surface activity of the un-reacted monomer from the gels and found no change in surface tension of water.

To validate the model developed above, it was decided to explore the effects of gel thickness and initial surfactant loading on release rates of the surfactant. Surfactant-laden gels with 8% surfactant by weight in dry state were prepared having two different thicknesses (100 and 200 μm). Also 200 μm thick gels were prepared with 4% surfactant loading by weight in dry state. The weights of both the thick and the thin gels were about the same because the cross sectional area of the thin gel was double that of the thick gel. Surfactant release data from all the

three sets of hydrogels is plotted in Figure 4-5 and we observe that the percentage release decreases with an increase in surfactant loading, which agrees with the model proposed above. Also, the release rates decrease with an increasing thickness, which is expected. Equation 4-25 predicts that a plot of cumulative percentage vs. $\theta \equiv \sqrt{\frac{t}{C_p h^2}}$ should be a straight line with slope $\sqrt{2D_S C^*} \times 100$. To quantitatively validate the model, in Figure 4-6, the percentage release is plotted against θ. All the release curves match and are linear at short times validating the model. The slope indicated in the figure has a value of 1.1 ± 0.03. The model predicts that the plot in Figure 4-6 must stay linear till the boundary layer thickness δ becomes equal to h. At this time the gel does not contain any micelles and so the concentration in the entire gel is less than or equal to C*. For cases in which C* is much less than C_p, the amount of surfactant in the gel after all the micelles are broken is a very small fraction of the initial surfactant loading. This is clearly evident in Figure 6 as the plot deviates from linear behavior after the percentage release exceeds 95%. The slope of the line in Figure 4-6 depends only on the parameter ($D_S C^*$) and so we cannot determine both D_S and C*. The non-linear part of the curve depends on these parameters individually, but since the non-linear part of the curve contributes to a very small fraction of the release, it is not prudent to use that limited data to determine D_S and C* individually. The value of surfactant diffusivity can be obtained by techniques such as nuclear magnetic resonance or by measuring surfactant release rates with low surfactant loading, and then the value of C* can be obtained from the slope of the data in Figure 4-6. Later in chapter 7 we will also discuss two model techniques to determine the CAC of surfactants. However it is shown later that the drug transport from the gels does not depend on DS and C* individually, but only on the product.

4.3.3 Drug Release from Surfactant Laden Gels

4.3.3.1 Model

As described in the previous section, diffusion and breakup of micelles leads to creation of two zones: the first zone contains free surfactant below the critical aggregation concentration, C* and the second zone contains micelles at concentration C_p and free surfactant at concentration C*. The drug in region I can exist either as free or bound to the polymer and both of these forms can diffuse with respective diffusivities. Accordingly, the mass balance in region I can be described by the following equation:

$$\frac{\partial C_I}{\partial t} = D\frac{\partial^2 C_I}{\partial y^2} \quad \text{for } 0 \le y \le \delta(t) \tag{4-26}$$

Where C_I is the total drug concentration in region I, which includes both free and polymer bound drug, and D is the average diffusivity that includes contributions from both free and surface diffusion. Furthermore, it is assumed that surfactant and drug transport are uncoupled in this region, which may be a reasonable assumption due to small drug concentrations explored here. It is noted that the drug diffusivity in the above equation is assumed to be the same as obtained from the experiments of drug release from pure p-HEMA gels in section 4.3.1. In region II, a fraction of the drug partitions inside the micelles and this fraction is not available for diffusion. Assuming that the time scale of drug transport from inside the micelle to outside is rapid, the concentration of drug inside the micelle is denoted by $K_m C_{II}$, where K_m is the partition coefficient of the drug. The average concentration of micelle bound drug can then be given by $\frac{K_m C_{II} C_p MW_S f_h}{\rho}$ where C_p is the concentration of surfactant present as micelles, 'MW_S' is the molecular weight of the surfactant, 'ρ' is the density of micellar core inside the gel volume and 'fh' is the fraction of the surfactant length which is hydrophobic in nature. For Brij 98

surfactant, fh can be approximated as 0.3. This expression can then be written as KC_pC_{II} where $K \equiv \frac{K_m MW_S f_h}{\rho}$. Thus, the total concentration of the drug in region II is $(1 + KC_p)C_{II}$. However, only the drug present outside the micelles can diffuse towards region I. Thus, mass balance in region II can be described by

$$\frac{\partial(1 + KC_P)C_{II}}{\partial t} = D\frac{\partial^2 C_{II}}{\partial y^2} \quad \text{for } \delta(t) \le y \le h \tag{4-27}$$

The average diffusivity in the above equation is assumed to be the same as the average drug diffusivity in region I. The boundary and the initial conditions for the mass balance equation are,

$$C_I(t, y = 0) = 0 \tag{4-28}$$

$$\frac{\partial C_{II}}{\partial y}(t, y = h) = 0 \tag{4-29}$$

$$C_I(t, y = \delta) = C_{II}(t, y = \delta) \tag{4-30}$$

$$D\frac{\partial C_I}{\partial y} = D\frac{\partial C_{II}}{\partial y} + KC_p C_{II}\frac{d\delta}{dt} \quad \text{at } y = \delta \tag{4-31}$$

$$C_{II}(t = 0, y) = C_f \tag{4-32}$$

Where, C_f is the initial free drug concentration in the gel, and it equals $C_i/(1 + KC_p)$, where C_i is the initial total drug concentration. The first boundary condition (Equation 4-28) assumes perfect sink conditions in the release medium and the second boundary condition (Equation 4-29) assumes symmetry at the gel center. The third (Equation 4-30) and the fourth boundary conditions (Equation 4-31) arise from assumptions of continuity of free concentration and total drug flux, with the second term on the RHS of the last boundary condition (Equation 4-31) accounting for the drug flux due to breakup of micelles.

To facilitate analytical solutions at short times, i.e., times in which the thickness of the drug concentration boundary layer is less than the half gel thickness, we replace Equation 4-29 by the following equivalent equation

$$C_{II}(t, y = h) = C_f \tag{4-33}$$

The above set of equations admits a similarity solution at short times of the form $C_I^{'} \equiv \frac{C_I}{C_f} = C_I^{'}(\eta)$ and $C_{II}^{'} \equiv \frac{C_{II}}{C_f} = C_{II}^{'}(\eta)$ where $\eta = y/\sqrt{4D_S t}$ and as shown in the previous section, $\delta = \alpha\sqrt{4D_S t}$. This transformation leads to the following equations and the boundary conditions,

$$2\eta \frac{D_s}{D} \frac{dC_I^{'}}{d\eta} + \frac{d^2 C_I^{'}}{d\eta^2} = 0 \tag{4-34}$$

$$2\eta \frac{(1 + KC_p)D_s}{D} \frac{dC_{II}^{'}}{d\eta} + \frac{d^2 C_{II}^{'}}{d\eta^2} = 0 \tag{4-35}$$

$$C_I^{'}(\eta = 0) = 0 \tag{4-36}$$

$$C_{II}^{'}(\eta \to \infty) = 1 \tag{4-37}$$

$$C_I^{'}(\eta = \alpha) = C_{II}^{'}(\eta = \alpha) \tag{4-38}$$

$$\frac{dC_I^{'}}{d\eta} = \frac{dC_{II}^{'}}{d\eta} + \frac{2KC_p C_{II}^{'} D_s \alpha}{D} \text{ for } \eta = \alpha \tag{4-39}$$

Solving the above set of equations utilizing the first three boundary conditions (Equations 4-36,4-37,4-38) yields the following solutions,

$$C_I^{'} = B\int_0^{\eta} e^{-\frac{D_s}{D}\xi^2} d\xi \tag{4-40}$$

$$C_{II}^{'} = 1 - \left(\frac{1 - B\int_{0}^{\alpha} e^{-\frac{D_s}{D}\xi^2} d\xi}{\int_{\alpha}^{\infty} e^{-\frac{D_s}{D}\left(1+Kc_p\right)\xi^2} d\xi} \right) \int_{\eta}^{\infty} e^{-\frac{D_s}{D}\left(1+Kc_p\right)\xi^2} d\xi \tag{4-41}$$

As shown above, for case of $\frac{C_p}{C^*} >> 1$, $\alpha = \sqrt{\frac{C^*}{2C_p}}$. In this limit the expression for the concentration simplify to yield

$$C_{I}^{'} = B\int_{0}^{\eta} e^{-\frac{D_s}{D}\xi^2} d\xi \tag{4-42}$$

$$C_{II}^{'} = 1 + \left(\frac{\left(1 - B\alpha\right)}{\sqrt{\frac{D\pi}{4D_S\left(1+Kc_p\right)}} - \alpha} \right) \left[\int_{0}^{\eta} e^{-\frac{D_s}{D}\left(1+Kc_p\right)\xi^2} d\xi - \sqrt{\frac{D\pi}{4D_S\left(1+Kc_p\right)}} \right] \tag{4-43}$$

Applying the flux equality boundary condition (Equation 4-39) at $\eta = \alpha$, gives the following expression for B

$$B = \frac{1}{\sqrt{\frac{D\pi}{4D_S\left(1+KC_p\right)}} - KC^* \sqrt{\frac{D_S\pi}{4D\left(1+KC_p\right)}} + KC^* \frac{D_s}{D}\sqrt{\frac{C^*}{2C_P}}} \tag{4-44}$$

Assuming that a major fraction of the drug in Region II is inside the micelles $KC_p >> 1$, and thus the expression for B simplifies to

$$B = \frac{1}{\sqrt{\frac{D\pi}{4D_S KC_P}} - C^* \sqrt{\frac{KD_S\pi}{4DC_P}} + KC^* \frac{D_s}{D}\sqrt{\frac{C^*}{2C_P}}} \tag{4-45}$$

The flux from the gel to the fluid can than be calculated as

$$j = D\frac{\partial C_I}{\partial y}\Big|_{y=0} = \frac{DC_f B}{\sqrt{4D_s t}} \tag{4-46}$$

The total amount of drug released from a gel can be calculated by integrating the flux in time and then multiplying by the total surface area '2A' to give

$$N = \frac{2DC_f\sqrt{t}A}{\sqrt{D_s}} \frac{1}{\sqrt{\frac{D\pi}{4D_S KC_P}} - C^* \sqrt{\frac{KD_S\pi}{4DC_P}} + KC^* \frac{D_s}{D}\sqrt{\frac{C^*}{2C_P}}} \tag{4-47}$$

The amount of drug initially loaded into the gel is $2AhC_i$ and thus the percentage drug release R_D(%) from the system is given by

$$R_D(\%) = \beta\sqrt{\frac{t}{C_p h^2}} \times 100 \tag{4-48}$$

Where,

$$\beta = \frac{1}{\sqrt{\frac{K\pi}{4D}} - (C^* D_S)\sqrt{\frac{\pi}{4}}\left(\frac{K}{D}\right)^{3/2} + \frac{(C^* D_S)^{3/2}}{\sqrt{2}}\left(\frac{K}{D}\right)^2} \tag{4-49}$$

4.3.3.2 Experimental results

4.3.3.2.1 Experiments with Daily PBS Replacement

To validate the model developed above, it was decided to explore the effects of initial surfactant loading on release rates of the drug. In these experiments, the release medium was replaced daily to simulate perfect sink conditions. Experiments were performed with three different surfactant loadings and thickness of gel was also varied for all the systems to validate the model. Release profiles from the thick and the thin gels are shown in Figures 4-7 and 4-8. As expected, surfactant loading inside the gel phase significantly affects the release rates of the drug. Based on the above model, a plot of percentage release vs. $\sqrt{\frac{t}{C_p h^2}}$ should be a straight line with slope $\beta \times 100$. The plots are shown in Figures 4-9 and 4-10 after rescaling the time

scale for both, the thin and the thick gels, respectively. For each case, the release curves match for the 2, 4 and 8% surfactant loadings. The slopes indicated in each figure represent the values of $\beta \times 100$. The values of slope are 1.47±.018 and 1.1±0.12 for the thick and the thin gels, respectively. The small difference in these values for the gels of two different thicknesses implies that the data does not satisfy the thickness scaling as predicted by the model. This difference likely arises from the fact that the PBS in the release medium was replaced every 24 hours for both the thick and the thin gels. Since the amount of drug released from the thin gels in a 24 hour period is double the amount released by the thick gels, the perfect-sink condition is perhaps not satisfied for the case of release from the thin gels. For the experiments from the thick and the thin gels to be equivalent, the PBS has to be replaced every 6 hours for the case of thin gels, which is a more difficult schedule to maintain. So it was decided to conduct release experiments without PBS replacement to validate the thickness scaling predicted by the model (data shown in Section 4.3.3.2.2). The release from thick gels was in perfect sink conditions and so the model developed above is valid. Accordingly, the slope value of 1.47±.018 $\sqrt{\frac{M\mu m^2}{s}}$ obtained from the thick gel data can be equated to 100xβ. Since both D and $\sqrt{D_S C^*}$ are known from the fits in the previous sections, we can now obtain the value of K. By using values of 1.44 x 10^{-14} m^2/s and 0.0078 $\sqrt{\frac{M\mu m^2}{s}}$ for D and $\sqrt{D_S C^*}$, respectively, and a value of 1.47 $\sqrt{\frac{M\mu m^2}{s}}$ for $\beta \times 100$, we determine K to be 142.9 M^{-1}. The molecular weight of the surfactant is 1149.5 and if we approximate ρ to be 1000 kg/m^3, we can determine the approximate partition coefficient K_m of the drug from the expression $K_m = \frac{K\rho}{MW_S f_h}$ to be 414.4.

The partition coefficient K_m is the ratio of the drug concentration inside the micelle and the mean concentration outside, which includes both the free concentration in the aqueous phase and the bound concentration. A high value of partition coefficient is responsible for the significant increase in release duration.

4.3.3.2.2 Experiments without Replacing the Release Medium (Equilibrium Release)

The model developed above can be extended to apply to experiments in which the release medium is not replaced, and eventually equilibrium is achieved. However that extension requires the partition coefficients between gel and PBS for both the surfactant and the drug. While the percentage release prediction of Equation 4-48 is not valid for equilibrium experiments, the thickness scaling predicted by the model is still valid if the volume of the fluid to the gel is kept the same for both the thin and the thick gels. The thickness scalings are verified by the data in Figure 4-11 in which the drug release rates are plotted against 'τ' where $\tau = \sqrt{\frac{t}{h^2}}$. The results overlap for the thick and thin gels validating the thickness scalings predicted by the model. It is also observed that the time required to reach equilibrium is much greater for surfactant laden gels then for pure p-HEMA gels.

4.3.4 Model Comparison with Published Data

To further validate the model it was decided to utilize the data from the work of Liu et al [94, 95] and compare it to the model developed for drug release from surfactant laden hydrogels. In [94], Liu et al explored the effect of changing surfactant (SDS) concentration on release of a hydrophobic drug CPT from agarose hydrogels. Specifically, they measured drug release from gels with 0.2, 0.4, 0.6, 0.8 and 1 wt% surfactant. The drug release data was obtained from their published work by a digitalization program and was re-plotted in Figure 4-12 as fraction drug

release vs. $\sqrt{\frac{t}{C_{SDS}}}$ where C_{SDS} represents the concentration of surfactant (%wt) inside the hydrogel. The release profiles match for 0.4, 0.6, 0.8 and 1 wt% surfactant, whereas the profile for 0.2% loading deviates. It is noted that the analytical solution developed for the drug release is based on the assumption that the concentration of surfactant present as micelles (C_p) is substantially larger than the CAC (C*). The value of CMC of SDS is about 0.24 wt% in the presence of the drug, and since the gels prepared by the authors had only about 3% polymer by weight, it can be assumed that the critical aggregation concentration inside the gel (C*) is close to the CMC. A surfactant loading of 0.2% would then be very close in value to C*, and thus the profiles for the 0.2% loading are in fact not expected to overlap those for the higher surfactant loadings. Liu et al also explored the effect of surfactant (DTAB) concentrations on release of CPT from agarose hydrogels [95]. They measured drug release rates from gels with 10mM, 30mM, 40mM and 50mM DTAB. The data obtained by Liu et al. for the four surfactant loadings is re-plotted in Figure 4-13 as fraction drug release vs. $\sqrt{\frac{t}{C_{DTAB}}}$ where C_{DTAB} represents the concentration of surfactant inside the hydrogel. Again, the results in Figure 4-13 show that the profiles for 30mM, 40mM and 50mM DTAB are very similar while the profile for 10mM DTAB is significantly different. The value of CMC of DTAB is about 7mM in the presence of the drug and therefore the profiles for the 10mM loading are expected to not match those for the higher loadings. It should be noted that even though the analytical solution developed here is not valid in conditions where the total surfactant concentration is close to the critical aggregation concentration, the general model developed here is still valid and it can be solved numerically to fit the data.

4.4 Conclusion

We have explored the mechanisms of transport of drugs and surfactants in hydrogels loaded with CyA and Brij 98. Transport models were developed for both the surfactant and the drug, and the results of the model were verified by measuring release rates of both surfactant and drug from hydrogels. The experimental results are in good agreement with the model. The model of drug release from surfactant laden hydrogels seems to be in good agreement with the published work of Liu et al [94, 95].

The transport of both the drug and the surfactant is controlled by diffusion through the gel. At concentrations above the critical aggregation concentration, excess surfactant forms micellar aggregates, into which hydrophobic drugs can partition preferentially. The diffusion of surfactant leads to breakup of micelles causing formation of a depletion zone near the surface. The plots of percentage release vs. $\sqrt{\frac{t}{C_p h^2}}$ should be a straight line with slope $\sqrt{2D_S C^*} \times 100$. This result sharply contrasts with the result for pure Fickian diffusion without any aggregate formation for which case the release rates scale linearly with loading and so the percentage release is independent of the initial surfactant loading.

The drug transport is strongly coupled to the surfactant transport. As the micelles break, the drug is released into the gel, and becomes available for diffusion. The model predicts that the percentage drug release is linear with $\sqrt{\frac{t}{C_p h^2}}$, and thus a four fold increase in surfactant loading leads to a two fold reduction in percentage release for drug at a given time. The model can be fitted to the experimental data to determine important physical parameters such as the partition coefficient between the hydrophobic core of the micelle and the hydrogel.

The model developed here neglect a number of issues including interactions between the drug and the micelle, concentration dependence of drug and surfactant adsorption on the polymer, etc. Also, the surfactant laden gel matrix is assumed to be homogenous on the length scales relevant to transport. A good agreement between the model and the experiments suggest that the assumptions are perhaps valid. The geometry for the gel is considered to be two-dimensional, which is a good assumption. The models can be applied in general to any arbitrary geometry by including diffusive flux in other directions in the mass balance equations.

The transport models developed here can be very helpful in tuning the drug release rates from hydrogels by controlling the surfactant concentration. The results also show that Brij 98 loaded p-HEMA exhibit an extended release of CyA and so contact lenses made with this material can be used for extended ocular delivery of CyA.

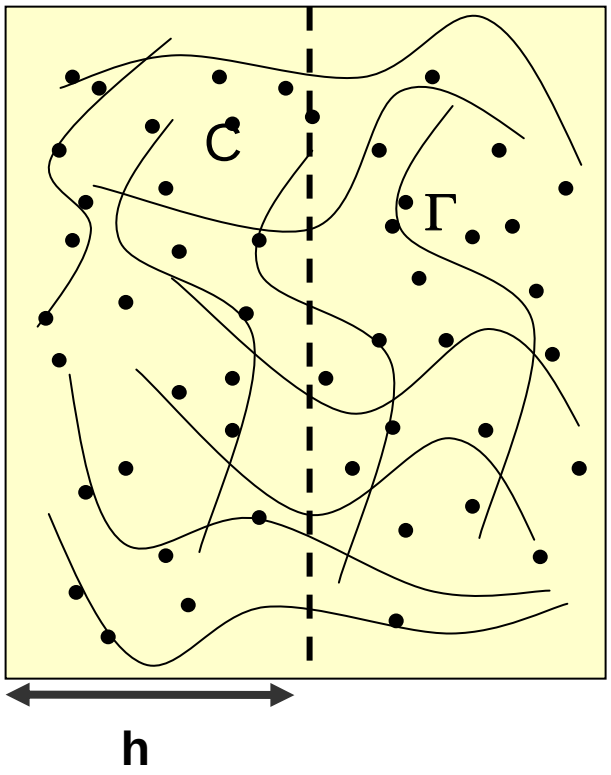

Figure 4-1. Transport of drug in the p-HEMA hydrogel. A large fraction of the drug (denoted by circles) is bound to the polymer (Γ) and a small fraction is present in the water phase of the hydrogel (C). The free and the bound drug are in equilibrium.

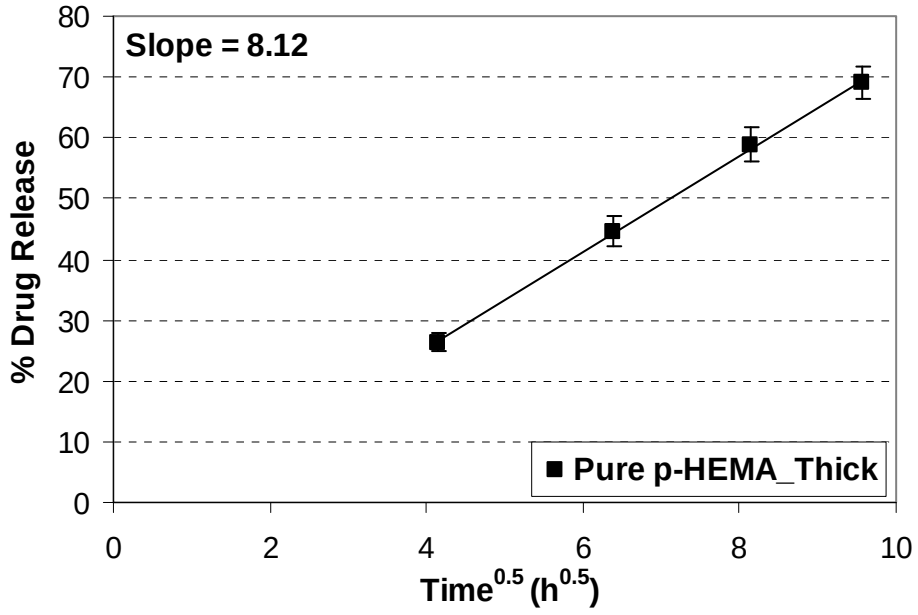

Figure 4-2. Percentage release of drug from pure p-HEMA gels. All the gels contained about 50 μg of drug. Data are plotted as mean ± SD (n = 3).

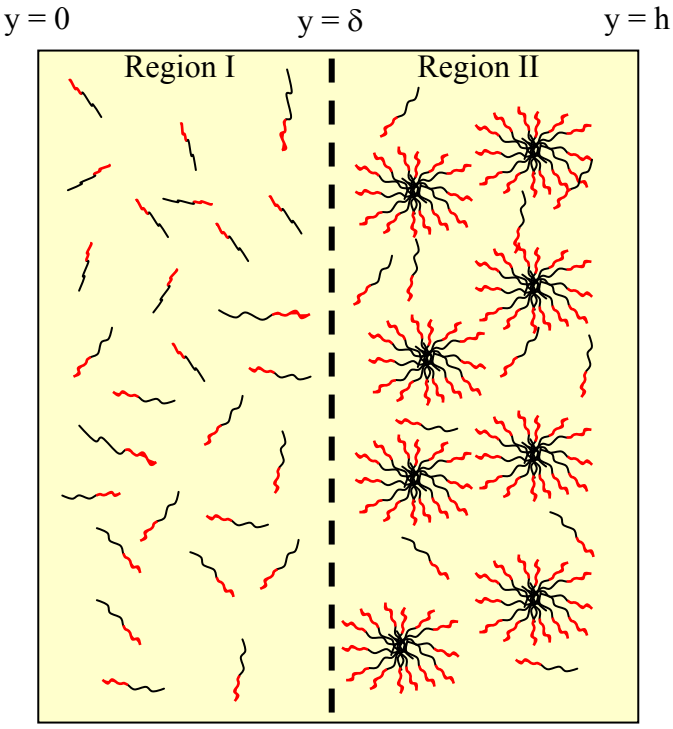

Figure 4-3. Transport from surfactant laden hydrogel. Region I represent the depletion zone with no micelles because the surfactant concentration is below the critical aggregation concentration. Region II contains surfactant aggregates along with free surfactant.

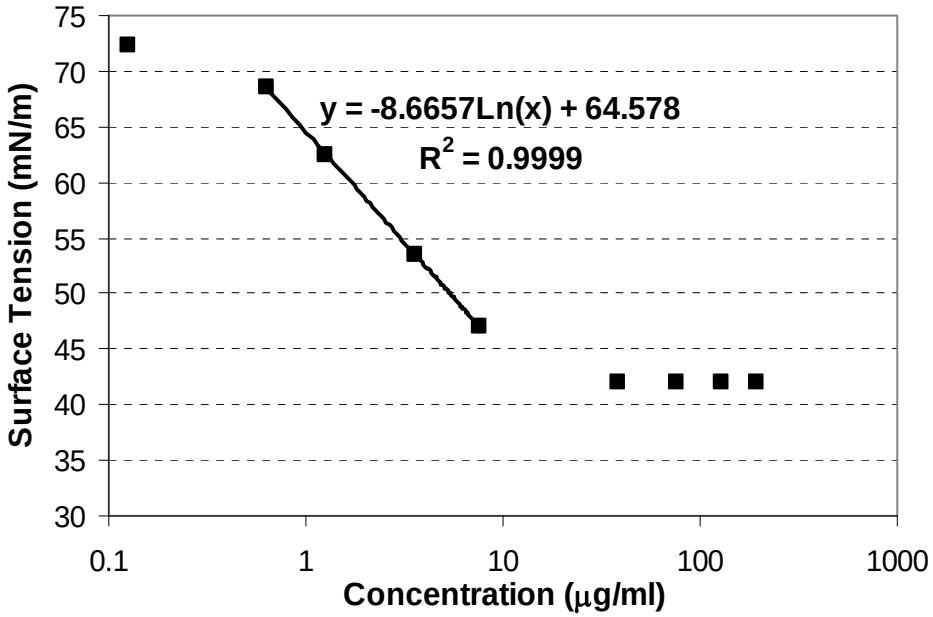

Figure 4-4. Dependence of surface tension on the bulk surfactant concentration for Brij 98 surfactant

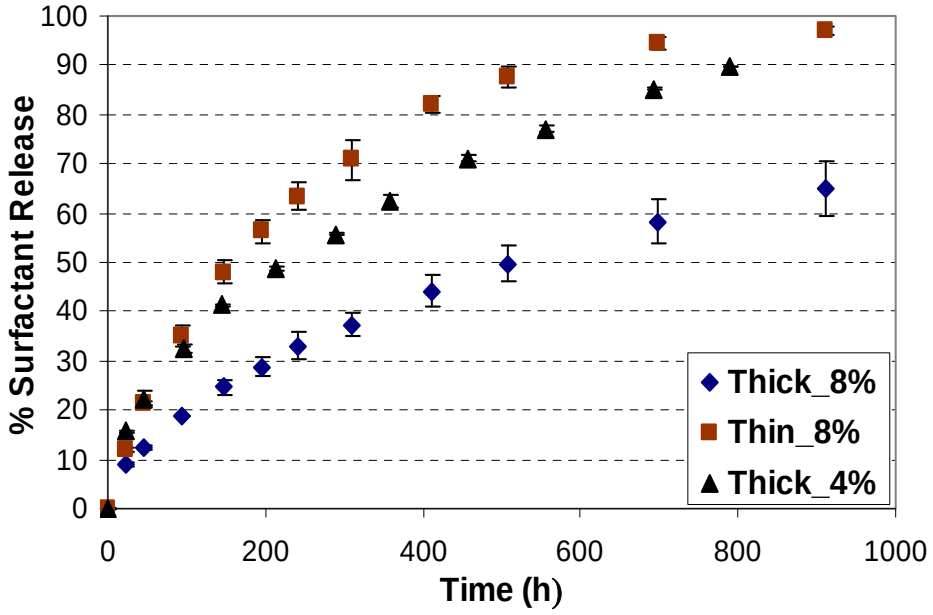

Figure 4-5. Cumulative percentage release of surfactant from hydrogels. Data are plotted as mean ± SD (n = 2).

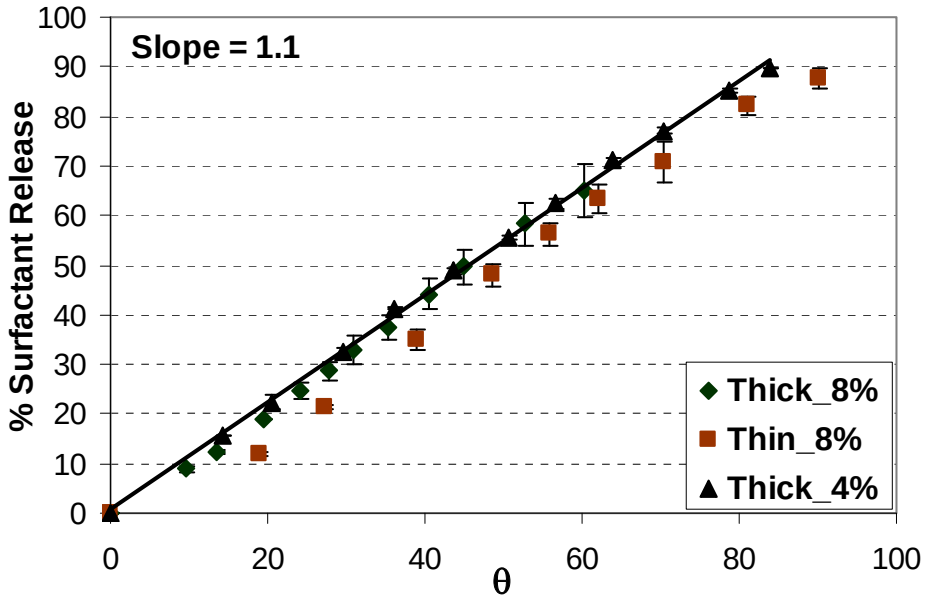

Figure 4-6. Cumulative percentage release of surfactant from the hydrogels after rescaling the time. θ represents $\sqrt{t/C_P h^2}$, where t is time in seconds, C_p is surfactant concentration in M, and h is half thickness of the gel in μm. Data are plotted as mean ± SD (n = 2).

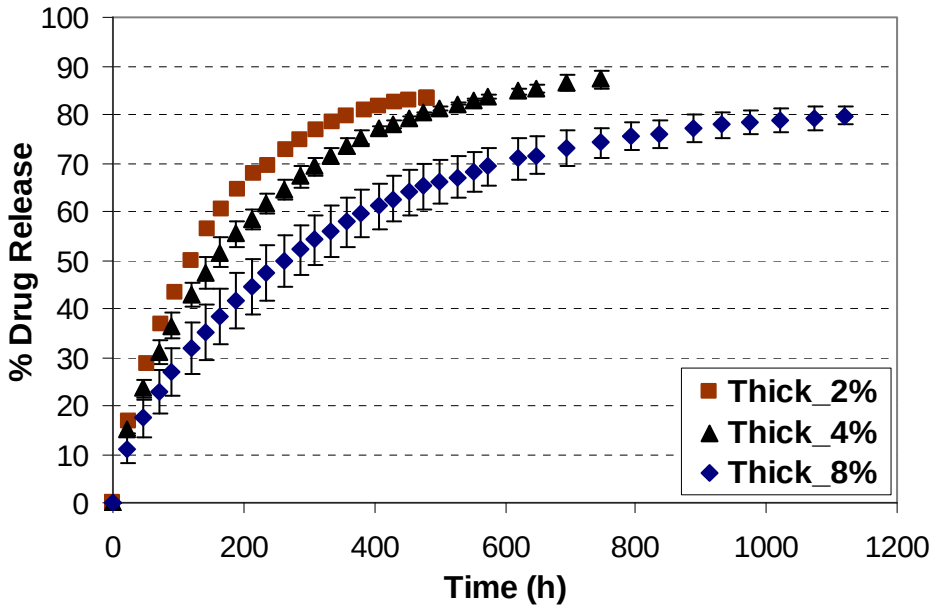

Figure 4-7. Effect of surfactant loading on cumulative percentage release of the drug for surfactant laden thick (200 µm) gels during PBS change experiments. All the gels contained nearly 50 µg of drug. Data is plotted as mean ± SD (n = 2).

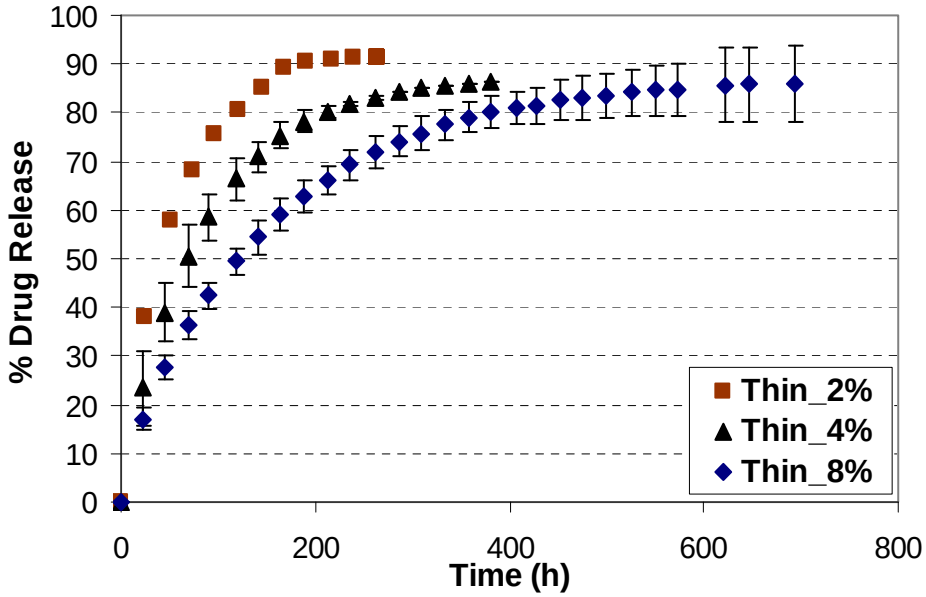

Figure 4-8. Effect of surfactant loading on cumulative percentage release of the drug for surfactant laden thin (100 µm) gels during PBS change experiments. All the gels contained nearly 50 µg of drug. Data is plotted as mean ± SD (n = 2).

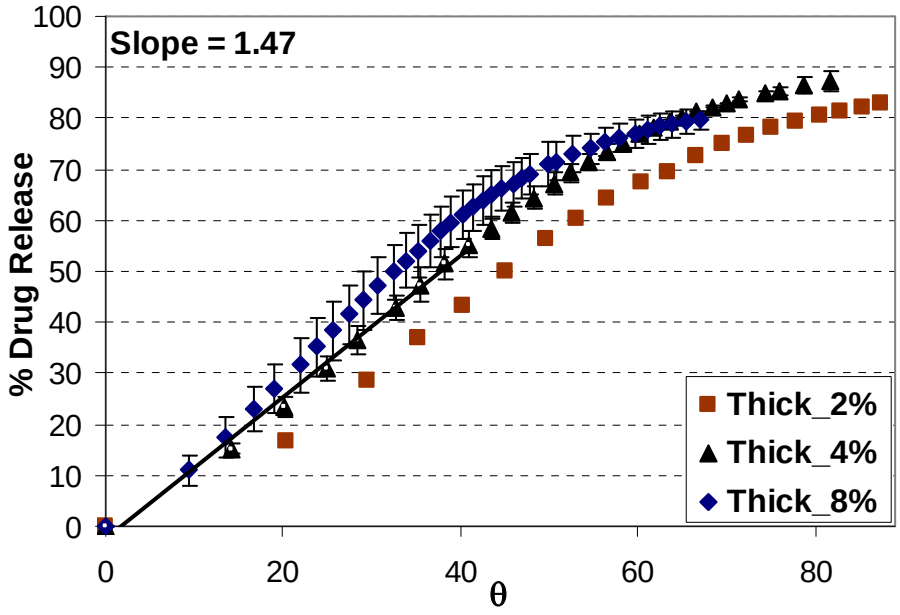

Figure 4-9. Cumulative percentage release of drug for surfactant laden thick (200 μm) gels during PBS change experiments after rescaling the time of release. θ represents $\sqrt{t/C_p h^2}$, where t is time in seconds, C_p is surfactant concentration in M, and h is half thickness of the gel in μm. Data is plotted as mean ± SD (n = 2).

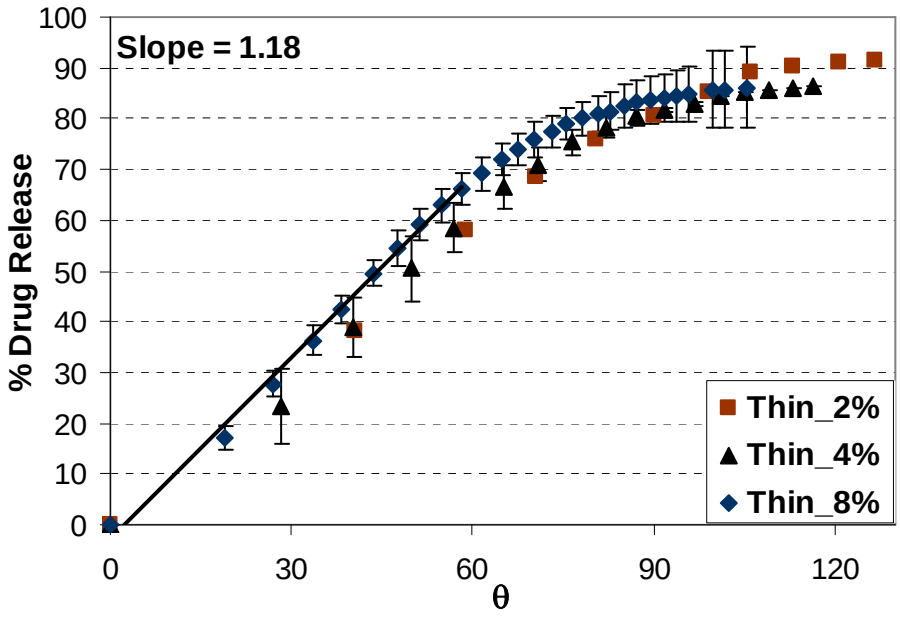

Figure 4-10. Cumulative percentage release of drug for surfactant laden thin (100 μm) gels during PBS change experiments after rescaling the time of release. θ represents $\sqrt{t/C_P h^2}$, where t is time in seconds, Cp is surfactant concentration in M, and h is half thickness of the gel in μm. Data is plotted as mean ± SD (n = 2).

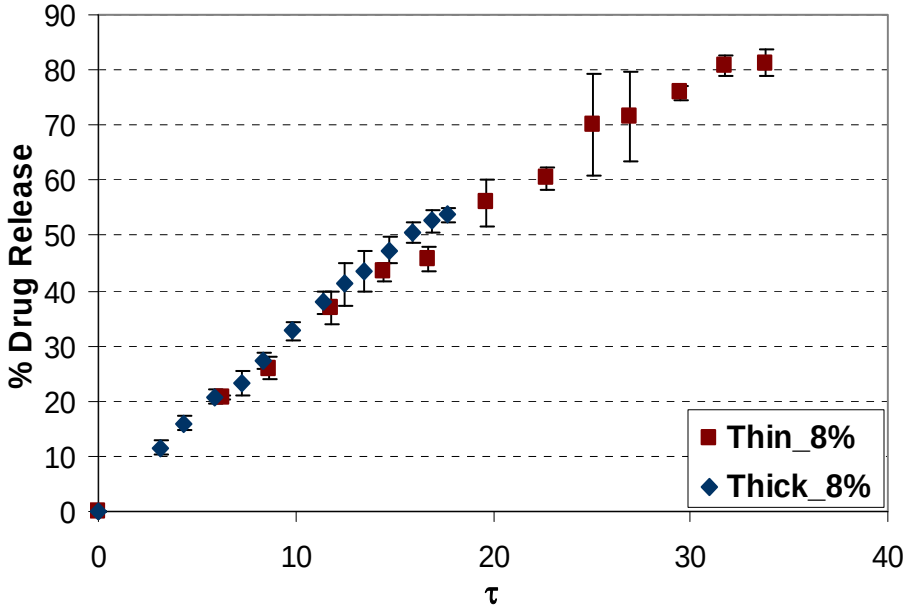

Figure 4-11. Drug release from surfactant laden gels for equilibrium (no PBS change) experiments. τ represents $\sqrt{t/h^2}$, where t is time in seconds and h is half thickness of the gel in μm. All the gels contained about 50 μg of drug. Data are plotted as mean ± SD (n = 2).

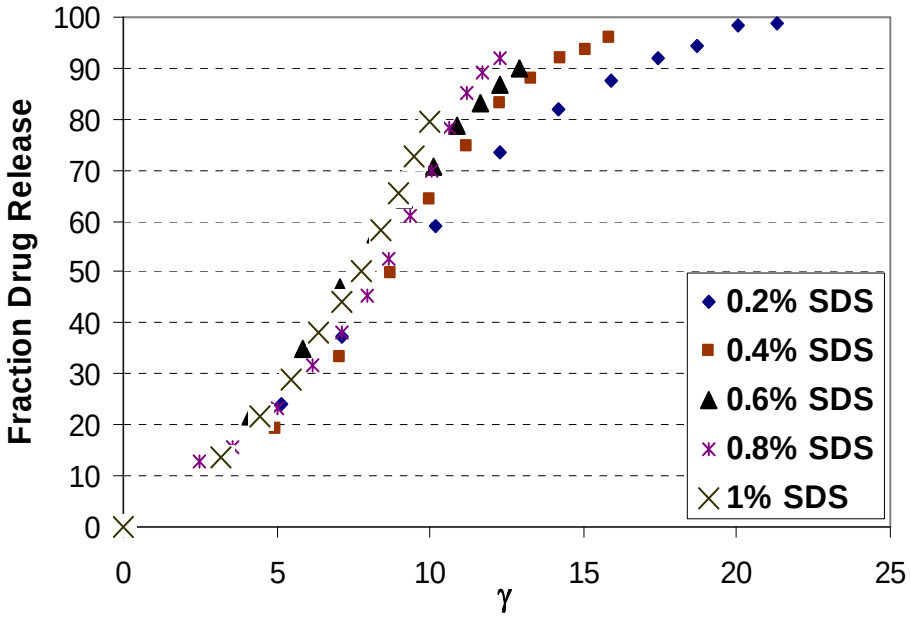

Figure 4-12. Drug release from agarose hydrogels containing SDS surfactant obtained from Liu et al. [94]. γ represents $\sqrt{t/C_{SDS}}$, where t is time in minutes and C_{SDS} is percentage of surfactant.

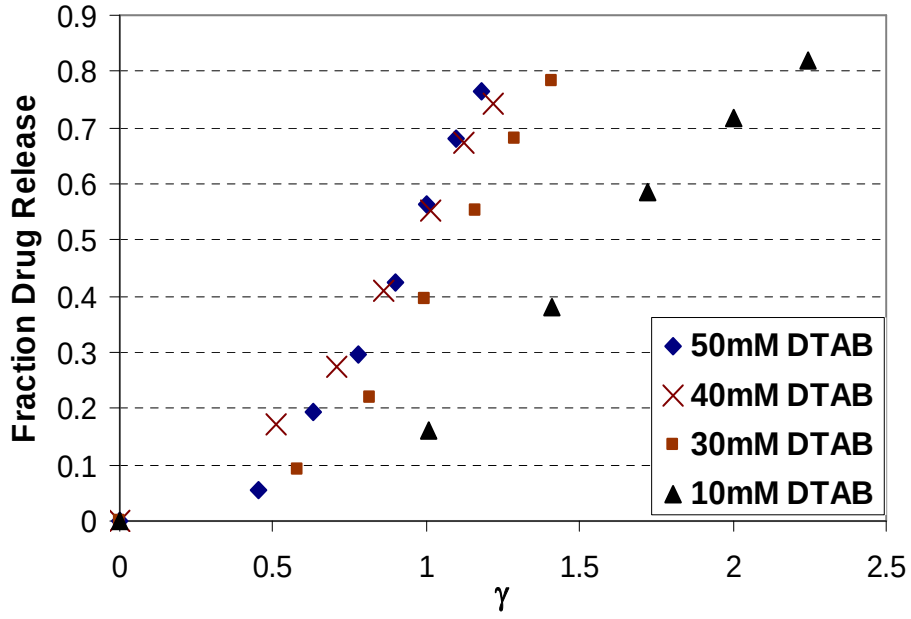

Figure 4-13. Drug release from agarose hydrogels containing DTAB surfactant obtained from Liu et al. [95]. γ represents $\sqrt{t/C_{DTAB}}$, where t is time in minutes and C_{DTAB} is surfactant concentration in mM.

CHAPTER 5
SURFACTANT LADEN HYDROGELS FOR OPHTHALMIC DRUG DELIVERY WITH INCREASED WETTABILITY AND WATER CONTENT

5.1 Introduction

Hydrogel contact lenses typically have about 60% polymer in the swollen state which competes with the surfactant-aggregates for drug binding. It is thus essential that in order for the surfactants to retard drug transport in contact lenses, the surfactant aggregates must have a very high affinity for the drug compared to the hydrogel. Accordingly, to develop a contact lens suitable for extended delivery of a given drug, it is important to investigate the microstructure of the gel with particular focus on the micellar-aggregates, and also investigate the mechanisms that impact the partitioning of the drugs in the aggregates. It is also equally important to investigate the effect of surfactant loading on gel physical properties relevant to contact lenses such as transparency, modulus, protein binding, wettability, and water content.

This chapter is an exhaustive study that focuses on each of the issues listed above. The results of this study will be helpful in delivering CyA to eyes through contact lenses, and also in designing suitable contact lenses for delivering other ophthalmic drugs. This is the first study that reports the microstructure and physical characterization of the surfactant-laden hydrogels with a large polymer fraction as large as 60%.

5.2 Materials and Methods

5.2.1 Materials

Hydroxy ethyl methacrylate (HEMA) monomer, ethylene glycol dimethacrylate (EGDMA), Dulbecco's phosphate buffered saline (PBS), dexamethasone (DMS), dexamethasone acetate (DMSA), Acetonitrile, lysozyme from chicken egg white, HPLC grade water, Brij 97, Brij 98, Brij 78 and Brij 700 were purchased from Sigma-Aldrich Chemicals (St Louis, MO). 2,4,6-Trimethylbenzoyl-diphenyl-phophineoxide (Darocur TPO) was kindly

provided by Ciba (Tarrytown, NY). Cyclosporine A (CyA) was purchased from LC Laboratories (Woburg, MA). All the chemicals were reagent grade. Acetonitrile was filtered before use and all the other chemicals were used without further purification.

5.2.2 Preparation of Surfactant Laden Gels

Surfactant laden gels were prepared by polymerizing the monomer solution containing surfactant and drug mixed in specific ratio. Briefly, 0.25, 0.6, 1.5 g of surfactant was dissolved in 10 ml DI water to make three different surfactant solutions (corresponding to 2%, 4%, 8%, surfactant in dry gel respectively). Separately, 3.5 mg of drug was dissolved in 2.7 ml of HEMA monomer and stirred at 600 rpm for a period of 5 hours. Next 15 μl of the crosslinker and 2ml of surfactant solution were added to the 2.7 ml of drug loaded monomer. The solution was degassed by bubbling nitrogen gas through it for 10 minutes followed by addition of 6 mg of UV initiator (TPO) and stirring the solution for 10 minutes. The solution was then poured between two glass plates separated by a spacer and the gel was cured by irradiating UVB light (305 nm) for 40 min from an Ultraviolet transilluminiator UVB-10 (Ultra Lum, Inc.). Four different spacers, 100, 200, 400 and 800 μm in thickness were utilized to synthesize gels of various thicknesses. Control, drug loaded p-HEMA gels without surfactants were prepared by following procedures identical to those described above except that the 2 ml surfactant solution was replaced by 2 ml DI water.

5.2.3 Drug Release Experiments

After polymerization, each gel was removed from the glass mold and was cut into smaller pieces that weighed about 40 mg in the dry state. These 40 mg gels were used in all experiments described in this chapter. As the thickness of the gel was varied, the size of the gel piece was adjusted to maintain similar weight for all the gels used in the study. Two sets of experiments were performed for the drug release studies. In the first set of experiments, gel was soaked in 3.5

ml of PBS and measurements were taken until equilibrium was reached for the drug. In the second set, gel was soaked in 3.5 ml of PBS and PBS was replaced every 24 hours, mimicking perfect sink conditions for the release experiments. Equilibrium experiments were conducted for all the three drugs explored in this study (CyA, DMS, and DMSA), whereas, PBS replacement experiments were performed for CyA only.

5.2.4 Drug Detection

CyA concentration was measured using a HPLC (Waters, Alliance System) equipped with a C18 reverse phase column and UV detector. The mobile phase composition was 70% acetonitrile and 30% DI water, and the column was maintained at 60°C. The flow rate was fixed at 1.2 ml/min and the detection wavelength was set at 210 nm[114]. The retention time for CyA under these conditions was 4.5 minutes, and the calibration curve for the area under the peak vs. concentration was linear ($R^2 = 0.995$). DMS and DMSA were detected using a UV-Vis spectrometer (Thermospectronic Genesys 10 UV) by measuring the absorbance spectra over a range of 190-290 nm. The absorbance data for the release experiments of DMS and DMSA were converted to the respective concentration value by a de-convolution technique as reported earlier [125].

5.2.5 Surfactant Release Experiments

The rates of surfactant release were measured in 3.5 ml of DI water with water replacement after each measurement to maintain perfect sink conditions. The surfactant concentration in the release medium was determined by measuring surface tension, which was then related to the concentration through a calibration curve. The surface tension was measured by using a Wilhelmy plate (sand blasted platinum plate) attached to a Scaime France Microbalance which was further connected to a Stathan Universal transducer (SC001). A

detailed description of the process for measuring surfactant concentration by surface tension measurements has also been reported earlier in chapter 3 (Section 3.2.11).

5.2.6 Lysozyme Sorption

A lysozyme solution was prepared by adding 40 mg of lysozyme to 40 ml of PBS. The 8% surfactant laden gels (about 40 mg in weight) were soaked in 3.5 ml of lysozyme solution and the amount of lysozyme that was taken up by the hydrogels was monitored by UV detection in the wavelength range 240-340 nm. The concentration of lysozyme was evaluated following a similar protocol as reported above for DMS and DMSA.

5.2.7 Preparation and Cryo-SEM of Hydrogels

All samples were soaked in 1x PBS buffer for at least 24 hours. The hydrogel samples were trimmed down to approximately 1 cm x 1 cm in size and mounted vertically on the cryo-SEM sample holder with a small amount of Tissue-Tek adhesive (Sakura). The samples were rapidly plunged into liquid nitrogen at a temperature below –190 ^{o}C (Gatan, Alto 2500), withdrawn into a vacuum transfer device under the protection of high vacuum, and transferred into the cryo-preparation chamber where the temperature was maintained at -130 ^{o}C and the anticontaminator at around –188 ^{o}C. The hydrogel samples were freeze fractured using the flat edge of a cold knife maintained at -130 ^{o}C and sublimated for 5 minutes at -95 ^{o}C to etch away surface water and expose the internal structural features. After sublimation, the temperature of the stage was adjusted back to –130 ^{o}C and the samples were sputter coated with platinum at 11 mA for 100 seconds. The samples were then transferred into the main chamber of the Field Emission SEM (Hitachi S-4800) via an interlocked airlock and mounted onto a cold stage module (–130 ^{o}C) fitted to the SEM stage. Images were acquired at a voltage of 2 kV.

5.2.8 Dynamic Mechanical Analysis

A dynamic mechanical analyzer (DMA Q800, TA instruments) was used to determine the mechanical properties of different surfactant laden systems synthesized above. For this study 400 μm and 800 μm thick gels were utilized to avoid breaking of the gel during the experiment. A hydrated gel was mounted on the clamp and the gel was kept submerged in DI water at room temperature during the experiment. Gel response in the form of storage and loss modulus of the gel was determined by applying tensile force in the longitudinal direction while keeping the gel tightly screwed between the clamps by applying a preload force of 0.01 N. To determine the linear viscoelastic range, strain test were first conducted at a frequency of 1 Hz followed by frequency sweep (1-35 Hz) measurements performed for all the samples at 20 μm strain.

5.2.9 Surface Contact Angle Measurements

Surface contact angles were measured for all the surfactant laden systems with 8% loading to investigate the effect of surfactant release on wettability. The contact angles were measured by captive bubble technique with a Drop Shape Analyzer (DSA100, KRÜSS). This technique was preferred over the sessile drop technique to eliminate contact angle change due to sample drying during measurements. A 200 μm thick gel was mounted on a glass slide which was then placed on a water filled cuvette with the lens submerged in water. An air bubble was created by an inverted syringe inside the cuvette, and allowed to detach and rise till it came in contact with the gel, and then the contact angle (θ) was measured. The gels were presoaked in a PBS buffer solution for one day before the experiment.

5.2.10 Transmittance Measurements

The transparency of all the surfactant laden hydrogels was quantified by measuring the transmittance of 100 μm thick hydrated gels at 600 nm using a UV-VIS spectrophotometer (Thermospectronic Genesys 10 UV).

5.2.11 Equilibrium Water Content

The gels of known weight were soaked in 3.5 ml of DI water, and the dynamic weight was measured as a function of time. The excess water from the gel surface was removed before each measurement by dabbing with Kimwipes (Fischer Scientific). The equilibrium water content (EWC) of the surfactant laden gels was calculated by determining the amount of water uptake per dry gel weight, i.e.,

$$\%EWC = \frac{W_{WET} - W_{DRY}}{W_{DRY}} \times 100 \tag{5-1}$$

5.2.12 Statistical Analysis

Linear regression analysis to determine slopes, correlation coefficients and confidence intervals was performed in JMP developed by SAS (Cary, North Carolina). The 95% confidence intervals (CI) were utilized to compare release rates.

5.3 Results and Discussion

5.3.1 Surfactant Release from the Hydrogels

Table 1 lists the surfactants utilized in this study and their relevant physical properties obtained from the literature. We also list the value of 'fh' which is defined as the fraction of hydrophobic chain length of the surfactant and is calculated by taking the ratio of number of carbons in the hydrophobic tail of the surfactant to the total number of carbons present in the surfactant.

The rate of surfactant release from surfactant-laden contact lenses needs to be measured because an excessive release could lead to toxicity. Additionally, the rate of surfactant release impacts drug release. As described in the previous section, the surfactant concentration in the release medium was determined by measuring the surface tension of the solution, which is related to the bulk concentration. Figure 5-1A-B shows the calibration curves for Brij 78 and Brij 700 surfactants. Calibration curves for Brij 98 and Brij 97 have been shown earlier (Figure 3-10 and Figure 4-4). A model for surfactant release from hydrogels laden with surfactant aggregates has been proposed earlier (Chapter 4), and it predicts the following equation to describe surfactant release at short times,

$$\%\text{Surfactant Release} = \sqrt{2D_S C^*}\sqrt{\frac{t}{C_P h^2}} \times 100 \tag{5-2}$$

where D_S is the surfactant diffusivity, C* is the critical aggregation concentration (CAC), i.e., the concentration beyond which the surfactant forms aggregates inside the gel, 't' is time, C_p is the concentration of the surfactant present as aggregates inside the hydrogel, and 'h' is the half-thickness of the hydrogel. The above equation is valid for diffusion of any solute that is loaded in the gel above saturation limit and so a fraction of the solute precipitates into aggregates. This equation is the equivalent of the Higuchi equation that is commonly utilized to model drug release from ointments when drug is present as a suspension [89].

To validate the model and to understand the mechanism of surfactant transport, surfactant release studies were conducted from gels of different surfactant loadings (approximately 2%, 4% and 8% w/w in drug gel) and different gel thicknesses (~ 100 and 200 μm in the dry state). Figure 5-2A-C shows the surfactant release from 100 μm thick and 200 μm thick gels with three different surfactant concentrations explored for 200 μm thick gels. The data is re-plotted in

Figure 5-3A-C with the time axis rescaled to $\theta \equiv \sqrt{\frac{t}{C_p h^2}}$, where t is time in seconds, C_p is the concentration in moles per liter and h is half-thickness of the gel in μm. The model (Equation 5-2) predicts that the rescaled plots should overlap for all thicknesses and surfactant loadings, and the plots should be linear with the slope $\sqrt{2D_S C^*} \times 100$, which agrees with all the experimental results for Brij 97 and Brij 78 laden hydrogels within 95% CI. However, for the Brij 700 surfactant, the data matches the model only for 4% and 8% surfactant loading, while thickness scaling and surfactant release from gels containing 2% surfactant in dry gel do not follow the predicted behavior. We speculate that association of Brij 700 with the gel matrix is strongly dependent on the gel thickness maybe due to large number of ethylene oxide (EO) units in the surfactant. Also, the CAC values for the Brij 700 laden system might be closer to 2% surfactant loading where the model assumption that $C^* << C_p$ does not hold.

To verify the hypothesis that CAC for Brij 700 is close to 2% surfactant loading, Brij 700 release was also conducted from gels with 1% surfactant loading and the results are plotted in Figure 5-2C. The percentage release from both 2% and 1% surfactant loaded gels overlapped within 95% CI showing that the release of surfactant at these concentrations is independent of the initial surfactant loading suggesting that there are no or an insignificant number of aggregates inside the gel for surfactant loadings as large as 2%, validating our hypothesis.

The slope indicated in Figure 5-3A-C represents the value of $\sqrt{2D_S C^*} \times 100$. We calculated the value of $D_S C^*$ for all the systems and they are reported in Table 5-2. The value of this parameter for Brij 98 surfactant was calculated earlier in Chapter 4, and is also reported in Table 5-2 for comparison. We currently do not have the value for the diffusivity of surfactants (Brij 78, 97 and 98) from these hydrogels or the critical aggregation concentrations of the

surfactants inside the gels to estimate both the parameters individually. We discuss some novel methods to evaluate CAC for surfactant laden hydrogels in chapter 7. As mentioned above, the critical aggregation concentration for Brij 700 in p-HEMA gels is more than 1%, and so the release data from gels loaded with 1% (w/w) can be fitted to the following equation to obtain the surfactant diffusivity [87],

$$\% \text{ Release} = \sqrt{\frac{4D_S t}{\pi h^2}} \times 100 \tag{5-3}$$

Here D_S is the diffusivity of the surfactant and 'h' is the half-thickness of the gel. The diffusivity of Brij 700 from these hydrogels was determined to be 7.85×10^{-17} m^2/s and subsequently the value of C* was evaluated from the already determined parameter 'DsC*' (Table 5-2) to be 2.4±1.1 mM, which is equivalent to 1.12±0.51% surfactant in a dry gel. This value is in reasonable agreement with our prior hypothesis that the C* for Brij 700 is approximately 2%, which was based on the overlapping percentage release data for 1% and 2% Brij 700 loaded gels.

5.3.2 CyA Release: Equilibrium Experiments

A large fraction of hydrophobic drugs such as CyA are expected to partition inside the surfactant aggregates. During the drug release process, the drug molecules have to first diffuse through the surfactant head region into the p-HEMA gel, and subsequently diffuse through the gel. The head group of the surfactants may offer resistance to transport of the molecules, and this transport could potentially be rate limiting. However if the resistance to transport from the surfactant aggregates to the p-HEMA gel is small, the concentrations inside the aggregates will be in equilibrium with that in the p-HEMA gel, and in this case, diffusion through the p-HEMA gel will be rate controlling. If transport through the gel is rate controlling, the time scale for drug release scales as the square of the gel thickness, and if the transport across the aggregates is rate

controlling, the time scale for release should be independent of the gel thickness. To investigate the rate limiting step, drug release studies were conducted from 100 μm and 200 μm thick gels with 8% surfactant loading. It is noted that the gel weight and the fluid volume in the release medium was kept the same for gels of both thicknesses. To determine the rate limiting process, we plot percentage release of the drug against 'τ' where, $\tau = \sqrt{\frac{\text{Release Time}}{i^2}}$ i = 1 for 100 μm thick gels and 2 for 200 μm thick gels in Figures 5-4A-B. It has been shown earlier that the rate limiting step in drug diffusion from p-HEMA, Brij 97 and Brij 98 laden gels is also diffusion controlled (Figure 3-8 and Figure 4-11). The data for different thicknesses for all the systems overlaps proving that the transport of drug in all cases is controlled by diffusion through the gel, and that the drug concentrations inside the aggregates and in the p-HEMA gel are in equilibrium.

The data in Figures 5A-B, Figure 4-11 and Figure 3-8 also show that the time required to reach equilibrium is much greater for surfactant laden gels then for pure p-HEMA gels and Brij 78 systems take the longest time to equilibrate. Also, the percentage of drug that diffuses out, till equilibrium is attained, is different for each system, with the relative order Brij 97 laden gels < Pure p-HEMA < Brij 78 <Brij 700 <Brij 98. To explain these observations, we propose a qualitative picture of the system in Figure 5-5. In the gel matrix, surfactants can exist in three forms: a) free form, not interacting with other surfactants or the polymer b) as micellar aggregates or c) interacting with the polymer matrix. Similarly, the drug also exists in three different forms: a) free form, b) inside micellar aggregates, c) adsorbed on the polymer. Although diffusion of drug through the gel is the rate controlling step, only the drug present in the matrix, which is a small fraction of the total drug, can directly diffuse. This creates a depot effect which prolongs the total release duration. The partitioning of the drug will likely depend on the hydrophobicity of the core of the surfactant aggregates, which will depend on the

surfactant chain length and the packing in the aggregates. Also, due to surfactant diffusing out during equilibrium experiments, the drug solubility can also increase in the release medium. It is thus probable that the presence of surfactants in the release medium can affect the amount of drug diffusing out. This interaction between the drug and the surfactant in the release medium should be dominant only above CMC values and it is possible that for Brij 97 system, the surfactant concentration in the bulk phase does not reach CMC, while for other systems it does reach above CMC value, leading to smaller percentage drug release for Brij 97 laden gels than pure p-HEMA systems. Essentially, the combined interactions of drug molecules with the surfactants present inside the gel matrix and outside in the release medium would then determine the equilibrium percentage release from the hydrogel.

5.3.3 Effect of Surfactant Dissolved in the Release Medium

To understand the effect of surfactants (present in the release medium) on the release rates and amount of drug released from the gel system, we conducted experiments in which pure p-HEMA gels (loaded with drug) were soaked in release mediums containing varying surfactant concentration. Three different surfactant concentrations were explored for each surfactant based on the theoretical value of their CMC as shown in Table 5-3. Specifically, concentration of surfactant was chosen as C1 (CMC/3), C2 (CMC) and C3 (3*CMC) for all the systems studied and the results from all the experiments are shown in Figure 5-6 A-D. It was observed in all the experiments that as we increase the surfactant concentration in the release medium, amount of drug and its release rates also increase. We also observe that at short time scales, drug release rates from all the surfactant containing systems are slower than from systems containing no surfactants. This observation can be explained by taking into consideration the initial uptake of surfactants by the gel matrix which then can give rise to drug-surfactant interaction at the periphery of the gel resulting in slower release rates of the drug. It is also observed that amount

of drug released at equilibrium for pure HEMA gel is nearly same for Brij 78 and Brij 700 containing release medium when the concentration of surfactant is below its CMC value (C1). This shows that there is no effect of surfactant concentration on the release percentage of the drug when concentration of surfactant is below its CMC value. We do not observe this when Brij 98 and Brij 97 surfactants are dissolved in the release medium at concentrations below CMC and we speculate that the theoretical value of CMC for these two surfactants might not be accurate which may lead to an erroneous assumption that C1 concentration for these surfactants is below CMC. Researchers have also shown a wide range of CMC being reported in the literature for these non-ionic surfactants [119,120]. As we start increasing the surfactant concentration to a value above CMC, there is more drug released at equilibrium indicating that the drug is interacting with the micelles present in the release medium. Also, we observe that there is not much change in release rates and release percentage of the drug for concentration C2 and C3 for Brij 98 surfactant. This may be because at much higher concentrations of surfactant in the release medium, rod shaped micelles may also start forming and so at concentrations C2 and C3 we observe similar release behavior of the drug.

5.3.4 CyA Release: PBS Change Experiments

Figures 5-7A-C show the percentage release of the drug with different surfactant loading for all the surfactant laden gels that are 200 μm in thickness and loaded with 50 μg of drug. As expected, the percentage release of the drug decreases as the surfactant loading is increased inside the hydrogel. A model for drug release from hydrogels laden with surfactant aggregates has been proposed earlier in Chapter 4, and it predicts the following equation to describe drug release at short times,

$$\%\text{Drug Release} = \beta^* \sqrt{\frac{t}{h^2}} \times 100 \tag{5-4}$$

$$\beta^* = \frac{1}{\sqrt{\frac{\pi(1+KC_P)}{4D}} - (C^* D_S)\frac{K}{D}\sqrt{\frac{\pi(1+KC_P)}{4D}} + (C^* D_S)^{3/2}\frac{K(1+KC_P)}{D^2\sqrt{2C_P}}} \quad (5\text{-}5)$$

$$K = \frac{K_m MW_S f_h}{\rho} \quad (5\text{-}6)$$

Here,

D = Diffusivity of drug
Km = Partition coefficient of the drug defined as ratio of drug concentration inside the micelle to drug concentration in the hydrogel
MW_S = Molecular weight of the surfactant
ρ = Density of micellar core

To establish the validity of the model and to determine all the model parameters, we re-plotted the percentage release of the drug against 'γ' where $\gamma = \sqrt{\frac{t}{h^2}}$ where t is the time in seconds and h is half thickness of the gel in μm. We have also included the re-plotted data for systems loaded with Brij 98 surfactant and the results are shown in Figures 5-8A-D. The slopes between various surfactant loadings for each system differ as the 95% CI for the slopes do not overlap. We fitted the release data to a straight line to obtain β* and then used Equations 5-5 and 5-6 to obtain K_m. The parameters determined for each system are listed in Table 5-4. The values of K_m are relatively independent of the surfactant loading, thus validating the model. In these calculations, the diffusivity of the drug was taken to be 1.44×10^{-14} m^2/s and ρ was taken to be 1000 kg/m^3. The value of K for 2% Brij 700 loading in the system could not be determined which is expected since it was shown earlier that at this concentration is close to the CAC value for this surfactant. Furthermore, in Figure 5-7C we observed the percentage release of CyA from p-HEMA gels overlapping that from the 2% Brij 700 loaded gels, again suggesting that there was no significant partitioning inside the surfactant aggregates due to an insignificant number of such aggregates inside the hydrogel.

The partition coefficient of the drug between the surfactant aggregates and the p-HEMA gels is highest for the Brij 700 laden gels and smallest for the Brij 97 laden hydrogels. Even though the value of K_m is highest for Brij 700, these systems do not attenuate drug release significantly for two reasons. First, the value of C* is large (~2%) implying that only a small amount of surfactant is available for forming aggregates. Second, due to the large molecular weight, the volume fraction of the hydrophobic core which provides the site for drug partitioning is small.

The values of the partition coefficients clearly suggest that an increase in the hydrophilic chain length leads to an increase in the partition coefficient. This is most likely due to an improved shielding of the hydrophobic core from water on increasing the hydrophilic chain length. Also, a comparison of Brij 78 and Brij 98 systems shows that there is a significant increase in the partition coefficient of the drug if the hydrophobic tail of the surfactant is saturated (Brij 78). This could be attributed to the fact that an unsaturated chain is more rigid than a saturated chain, and an increase in rigidity will likely lead to reduced packing resulting in a reduced shielding of the core from water, and a consequent reduction in the partitioning of hydrophobic drugs.

The results reported above show that amongst the systems explored, Brij 78 is the most suitable candidate for extended drug delivery. The toxicological response of this surfactant on the ocular surface has been investigated in rabbits and it is reported that administration of 0.1 ml of 2% (20000 μg/ml) eye drops does not cause toxic effects [67]. Assuming a bioavailability of about 2%, about 40 μg of the surfactant delivered in the drop reaches the cornea without causing any toxicity. The same study also showed that exposure to 0.05% Brij 78 solution for about 5 hours does not lead to any significant increase in corneal hydration again suggesting that Brij 78

has negligible toxicity even with extended exposure. The surfactant release studies reported here demonstrate that about 10% of the Brij 78 loaded in the 100 μm thick gel with 8% loading is released in a period of 10 days, which corresponds to around 300 μg of surfactant or equivalently an average release of about 30 μg/day. When a contact lens is placed on an eye, at the most half this amount, i.e., 15 μg/day will be released into the post lens tear film, which is the thin tear film in between the cornea and the contact lens. Ocular conditions are likely not perfect-sink conditions and so the amounts released would be less than this level. Thus, it might be expected that the lenses loaded with Brij 78 will not cause any toxicity even if the lenses are worn continuously for a few days.

5.3.5 DMS and DMSA Release: Equilibrium Experiments

Since Brij 78 laden hydrogels were found to be most effective in attenuating CyA release rates, these systems were explored for delivering other hydrophobic drugs such as DMS and DMSA. All the gels prepared for DMS and DMSA were 100 μm in thickness and weighed about 40 mg. In Figure 5-9 and Figure 5-10 we plot the percentage release of these drugs over a period of one day from hydrogels loaded with varying Brij 78 loading. The data shows no significant difference between release times of the drugs from the surfactant laden gels when compared to release from control p-HEMA gels. To explain the negligible effect of surfactant loading on release times, we calculated the partition coefficient of the drug between the gel and the release medium (Table 5-5). These release experiments equilibrated in less than a day, and it could be assumed that during this time there was negligible surfactant loss from the hydrogel. We can then calculate the contribution of micelles inside the hydrogel to the overall partition coefficient by the following equation,

$$K_{Avg} = K_{p-HEMA}(1-\varphi) + K_{Micelle} f_h \varphi \tag{5-7}$$

Where,

K_{Avg} = Calculated partition coefficient in gel with respect to PBS
$K_{p\text{-}HEMA}$ = Partition coefficient of the drug in control p-HEMA gels with respect to PBS
$K_{Micelle}$ = Partition coefficient of the drug in the cores of the surfactant aggregates with respect to PBS
ϕ = Fraction of surfactant inside the hydrogel, and thus '$fh\phi$' is the fraction of the hydrophobic cores inside the gel

The values of $K_{Micelle}$ calculated from Equation 5-7 are listed in Table 5-5 for both drugs. The partition coefficient of the drug in the hydrophobic cores with respect to the p-HEMA matrix is simply the ratio $K_{Micelle}/K_{p\text{-}HEMA}$, defined earlier as K_m. The values of this ratio are 7.5±0.8 and 18.0±5.0 for DMS and DMSA, respectively, which are both much less than the value of 458.9±61.5 obtained earlier for CyA. This implies that the cores of the surfactant aggregates have a much larger affinity for CyA than DMS and DMSA. These results also suggest that the ratio $K_{Micelle}/K_{p\text{-}HEMA}$, which can be determined relatively easily, is the most critical parameter for the successful attenuation of drug release from the surfactant-laden hydrogels.

5.3.6 Uptake of Lysozyme in the Hydrogels

Binding of tear proteins to contact lenses is undesirable as it can lead to increased bacterial binding to the lenses. Lyzozyme is the main protein present in tears, and it is frequently used as the test protein to investigate protein binding to contact lenses [126]. It may be speculated that the presence of hydrophobic regions inside the surfactant-laden contact lenses can lead to increased protein binding. To test this hypothesis, hydrogels (200 μm thick) were soaked in lyzozyme solution, and the mass of lysozyme bound to the lens was determined by assaying the free lyzozyme concentration through UV-Vis spectrophotometry. Lysozyme uptake by the surfactant laden gels (8% w/dry gel w) and pure p-HEMA gels is shown in Figure 5-11. It is

observed that the presence of surfactant in the gels does not have any significant effect on lysozyme adsorption in the gel matrix.

5.3.7 Microstructure of Hydrogels: Cryo-SEM Imaging

Figures 12 A-O show a series of SEM images of the cross-sections of p-HEMA and surfactant laden gels (8% w/dry gel w). The pure p-HEMA gels have a uniform structure with no visible pores, which is expected because pores in p-HEMA gels are a few nm in size. The microstructure of surfactant laden gels is in sharp contrast to pure p-HEMA gels, as they show a uniform distribution of pores with pore sizes ranging from 40-50 nm. The sizes of these pores are much larger than the expected micelle size suggesting that the structure of the surfactant aggregates inside these pores is likely more complex than micelles. The volume fraction of the pores is much larger than the surfactant loading, which implies that these pores are likely water rich environments, and so the presence of these pores should lead to increased water content in the gels. To investigate this issue further, the area fraction of pores in the hydrogels was determined by image analysis using ImageJ (National Institute of Health) software and these values are listed in Table 5-6. If we assume that after hydration these pores are filled with water, then the equilibrium water content of the systems can be predicted by the following equation

$$EWC_{pred}(\%) = \left(\frac{EWC_{p-HEMA}(1-\alpha)}{100} + \alpha\right) \times 100 \qquad (5\text{-}8)$$

Where,

α = Fraction of area occupied by pores

$EWC_{p\text{-}HEMA}$ = Water uptake in pure p-HEMA hydrogel

The values of water content (EWC_{Pred}) from Equation 5-8 are also listed in Table 5-6. A quantitative analysis of the pore structure along with the equilibrium water content (see 5.3.8.2) shows that these pores are essentially filled with water when the gels are hydrated. Together with the 50 nm size this suggests that the surfactant structures could possibly be vesicles.

5.3.8 Physical Properties

The surfactant-laden gels were characterized by several techniques to investigate the impact of surfactant loading and the resulting porous structure and also to determine the suitability of these systems as a typical contact lens. It should be noted that in all the studies in this section we used gels which contained 8% surfactant per dry gel weight.

5.3.8.1 Mechanical properties

The storage moduli (G') and the loss moduli (G'') for all the five systems explored in this study are plotted as a function of frequency in Figure 5-13A-B. All the gels explored for studying the mechanical properties were 400 μm and 800 μm thick. The results show a negligible effect of surfactant loading on the mechanical properties. The elastic modulus G' continuously increases with increasing frequency and the values of the modulus at frequencies approaching zero for all the systems is close to the desired value for commercial lenses [46]. The loss modulus first increases and then decreases with frequency. The mechanical response of a contact lens plays an important role in lens settling, lens shape, and the pressure distribution on the post-lens tear film. It may thus be useful to obtain a model that can describe the mechanical properties of the lenses so that this model can be utilized in modeling lens deformation in the eyes due to application of the forces during blinking. To model the frequency dependence of the storage and loss modulus, we used a three parameter 'Standard Linear Solid Model' which is shown in Figure 5-14. In this model there is an elastic spring connected to a viscous dashpot in series like a Maxwell model, with an addition of an elastic spring in parallel. To determine the expressions for G' and G", it is instructive to consider application of a periodic strain. The stresses and strains in the individual elements are then related by the following expressions

$$\varepsilon_1 = \varepsilon_2 + \varepsilon_3 = \varepsilon_0 e^{i\omega t} \tag{5-9}$$

$$\varepsilon_2 E_2 = \dot{\varepsilon}_3 \mu \tag{5-10}$$

The complex modulus G (=G' + iG") is the ratio of the stress and the strain, and it can be obtained from the following expression

$$G' + iG'' = \frac{\varepsilon_1 E_1 + \varepsilon_2 E_2}{\varepsilon_0 e^{i\omega t}} \tag{5-11}$$

Using Equations 5-9, 5-10 and 5-11 we can evaluate G' and G'' to be,

$$G' = \frac{E_1 E_2^2 + (E_2 + E_1)\omega^2 \mu^2}{E_2^2 + \omega^2 \mu^2} \tag{5-12}$$

$$G'' = \frac{E_2^2 \omega \mu}{E_2^2 + \omega^2 \mu^2} \tag{5-13}$$

The experimental data averaged from all the systems was fitted to the model, and the model fit is also plotted in Figure 5-13A-B, and the parameters are listed in Table 5-7. The data fits the model reasonably for lower frequencies, while there is a clear deviation from the model at frequencies greater than 25 s^{-1}. A more generalized Maxwell model is needed for the data at higher frequencies but physiological blink frequencies are about 10 s^{-1} and so the model proposed above may be adequate. The loss moduli of the gels may partially be attributed to water flow during the gel stretching. The contribution of water flow to the moduli could be explored by measuring the moduli for gels of different thicknesses. Since water transport depends on the gel thickness, a significant dependence of the loss modulus on the thickness will indicate that water transport is an important contributor to the loss modulus. The storage and the loss modulus for pure p-HEMA gels are relatively independent of the gel thickness as shown in Figure 5-15. This suggests that water transport during gel stretching does not contribute to the loss modulus for the p-HEMA gels. The results were similar for the surfactant-laden gels and are not shown in Figure 5-15 for clarity of presentation.

5.3.8.2 Transparency, equilibrium water content, and surface contact angle of gels

All the gels explored in this study were visibly transparent and clear, and 100 μm thick hydrated gels had transmittance values larger than 98.5% (Table 5-6) at a wavelength of 600 nm, and so are suitable for contact lens application. It was also observed that the surfactant laden gels had a higher transparency than the pure p-HEMA gel likely due to the higher water content.

The EWC of contact lenses is crucial as it likely impacts comfort, and also an increase in the EWC leads to an increase in the oxygen permeability of p-HEMA contact lenses. The EWC values of all the gels obtained by hydrating 200 μm thick gels are listed in Table 5-6. All the surfactant systems had higher water content than pure p-HEMA gels, and thus are more suitable for contact lens application. The water content appears to be a function of length of hydrophilic part of the surfactants and it increases as the length of (EO) groups of the surfactants increase. The measured values match the EWC predictions based on analysis of SEM images. This suggests that water content inside the hydrogel increases due to formation of pores which are filled with water and since the pore size is less than 40 nm for all the surfactant laden hydrogels, these remain visibly transparent after polymerization.

The contact angles were measured for all systems to determine the effect of surfactants on the wettability of the hydrogels. Thickness of the gels utilized for measuring the contact angle was 200 μm. It has been shown previously that surfactants can significantly alter the contact angles of hydrogels [127,128]. The captive bubble technique was utilized to determine the contact angle to ensure that the gel remains hydrated during the measurements. The values of contact angles listed in Table 5-6 are all lower than those for the p-HEMA gels likely due to the presence of surfactant on the surface making surfactant laden gels more suitable for contact lens application.

5.4 Conclusion

We have explored Brij surfactant laden p-HEMA hydrogels for ophthalmic drug delivery by contact lenses. The surfactants explored here have the same length of the hydrophobic group but differed in chain length of the hydrophilic unit (EO) and in presence of an unsaturated group in the tail region of the surfactant. Ophthalmic drugs were loaded in these systems by direct addition to the polymerizing mixture. The results reported here clearly prove that the duration of CyA release can be significantly reduced by incorporation of surfactants inside the gel matrix by as much as a factor of five compared to pure p-HEMA gels. The mechanism of reduction in release rates is through a preferential partitioning of the drug into the surfactant domains that form inside the gels. The rate controlling step is diffusion through the gel but its rate is reduced due to a reduction in the free drug concentration. The concentration and type of the surfactant plays an important role as an increase in the hydrophilic chain length increases partitioning into the hydrophobic cores of the surfactant aggregates and the presence of a double bond in the hydrophobic chain reduces the partitioning. Both these effects likely occur due to the impact of these factors on shielding of the hydrophobic core from the water molecules. Amongst the surfactants explored here, Brij 78 is most promising for extended release of CyA from p-HEMA contact lenses due to a high partition coefficient of 458.9±61.5 for partitioning between the hydrophobic cores and the p-HEMA matrix. The partition coefficient is even higher for Brij 700 due to the large hydrophilic chain length but the total partitioning is small due to a smaller fraction of the hydrophobic segment and also due to a relatively large value of the critical aggregation concentration in the gel. Furthermore, Brij 78 surfactants have been used in ocular studies as cornea permeability enhancers, and have been shown to have negligible toxicity at concentrations as large as 2% (w/w) [67]. Even though Brij-78 laden gels showed promising results for the drug CyA, these could not significantly attenuate release of two other hydrophobic

drugs, DMS and DMSA, due to a lower partition coefficient of these drugs inside the Brij 78 aggregates.

Freeze fracture SEM imaging provides a direct evidence of the presence of pores in the surfactant-laden hydrogels. The pores are about 50 nm in size and are filled mostly with water, which suggests that the surfactant aggregates are perhaps more complex than micelles, and could possibly be vesicles.

The surfactant-laden gels were characterized to determine their suitability as contact lenses materials. All the systems were clear and transparent, and had storage moduli suitable for contact lens applications. The water content for all the surfactant laden gels was much higher than that for pure p-HEMA hydrogel, which is encouraging as it will increase oxygen permeability and perhaps comfort. The wettability of the lenses also improved due to surfactant entrapment with maximum improvement with Brij 78, which could also have beneficial effects.

While the results reported here are very encouraging, they need to be supplemented with animal studies to explore the potential toxicity due to continuous exposure to surfactants. Also, even though incorporation of the surfactants is likely to increase the oxygen permeability, it may not be sufficient for extended wear applications, and so it will be desirable to conduct studies similar to those reported here for silicone hydrogels. Since silicone hydrogels are a mix of silicone and hydrogel materials, it may be possible to create both hydrophobic and hydrophilic domains, which may be useful for extended release of both hydrophobic and hydrophilic drugs. In addition to the surfactants explored here, other surfactants and self assembling molecules such as lipids, and block-co-polymers could be used to create domains that could trap and slowly release hydrophobic and/or hydrophilic drugs. Thus, while issues related to toxicity still need to be explored, this study provides conclusive evidence that p-HEMA contact lenses loaded with

Brij 78 surfactant have physical properties suitable for contact lens applications, and also for extended drug delivery.

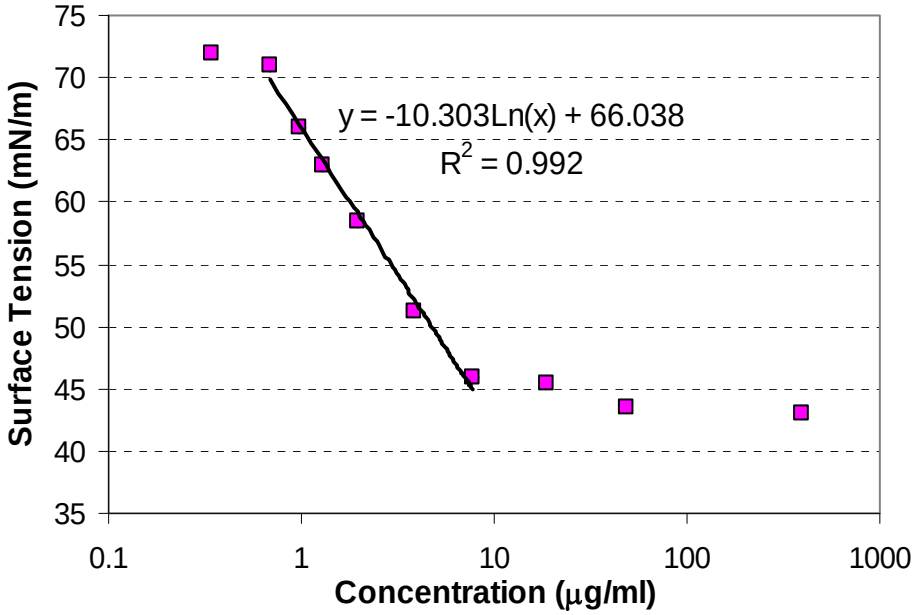

A

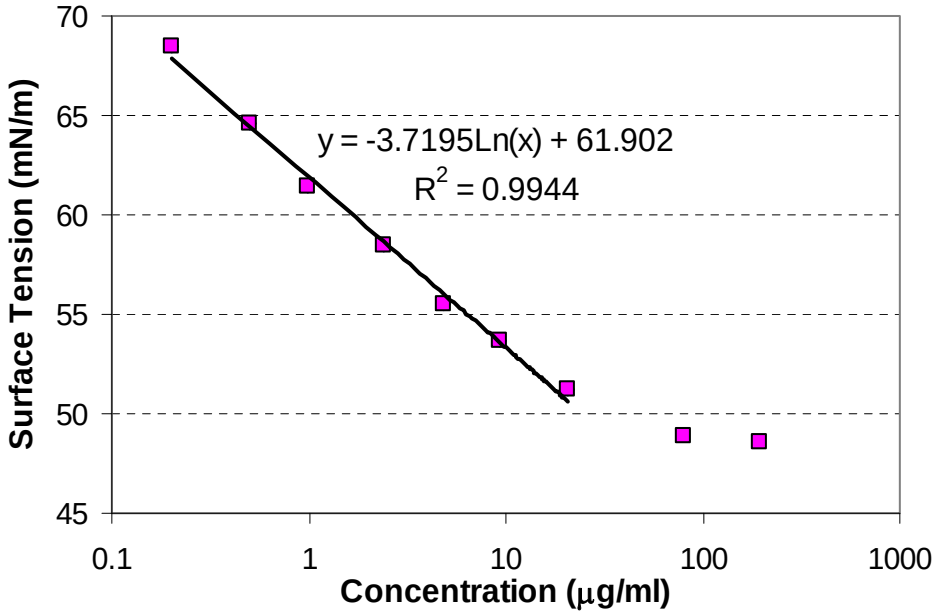

B

Figure 5-1. Dependence of surface tension on the bulk surfactant concentration A) Brij 78 surfactant B) Brij 700 surfactant

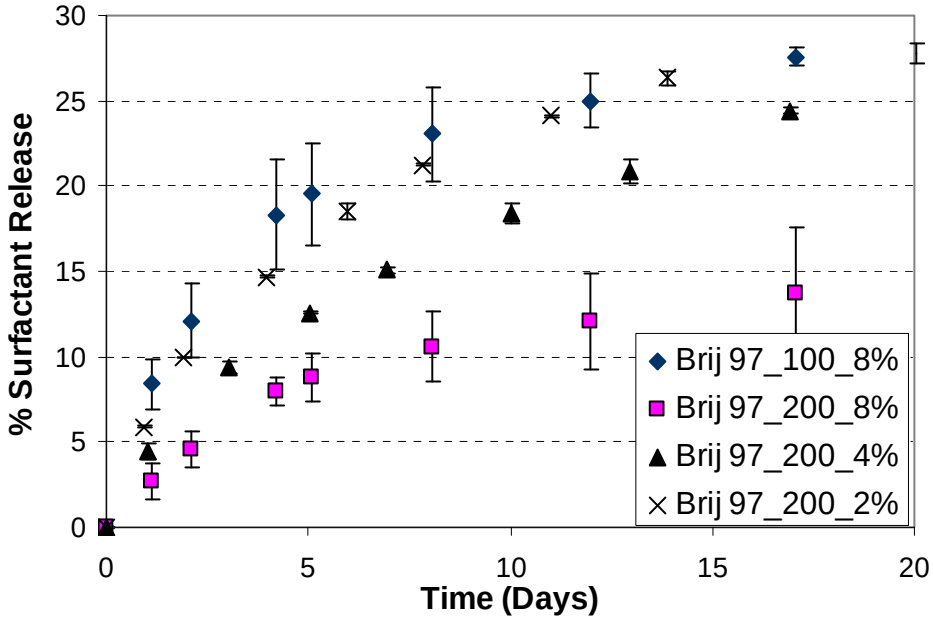

A

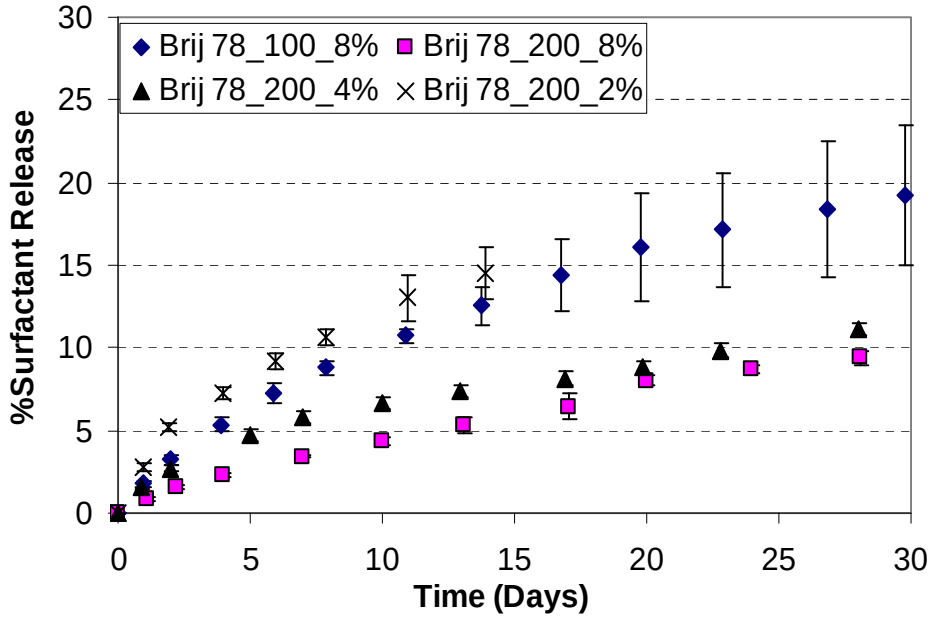

B

Figure 5-2. Percentage release of surfactant during water change experiments. The gel thicknesses in μm and the percentage of surfactant loaded in the gel are indicated in the legend. A) Brij 97 surfactant system B) Brij 78 surfactant system C) Brij 700 surfactant system.

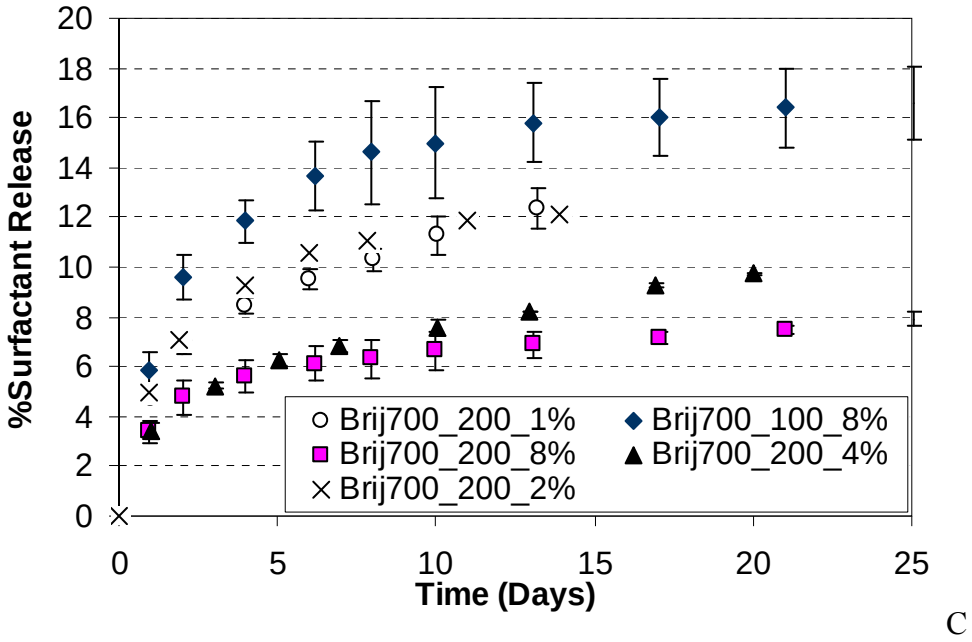

C

Figure 5-2. Continued

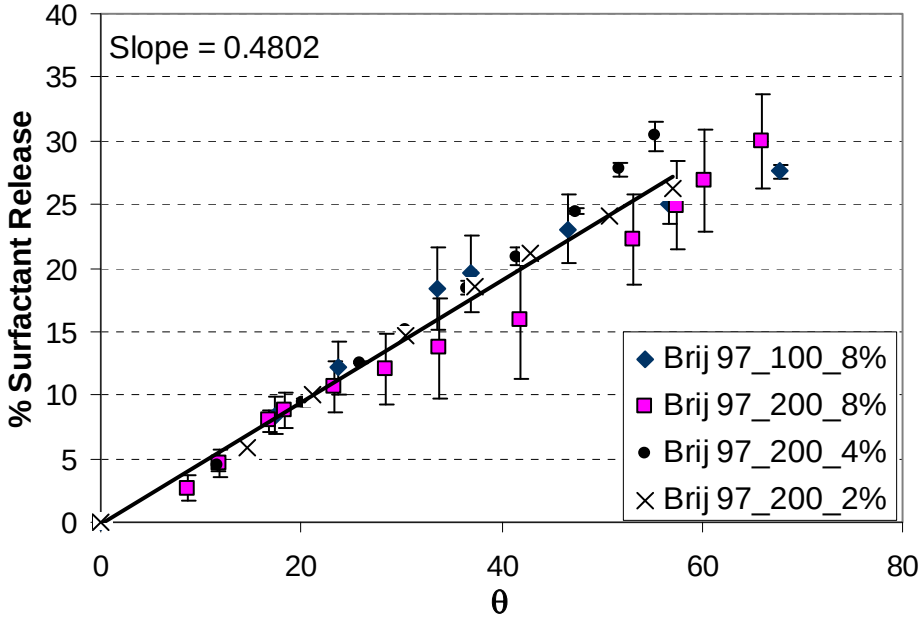

A

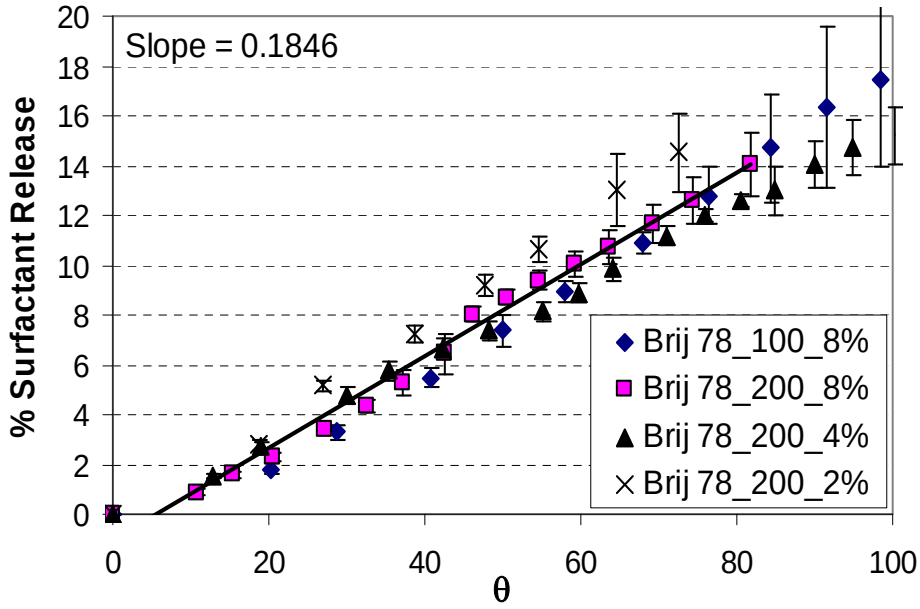

B

Figure 5-3. Cumulative percentage release of surfactant from the hydrogels after rescaling the time. θ represents $\sqrt{t}/C_p/h^2$ where t is time in seconds, C_p is surfactant concentration in M, and h is half thickness of the gel in μm. A) Brij 97 surfactant system B) Brij 78 surfactant system C) Brij 700 surfactant system.

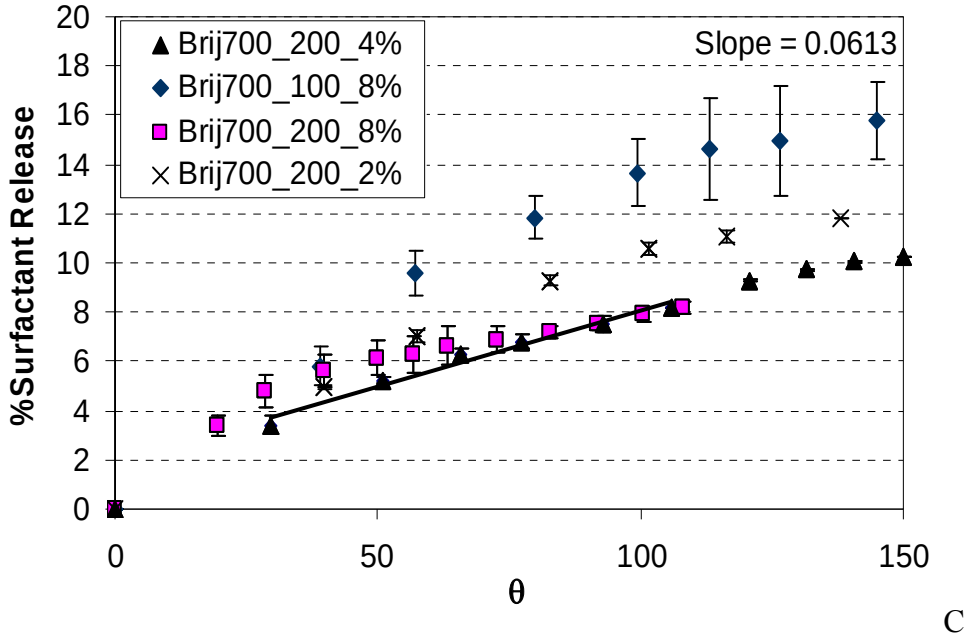

Figure 5-3. Continued

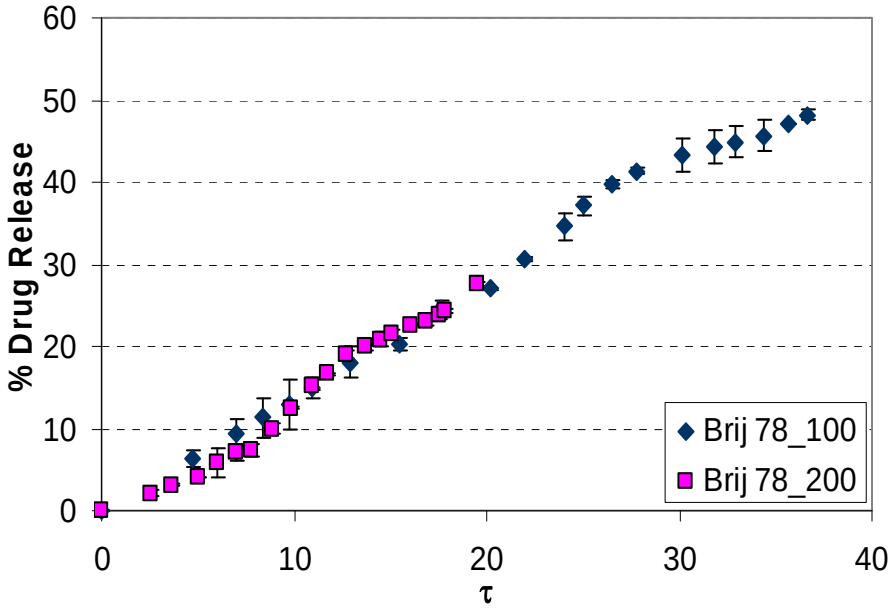

A

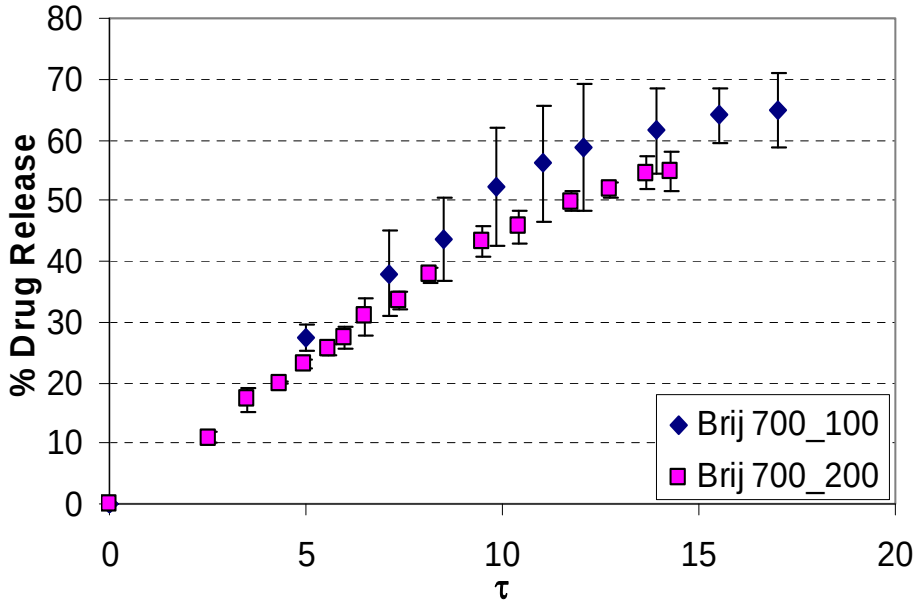

B

Figure 5-4. Effect of thickness on percentage release of drug during equilibrium experiments. τ represents $\sqrt{t}/i^2$ where t is release time in hours and i = 1 for thin gels and i = 2 for thick gels. All the gels contained 50 μg of drug. A) Brij 78 surfactant system B) Brij 700 surfactant system.

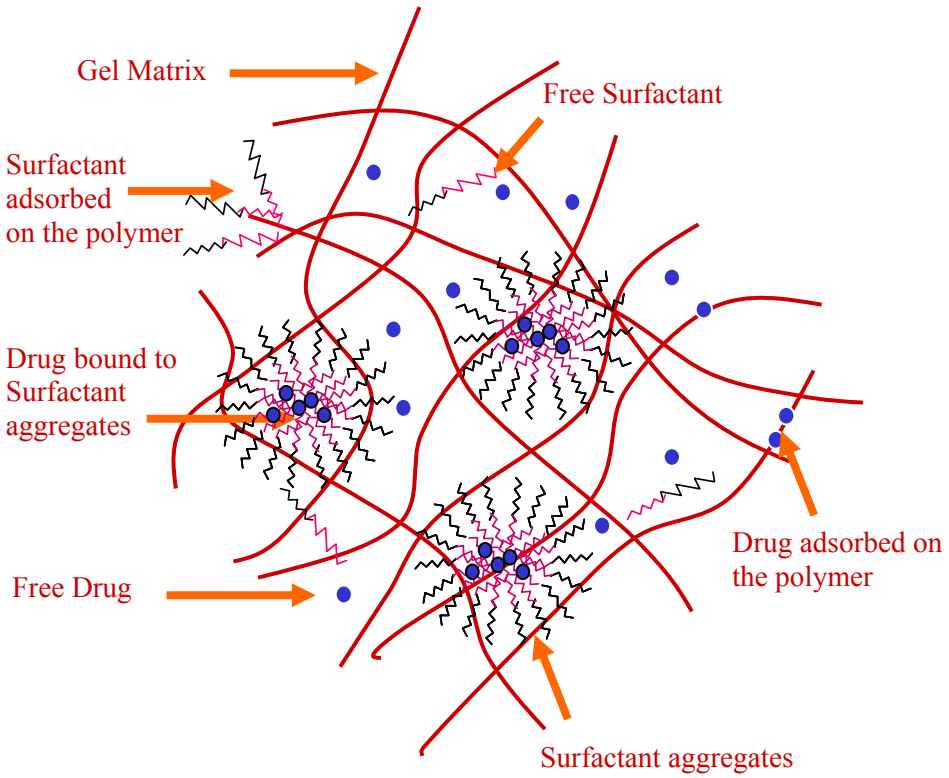

Figure 5-5. Microstructure of the surfactant-laden gel

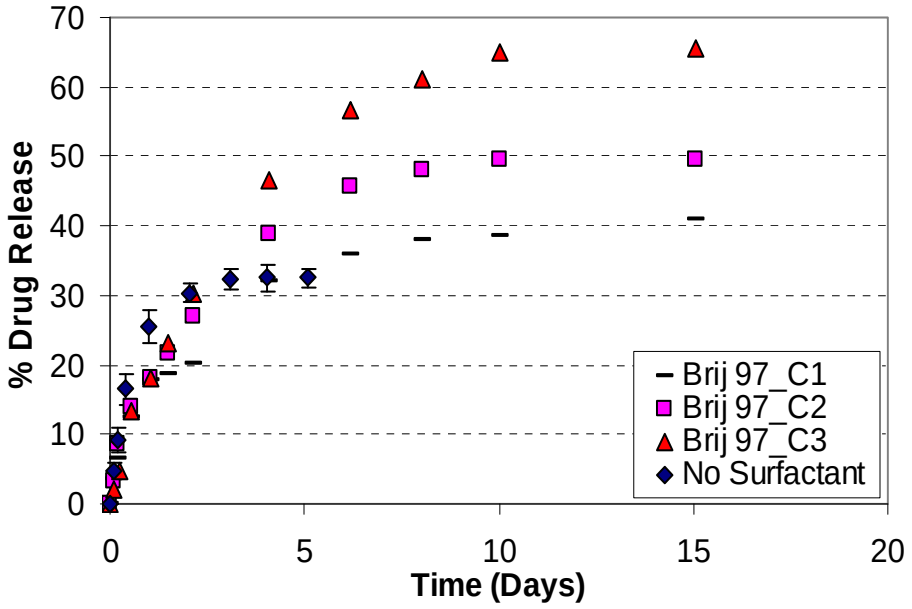

A

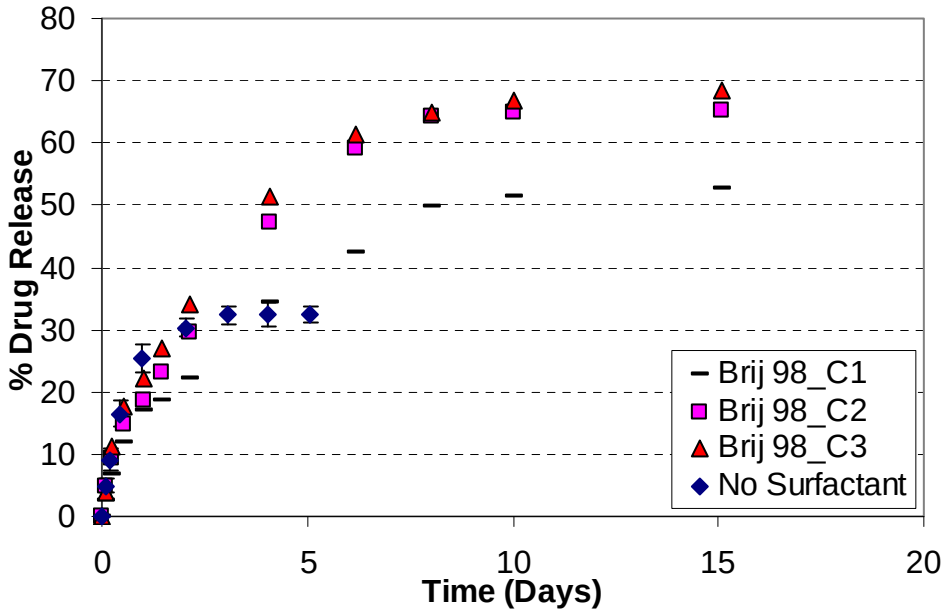

B

Figure 5-6. Effect of surfactant dissolved in the release medium on cumulative percentage release of the drug during equilibrium experiments. All the gels contained nearly 55 μg of drug and were around 200 μm thick. A) Brij 97 surfactant system B) Brij 98 surfactant system C)Brij 78 surfactant system D) Brij 700 surfactant system.

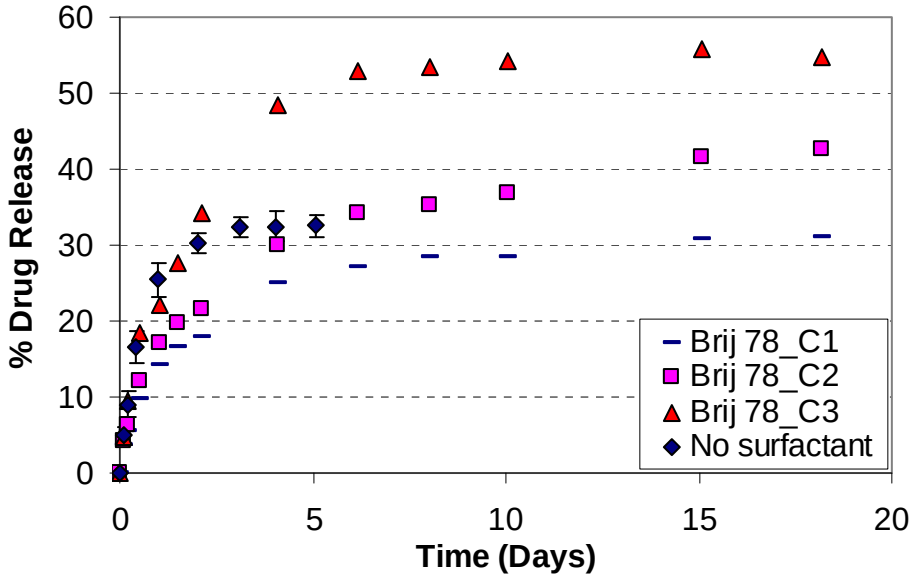

C

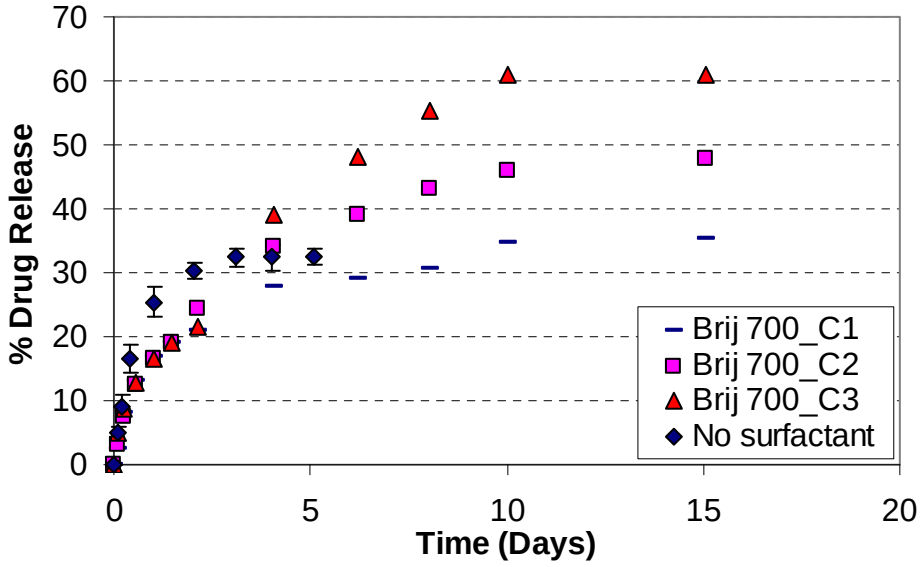

D

Figure 5-6. Continued

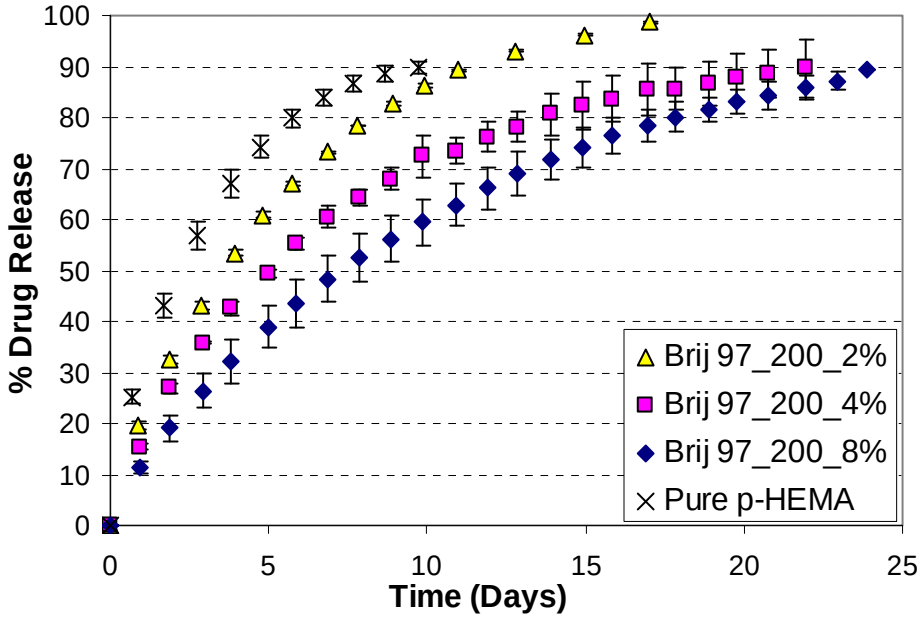

A

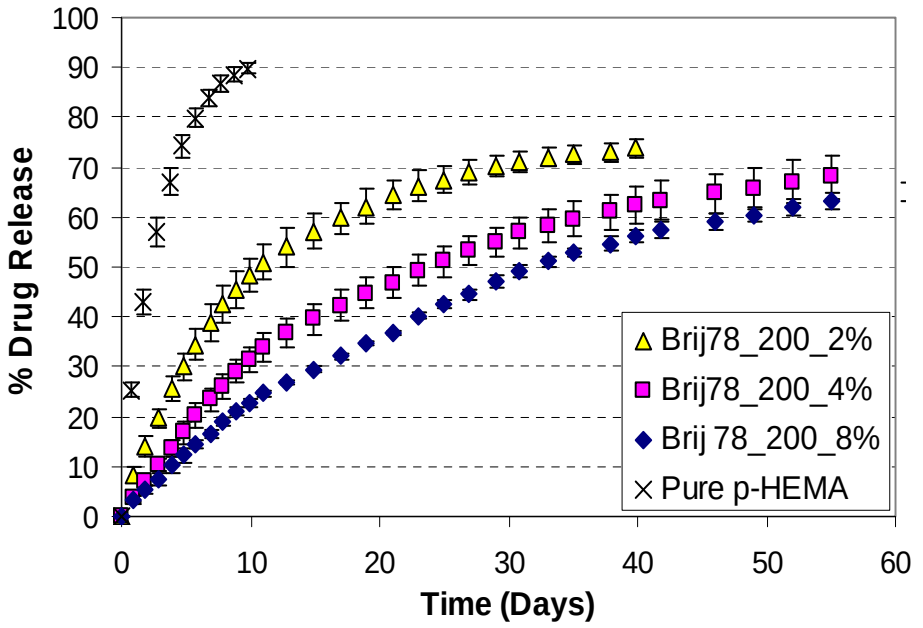

B

Figure 5-7. Effect of surfactant loading on cumulative drug release from surfactant-laden gels in PBS change experiments. All the gels were 200 μm thick and contained 50 μg of drug. A) Brij 97 surfactant system B)Brij 78 surfactant system C) Brij 700 surfactant system.

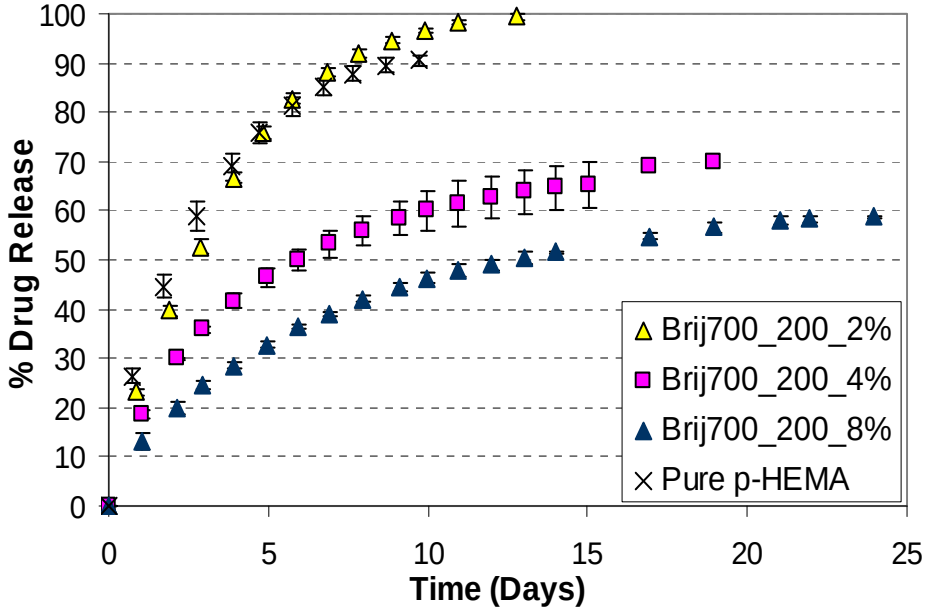

C

Figure 5-7. Continued

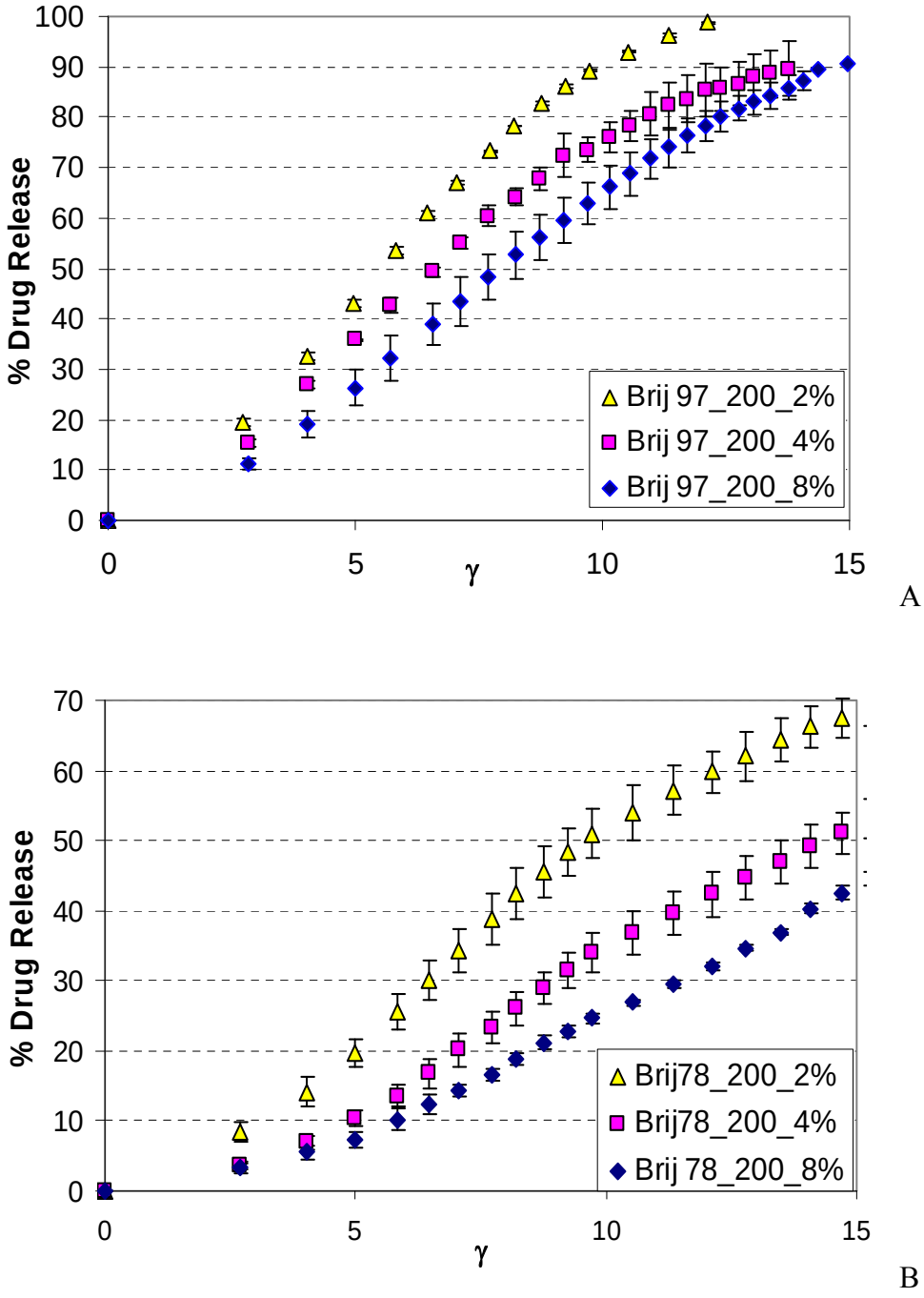

Figure 5-8. Cumulative percentage release of drug from 200 μm thick surfactant-laden gels in PBS change experiments after rescaling the time. γ represents $\sqrt{t}/h^2$ where t is time in seconds and h is half thickness of the gel in μm. A) Brij 97 surfactant system B) Brij 78 surfactant system C) Brij 700 surfactant system D) Brij 98 surfactant system.

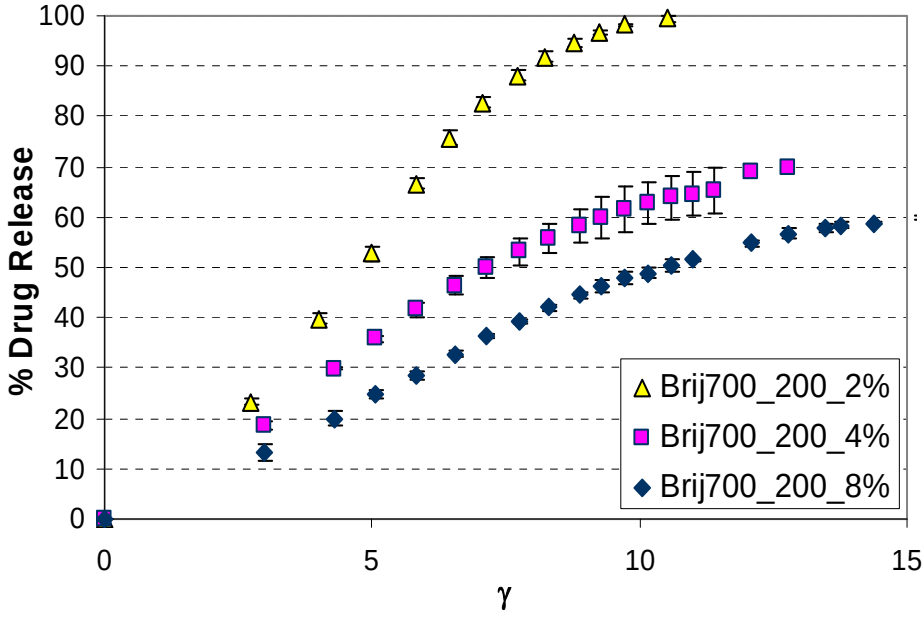

C

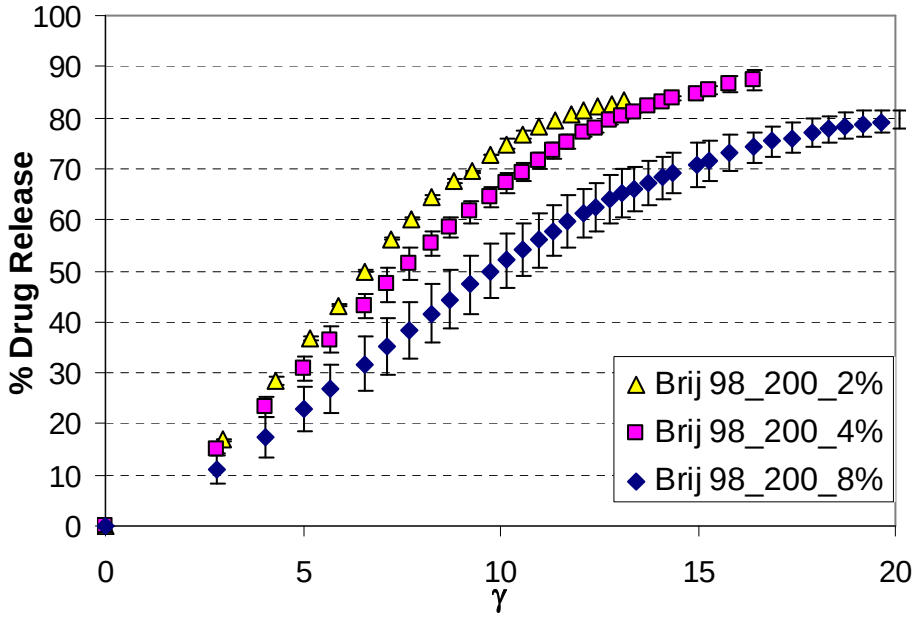

D

Figure 5-8. Continued

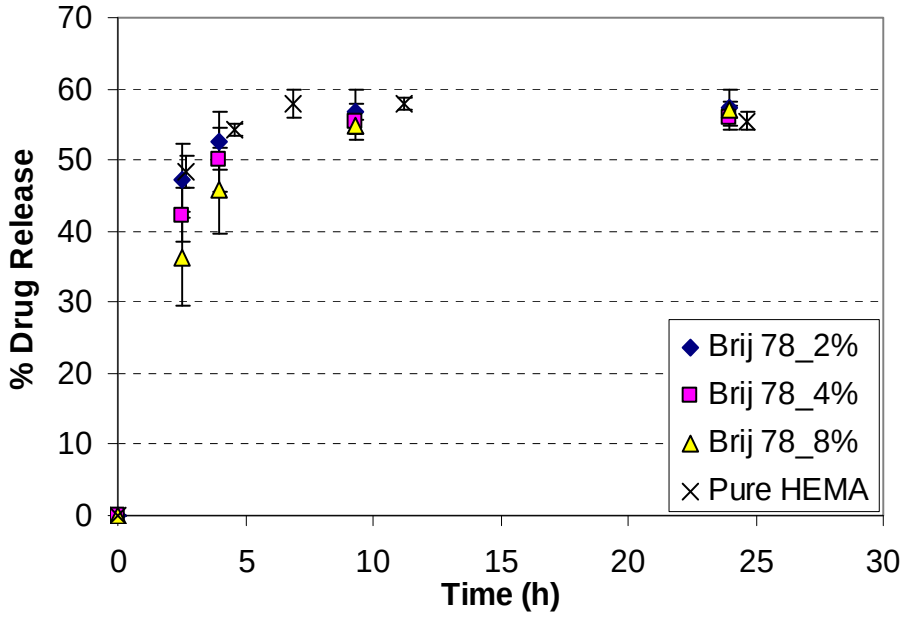

Figure 5-9. Percentage release of DMS from 100 μm thick p-HEMA and Brij 78 laden in equilibrium experiments

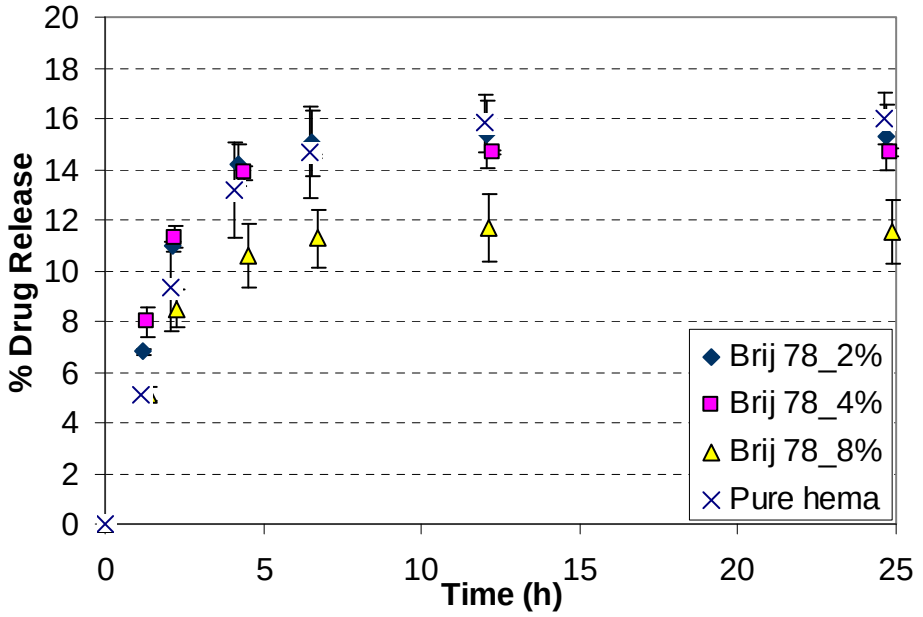

Figure 5-10. Percentage release of DMSA from 100 μm thick p-HEMA and Brij 78 laden gels in equilibrium experiments

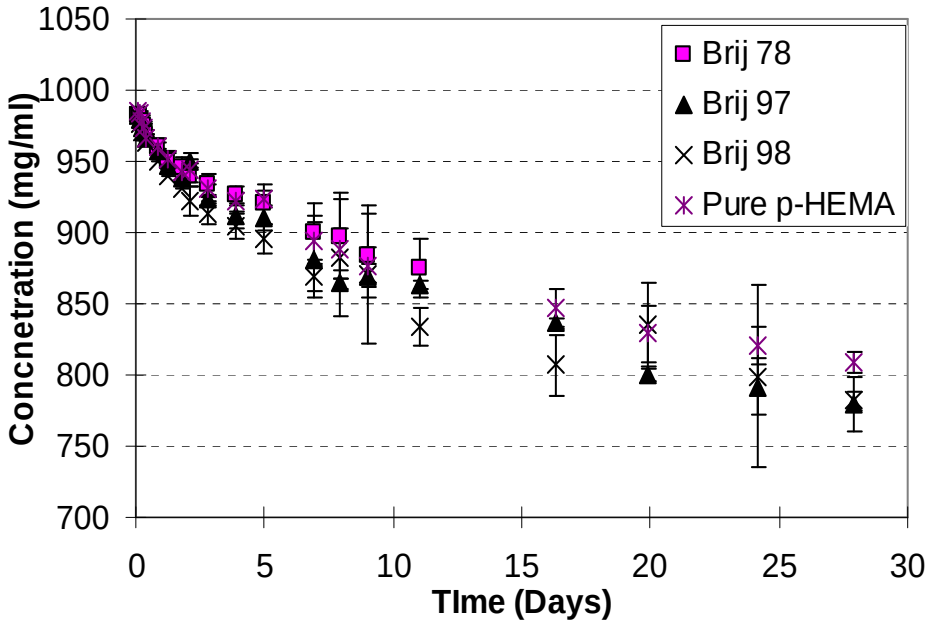

Figure 5-11. Lysozyme sorption in surfactant laden and pure p-HEMA hydrogels

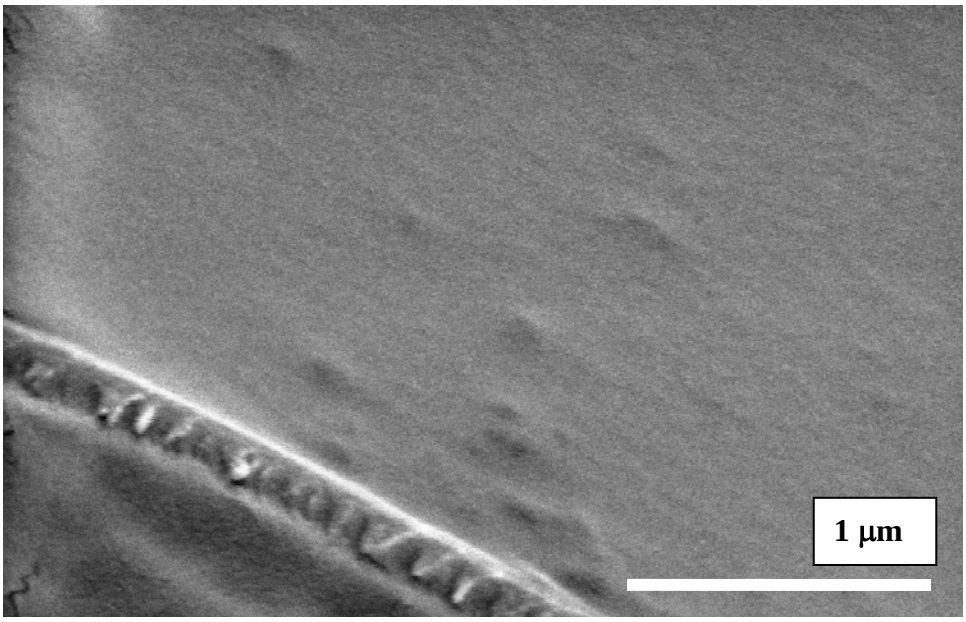

A

Figure 5-12. Cryo-SEM image for 200 μm thick gels. A) pure p-HEMA gels:Scale-1μm B) pure p-HEMA gels:Scale-2μm C) pure p-HEMA gels:Scale-5μm D) Brij 98 laden gels:Scale-1μm E) Brij 98 laden gels:Scale-2μm F) Brij 98 laden gels:Scale-5μm G) Brij 97 laden gels:Scale-1μm H) Brij 97 laden gels:Scale-2μm I) Brij 97 laden gels:Scale-5μm J) Brij 78 laden gels:Scale-1μm. K) Brij 78 laden gels:Scale-2μm L) Brij 78 laden gels:Scale-5μm M) Brij 700 laden gels:Scale-1μm N) Brij 700 laden gels:Scale-2μm O) Brij 700 laden gels:Scale-5μm.

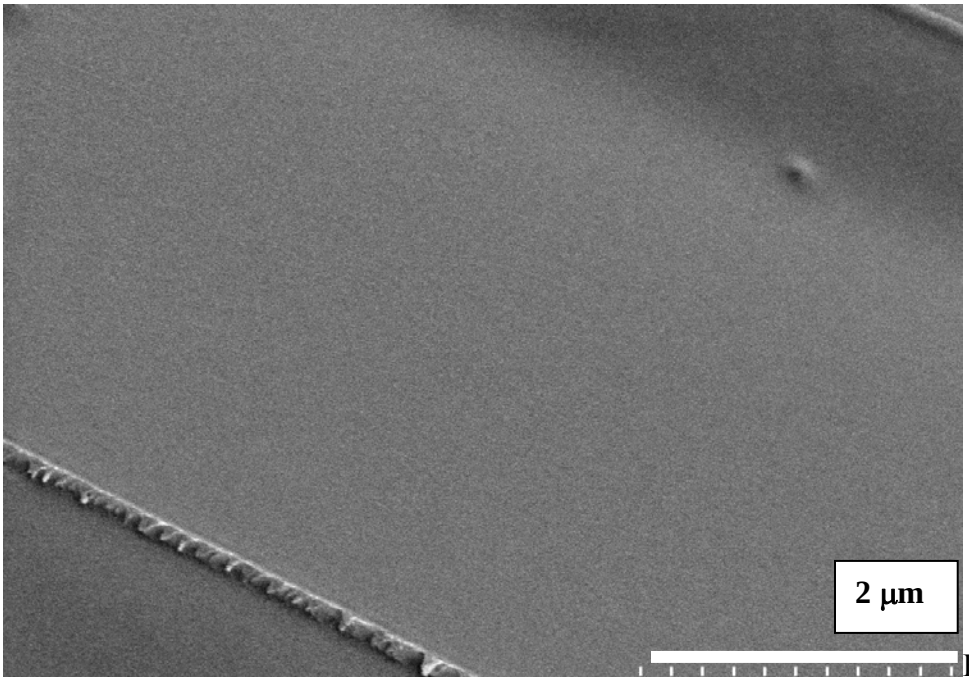

B

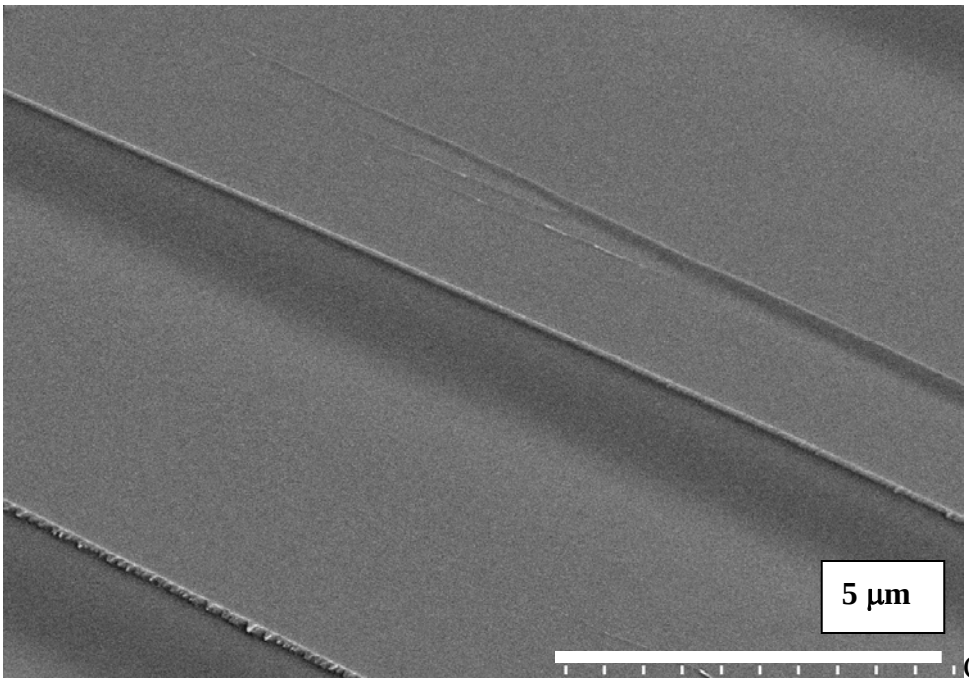

C

Figure 5-12. Continued

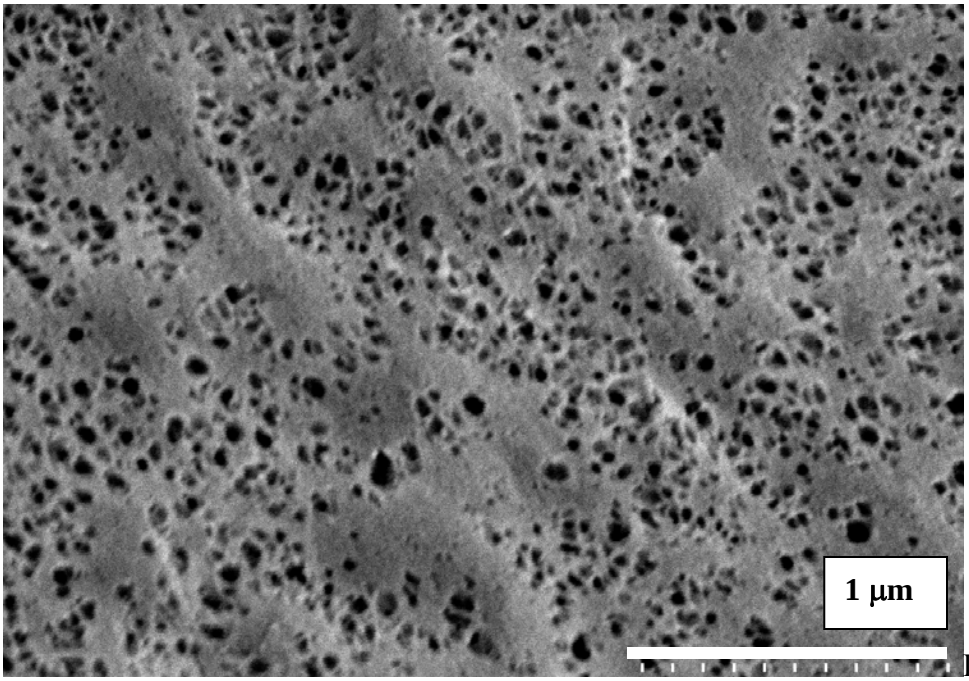

D

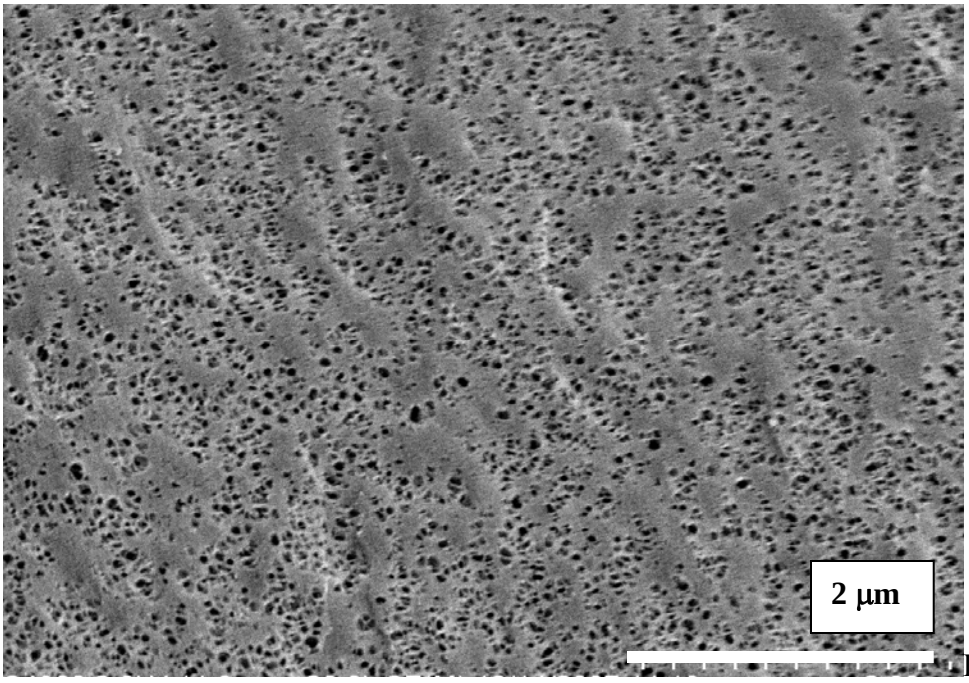

E

Figure 5-12. Continued

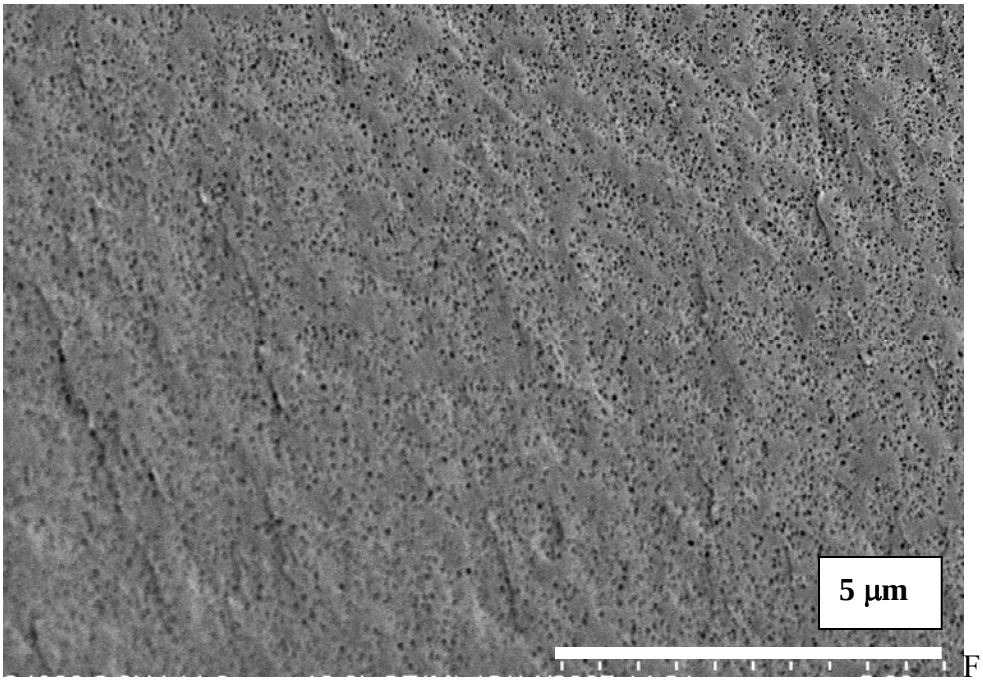

F

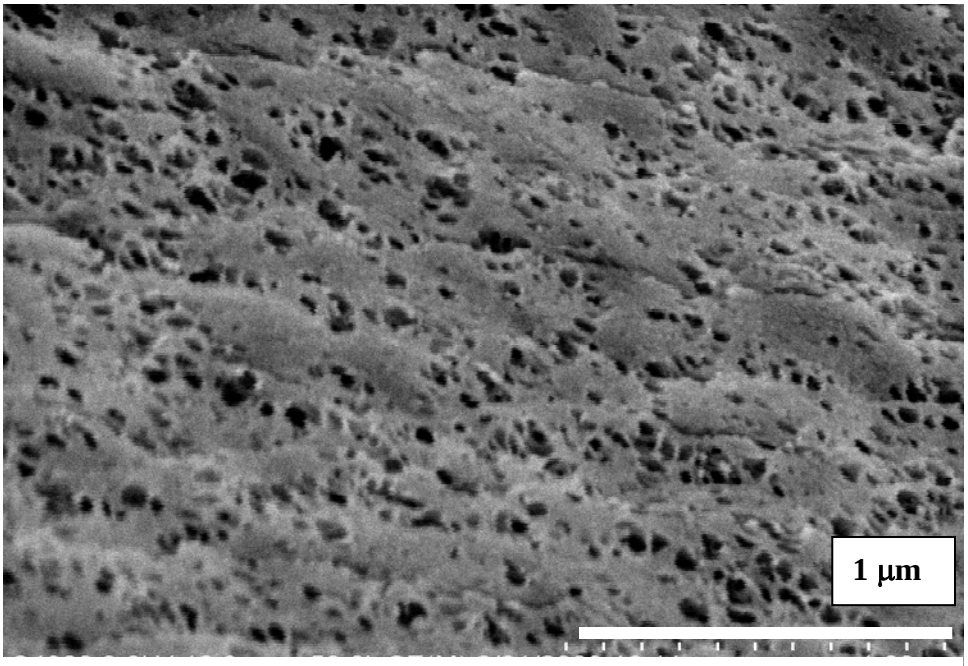

G

Figure 5-12. Continued

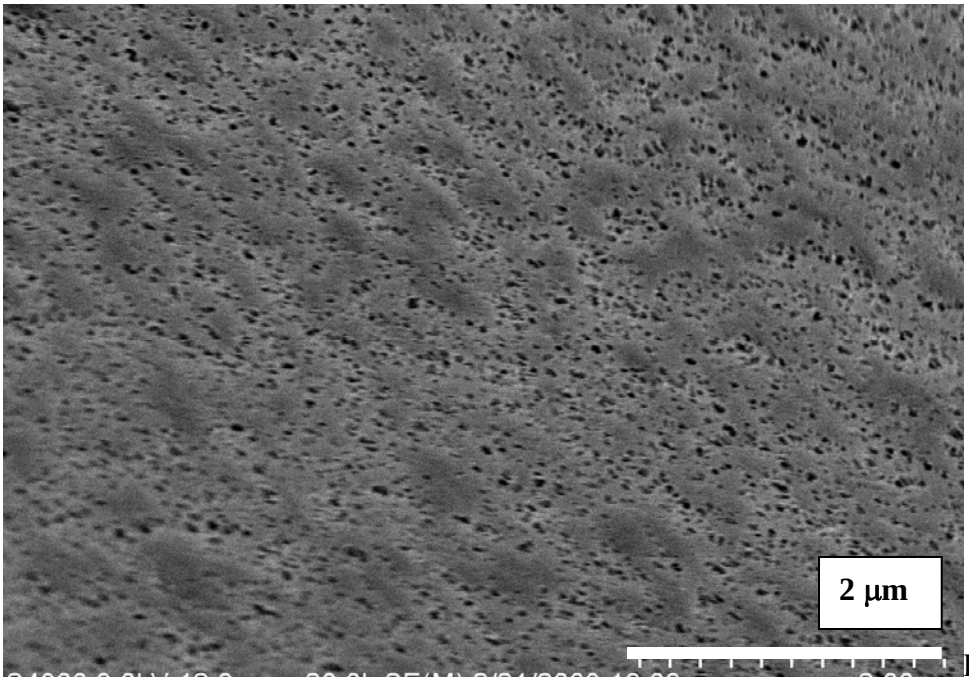

H

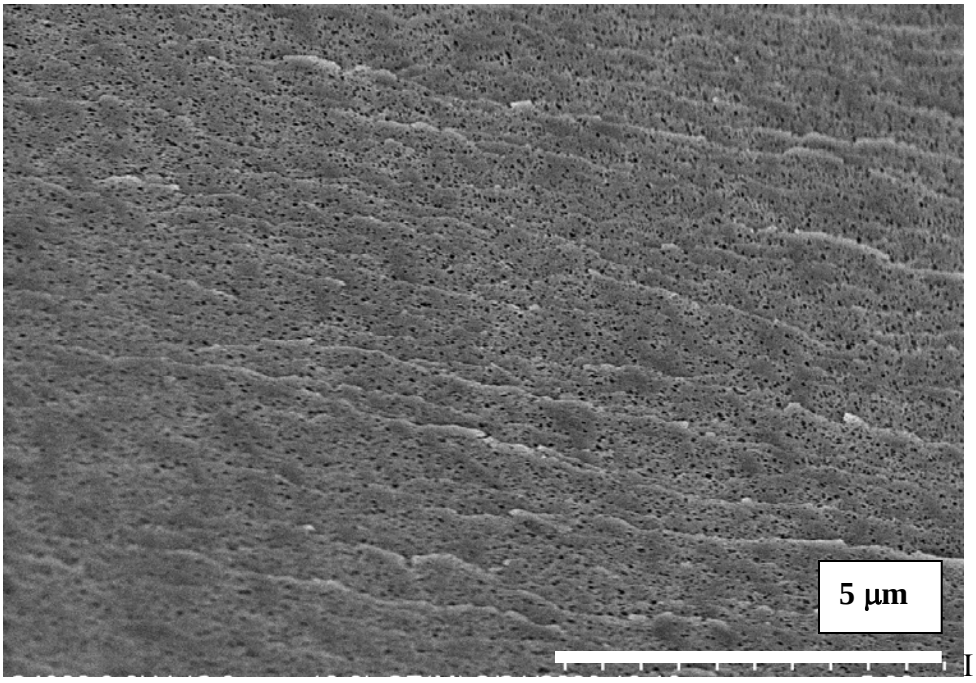

I

Figure 5-12. Continued

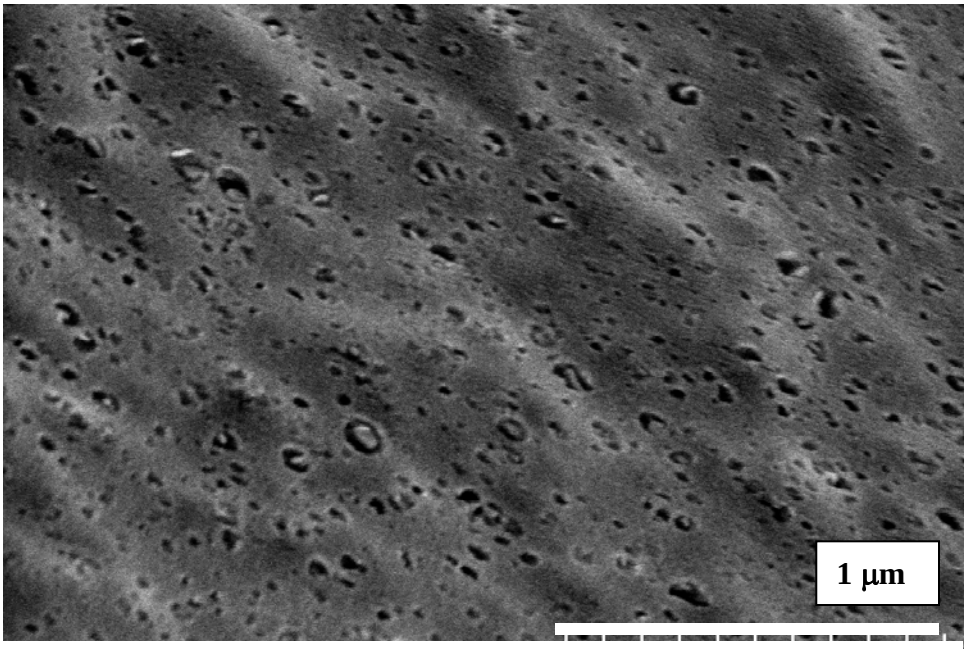

J

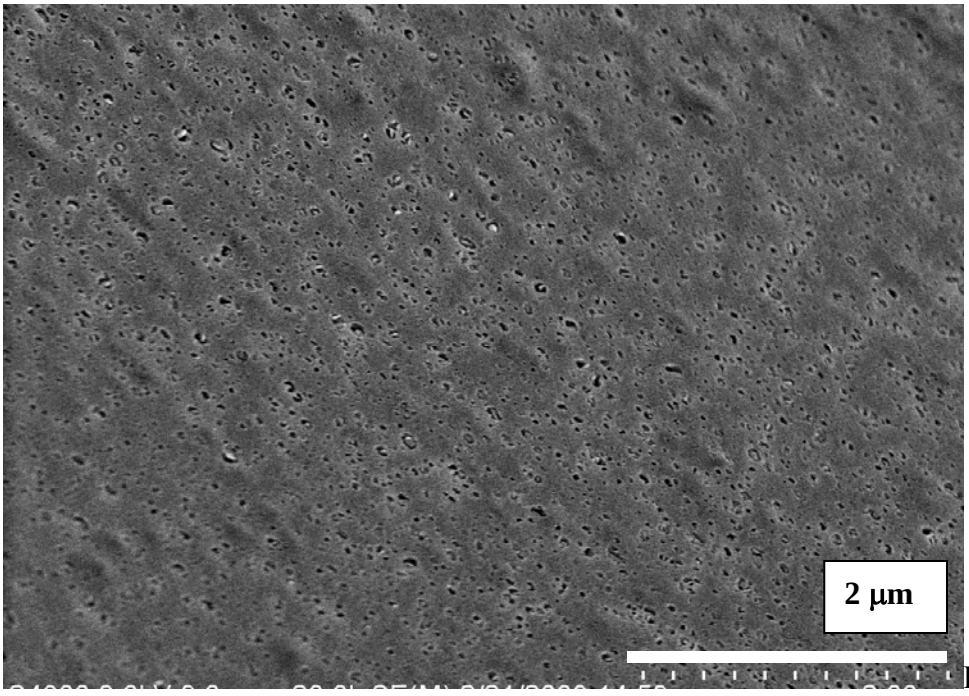

K

Figure 5-12. Continued

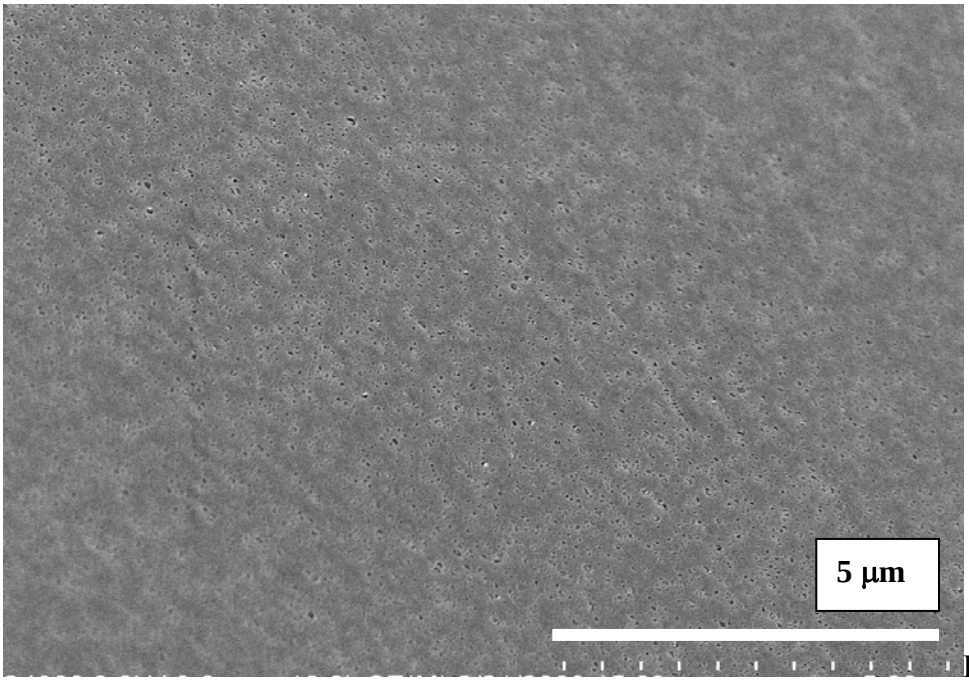

L

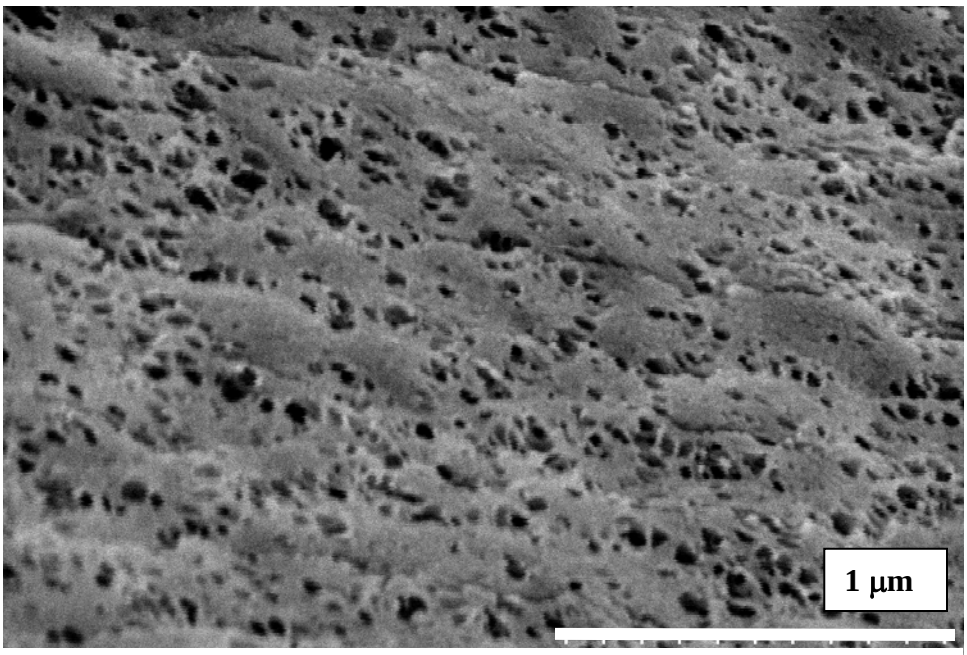

M

Figure 5-12. Continued

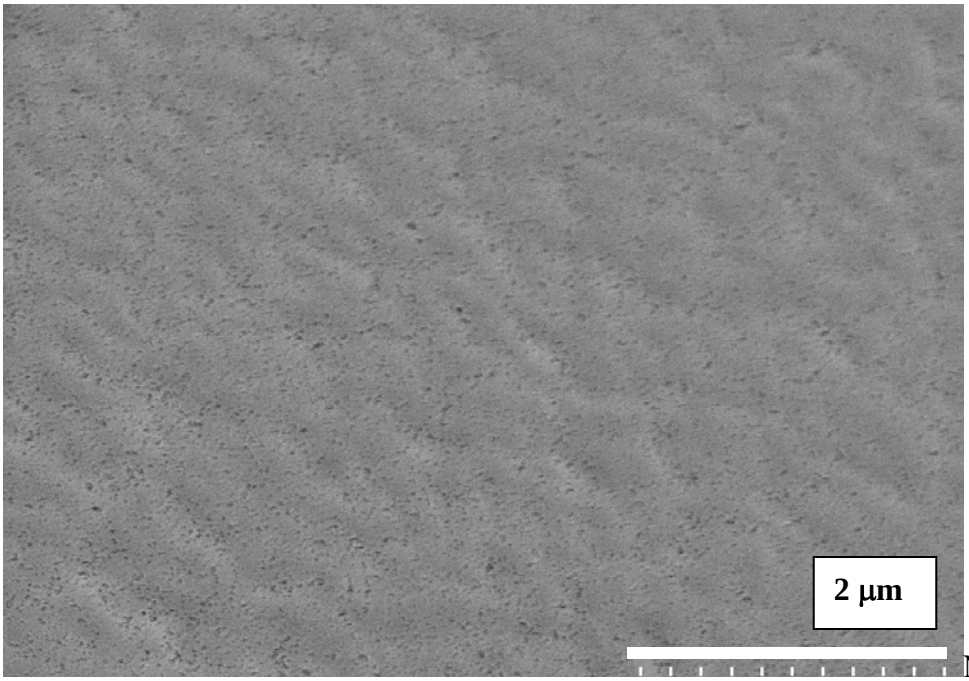

N

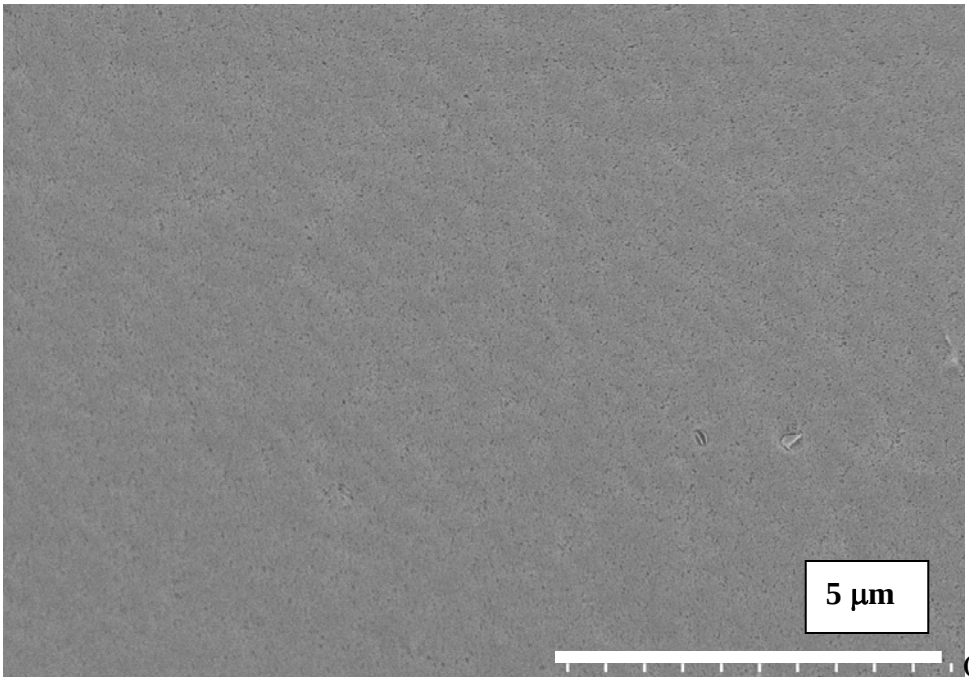

O

Figure 5-12. Continued

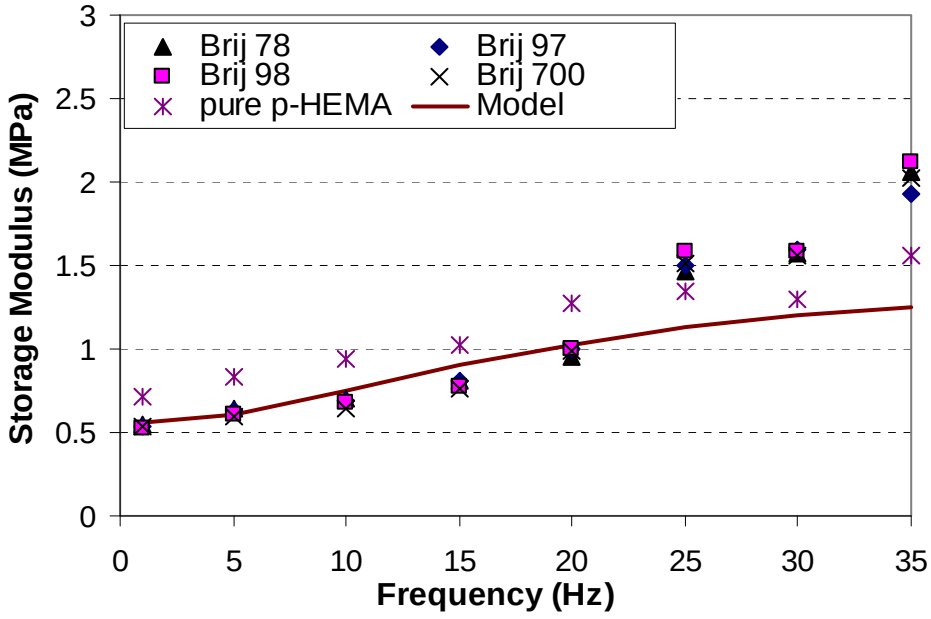

A

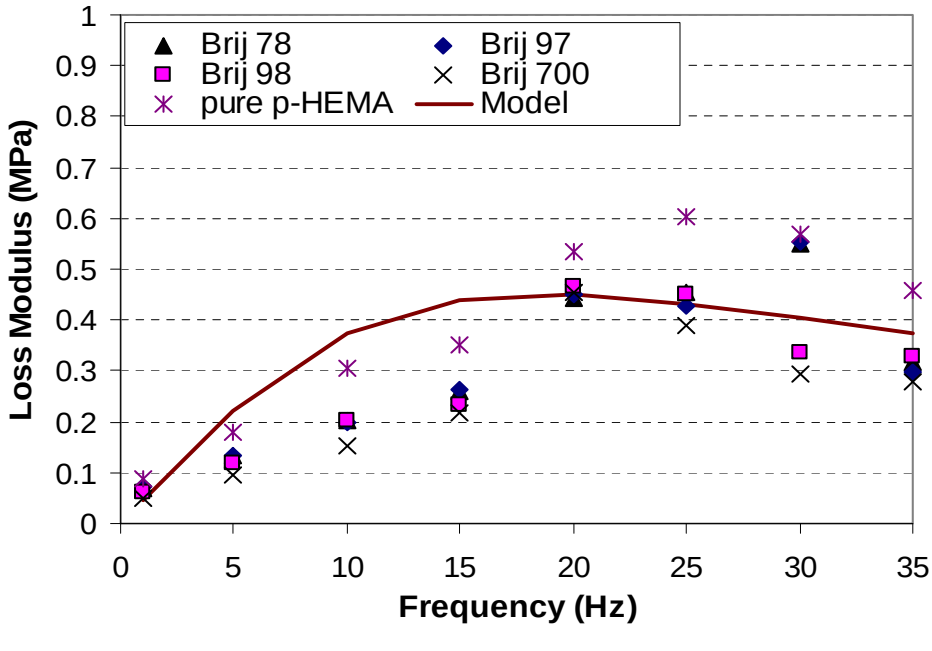

B

Figure 5-13. Frequency dependence of moduli for 800 μm thick surfactant laden and pure p-HEMA gels. A) Storage Modulus B) Loss Modulus

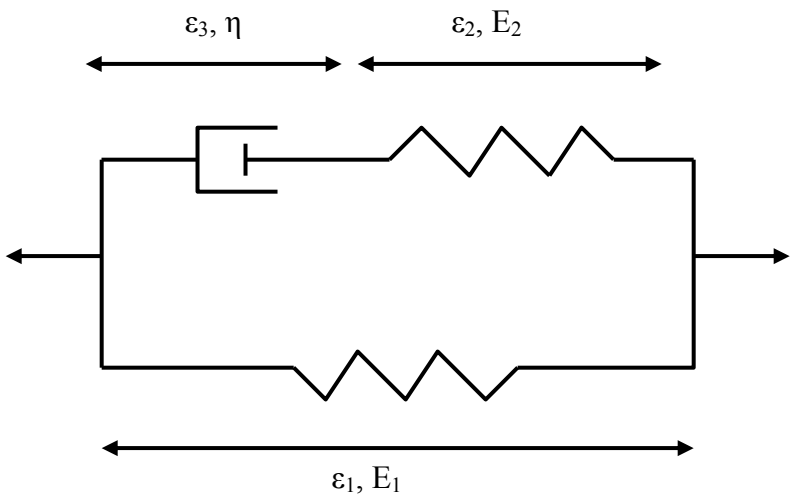

Figure 5-14. Standard Linear Solid Model used for fitting the viscoelasticity data of the surfactant-laden gels

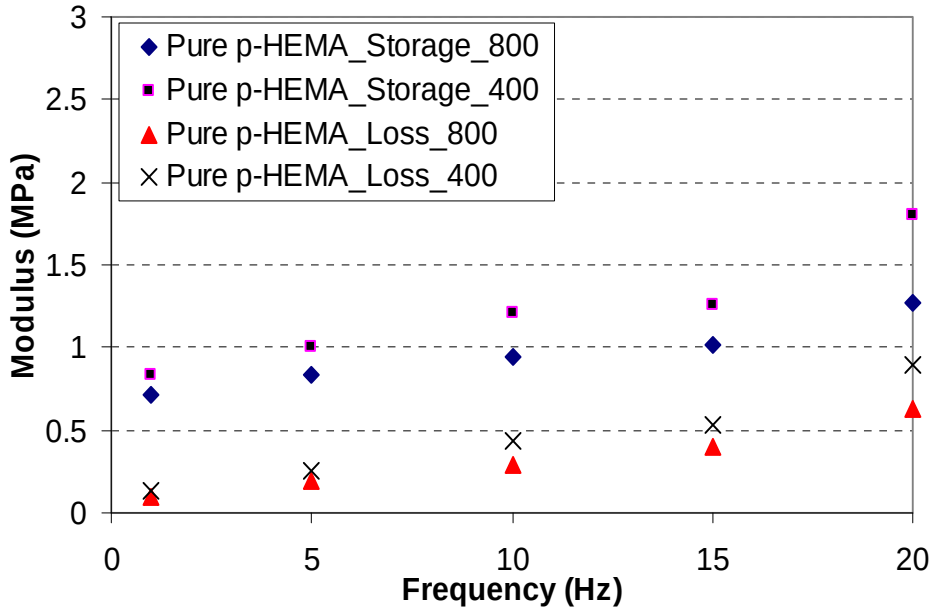

Figure 5-15. Effect of thickness on the storage and loss moduli of pure p-HEMA gels. The gel thicknesses in μm are indicated in the legends.

Table 5-1. Physical properties of the surfactants explored in this study

System	Name	Chemical Formula	Molecular weight	HLB [120]	fh
Brij 97	POE (10) oleyl ether	$C_{18}H_{35}(OCH_2CH_2)_{10}OH$	709.0	12.4	0.47
Brij 98	POE (20) oleyl ether	$C_{18}H_{35}(OCH_2CH_2)_{20}OH$	1149.5	15.0	0.31
Brij 78	POE (20) stearyl ether	$C_{18}H_{37}(OCH_2CH_2)_{20}OH$	1151.5	15.0	0.31
Brij 700	POE (100) stearyl ether	$C_{18}H_{37}(OCH_2CH_2)_{100}OH$	4670.0	18.8	0.08

Table 5-2. D_SC^* for all systems obtained from fitting of the surfactant release data

System	Slope	D_SC^* $(\mu m)^2M/s \times 10^6$
Brij 97	0.4802 ± 0.010	11.52
Brij 98	1.1000 ± 0.013 [39]	60.80
Brij 78	0.1846 ± 0.050	1.70
Brij 700	0.0613 ± 0.013	0.19

Table 5-3. Concentration of surfactants dissolved in the release medium

System	CMC (μg/ml)	C1 (μg/ml)	C2 (μg/ml)	C3 (μg/ml)
Brij 97	290.0	100	286	861
Brij 98	304.5	101	307	924
Brij 78	53.0	18	53	159
Brij 700	93.4	31	93	270

Table 5-4. Partition coefficient of CyA for all the surfactant systems

System	Amount of surfactant	Slope	K (M^{-1})	Km
	2%	11.08 ± 0.83	14.14	
Brij 97	4%	9.22 ± 0.20	18.35	48.9± 6.3
	8%	7.76 ± 0.33	16.40	
	2%	6.37 ± 0.43	142.20	
Brij 78	4%	4.51 ± 0.40	163.10	458.9±61.5
	8%	3.19 ± 0.33	186.10	
	2%	9.17 ± 0.20	99.46	
Brij 98	4%	7.46 ± 0.16	96.46	261.0±24.4
	8%	5.71 ± 0.07	83.10	
	2%	13.87 ± 2.32	-	
Brij 700	4%	7.26 ± 0.67	258.48	675.8±11.4
	8%	5.33 ± 0.17	252.47	

Table 5-5. Partition coefficient of DMS and DMSA in p-HEMA and Brij 78 surfactant laden hydrogels

System	DMS		DMSA	
	K_{Avg}	$K_{Micelle}$	K_{Avg}	$K_{Micelle}$
Pure p-HEMA	54.5	-	341.3	-
Brij 78 (2%)	55.3	366.8	368.0	5885.4
Brij 78 (4%)	57.0	399.5	384.2	4563.6
Brij 78 (8%)	61.4	456.9	503.7	7950.4

Table 5-6. Physical properties of the surfactant laden and pure p-HEMA hydrogels

System	α	EWC_{Pred} (%)	EWC (%)	Transmittance (%)	Contact Angle
Brij 97 (8%)	31.0	67.6	64.1	99.8	27.9±1.06
Brij 98 (8%)	29.1	66.7	67.2	99.2	24.9±1.40
Brij 78 (8%)	41.0	72.3	70.3	99.9	19.8±0.78
Brij 700 (8%)	46.4	74.8	70.4	99.5	27.2±0.59
Pure p-HEMA	-	-	53.0	98.9	30.3±0.18

Table 5-7. Parameters obtained by fitting Standard Linear Solid Model to the experimental data

Parameter	Value
E_1	0.55 MPa
E_2	0.90 MPa
μ	0.0076 MPa.s

CHAPTER 6
LIPOSOME ASSAY FOR EVALUATING OCULAR TOXICITY OF SURFACTANTS

6.1 Introduction

One in vitro method of assessing ocular toxicity is the utilization of liposomes to mimic cell permeation by the test substance. The advantages of using liposome leakage to assess ocular toxicity include low cost and the ability to assess many compounds rapidly. Additionally, the test is quantitative and so lacks the unpredictability that can be associated with using live cells. This test is based on the idea that the permeation of a test substance through lipid bilayers is the root cause of inducing ocular toxicity, with toxicity being caused by the leakage of cellular components, which increases substantially on binding of the test substance to the bilayer. The liposome based assay is designed so that the lipid composition of the bilayers imitates the composition of corneal epithelial cells. The test measures the leakage of fluorescent dye from the liposome core upon interaction with a test substance. The maximum score of the Draize eye test is 110, with 80 out of 110 coming from the cornea alone, suggesting that the assessment of corneal toxicity should be the main focus of an in vitro alternative. This fact first inspired researchers to test liposomes as a possible means of assessing the ocular toxicity of surfactants [111,112]. Since that time, a few others have examined liposome leakage as well [108,113]. Good correlations to in vivo data were obtained in some cases for some surfactants, with gross outliers sometimes present.

In this Chapter, we propose that the lack of good correlation in some studies between the liposome based assay and the Draize test was due to neglect of mechanistic issues, and that a better correlation can be obtained by designing the liposome assay after mechanistic considerations. Specifically, while comparing the Draize test to increases in liposome permeability upon exposure to surfactants, most researchers evaluated the liposome permeability

at a fixed surfactant concentration or at a concentration which induced 50% dye leakage, and the concentrations were significantly below the concentration used in the Draize test. Herein, we first show that the liposome permeability in the presence of surfactants at a fixed surfactant concentration does not correlate well with the Draize scores. We then show that the correlations are significantly improved when the surfactant concentration in the liposome assay is chosen to be CMC/200, where CMC is the critical micelle concentration, which varies significantly across the surfactants explored in this study. We also show the rationale for this choice of surfactant concentration in the liposome assay based on mechanistic considerations. Finally, we utilize the liposome assay developed here to determine the ocular toxicity of several Brij surfactants for which available ocular toxicity data was very limited or nonexistent and have been used previously to attenuate drug release from contact lenses.

6.2. Materials and Methods

6.2.1 Materials

Methanol, chloroform, Dulbecco's Phosphate Buffered Saline (PBS) without calcium chloride and magnesium chloride, Sephadex G-50 (fine), cholesterol (CH), sodium dodecyl sulfate (SDS), polyoxyethylene sorbitan monolaurate (Tween 20), polyoxyethylene sorbitan monooleate (Tween 80), hexadecyltrimethylammonium bromide (CTAB), cetyl pyridinium chloride (CPC), benzalkonium chloride (BKC), Brij 56, Brij 58, Brij 98, Brij 76, Brij 78, Brij 97, and Brij 700 were purchased from Sigma Aldrich. Whatman GF/B glass microfiber filters, calcein dye (fluorexon), polyoxyethylene sorbitan monopalmitate (Tween 40), myristyltrimethylammonium bromide (MTAB), and Triton X-100 were purchased from Fisher Scientific. Octadecyltrimethylammonium bromide (OTAB) was purchased from K & K Laboratories. The lipids 1,2-Dioleoyl-sn-Glycero-3-Phosphoethanolamine (DOPE), dissolved in chloroform, 1,2-Dimyristoyl-sn-Glycero-3-[Phospho-rac-(1-glycerol)] (Sodium Salt) (DMPG),

in powder form, and 1,2-Dimyristoyl-sn-Glycero-3-Phosphocholine (DMPC), in powder form, were purchased from Avanti Polar Lipids, Inc. A Mini-Extruder kit for liposome preparation was also purchased from Avanti Polar Lipids, Inc.

6.2.2 Liposome Preparation for Calcein Leakage Studies

Liposomes composed of a molar ratio of 8:6:1.5:1.5 of DMPC:DOPE:DMPG:CH encapsulating an aqueous 100 mM calcein dye solution were prepared via a combination of mixing, sonication, and extrusion. The ratio of lipids was chosen based on the composition of the corneal epithelium [113]. Lipids were combined in their respective molar ratios and then dissolved in a 9:1 mixture (by volume) of chloroform:methanol such that a 20 mg/mL concentration of lipids was obtained. The organic solvent was then evaporated under a stream of nitrogen. After an even and uniformly dried lipid film was obtained, the dried lipid layer was hydrated with 100 mM calcein dye dissolved in PBS such that the lipid concentration was 25 mg lipid/mL. The lipid suspension was then mixed using a Fisher vortex mixer for 1-2 minutes, followed by bath sonication for 20 minutes. The vesicles were then gently stirred overnight at 30°C for approximately 20 hours, due to the increase in entrapped aqueous volume of liposomes with increased stir times [129]. After stirring, the liposome solution was extruded through a 100 nm membrane 15 times. To remove excess dye from the bulk, the liposome solution was passed through a mini-column of Sephadex G-50 (fine) using the centrifugation method to ensure that a large portion of the lipids added to the Sephadex bed were recovered [130]. The resulting liposome solution was diluted by a factor of 1001 based on the observation that the calcein release at the subsequent concentration fell in the linear detection regime.

6.2.3 Liposome Leakage Studies

Surfactant induced calcein leakage from liposomes was used to mimic surfactant permeation into corneal epithelial cells *in vivo*. The 100 mM calcein solution inside the

liposomes was in the quenched state, as is the case for highly concentrated calcein and carboxyfluorescein, so that only the diluted dye which leaked into the bulk medium gave a signal [130]. The baseline fluorescence of the liposome solution prior to leakage was first measured using a Quantech Digital Filter Fluorometer with excitation and emission filters at 490 and 515 nm, respectively. A concentrated surfactant solution was then added such that the final surfactant concentration was either 1 μg/mL or the critical micelle concentration (CMC) of the surfactant divided by 200 (discussed later). The liposome solution was kept at room temperature in between subsequent fluorescent measurements. To compute the percent release, the following formula was used,

$$\%\text{Release} = \frac{F_t - F_o}{F_{total} - F_o} \times 100 \tag{6-1}$$

Where F_t was the fluorescence measurement at time t (10 minutes), F_o was the fluorescence at time zero, and F_{total} was the total calcein released, which was determined by breaking the liposomes with 100 μL of 20% (v/v) Triton X-100. Corrections were made to account for the dilution upon addition of the surfactant and Triton X-100 solutions. All release experiments were carried out at least twice.

6.2.4 Draize Scores

Draize scores for ten of the surfactants tested (SDS, Tween 20, Tween 40, Tween 80, Triton X-100, MTAB, CTAB, OTAB, CPC, BKC) were obtained from three independently published studies [105,131,132]. Kennah et al. published 24 h average Draize scores for multiple concentrations of surfactants, enabling two correlations from their publication [131]. Their scores for concentrations of 10% and 1% (vol %) were used. For SDS, authors reported Draize scores for 30%, 15%, and 3% surfactant concentrations, and their data was fitted to a calibration curve to compute the corresponding Draize scores at 10% and 1%. Tachon et al.

reported the maximum Draize score after 1 h or 24 h at 10% w/v surfactant concentrations [132]. Finally, Matsukawa et al. reported both the maximal average scores and the 24 h average scores for 10 % solutions, and the latter was used for consistency [105]. Table 6-1 shows the surfactants used for the *in vitro/in vivo* correlations and their corresponding Draize scores from each publication. Note that not all surfactants were studied in each published work.

6.2.5 Data Analysis

Draize scores and percentage of calcein release from liposomes after 10 minutes were correlated using Pearson's correlation coefficient (r) and the coefficient of determination (R^2), as well as Spearman's rank correlation coefficient. Both types of measures were computed based on the variety of coefficients used in the literature and the question of validity associated with using ordinal data for Pearson's coefficient. The prediction equations calculated from Draize data at 10% from Kennah et al., Tachon et al., and Matsukawa et al. [105,131,132] were compared using 95% confidence intervals for mean Draize scores as a function of percentage calcein leakage generated in JMP (SAS, Cary NC). Also, the predicted Draize scores from the correlations were compared to the actual values qualitatively to determine the percentage of surfactants correctly categorized. One of three categories was assigned to each surfactant based on the following scale for Draize scores: mild/moderate (0-25), irritant (>25-50), severe (>50-110)

6.3 Results and Discussion

6.3.1 Draize Score / Leakage Correlations at a Constant Test Concentration

In some of the prior studies, researchers measured the leakage of dyes from liposomes after exposure to surfactants at a given fixed concentration and then attempted to correlate the leakage with the Draize score. In this section, we report results from a similar study in which the bulk concentration of surfactant in the liposome solution was fixed at 1 μg/ml, which was below the

CMC value of all the surfactants tested. It is a common belief that the Draize eye score, if reported from different labs, can have statistically significant differences [103]. To avoid this, we chose three publications with Draize eye scores available for most of the surfactants we utilized in our study (Table 6-1). In Figure 6-1 we plot the Draize scores from different authors versus the percentage dye leakage after 10 minutes at fixed surfactant concentrations. We used two different concentrations from the publication of Kennah et al. to obtain two correlations [131]. The correlation coefficients (Pearson and Spearman) and the coefficient of determination (R^2) for the fits at fixed concentrations are reported in Table 6-2. As expected, the correlation coefficients for all the publications do not show a promising relationship between the Draize test and the liposome study. We also did experiments at two higher concentrations (data not shown) and obtained poor correlations for the fits between the Draize data and the percentage dye leakage from the liposomes after 10 minutes.

6.3.2 Draize Score / Leakage Correlations at Adjusted Concentrations

As shown in the previous section, the liposome assay does not correlate well to the Draize scores for surfactants if the surfactant concentration in the liposome leakage studies is kept fixed. In this section, we report the results for leakage studies from liposomes with the surfactant concentration kept at CMC/200. Specifically, we correlate the Draize data with the percentage dye leakage from liposomes after 10 minutes when the concentration of the surfactant introduced in the solution was adjusted to be CMC/200. Table 6-3 shows the CMC values taken from literature and the concentrations utilized for the test. Figure 6-2 shows the correlations between the reported Draize scores and the percentage dye leakage after 10 minutes. Consequently, the following correlation equations for various sets of Draize scores obtained via different in vivo concentrations and from different groups were produced:

a) Kennah et al. [131], Concentration 1% v/v:
Draize score = 12.57 · Ln (% Leakage) + 3.76 (6-2)

b) Kennah et al. [131], Concentration 10% v/v:
Draize score = 16.19 · Ln (% Leakage) + 34.83 (6-3)

c) Matsukawa et al. [105], Concentration 10% w/v:
Draize score = 18.18 · Ln (% Leakage) + 21.64 (6-4)

d) Tachon et al. [132], Concentration 10% w/v:
Draize score = 13.75 · Ln (% Leakage) + 22.35 (6-5)

Correlation coefficients in Table 6-2 show a significant improvement over the correlations obtained by comparing the dye release at fixed surfactant concentrations. This is true of both the Spearman and Pearson coefficients. The Spearman coefficient is perhaps more significant in this case, despite the common practice of reporting the Pearson value, due to the ordinal nature of the data. Equally important for application purposes is the percent of surfactants categorized correctly, based on the system described in Section 6.2.5. Clearly, the number of surfactants correctly identified into one of three irritancy categories has improved in most cases. These observations are confirmation that the correction factor introduced does indeed provide a clearer understanding of the relationship between Draize scores and the percentage dye leakage from liposomes.

We also evaluated the 95% confidence intervals for the mean values for all the correlations at a fixed concentration of 10% for the Draize scores and the results are shown in Figure 6-3. The three confidence intervals overlap and this suggest that the correlations obtained from different sources with different surfactants may be used simultaneously in this case for Draize score prediction purposes.

6.3.3 Mechanism of Surfactant Toxicity

Surfactants have been shown to cause toxicity by penetrating the epithelial cell membrane, causing irreparable damage to the ocular tissue. Jester et al. suggested that the degree of ocular

irritation caused by surfactants depends on the initial area and depth of injury, suggesting that the area and volume both determine the toxicity levels of surfactants [133]. Tachon et al. pointed out that damaged cells release lysosomal enzymes, histamine, and inflammatory mediators and suggested that the ability to permeate cells was a major sign of toxicity [132]. Okahata and Ebato claimed that eye irritancy is due to the penetration of surfactant molecules into the lipid bilayer as they correlated Draize scores to the partition coefficients of surfactants [108]. Authors did not found a significant correlation between the hydrophilic-lipophilic balance (HLB) and the Draize score and concluded that mere lipophilicity arguments cannot determine the irritancy of a surfactant. Other properties such as electrostatic interactions, steric effects, and charge density significantly contribute to the interaction between the surfactant and the corneal epithelium. The liposomes used in our study have been designed to mimic the lipid composition of the corneal epithelium [113]. Based on this, an increase in the permeability of liposomes in the presence of surfactants should directly correlate with eye irritancy. The mechanism of surfactant toxicity is shown in Figure 6-4. Release of substances from the corneal epithelium is shown to be directly related to monomer surfactant penetrating inside the cells.

Liposome leakage as a toxicity assay to measure surfactant toxicity has been explored in the past with little understanding of the underlying criteria needed to correctly test the potential irritant [108,111-113]. The liposome composition is chosen to mimic the cornea lipid composition, and so the key parameters that need to be chosen for the liposome assay are the lipid loading, liposome size, and the surfactant concentration. Among these, the surfactant concentration is the most important parameter and must be chosen based on mechanistic considerations. Surfactant molecules will form micelles on the ocular surface if introduced at concentrations above their critical micelle concentration (CMC) and these micelles should have

little or no interaction with the epithelial layer due to thermodynamic considerations. Essentially, only the surfactant monomers should directly bind to the lipid bilayers of the corneal epithelium. This point was specifically addressed by Okahata and Ebato, who measured the absorption of surfactants onto a lipid-coated quartz microbalance and showed good correlation with Draize scores [108]. Absorption became saturated for nonionic and cationic surfactants above the CMC, pointing to a lack of micelle interaction with the membrane. Furthermore, this point was supported by the work of Hall-Manning et al., who found skin irritancy to be related to the amount of surfactant monomer on the surface (CMC), rather than the absolute concentration tested [134]. Thus, only the free surfactant, which is present at the CMC, should interact with the corneal epithelium. As the surfactant molecule starts to penetrate the epithelial bilayer, micelles on the ocular surface break and the concentration of free surfactant on the ocular surface is constantly maintained at the CMC until all the surfactant micelles have either drained or have been broken. Thus, if a surfactant is introduced at varying concentrations on the ocular surface, the drainage of surfactant micelles should affect the extent of ocular toxicity. As the concentration of surfactant introduced on the ocular surface increases, the total time for drainage of the surfactant from the ocular surface will also vary, leading to an increase in toxicity. Once the concentration of the surfactant introduced exceeds a critical value where the time of drainage is longer than the time at which the toxicity is assessed, ocular toxicity should saturate. These points are supported by Draize data given by Kennah et al. and Matsukawa et al., which show increases in Draize scores well above the CMC values of surfactants and then subsequent leveling off of those Draize scores [105,131]. Thus, residence time is a key factor to consider when comparing one Draize score to another for varying surfactant concentration. This point is quantitatively addressed in a later section. For this reason, we have used Draize data generated

from the same stock surfactant concentration for each of our correlations, rather than using any Draize data available at any concentration above the surfactant CMC. Draize data also varies widely from study to study, and so we have generated separate correlations for each study, rather than intermingling all of the available data.

The degree of surfactant penetration inside the ocular surface should also be proportional to the surface area available for the surfactant to diffuse in. Similarly, when liposomes are used as an alternative, the amount of surfactant penetrating the lipid bilayer should be directly proportional to the surface area of the liposomes present. This clearly suggests that experiments have to be designed with differences between liposomes and the corneal epithelium taken into consideration. To illustrate the importance of differences between liposome and corneal geometry, it is instructive to consider a mass balance on species such as lysosomal enzymes, histamine, and inflammatory mediators that begin to leak from inside the corneal cells due to the toxic effects of surfactant penetration into the bilayer of the corneal epithelium. The mass balance yields

$$V_{Cornea}\frac{dC_S}{dt} = -K_{Perm}\,A_{Cornea}\,C_S \tag{6-6}$$

where V_{Cornea} is the cellular volume of the corneal epithelium, K_{Perm} is the permeability of the corneal epithelium to the species that leaks out, A_{Cornea} is the corneal area available for penetration, and C_S is the concentration of the species of interest inside the corneal cells. The above equation treats the cornea epithelium as well-mixed, which is perhaps not a precise assumption. However this simpler treatment is sufficient to illustrate the approach for obtaining the surfactant concentration that should be used in the liposome assay. Similarly, a mass balance on a test component such as a dye present inside the liposomes can be given by

$$V_{Liposome}\frac{dC_{Dye}}{dt} = -K_{Perm,Lipo}\,A_{Liposome}\,C_{Dye} \tag{6-7}$$

Where $V_{Liposome}$ is the volume of the liposomes, $K_{Perm,Lipo}$ is the permeability of the liposomes, $A_{Liposome}$ is the liposome surface area available for penetration, and C_{Dye} is the concentration of the species that leaks out. The presence of surfactants is manifested in increased permeabilities for both the cornea and the liposomes. Based on the above equations, the time scale for the leakage of the molecules is $\frac{KA}{V}$. The surface area to volume ratio (A/V) is much larger for liposomes due to their small size. Thus, if the surfactant concentration for the liposome assay is chosen to be the same as that in the Draize test, or even the CMC, the time scale for dye leakage will be extremely small, and so the percentage leakage will be very large unless the measurements are done at extremely short times. Since short-time measurements are prone to artifacts due to issues such as mixing, it is more appropriate to ensure that the time scale for the leakage in the liposomes is comparable to that in the corneal cells. Since the time scale is $\frac{KA}{V}$, the higher values of A/V can be compensated by a lower K for the liposome assay. The permeability K is related to the amount of surfactant that binds to the liposomes, and so the value of K in the liposome assay can be controlled by controlling the surfactant concentration in the assay. Based on these arguments, Equation 6-8 can be used to evaluate the effective concentration that should be tested in the liposome assay to correctly predict the irritancy of surfactants in vivo,

$$C_{TEST} = \frac{A_{Cornea}\,V_{Liposome}}{V_{Cornea}\,A_{Liposome}}\,CMC \tag{6-8}$$

Equation 6-8 implicitly assumes that permeability is linearly related to the surfactant concentration, and also that the appropriate concentration that controls binding in the Draize test

is not the total concentration but the surfactant monomer concentration, which equals the CMC. In Table 6-4, we show the calculated values for the surface area to volume ratios for the corneal epithelium and the liposome system. From these values we can evaluate the test concentration for different surfactant systems based on their CMC's. Since the surface area to volume ratio is a rough calculation and the reported CMC values for surfactants can vary, we rounded the correction factor up to 200. Thus, we divided each CMC value by 200 to obtain the most physiologically relevant test concentration possible for our liposomal system. This surface area to volume ratio correction has not been done in previous reports and is crucial to ensuring that the two systems allow for a correct comparison. Our correction factor of 200 depends heavily on our liposomes having mean diameters of around 110 nm and new correction factors must be computed when working with liposomes of dramatically different sizes [135]. It is also noted that since the value of this ratio was obtained from several qualitative or partially quantitative arguments, there is likely a range of the value of this ratio, perhaps from about 100 to 1000, that could be used in the assay. The central hypothesis is that the test concentrations for the liposome assays for several different surfactants should be chosen such that the ratio of the test concentrations and the respective CMCs are the same for each surfactant, and that this ratio is around 200.

6.3.4 Comparison of Liposome Assay with other in Vitro Assays

Matsukawa et al. [105] used the EYTEX™ test as an in vitro model to predict ocular toxicity. They argued that since protein denaturation is one of the most important factors in determining the extent of ocular irritation, it could be used as an alternative. The overall correlation coefficient between Draize scores and the EYTEX™ test was reported as 0.313, which is very poor when compared to our values (Table 6-2). Also, using their technique had a major limitation of not being able to predict toxicity for cationic surfactants, whereas with the

liposome leakage technique we can accurately predict the irritancy of cationic surfactants. Vian et al. compared three different *in vitro* techniques to determine the ocular toxicity of various surfactants [104]. They utilized neutral red uptake assay, the MTT tetrazolium salt assay, and the total protein content assay for correlating in vivo Draize data and concluded that among the three techniques, neutral red uptake assay was best correlated with the Draize score though even this assay had insufficient correlation. Tachon et al. used cell mortality and inhibition of cell growth as assays to assess surfactant toxicity [132]. They got reasonable agreement with the Draize test score and concluded that penetration of surfactant in the cell lines was responsible for cell damage. Cottin et al. correlated toxicity to cell leakage using a fluorescent dye [109]. They measured the amount of surfactant needed to induce 20% leakage and related it to Draize scores via a non-linear relationship. They found strong correlations between *in vivo* and *in vitro* assays and suggested that this method could be another addition for an *in vitro* alternative to the Draize eye test. Kennah et al. have suggested in the past that there is a need for another *in vivo* alternative to the Draize test due to poor reproducibility and the subjective assessment which differs from one researcher to other [103,131]. They sought to accomplish this by measuring the corneal thickness of rabbit eyes before and after exposure. They found a linear relationship between their test and the Draize score with a reasonable correlation, but failed to comment on why a linear fit should be observed even though the Draize score saturates at a maximum value of 110. A reasonable logarithmic fit can also be obtained from their data and it remains unclear as to why the authors chose a linear relationship. All the relevant correlations, including our work, are compared in Table 6-5. As can be seen from the results, liposome leakage studies have potential to be used as one of the *in vitro* alternatives for early predictions of the irritancy of surfactants and possibly other substances as well.

6.3.5 Prediction of Ocular Toxicity for Non-ionic Surfactants

Surfactants have been actively explored in literature as potential permeability enhancers to increase the permeability of some common ocular drugs [67]. We have also shown previously that surfactants can be used to attenuate drug release from contact lenses and they can potentially diffuse from the lenses to the ocular surface and lead to potential toxicity. This is a first attempt at evaluating the potential ocular toxicity of similar surfactants for which Draize eye scores are currently unavailable. We predicted the ocular irritancy levels of these surfactants by performing similar experiments as before, where the test concentration of surfactant was adjusted according to Equation 6-8. Leakage from liposomes was evaluated as discussed in the previous section and Draize scores were predicted from the correlations (Equations 6-2 to 6-5) obtained by fitting Draize scores from various sources. In Table 6-6, Draize score predictions for six non-ionic surfactants are presented. Since all the predictions were made for a surfactant concentration of 10% (w/v) on the ocular surface, the predicted Draize scores should correspond to the same tested concentration. Similarly, predicted values for ocular irritancy at 1% surfactant loading were obtained by using the correlation from the data of Kennah et al. and is shown in Table 6-7 [131]. As expected, the predicted Draize scores are higher for the higher concentration with Brij 78, Brij 700, Brij 56 and Brij 58 showing negligible toxicity for the 1% concentration correlation.

The mechanism of toxicity should be identical for a particular class of surfactants. For non-ionic surfactants the determining factor in toxicity should be the hydrophobic interaction of the surfactant with the lipid bilayer. Hydrophobic interaction of stearyl and cetyl chains should be stronger than oleyl chains because of the double bond of the oleyl chain, which makes oleyl surfactants more hydrophilic. This would suggest that Brij 78 ($C_{18}H_{37}(OCH_2OCH_2)_{20}OH$), Brij 700 ($C_{18}H_{37}(OCH_2OCH_2)_{100}OH$), Brij 56 ($C_{16}H_{33}(OCH_2OCH_2)10OH$), and Brij 58

($C_{16}H_{33}(OCH_2OCH_2)_{20}OH$) should be more toxic compared to Brij 97 ($C_{18}H_{35}(OCH_2OCH_2)_{10}OH$) and Brij 98 ($C_{18}H_{35}(OCH_2OCH_2)_{20}OH$). On the other hand, the CMC values of Brij 97 and Brij 98 surfactants are much higher than the other surfactants (Table 6-3). Thus, when present at concentrations higher than the CMC, the number of monomers for Brij 98 and Brij 97 surfactants would be much larger than the other surfactants, leading to more toxicity. This explains why we get a higher Draize score for Brij 97 and Brij 98 compared to other surfactants at both 10% and 1% surfactant loading. Since no Draize data is available for these systems, we can at best speculate that the oleyl series of surfactants should be more toxic than the stearyl and cetyl groups of surfactants if administered on the ocular surface above their respective CMC's due solely to the larger number of monomers available for epithelial cell penetration for the oleyl series.

Draize scores for Brij 78 have been reported previously and the authors found that the Draize score at 1% w/v surfactant loading was 2 [67]. This value is in agreement with what we observe (Table 6-7) for this surfactant at similar concentrations. It is noted here that we try to predict the overall Draize score from liposomes mimicking only the corneal epithelium whereas there is a contribution from both the iris and conjunctiva in the overall Draize score, which can result in prediction errors. Our correlations, on the other hand, suggest that reasonable predictions can be derived by correlating the overall Draize data with percentage liposome leakage.

6.3.6 Model for Micelle Depletion from the Ocular Surface

In the previous sections we have proposed that the interaction of surfactants and the epithelial layer occurs at a constant concentration which corresponds to the CMC of the surfactant. The surfactant micelles on the ocular surface have little interaction with the ocular tissues and either break due to surfactant adsorption inside the corneal epithelium and

conjunctiva to maintain the free surfactant concentration at the CMC, or drain from the ocular surface through the nasal route. Researchers have shown that as the concentration of the test material on the ocular surface is increased to concentrations above CMC, the corresponding Draize scores also increase, whereas at really higher concentrations there is a saturation of Draize scores [131]. At first glance, this appears to be a conundrum, in that though the interaction between surfactants and the ocular surface occurs at a maximum concentration corresponding to the surfactant CMC, the toxicity still increases with increasing surfactant concentration. This seems to be a direct effect of the residence time of surfactant micelles on the ocular surface, which should vary with increasing surfactant concentration. This can be explained more clearly by looking closely at the mass balances on the tears and surfactant on the ocular surface. A mass balance on the surfactant on the ocular surface can be given by,

$$\frac{d(VC_{Micelle})}{dt} = -q_{Drainage}(C_{Micelle} + CMC) - k_{Cornea}\,A_{Cornea}\,CMC - k_{Conj}\,A_{Conj}\,CMC \tag{6-9}$$

And the tear balance on the ocular surface can be given by,

$$\frac{dV}{dt} = q_{Secretion} - q_{Drainage} - q_{Conjunctiva} - q_{Evaporation} \tag{6-10}$$

Where

$C_{Micelle}$ = Concentration of micelles on the ocular surface
CMC = Critical micelle concentration
A_{Cornea} = Area of the cornea
A_{Conj} = Area of the conjunctiva
k_{Cornea} = Permeability of the surfactant in the cornea
k_{Conj} = Permeability of surfactant in the conjunctiva
$q_{Secretion}$ = Rate of tear production
$q_{Drainage}$ = Rate of tear drainage
$q_{Conjunctiva}$ = Rate of tear penetration inside the conjunctiva
$q_{Evaporation}$ = Rate of tear evaporation from the ocular surface
V = Volume of tears on the ocular surface

These coupled equations show that the residence time of the surfactant micelles on the ocular surface should be a function of surfactant concentration.

It is instructive to consider an extreme case in which the dominant mechanism for surfactant loss from the tear film is canalicular drainage. This is a likely scenario at surfactant concentrations much above CMC. In this case, the time for the surfactant concentration in the tear film to go from the initial concentration C_i to CMC is equal to $\frac{V}{q_{Drainage}} \ln \frac{C_i}{CMC}$. Thus, a higher initial C_i will lead to a larger duration in which the surfactant concentration in the tear volume is larger than CMC, and the larger time will lead to a larger influx of the surfactant into the cornea, causing higher toxicity. This clearly indicates that the Draize eye score, which should be indicative of the amount of surfactant monomer diffusing inside the cornel epithelium, should increase with increasing surfactant concentrations due to increased residence times.

6.4 Conclusion

Damage to the corneal epithelium can be attributed to the disruption of membrane fluidity due to the penetration of external agents such as surfactants, and the subsequent release of lysosomal enzymes, histamine, and inflammatory mediators. Interactions between surfactants and the corneal surface are governed by their respective CMC's, as micelles are not expected to interact with lipid bilayers. This has been indicated indirectly in the past by researchers who have tried to correlate Draize scores with specific surfactant concentrations resulting in 20% to 50% leakage of fluorescent dyes from liposomes [111,113]. Thus, it has been shown that different surfactants interact differently with the corneal epithelium, and the interaction is dependant on, but not limited to, the concentration of the surfactants on the ocular surface.

We propose that this concentration is the CMC of different surfactants, and that to successfully develop an in vitro alternative to the Draize eye test using liposomes, it is imperative to account for CMC differences. Moreover, liposomes mimicking the corneal epithelium can be successfully utilized to assess the toxicity of various surfactants if a correction

factor is introduced to account for the increased surface area to volume ratio of liposomes compared to the corneal epithelium. Once this factor was introduced, the correlations between dye leakage from liposomes and Draize scores improved significantly. This method can be used to evaluate the initial toxicity of various surfactants, and could thus become a key method to assess ocular toxicity *in vitro*. Accordingly, the correlations between Draize eye scores and liposome leakage produced were used to predict the ocular toxicity of six non-ionic surfactants for which ocular toxicity data was non-existent. We predict that Brij 78, Brij 700, Brij 56, and Brij 58 are mildly/moderately comfortable when placed in the eye at concentrations of 10% (w/v), while Brij 97 and Brij 98 appear to be irritating at similar concentrations. At 1% (w/v), all of the surfactants examined are most likely in the mild/moderate category, causing little to no discomfort.

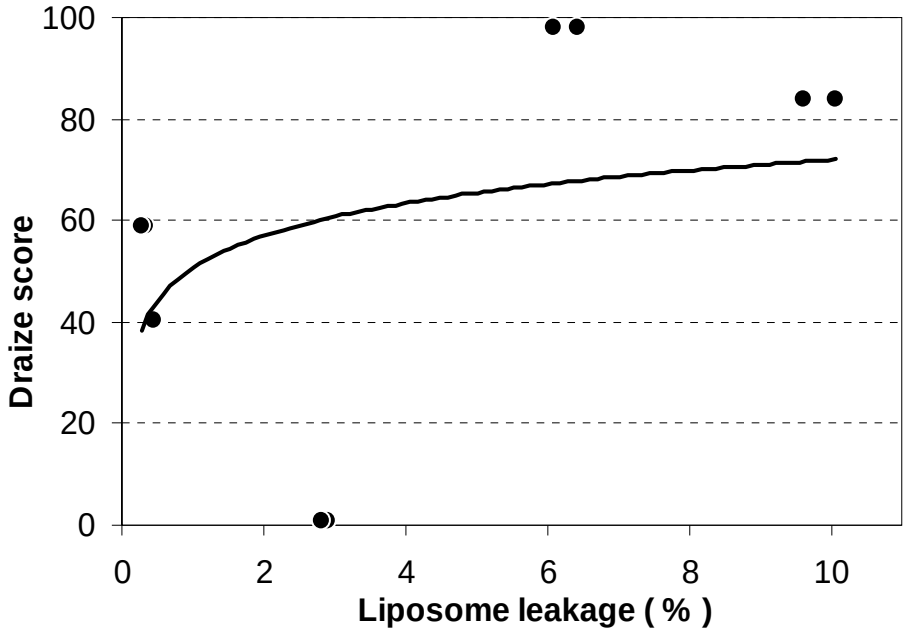

A

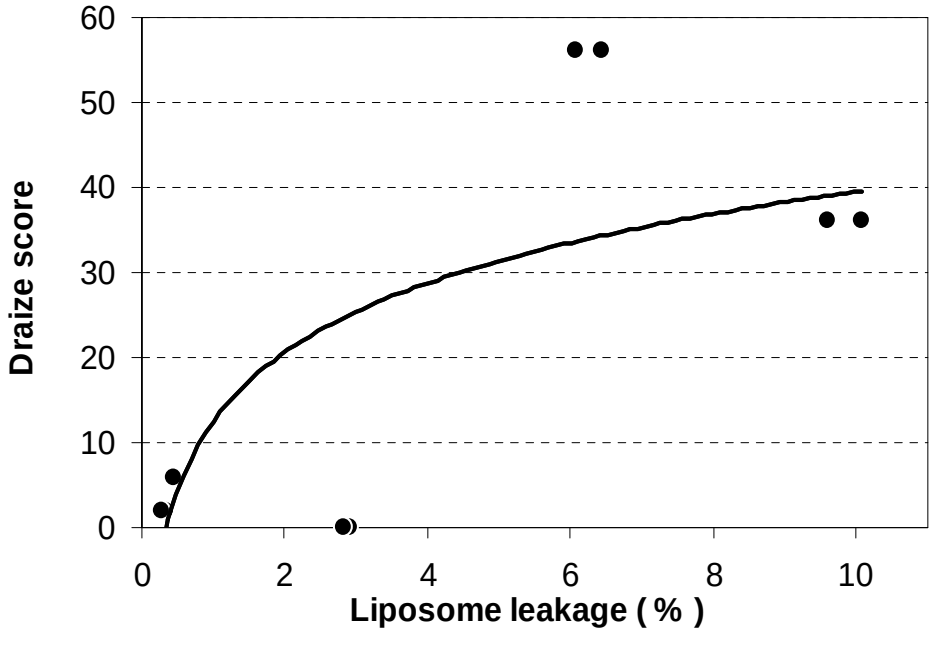

B

Figure 6-1. Draize scores versus liposome leakage after 10 minutes induced by surfactants at concentrations of 1 μg/mL and logarithmic correlations for A) Draize scores from Kennah et al. [131] evaluated at 10% (v/v) with $r_p = 0.38$, $r_s = 0.49$, B) Draize scores from Kennah et al. [131] evaluated at 1% (v/v) with $r_p = 0.74$, $r_s = 0.59$, C) Draize scores from Tachon et al.[132] evaluated at 10% (w/v) with $r_p = 0.26$, $r_s = 0.43$, d) Draize scores from Matsukawa et al.[105] evaluated at 10% (w/v) with $r_p = 0.74$, $r_s = 0.63$.

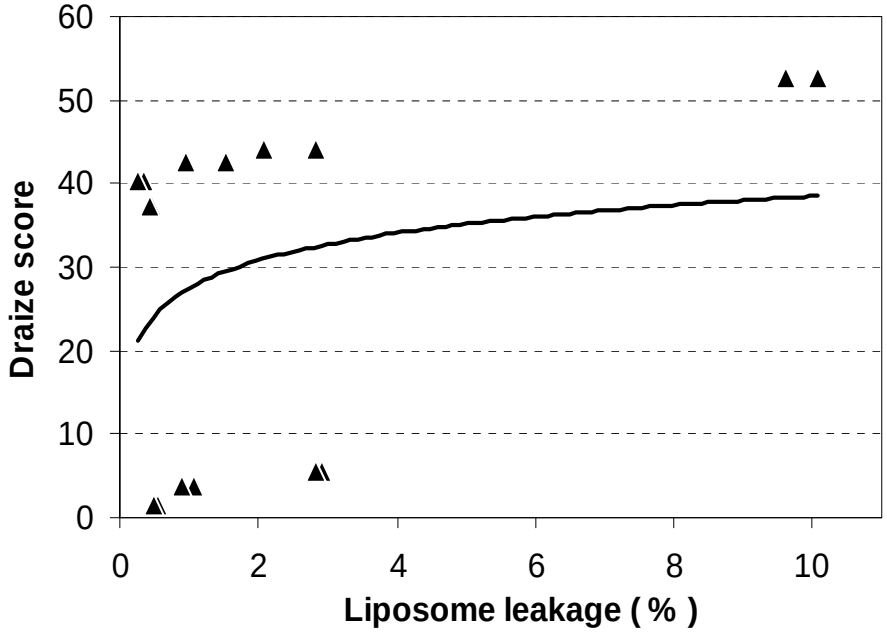

C

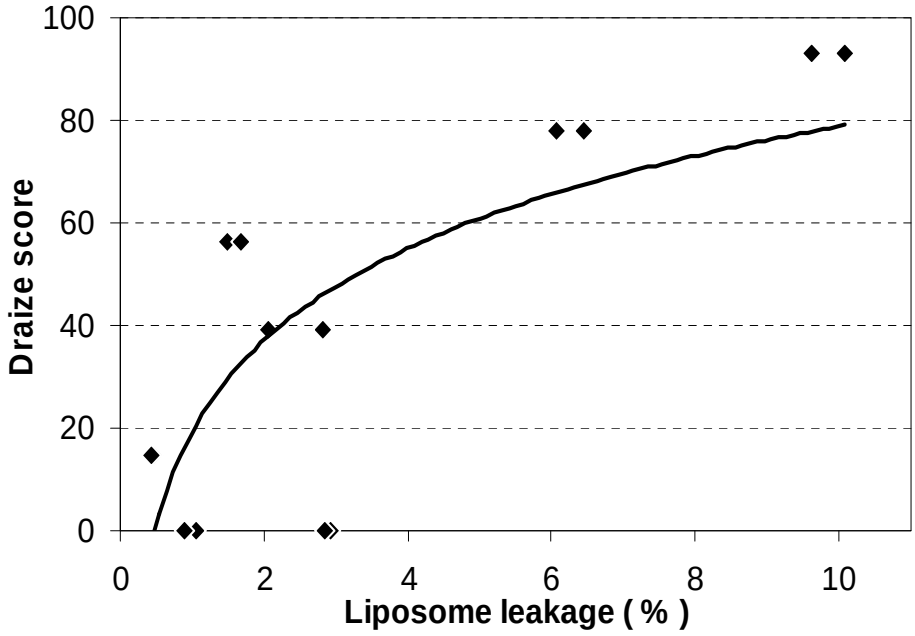

D

Figure 6-1. Continued

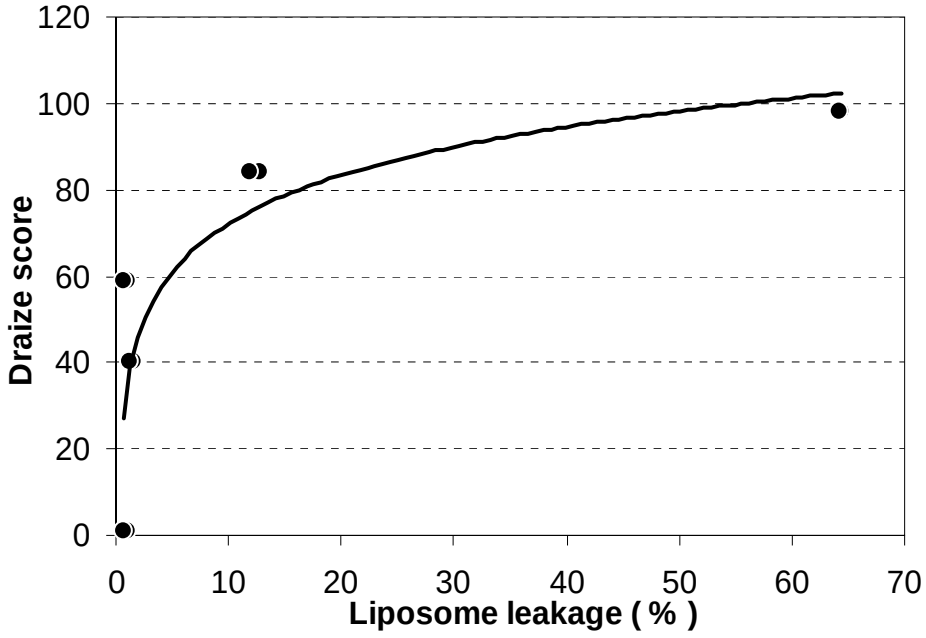

A

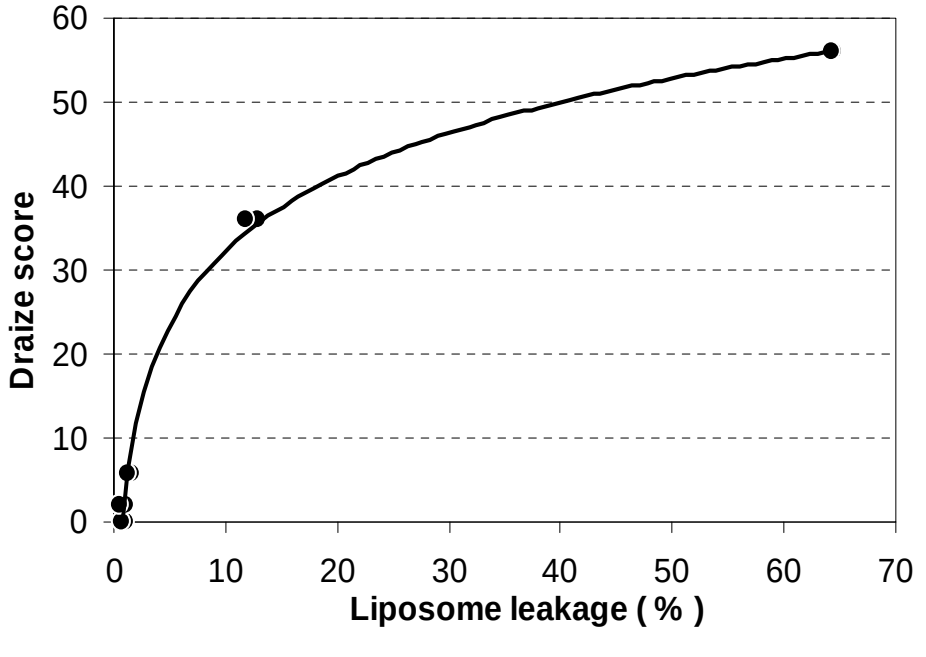

B

Figure 6-2. Draize scores versus liposome leakage after 10 minutes induced by surfactants at CMC/200 and logarithmic correlations for A) Draize scores from Kennah et al. [131] evaluated at 10% (v/v) with r_p = 0.82, r_s = 0.79, B) Draize scores from Kennah et al.[131] evaluated at 1% (v/v) with r_p = 0.99, r_s = 0.94, C) Draize scores from Tachon et al. [132] evaluated at 10% (w/v) with rp = 0.74, rs = 0.85, D) Draize scores from Matsukawa et al.[105] evaluated at 10% (w/v) with r_p = 0.78, r_s = 0.79.

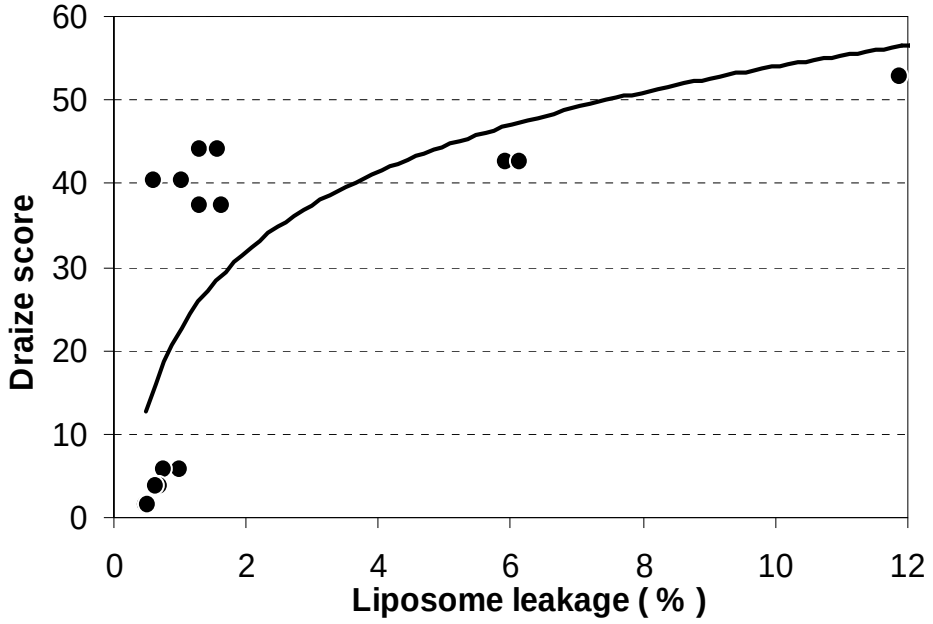

C

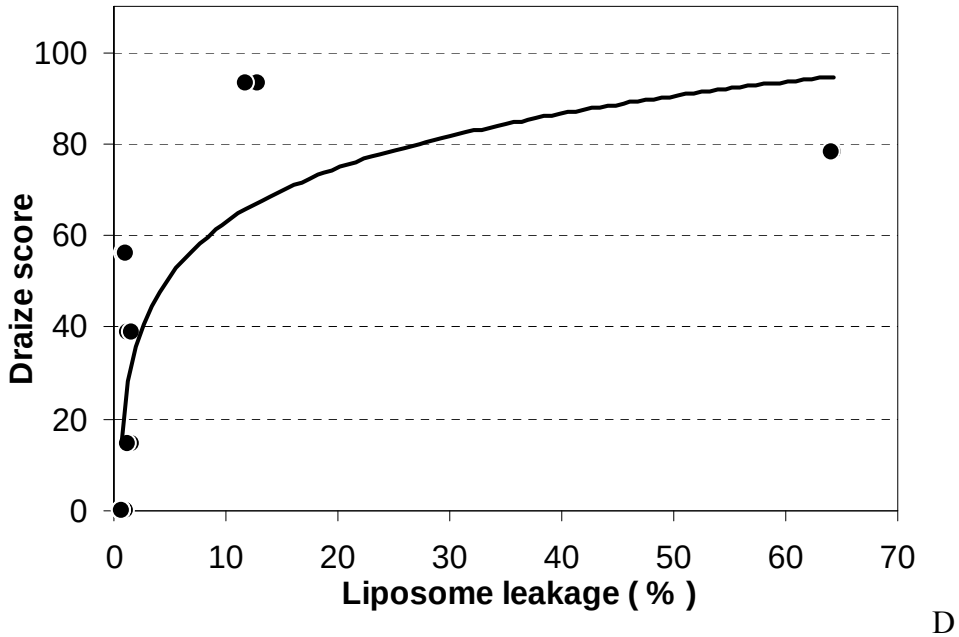

D

Figure 6-2. Continued

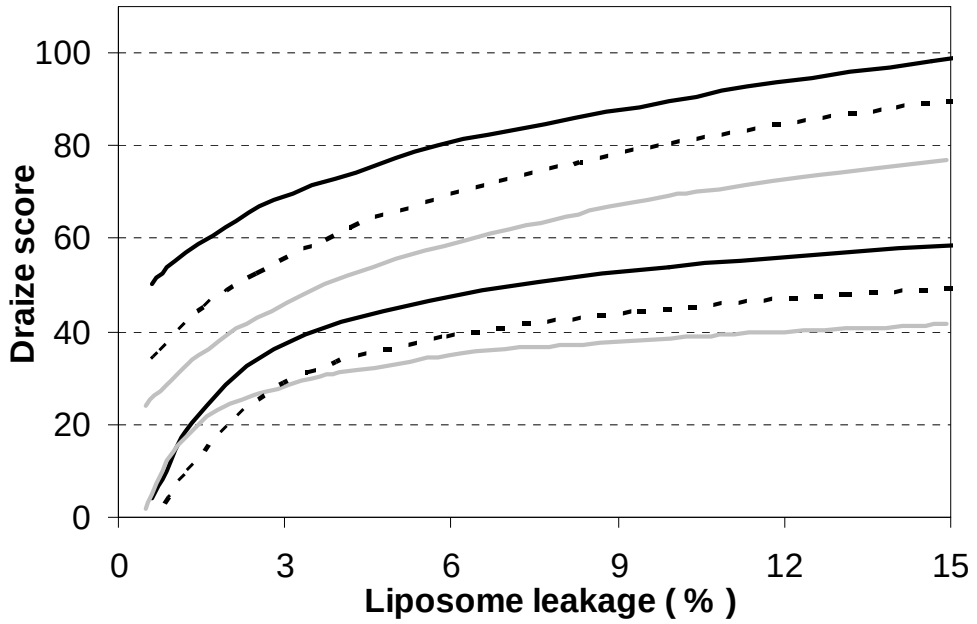

Figure 6-3. The 95% confidence intervals for mean Draize scores at 10% ocular loading for surfactants based on logarithmic corrleations from percent dye leakage from liposomes after ten minutes at surfactant CMC/200. Kennah et al. [131] (——); Tachon et al. [132] (——); Matsukawa et al. [105] (- - - -).

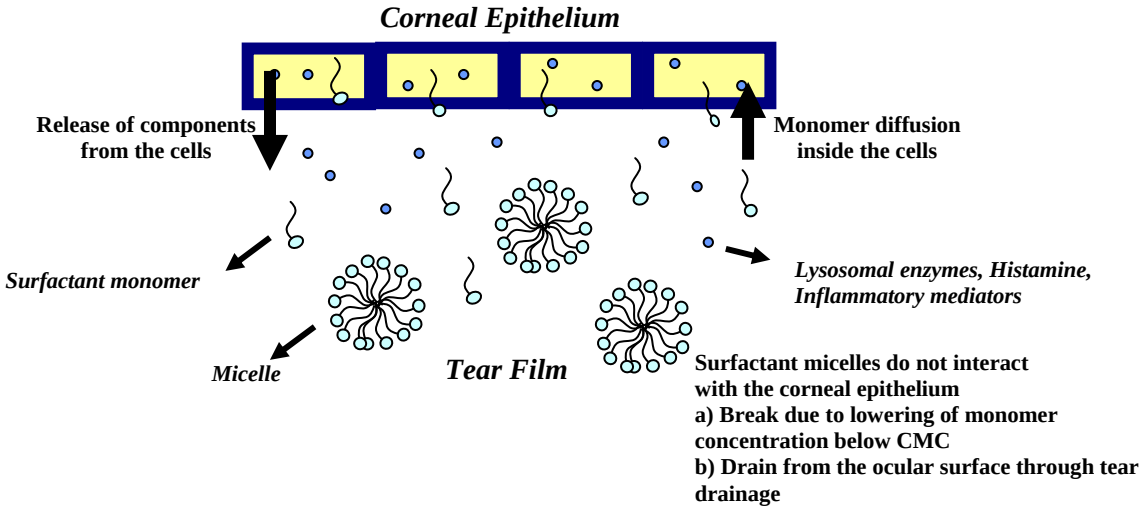

Figure 6-4. Surfactant induced toxicity on the corneal surface

Table 6-1. Draize scores used for in vitro/in vivo correlations

Surfactant	Tachon et al. Draize Scores (10%) [132]	Matsukawa et al. Draize Scores (10%) [105]	Kennah et al. Draize Scores (10%) [131]	Kennah et al. Draize Scores (1%) [131]
SDS	37.34	14.70	40.33 [b]	5.83 [b]
Tween 20	5.67	0.01 [a]	1.00	0.01
Tween 80	3.83	0.01	-	-
Triton X 100	40.33	-	59.00	2.00
CPC [c]	52.67	93.00	84.00	36.00
Tween 40	1.50	-	-	-
MTAB	42.66	-	-	-
CTAB	44.00	39.00	-	-
BKC	-	78.00	98.00	56.00
OCTAB	-	56.30	-	-

[a]Values of 0.01 were used in place of 0 for nonlinear correlation purposes. [b]Interpolated from a linear relationship for concentrations of 0, 3, and 15%. [c]Cetyl pyridinium bromide was tested in Kennah et al. [131] and Tachon et al. [132] and assumed to behave similarly to cetyl pyridinium chloride which was tested here.

Table 6-2. Correlation comparisons for Draize scores and leakage experiments performed at surfactant concentrations of 1 μg/mL and CMC/200

Source	Pearson	Spearman	R^2	Percent Categorized Correctly
Kennah et al. [a] (10% - 1 μg/mL) [131]	0.38	0.49	0.14	50.0
Kennah et al. [b] (10% - CMC/200) [131]	0.82	0.79	0.68	60.0
Kennah et al. [c] (1% - 1 μg/mL) [131]	0.74	0.59	0.54	100.0
Kennah et al. [d] (1% - CMC/200) [131]	0.99	0.94	0.99	100.0
Matsukawa et al. [a] (10% - 1 μg/mL) [105]	0.74	0.63	0.55	71.4
Matsukawa et al. [b] (10% - CMC/200) [105]	0.78	0.79	0.61	71.4
Tachon et al. [a] (10% - 1 μg/mL) [132]	0.26	0.43	0.07	62.5
Tachon et al. [b] (10% - CMC/200) [132]	0.74	0.85	0.55	87.5

[a]Draize scores were evaluated at stock surfactant concentrations of 10%, while leakage experiments were evaluated at a final concentration of 1 μg/mL. [b]Draize scores were evaluated at stock surfactant concentrations of 10%, while leakage experiments were evaluated at a final concentration of CMC/200. [c]Draize scores were evaluated at stock surfactant concentrations of 1%, while leakage experiments were evaluated at a final concentration of 1 μg/mL. [d]Draize scores were evaluated at stock surfactant concentrations of 1%, while leakage experiments were evaluated at a final concentration of CMC/200.

Table 6-3. Critical micelle concentrations for surfactants studied and subsequent test concentrations for liposome leakage

Surfactant	MW	CMC (mM)	CMC (μg/mL)	Test Concentration - CMC/200 (μg/mL)	Source
Triton X-100	647.0	0.200	129.40	0.647	Roche Applied Science
SDS	288.4	8.200	2364.72	11.824	Rosen [136]
Tween 20	1226.0	0.050	61.30	0.307	Hait and Moulik [120]
Tween 40	1283.6	0.023	29.52	0.148	Hait and Moulik [120]
Tween 80	1309.7	0.010	13.10	0.065	Hait and Moulik [120]
BKC	340.0	8.800	2992.00	14.960	Rosen [136]
OTAB	391.9	0.310	121.49	0.607	Rosen [136]
CTAB	364.5	0.980	357.19	1.786	Rosen [136]
MTAB	308.0	3.600	1108.80	5.544	Rosen [136]
CPC	340.0	0.900	305.99	1.530	Rosen [136]
Brij 58	1120.0	0.007	7.84	0.039	Hait and Moulik [120]
Brij 56	682.0	0.002	1.36	0.007	Hait and Moulik [120]
Brij 97	709.0	0.400	283.60	1.418	Hait and Moulik [120]
Brij 98	1153.5	0.265	305.69	1.528	Hait and Moulik [120]
Brij 78	1151.5	0.006	6.56	0.033	Hait and Moulik [120]
Brij 700	4670.0	0.020	93.40	0.467	Hait and Moulik [120]

Table 6-4. Surface area to volume ratio comparisons for liposomes and epithelial cells

	Liposome (SA / V) Ratio (m^2/L)	Epithileal Cell (SA / V) Ratio (m^2/L)
	54545 [a]	314 [d]
	66439 [b]	375 [e]
	68412 [c]	-
Mean (SA / V) ratios	63132	345
Ratio of (SA / V)	**183**	

[a]Calculated from the average surface area, 62 $Å^2$, occupied by a single lipid [130,137,138] and the entrapped volume [139] based on a liposome radius of 55 nm.[135]. [b]Calculated based on a unilamellar bilayer thickness of 35 Å and a liposome radius of 55 nm [135,138]. [c]Calculated based on a unilamellar bilayer thickness of 40 Å and a liposome radius of 55 nm [140]. [d]Taken from Maric et al. for epithelial cells [141]. [e]Taken from Farinas and Verkman for epithelial cells [142].

Table 6-5. Correlation comparisons between the liposome leakage method of assessing toxicity and other published methods

Source	Study	Pearson	Spearman	% Correct
Matsukawa et al. [105]	EYETEX™	0.20 - 0.40	N / A	61 - 70
Vian et al. [104]	Cell Studies	0.48 - 0.62	0.53 - 0.64	75
Kennah et al. [131]	Corneal Thickness	0.86	N / A	76
Tachon et al. [132]	Cell Growth Inhibition	N / A	0.65 - 0.85	N / A
Cottin and Zanvit [109]	Cell Leakage	0.94	0.92	93
Current Study	Liposome Leakage	0.74 - 0.99	0.79 - 0.94	60 - 100 [a]

[a]Based on the three class system described in section 6.2.5.

Table 6-6. Predicted Draize scores for 10% stock solutions of selected Brij surfactants

Surfactant	Kennah et al. (10%) [a] [131]	Matsukawa et al. (10%) [a] [105]	Tachon et al. (10%) [a] [132]	Average	Standard Deviation	Irritation Class [b]
Brij 97	45.1	34.5	31.1	36.9	7.3	Irritant
Brij 98	42.9	32.1	29.2	34.7	7.2	Irritant
Brij 78	29.8	18.3	18.1	22.1	6.7	Mild / Moderate
Brij 700	32.2	20.9	20.1	24.4	6.8	Mild / Moderate
Brij 56	29.3	17.8	17.6	21.6	6.7	Mild / Moderate
Brij 58	34.3	23.1	21.9	26.4	6.8	Mild / Moderate

[a]Draize scores were evaluated at surfactant concentrations of 10%, while liposome leakage was evaluated at CMC/200 for each surfactant. [b]Based on the scale presented in section 6.2.5.

Table 6-7. Predicted Draize scores for 1% stock solutions of selected Brij surfactants

Surfactant	Kennah et al.(1%) [a] [131]	Irritation Class [b]
Brij 97	11.0	Mild / Moderate
Brij 98	9.2	Mild / Moderate
Brij 78	0.0 [c,d]	Mild / Moderate
Brij 700	0.8	Mild / Moderate
Brij 56	0.0 [c]	Mild / Moderate
Brij 58	2.5	Mild / Moderate

[a]Draize scores were evaluated at surfactant concentrations of 1%, while liposome leakage was evaluated at CMC/200 for each surfactant. [b]Based on the scale presented in section 2.5. [c]In cases where predictions were slightly negative, the Draize score was taken to be zero. [d]Compares well with the work of Saettone et al., who reported a score of 2 for Brij 78 at a concentration of 1% [67]. They also showed an increase at 2%, which supports our finding of a higher score at 10% (Table 6-6).

CHAPTER 7
ASSESING CRITICAL AGGREGATION CONCENTRATION FOR SURFACTANTS IN HYDROGELS

7.1 Introduction

It is important to determine the CAC values for surfactants in hydrogels to design and tune drug release. In this chapter we discuss two methods of determining the critical aggregation concentration (CAC) inside p-HEMA matrix for the surfactants used in this work. In chapter 5 we determined the CAC of Brij 700 and here we obtain the CAC values for Brij 97, Brij 98 and Brij 78. The first method for determining CAC relies on the fact that the formation of the surfactant aggregates leads to a slowdown of drug transport due to drug partitioning into the surfactant aggregates. Thus gels with fixed drug loading and different surfactant loadings were prepared and drug diffusion from these gels was measured. The second method relies on the fact that the water content of the gels increase with increasing surfactant amount. However the rate of increase will likely be discontinuous at the critical aggregation concentration signaling a first order phase transition. Thus gels with varying surfactant loading were prepared, and their water content was measured.

7.2 Materials and Methods

7.2.1 Materials

2-Hydroxyethyl methacrylate (HEMA) monomer, ethylene glycol dimethacrylate (EGDMA), Dulbecco's phosphate buffered saline (PBS), acetonitrile, polyoxyethylene(20) stearyl ether (Brij 78), polyoxyethylene(10) oleyl ether (Brij 97), polyoxyethylene(20) oleyl ether (Brij 98) and HPLC grade water were purchased from Sigma-Aldrich Chemicals (St Louis, MO). 2,4,6-trimethylbenzoyl-diphenyl-phophineoxide (TPO) was kindly provided by Ciba (Tarrytown, NY). CyA was purchased from LC Laboratories (Woburg, MA). All the chemicals

were reagent grade. Acetonitrile was filtered before use and all the other chemicals were used without further purification.

7.2.2 Synthesis of Surfactant and Drug Laden Gels

The surfactant laden gels were prepared by polymerizing the monomer solution containing surfactant and drug mixed in specific ratio. Briefly, specific amounts of surfactants were dissolved in DI water to make surfactant solutions of compositions such that the surfactant loadings in the dry gel ranged from 0.05% to 8%. Separately, 3.5 mg of drug was dissolved in 2.7 ml of HEMA monomer and stirred at 600 rpm for a period of 5 hours. Next 15 μl of the crosslinker and 2ml of surfactant solution were added to 2.7 ml of drug loaded monomer. The solution was degassed by bubbling nitrogen gas through it for 10 minutes followed by addition of 6 mg of UV initiator (TPO) and stirring for 10 minutes. The solution was then poured between two glass plates separated by a spacer and the gel was cured by irradiating UVB light (305 nm) for 40 min from an Ultraviolet transilluminiator UVB-10 (Ultra Lum, Inc.). Control drug loaded p-HEMA gels without surfactants were prepared by following procedures identical to those described above except that the 2 ml surfactant solution was replaced by 2 ml DI water. Control gels without any drug were synthesized in a similar manner as described above except that the drug was not mixed in the monomer solution before polymerization. After polymerization, each gel was removed from the glass mold, and was cut into smaller square pieces that were dried at room temperature for two days before being used for any experiments.

7.2.3 Drug Detection: HPLC Assay

CyA concentration was measured using a HPLC (Waters, Alliance System) equipped with a C_{18} reverse phase column and a UV detector. The mobile phase composition was 70% acetonitrile and 30% DI water, and the column was maintained at 60°C. The flow rate was fixed at 1.2 ml/min and the detection wavelength was set at 210 nm. The retention time for CyA under

these conditions was 4.55 minutes, and the calibration curve for area under the peak vs. concentration was linear ($R^2 = 0.995$).

7.2.4 Drug Release

Square gel pieces about 1.5X1.5 cm in size and 40 mg in weight were utilized for drug release experiments. Drug release kinetics was measured by soaking the gel in 3.5 ml PBS buffer, which was replaced every 24 hours and all the measurements were done at room temperature. These experiments were conducted till 60% of the drug diffused from the gel matrix.

7.2.5 Equilibrium Water Content

The gels of known weight with varying surfactant loading but no drug were soaked in 3.5 ml of PBS, and the dynamic weight was measured as a function of time. The excess water from the gel surface was removed before each measurement by dabbing with Kimwipes (Fischer Scientific). The equilibrium water content (EWC) of the surfactant laden gels was calculated by determining amount of water uptake per dry gel weight, i.e,

$$\%EWC = \frac{W_{WET} - W_{DRY}}{W_{DRY}} \times 100 \tag{7-1}$$

For PBS uptake experiments, surfactants laden gels without the drug were utilized.

7.3 Results and Discussion

7.3.1 Method I: Drug Release

We have earlier developed a model for drug transport from surfactant laden hydrogels (Chapter 4, Section 4.3.3.1). Here we propose a new method to determine CAC for various surfactants by performing drug release from the surfactant laden hydrogels by varying surfactant concentration and using the model. To understand this method, we first need to clearly decipher the role of surfactant in drug release from hydrogels. When surfactants are introduced inside the

gel matrix containing a drug, their interaction with the drug solute depends strongly on surfactant concentration. Below their respective CAC, surfactants have only minor interactions with the drug solute but as the concentration of the surfactant is increased beyond the CAC, surfactant starts aggregating, and the hydrophobic interaction between the drug and the hydrophobic interior of the surfactant aggregates becomes pronounced. Hydrophobic drug molecules such as CyA partition inside the hydrophobic interior of the surfactant aggregates, and this leads to a slowdown in the drug release from the hydrogel. This phenomenon can be utilized to determine the CAC for various surfactants, especially if the presence of surfactants can significantly slow down the drug release above their CAC. Firstly, we conducted drug release from gels containing varying amount of surfactant loading. The rate of release scales as $t^{1/2}$, and so we determined the slope ($Slope_{EXP}$) of the linear fit between % Drug Release and $\sqrt{\frac{t}{(2h)^2}}$ where 't' is time in hours and 'h' is half-thickness of the gel. This slope is relatively unaffected by surfactant addition till the surfactants begin to form aggregates, and thus the surfactant concentration at which the slope begins to decrease equals the critical aggregation concentration. A better and more quantitative value of the CAC can be determined by utilizing the model for drug release from surfactant-laden gels proposed earlier and briefly described below.

Drug release from the surfactant laden hydrogels was discussed in chapter 4 and the following concentration profiles were determined for solute diffusion from surfactant laden hydrogels.

$$C_I^{'} = B\int_0^{\eta} e^{-\frac{D_s}{D}\xi^2}\, d\xi \tag{7-2}$$

$$C_{II}^{'} = 1 - \left(\frac{1 - B\int_{0}^{\alpha} e^{-\frac{D_s}{D}\xi^2} d\xi}{\int_{\alpha}^{\infty} e^{-\frac{D_s}{D}(1+KC_p)\xi^2} d\xi} \right) \int_{\eta}^{\infty} e^{-\frac{D_s}{D}(1+KC_p)\xi^2} d\xi \tag{7-3}$$

In Equation 7-2 and 7-3, D is the diffusivity of the drug (1.44×10^{-14} m^2/s), D_S is the diffusivity of the surfactant, C_p is the concentration of surfactant present as aggregates inside the hydrogel defined as C_i-C* (C_i = Initial surfactant concentration inside the hydrogel, C* = CAC) and K is a constant related to the partition coefficient of the drug when partition coefficient is defined as the ratio of drug concentration inside the micelles and drug concentration inside the gel matrix. Equation 7-2 is the solution for drug diffusion from region inside the gel matrix which does not contain any surfactant aggregates whereas Equation 7-3 is the concentration profile of the drug in region II, i.e., the region with surfactant aggregates (See Figure 4-3). α is given by the solution to following equation,

$$2\alpha \frac{C_p}{C^*} = \frac{e^{-\alpha^2}}{\int_{0}^{\alpha} e^{-\xi^2} d\xi} \tag{7-4}$$

In Equation 7-2 and 7-3, η is defined as $y/\sqrt{4D_St}$ and the thickness of region I by $\alpha\sqrt{4D_St}$ (=δ). The unknown B in the above equations can be determined by using the following flux balance at y = δ (or η = α),

$$\frac{dC_I^{'}}{d\eta} = \frac{dC_{II}^{'}}{d\eta} + \frac{2KC_pC_{II}^{'}D_s\alpha}{D} \tag{7-5}$$

Utilizing Equation 7-2, 7-3 and 7-5 we can evaluate the constant B as,

$$B = \frac{1}{\lambda}\left(\frac{e^{-\frac{D_D}{D}(1+KC_p)\alpha^2}}{\sqrt{\frac{D\pi}{4D_S(1+KC_p)}} - \int_0^{\alpha} e^{-\frac{D_D}{D}(1+KC_p)\xi^2} d\xi} \right) \tag{7-6}$$

Where,

$$\lambda = \left[e^{-\frac{D_D}{D}\alpha^2} + \frac{e^{-\frac{D_D}{D}(1+KC_p)\alpha^2} \int_0^{\alpha} e^{-\frac{D_D}{D}\xi^2} d\xi}{\sqrt{\frac{D\pi}{4D_S(1+KC_p)}} - \int_0^{\alpha} e^{-\frac{D_D}{D}(1+KC_p)\xi^2} d\xi} - \frac{2KC_p D_S \alpha \int_0^{\alpha} e^{-\frac{D_D}{D}\xi^2} d\xi}{D} \right] \tag{7-7}$$

The percentage release of drug from the gel can be determined by calculating the flux from the gel and integrating it over time (See Section 4.3.3.1) to give the following relation,

$$R(\%) = \frac{2DB}{(1+KC_p)\sqrt{D_S}} \sqrt{\frac{t}{(2h)^2}} \times 100 \tag{7-8}$$

And slope for a plot of % Drug Release vs. $\sqrt{\frac{t}{(2h)^2}}$ should be,

$$Slope_{TH} = \frac{2DB}{(1+KC_p)\sqrt{D_S}} \times 100 \tag{7-9}$$

For a given value of CAC, we can determine the theoretical slope for any value of initial surfactant loading, since all the other parameters in Equation 7-9 are known, and are listed in Table 7-1. The value of CAC can thus be determined by minimizing the differences between the measured and the theoretical slopes. This was accomplished by minimizing the Error between the model and the experiments defined as,

$$Error = \sum_{C_i} \left(\frac{Slope_{TH} - Slope_{EXP}}{Slope_{TH}} \right)^2 \tag{7-10}$$

In Figure 7-1A-C we plot the Error vs. CAC for the three surfactants and the minimum value for error in each graph corresponds to the CAC for different surfactant systems. The values of CAC for various surfactant systems are listed in Table 7-2. For the CAC corresponding to the minimum error, we also plot the theoretical and experimentally determined slopes for various initial surfactant loadings in Figure 7-2A-C where the x-axis represents$1/C_i$ where C_i is in mM. As can be seen from the plots, there is a good agreement between the theoretical and experimentally determined slopes for all the surfactant systems.

7.3.2 Method II: Water Uptake

It was observed earlier that presence of surfactants inside the hydrogel can significantly alter the microstructure of the gel (Chapter 5, Section 5.3.7). It was also shown that this change in microstructure can alter the water uptake properties of the gels. This change in water uptake properties of the hydrogels could be used to determine the CAC for these surfactants. This method assumes a direct correlation between the equilibrium water uptake (EWC) of hydrogels with the surfactant loading. We believe that as the concentration of the surfactant is increased beyond the CAC of the hydrogel, there is a significant alteration of the microstructure of the hydrogel, which should result in changes in the rate of increase in water content with increase in surfactant concentration. Figure 7-3A-C shows the water uptake by gels at varying surfactant loadings for the three surfactant of interest. As can be seen in all the systems, the water content increases with surfactant loading but there is a sudden change in the slope of EWC increase with increasing surfactant loading at critical surfactant loading, which likely corresponds to aggregation of surfactants into aggregates. The increase in water content is linear in both regimes (surfactant loading less or greater than CAC). Accordingly, the EWC vs. surfactant loading data (C_i) was fitted to two straight line relationships with discontinuous slope at the CAC. The CAC values calculated from these systems are listed in Table 7-2 for comparison with

the CAC determined from the previous method, and we see that both the methods lead to similar values except for Brij 98 surfactant system.

7.3.3 Surfactant Diffusivity

We had earlier fitted the surfactant release data to a model to determine the product $D_S C^*$ for all surfactants of interest. Now that we have also determined C^*, which is the critical aggregation concentration, we can determine the surfactant diffusivities. The values of $D_S C^*$ are listed in Table 7-1 and the diffusivities obtained by using the C* (=CAC) determined above are reported in Table 7-2. It is observed that the diffusivities of the surfactant are not a strong function of their molecular weight as the diffusivity for Brij 97 is smaller than that for Brij 98. This clearly shows that surfactant diffusivity, unlike solute diffusivity from theses hydrogels depends strongly on the surfactant-polymer interactions.

7.4 Conclusion

Drug release from hydrogels can be controlled only when surfactant concentration is above the CAC inside the hydrogel and hence it is important to know the value of CAC for various surfactant-polymer systems. Two methods for determining the CAC for Brij series surfactants are suggested in this chapter. Both the methods are based on the hypothesis that there is a significant change in gel properties as the surfactant concentration is increased beyond the CAC. Both methods yield relatively similar CAC values.

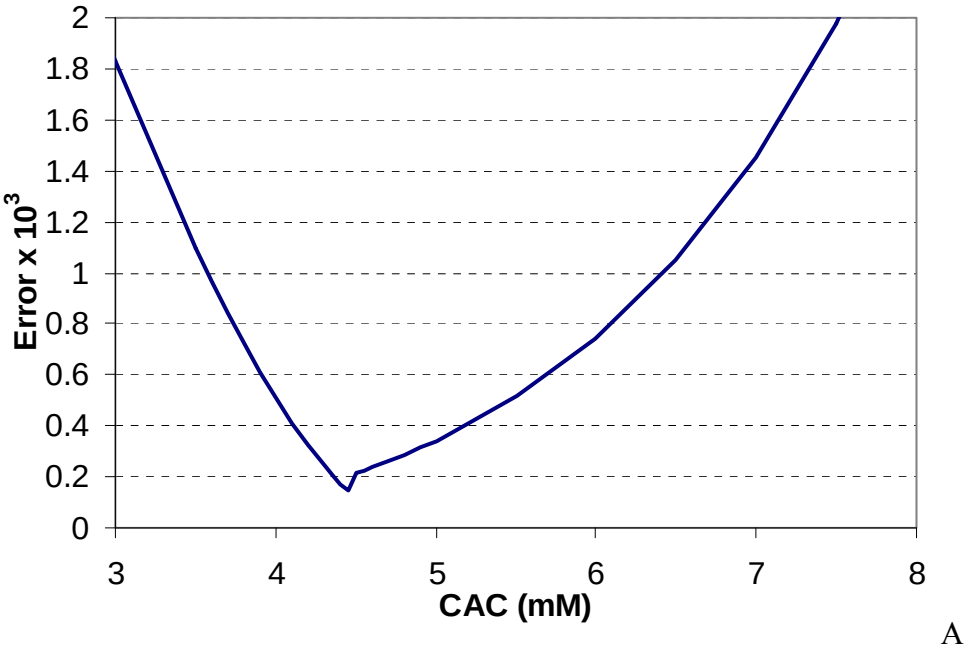

A

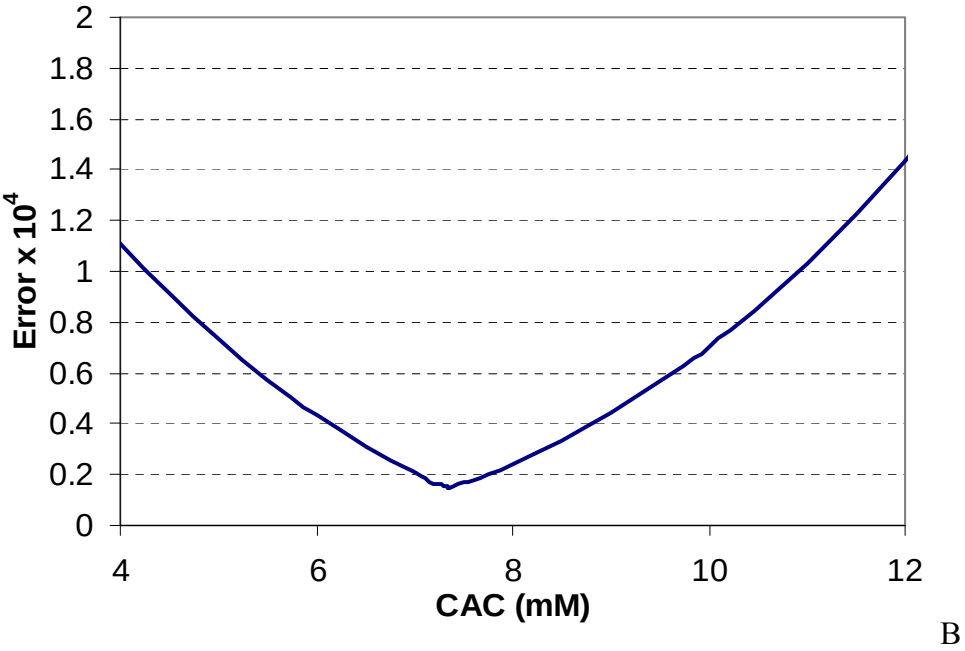

B

Figure 7-1. Error between theoretical and experimentally determined slope for drug release experiments from hydrogels containing varying surfactant loading against CAC. A) Brij 78 System B) Brij 97 system C) Brij 98 system

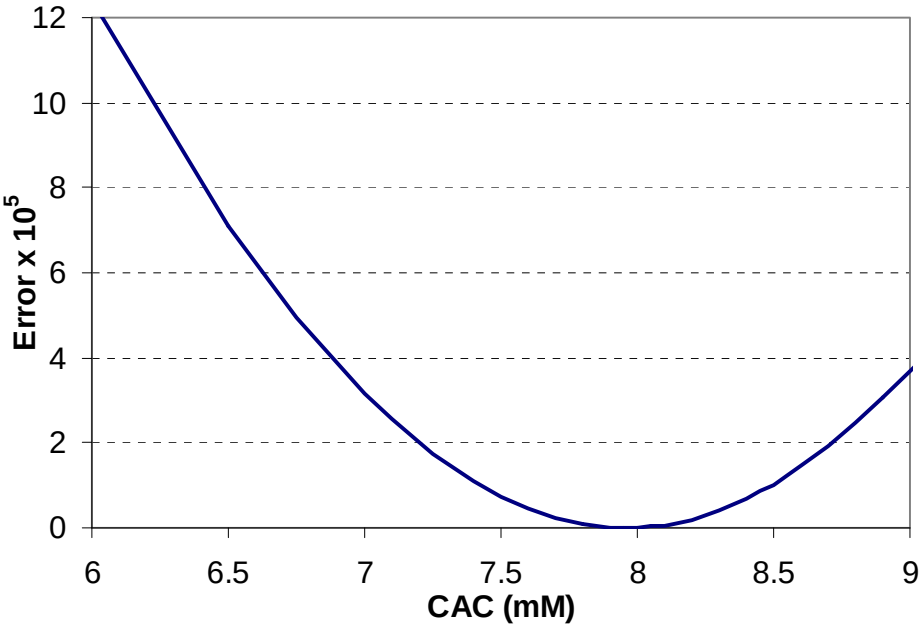

Figure 7-1. Continued

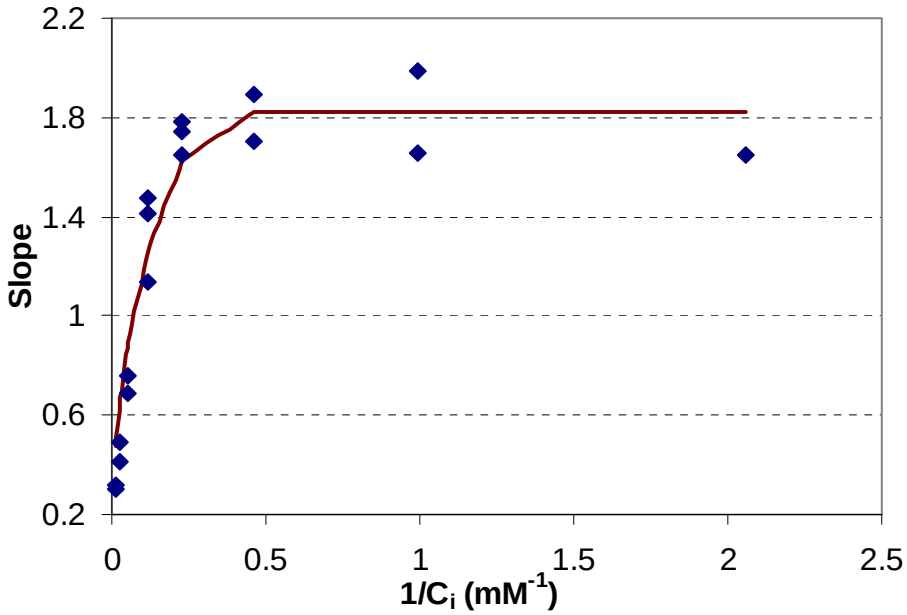

A

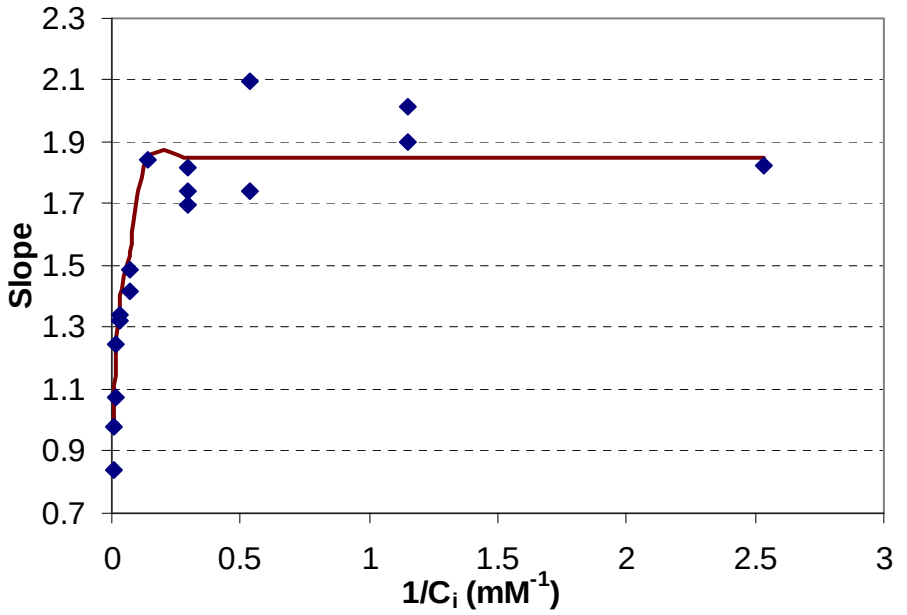

B

Figure 7-2. Plot of slope vs inverse of initial surfactant loading inside the hydrogels. Solid line is the theoretically determined slope from the model determined at the CAC with minimum error in fitting. A) Brij 78 system B) Brij 97 system C) Brij 98 system

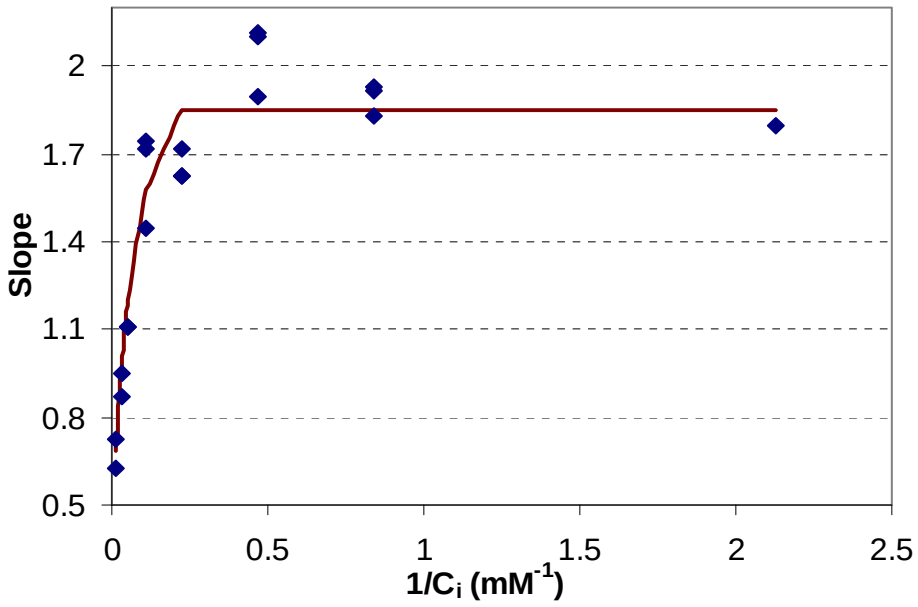

C

Figure 7-2. Continued

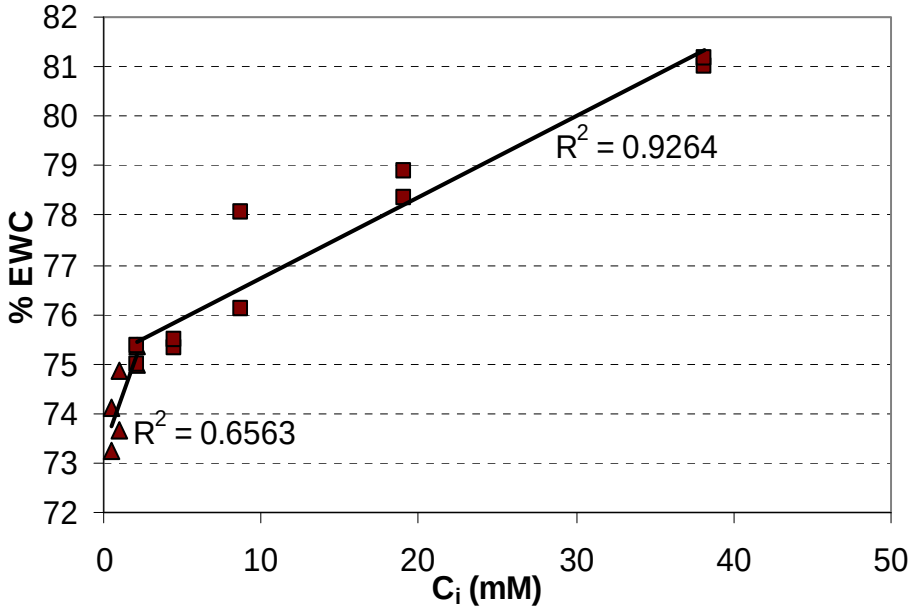

A

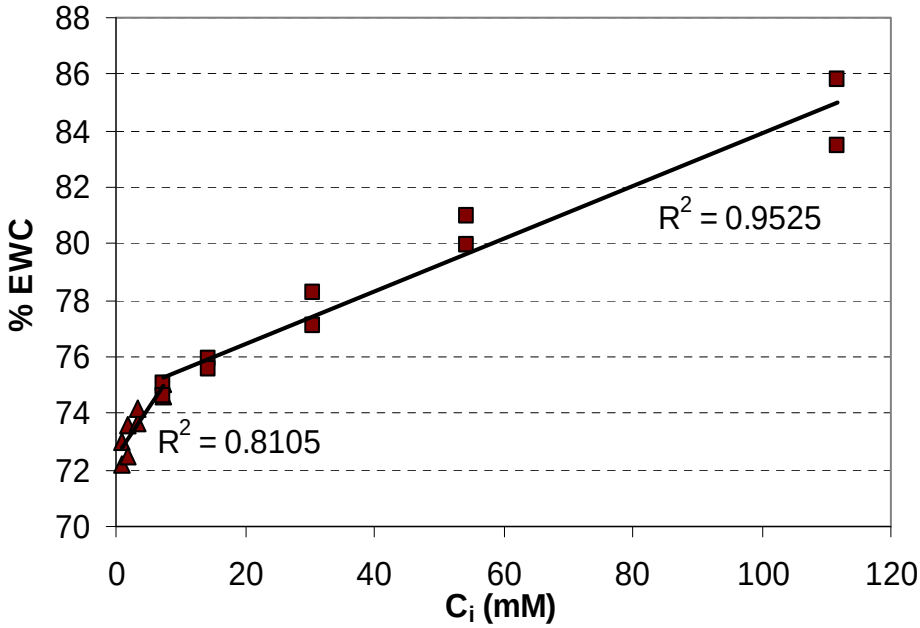

B

Figure 7-3. Equilibrium water content of surfactant laden hydrogels with varying initial surfactant loading inside the p-HEMA matrix. Change in slope in the plot should correspond to the CAC for different surfactant systems. A) Brij 78 system B) Brij 97 system C) Brij 98 system

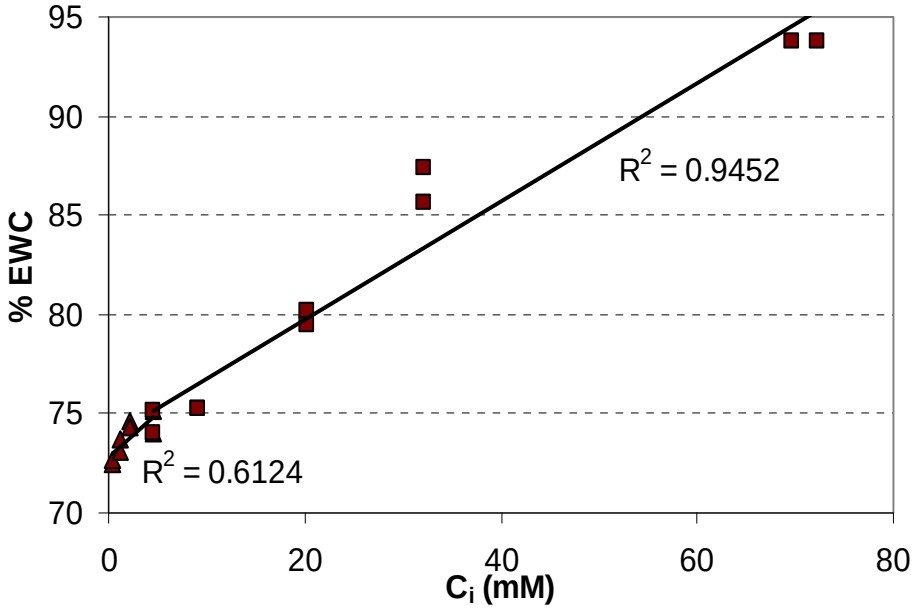

C

Figure 7-3. Continued

Table 7-1. Physical properties of the surfactant utilized in solving the drug release model

System	K (M^{-1})	D_SxCAC (m^2mM/s)	MW
Brij 97	16.3	$11.52x10^{-15}$	709.0
Brij 98	93.0	$60.80x10^{-15}$	1149.5
Brij 78	163.8	$1.70x10^{-15}$	1151.5

Table 7-2. Critical aggregation concentration for each surfactant system evaluated from two different techniques

System	CAC (mM)		Average CAC	D_S (m^2/s)
	Method I	Method II		
Brij 97	7.35	7.35	7.35	$1.57x10^{-15}$
Brij 98	7.95	4.48	6.22	$9.77x10^{-15}$
Brij 78	4.45	4.46	4.45	$3.82x10^{-16}$

CHAPTER 8
CONCLUSION

Ophthalmic drug delivery via contact lenses is beneficial for increasing the bioavailability of the drug and also reducing the side effects of ophthalmic drugs due to reduction in systemic uptake. Most commercially available contact lenses can be utilized to deliver various drugs to the ocular surface though the major drawback of these systems is a fast release from these lenses and most of the drug diffuses out within few hours of application. This work has focused on designing novel contact lenses which can increase the therapeutic efficiency of contact lenses by controlling drug release rates of common ophthalmic drugs. This is achieved by introduction of microemulsion and micelles inside the contact lenses.

In chapter 2 we show that by using drug nanoparticles inside the contact lenses, release rates of the drug CyA can be controlled and sustained delivery is possible for a week. Major advantage of this system is its easy availability and ease of application. It is also pointed out that as the concentration of drug is increased above the solubility limits of the p-HEMA gel network, the gel starts to loose its transparency. This means that though release rates of the drug can be controlled by increasing drug concentration, there is a significant compromise of gel properties such as transparency, making these systems redundant.

Chapter 3 focuses on developing microemulsion and surfactant-laden contact lenses that can deliver CyA for an extended period of time. A nonionic surfactant Brij 97 is used in these studies. Both surfactant and microemulsion-laden gels exhibit slow and extended drug release lasting for about 20 days. This is a significant improvement compared to the control (pure p-HEMA gels), which releases drug for less than 5 days at similar drug loadings. The duration of drug release depends on the surfactant loading, but it is similar for both surfactant and microemulsion-laden gels for similar surfactant loadings, particularly early in the release. There

are some differences in the release profiles at longer times and so further investigations are needed to conclusively determine the role of oil in these studies. The surfactant loadings in these studies are higher than the CMC and so the hydrated gels are expected to contain surfactant aggregates. Since CyA is a hydrophobic drug, it preferentially partitions into the hydrophobic domains leading to an increase in partition coefficient of the gel. The interaction of the drug with the hydrophobic domains and the resistance offered by the surfactants to transport of drug from inside the domains to the bulk gel leads to a slow down in transport rates from the gel. The gels release on an average about 2 μg of drug each day, which is sufficient to achieve therapeutic concentrations in cornea.

As shown in chapter 3, drug release profiles are unaffected by the method of drug loading. The gels which had CyA loaded by soaking in solutions behave similarly to those in which the drug is added before polymerization. It is however interesting to note that when the drug is loaded by soaking, the process equilibrates in less than 5 days but these gels release drug for more than 20 days. This also suggests that the drug has a large affinity for hydrophobic domains in the gel, which leads to a rapid uptake.

The duration of drug release is unaltered by processing conditions which include autoclaving and packaging. Additionally, the drug is not damaged by the autoclaving. These results are very encouraging and so it seems that surfactant or microemulsion-laden gels may be suitable for delivering CyA to eyes. In addition to treating ocular disorders, CyA has also shown promise in treating contact lens mediated dry eyes, and so these systems could also be very useful for a large population that is unable to wear contact lenses due to discomfort [124].

In chapter 4 we increased our understanding of this system by proposing models for both drug and surfactant transport from p-HEMA hydrogels and the results of the model were verified

by measuring release rates of both surfactant and drug from hydrogels. We explored Brij 98 surfactant laden p-HEMA hydrogels in this chapter. The experimental results were in good agreement with the models. The transport models developed here can be very helpful in tuning the drug release rates from hydrogels by controlling the surfactant concentration.

To further verify the model developed in chapter 4, we studied more surfactants and drugs in chapter 5. Similar classes of surfactant were utilized to comment on qualitative behavior of surfactants based on their molecular structure which was further verified by experiments. These surfactants had unsaturated and saturated carbon chains as hydrophobic segments with three different lengths of hydrophilic (EO) segment. Experiments were conducted to study the effects of gel thickness, surfactant type and concentration on release profiles. Mechanism of release of the drug from all the surfactant laden systems was diffusion controlled as was inferred from the study of two different thicknesses for each surfactant-laden system. We were able to determine partition coefficient of the drug for all the systems and quantitatively determine which system would provide maximum barrier to CyA transport from the hydrogels. Brij 78 systems seem to be the most promising because these systems release CyA for longer periods of time compared to other Brij systems and also seem to have the least amount of surfactant diffusing out in the release medium. The partition coefficient of the drug in these systems was determined to be 458.9±61.5 which shows that CyA had a very high affinity to Brij 78 aggregates present inside the hydrogel. Furthermore, Brij 78 surfactants have been used in ocular studies as cornea permeability enhancers, and so these are not expected to cause significant toxic response in the eyes [67]. Though Brij-78 laden gels showed promising results for the drug CyA, they could not be utilized to attenuate release of two other hydrophobic drugs, DMS and DMSA. This failure

was attributed to lower partition coefficient of these drugs inside Brij 78 micelles. Furthermore, these drugs are much smaller in size than CyA, leading to faster release from the hydrogel.

Chapter 5 also explored various properties of the hydrogels to determine their suitability as commercial contact lenses. All the systems showed very high transparency values along with a storage modulus suitable for contact lens applications. Water content for all the surfactant laden gels was much higher than that for pure p-HEMA hydrogel which can further be related to increased oxygen permeability with better patient compliance. Brij 78 laden gels showed the best wetting properties as was determined by the contact angle measurements on all the systems.

While the examples reported here were conducted with CyA, other drugs could also be dissolved in the HEMA monomer, but the release rates may not be as slow as those for CyA, particularly if the drug molecules are much smaller than CyA or if they are less hydrophobic in nature. It is also noted that in addition to surfactants, other self assembling molecules such as lipids, and block-co-polymers could be used to create domains that could trap and slowly release hydrophobic drugs.

After clearly establishing the concept and proving that micelle and microemulsion laden gels could potentially be used for delivering CyA at therapeutic dosages to the ocular surface, we also evaluated the potential damage of the studied non-ionic surfactants on the ocular surface by designing an in vitro toxicity assay as the data for potential ocular toxicity of these substances was scarce. This was discussed in chapter 6. Damage to the corneal epithelium can be attributed to the disruption of membrane fluidity due to the penetration of external agents such as surfactants, and the subsequent release of lysosomal enzymes, histamine, and inflammatory mediators. Interactions between surfactants and the corneal surface are governed by their respective CMC's, as micelles are not expected to interact with lipid bilayers. We successfully

developed an *in vitro* alternative to the popularly used eye irritation assay known as Draize eye test by using liposomes mimicking corneal epithelium and determining the release of a hydrophilic dye from liposome interior due to interaction with surfactants. We found that liposomes could be successfully utilized to assess the toxicity of various surfactants if a correction factor is introduced to account for the increased surface area to volume ratio of liposomes compared to the corneal epithelium. Once this factor was introduced, the correlations between dye leakage from liposomes and Draize scores improved significantly. This method can be used to evaluate the initial toxicity of various surfactants, and could thus become a key method to assess ocular toxicity in vitro. We predicted that Brij 78, Brij 700, Brij 56, and Brij 58 are mildly/moderately comfortable when placed in the eye at concentrations of 10% (w/v), while Brij 97 and Brij 98 appear to be irritating at similar concentrations. At 1% (w/v), all of the surfactants examined are most likely in the mild/moderate category, causing little to no discomfort.

CHAPTER 9
FUTURE WORK

9.1 Gels with Higher Surfactant Loading

This work has focused on maximum surfactant concentration of 8% w/dry gel w inside the hydrogel. It was observed that introduction of surfactants inside the hydrogel can significantly alter the microstructure of the hydrogel and this can lead to an improvement of water uptake properties of these hydrogels. To further investigate the effect of surfactant concentration on the gel properties it will be interesting to develop systems with much higher surfactant loading and determine the effect of high surfactant loading on the microstructure of the gel. We have successfully synthesized gels with 40% surfactant loading for Brij 97 and 25% surfactant loading for Brij 98 and Brij 78 systems in p-HEMA matrix. These gels remain transparent after introduction of such high surfactant concentration which suggests that the pores inside the hydrogels are not larger than 100 nm. We speculate that the pores inside these hydrogels will likely form an interconnected network, which could be verified by SEM imaging. Also, it may be possible to soak these gels in ethanol solution to remove all the surfactant from the gel matrix and then back-fill these gels with a silicone monomer. This will have a significant impact in terms of enhancing oxygen permeability of p-HEMA gels which can make these contact lenses suitable for extended wear. The wettability of these systems will also increase significantly due to high surfactant concentration, which may lead to better patient compliance. Surfactants have also been used as penetration enhancers through skin and high surfactant containing systems can be used to increase skin permeability in some other therapeutic applications.

9.2 Oxygen Permeability

We were unable to measure the oxygen permeability of surfactant laden gels in our lab due to lack of required setup. This work is currently in progress in the lab. In future, it might be

interesting to explore the effect of microstructure change due to surfactants inside the hydrogel on the oxygen permeability of these gels. The surfactant presence will certainly lead to increased oxygen transport due to increased water content but there may be other mechanisms related to the microstructure that impact oxygen transport. The oxygen permeability is defined in terms of Dk or barrers and it is suggested that the oxygen permeability of an extended wear contact lens should be larger than 110 barrers. Pure p-HEMA gels have an oxygen permeability of only 10 barrers and water has a maximum permeability of 80 barrers. This clearly suggests that some other component such as a silicone monomer, which has excessively large oxygen permeability (~600 barrers), has to be introduced along with surfactants to increase the permeability to desired levels. Surfactants inside the hydrogels can also act as an emulsifier in maintaining a co-continuous phase of HEMA and silicone in the hydrogels. Thus, there is an extensive possibility of changing oxygen permeability by introduction of surfactants inside the hydrogels and these need to be explored in detail in future studies.

9.3 Release of Bio-active Agents like Vitamin E from Contact Lenses

It was observed that release of surfactants from the hydrogels increases the partition coefficient of hydrophobic drugs and this can be potentially used to release highly insoluble agents such as a Vitamin E from the contact lenses, which can provide therapeutic advantages to commercially available contact lenses. Vitamin E can be loaded inside the gels using ethanol as the solvent as Vitamin E has negligible solubility inside water. It can also be loaded in the gels by mixing Vitamin E in the HEMA monomer before polymerization. In some preliminary results, we have shown that solubility of Vitamin E in water can be increased in presence of surfactants, and this suggests that surfactant laden hydrogels can potentially be used to deliver Vitamin E to the ocular surface. Also, we have successfully synthesized surfactant and Vitamin E loaded gels in our lab and the gels retain transparency on introduction of Vitamin E inside the

gel matrix. More rigorous experiments need to be conducted to explore surfactant laden gels to increase delivery of such highly hydrophobic substances.

9.4 Surfactant laden Silicone Contact Lenses

As seen previously, surfactants can enhance the surface properties of the hydrogels by increasing surface wettability and water content. Silicone contact lenses have very poor wettability and water content and it might be beneficial to study the property changes in these hydrogels on introduction of surfactants. We have done some preliminary studies on introduction of surfactants in silicone gels and the gels retained transparency if the surfactant concentration was below 4% surfactant loading inside the hydrogel. We also tried to measure the surfactant release from these silicone gels but realized that surface tension measurements are not suitable for measuring surfactant release from these gels as the control silicone gels should significant surface activity due to un-reacted monomer diffusion from these gels. Other surfactants which could be identified using techniques such as HPLC, UV-Vis spectrometry, Florescence, FTIR, NMR or refractive index measurements, need to be utilized inside these silicone gels if surfactant release needs to be measured.

9.5 Polymerizable Surfactants

Surfactants can potentially diffuse from the contact lenses and penetrate the ocular surface which might lead to toxicity. Thus, it might be beneficial to utilize surfactants which can polymerize inside the hydrogel matrix, and thus eliminating the risk of surfactant toxicity. It will also be very interesting if the surfactants could polymerize to form nanoparticles inside the hydrogel which could help reducing the transport of hydrophobic drugs and also eliminate the toxicity of an extra excipient like surfactant from these hydrogels.

9.6 In-vivo Experiments

In this work we have done rigorous in vitro analysis of surfactant laden hydrogels for controlled drug delivery of CyA, and we have shown that these systems could be potentially used for therapeutic use. In vivo studies still need to be performed to conclusively demonstrate the biocompatibility and efficacy of these systems for controlled delivery vehicle with increased bioavailability.

LIST OF REFERENCES

[1] Le Bourlais C, Acar L, Zia H, Sado PA, Needham T, Leverge R. Ophthalmic drug delivery systems - Recent advances. Prog Retin Eye Res 1998;17(1):33-58.

[2] Prausnitz MR, Noonan JS. Permeability of cornea, sclera and conjunctiva: A literature analysis for drug delivery to the eye. J Pharm Sci 1998;87(12):1479-1488.

[3] Snibson GR, Greaves JL, Soper NDW, Prydals JI, Wilson CG, Bron AJ. Precorneal residence time of sodium hyaluronate solutions studied by quantitative gamma scintigraphy. Eye 1990;4(4):594-602.

[4] Wilson CG, Zhu YP, Frier M, Rao LS, Gilchrist P, Perkins AC. Ocular contact time of a carbomer gel (GelTears) in humans. Brit J Ophthalmol 1998;82(10):1131-1134.

[5] Meadows DL, Paugh JR, Joshi A, Mordaunt J. A novel method to evaluate residence time in humans using a nonpenetrating fluorescent tracer. Invest Ophthalmol Vis Sci 2002;43(4):1032-1039.

[6] Ishibashi T, Yokoi N, Bron AJ, Tiffany JM, Komuro A, Kinoshita S. Retention of reversibly thermo-gelling timolol on the human ocular surface studied by video meniscometry. Curr Eye Res 2003;27(2):117-122.

[7] Yokoi N, Komuro A. Non-invasive methods of assessing the tear film. Exp Eye Res 2004;78(3):399-407.

[8] Lang JC. Ocular drug-delivery conventional ocular formulations. Adv Drug Deliver Rev 1995;16(1):39-43.

[9] Felt O, Einmahl S, Gurny R, Furrer P, Baeyens V. Polymeric systems for ophthalmic drug delivery. In: Dumitriu S, editor. Polymeric Biomaterials, New York, Marcel Dekker Inc., 2002. p. 377-421.

[10] Sintzel MB, Bernatchez SF, Tabatabay C, Gurny R. Biomaterials in ophthalmic drug delivery. Eur J Pharm Biopharm 1996;42(6):358-374.

[11] Ludwig A. The use of mucoadhesive polymers in ocular drug delivery. Adv Drug Deliver Rev 2005;57(11):1595-1639.

[12] Calvo P, Vila-Jato JL, Alonso MJ. Comparative in vitro evaluation of several colloidal systems,nanoparticles, nanocapsules, and nanoemulsions as ocular drug carriers. J Pharm Sci 1996; 85(5):530-536.

[13] Gavini E, Chetoni P, Cossu M, et al. PLGA microspheres for the ocular delivery of a peptide drug, vancomycin using emulsification/spray-drying as the preparation method: in vitro/in vivo studies. Eur J Pharm Biopharm 2004; 57(2): 207-212.

[14] McNamara NA, Polse KA, Brand RJ, Graham AD, Chan JS, McKenney CD. Tear mixing under a soft contact lens: Effects of lens diameter. Am J Ophthalmol 1999;127(6):659-665.

[15] Creech JL, Chauhan A, Radke CJ. Dispersive mixing in the posterior tear film under a soft contact lens. Ind Eng Chem Res 2001;40(14):3015-3026.

[16] Li CC, Chauhan A. Modeling ophthalmic drug delivery by soaked contact lenses. Ind Eng Chem Res 2006;45(10):3718-3734.

[17] Lemp MA. New strategies in the treatment of dry- eye states. Cornea 1999;18:625–632.

[18] Murube J, Paterson A, Murube E. Classification of artificial tears. I: Composition and properties. Adv Exp Med Biol 1998;438:693–704.

[19] Pflugfelder SC. Advances in the diagnosis and management of keratoconjunctivitis sicca. Curr Opin Ophthalmol 1998;9(4):50–53.

[20] Murube J, Murube E: Treatment of dry eye by blocking the lacrimal canaliculi. Surv Ophthalmol 1996;40(6):463–480.

[21] Pflugfelder SC, Jones D, Ji Z, Afonso A, MOnroy D. Altered cytokine balance in the tear fluid and conjunctiva of patients with Sjogrens syndrome keratoconjunctivitis sicca. Curr Eye Res 1999;19(3):201–211.

[22] Yen MT, Monroy D, Pflugfelder SC. Punctal occlusion decreases tear production, clearance, and ocular surface sensation. Invest Ophthalmol Vis Sci 1999;40:S980.

[23] Mathers WD, Dolney AM. Objective demonstration of tear stimulation with oral pilocarpine in dry eye patients. Invest Ophthalmol Vis Sci 2000;41:S60.

[24] Calonge M. The Treatment of Dry Eye. Surv Ophthalmol 2001;45(2):S227-S239.

[25] Walton RC, Nussenblatt RB, Whitcup SM. Cyclosporine therapy for severe sight-threatening uveitis in children and adolescents. Ophthalmology 1998;105(11):2028-2034.

[26] Gupta V, Sahu PK. Topical cyclosporin A in the management of vernal keratoconjunctivitis. Eye 2001;15(1):39-41.

[27] Georganas C, Ioakimidis D, Iatrou C, Vidalaki B, Iliadou K, Athanassiou P, Kontomerkos T. Relapsing Wegener's granulomatosis: successful treatment with cyclosporin-A. Clin Rheumatol 1996;15(2):189–192.

[28] Wiederholt M, Kossendrup D, Schulz W, Hoffman F. Pharmacokinetic of topical Cyclosporin A in rabbit eye. Invest Ophthalmol Vis Sci 1986;27(4):519-524.

[29] BenEzra D, Maftzir G, Courten C, Timonen P.Ocular penetration of cyclosporin A. III: the human eye. Brit J Ophthalmol 1990;74(6):350-352.

[30] Acheampong AA., Shackleton M, Tang-Liu D, Ding S, Stern M, Decker R. Distribution of cyclosporin A in ocular tissues after topical administration to albino rabbits and beagle dogs. Curr Eye Res 1999;18(2):91–103.

[31] Klang S, Abdulrazik M, Benita S. Influence of emulsion droplet surface charge on indomethacin ocular tissue distribution. Pharm Dev Technol 2000;5(4):521–532.

[32] Kanai A, Alba RM, Takano T, Kabayashi C, Nakajima A, Kurihara K, Yokoyama T, Fukami M. The effect on the cornea of alpha cyclodextrin vehicle for cyclosporin eye drops. Transplant P 1989;21(1):3150-3152.

[33] Bijl P, Eyk AD, Meyer D. Effects of three penetration enhancers on transcorneal permeation of cyclosporine. Cornea 2001;20(5):505-508.

[34] Kuwano M, Ibuki H, Morikawa N, Ota A, Kawashima Y. Cyclosporine A formulation affects its ocular distribution in rabbits. Pharm Res 2002;19(1):108-111.

[35] Milani JK, Pleyer U, Dukes A, Chou HJ, Lutz S, Ruckert D, Schmidt KH, Mondino BJ. Prolongation of corneal allograft survival with liposome encapsulated cyclosporine in the rat eye. Ophthalmology 1993;100(6):890-896.

[36] Felt O, Furrer P, Mayer JM, Plazonnet B, Buri P, Gurny R. Topical use of chitosan in ophthalmology: tolerance assessment and evaluation of precorneal retention. Int J Pharm 1999;180(2):185-193.

[37] De Campos AM, Sanchez A, Alonso MJ. Chitosan nanoparticles: a new vehicle for the improvement of the delivery of drugs to the ocular surface. Application to cyclosporin A. Int J Pharm 2001;224(1-2):159-168.

[38] El-Shabouri MH. Positively charged nanoparticles for improving the oral bioavailability of cyclosporin-A. Int J Pharm 2002;249(1-2):101-108.

[39] Reidy JJ, Gebhardt BM, Kaufman HE. The collagen shield: a new vehicle for delivery of cyclosporin A to the eye. Cornea 1990;9(3):196-199.

[40] Lallemand F, Furrer P, Felt-Baeyens O, Gex-Fabry M, Dumont JM, Besseghir K, Gurny R. A novel water-soluble cyclosporine A prodrug: Ocular tolerance and in vivo kinetics. Int J of Pharm 2005;295(1-2):7-14.

[41] Gallardo A, Fernandez F, Bermejo P, Rebuelta M, Cifuentes A, Diez-Masa JC, Roman J. Controlled release of cyclosporine from VP-HEMA copolymer systems of adjustable resorption monitorized by MEKC. Biomaterials 2000;21(9):915-921.

[42] Gallardo A, Fernandez F, Cifuentes A, Diez-Masa JC, Bermejo P, Rebuelta M, Roman J, Lopez-Bravo A.. Modulated release of cyclosporine from soluble vinyl pyrrolidone-hydroxyethyl methacrylate copolymer hydrogels - A correlation of 'in vitro' and 'in vivo' experiments. J Control Release 2001;72(1-3):1-11.

[43] Sedlavek J. Possibilities of application of ophthalmic drugs with the aid of gel contact lens. Cesk Oftalmol 1965;21:509-514.

[44] Jain MR. Drug delivery through soft contact lenses. Brit J Ophthalmol 1988;72(2):150-154.

[45] Karlgard CCS, Wong NS, Jones LW, Moresoli C. In vitro uptake and release studies of ocular pharmaceutical agents by silicon-containing and p-HEMA hydrogel contact lens materials. Int J Pharm 2003;257(1-2):141-151.

[46] Alvarez-Lorenzo C, Hiratani H, Gomez-Amoza JL, Martinez-Pacheco R, Souto C, Concheiro A. Soft contact lenses capable of sustained delivery of timolol. J Pharm Sci 2002;91(10):2182-2192.

[47] Hsiue GH, Guu JA, Cheng CC. Poly(2-hydroxyethyl methacrylate) film as a drug delivery system for pilocarpine. Biomaterials 2001;22(13):1763-1769.

[48] Tian X, Iwatsu M, Sado K, Kanai A. Studies on the uptake and release of fluoroquinolones by disposable contact lenses. CLAO J 2001;27(4):216-220.

[49] Hillman JS. Management of acute glaucoma with pilocarpine-soaked hydrophilic lens. Brit J Ophthalmol 1974;58(7):674-679.

[50] Ramer RM, Gasset AR. Ocular penetration of pilocarpine – effect on concentration on ocular penetration of pilocarpine. Ann Ophthalmol 1974;6(11):1160-1162.

[51] Ruben M, Watkins R. Pilocarpine dispensation for soft hydrophilic contact-lens. Brit J Ophthalmol 1975;59(8):455-458.

[52] Rosenwald PL. Ocular device. US Patent No. 4,484,922, 1981.

[53] Arthur BW, Hay GJ, Wasan SM, Willis WE. Ultrastructural effects of topical timolol on the rabbit cornea – outcome alone and in conjunction with a gas permeable contact –lens. Arch Ophthalmol 1983;101(10):1607-1610.

[54] Wilson MC, Shields MB. A comparison of the clinical variations of the iridocorneal endothelial syndrome. Arch Ophthalmol 1989;107(10):1465-1468.

[55] Schultz CL, Nunez IM, Silor DL, Neil ML. Contact lens containing a leachable absorbed material. US Patent No. 5,723,131, 1995.

[56] Fristrom B. A 6-month, randomized, double-masked comparison of latanoprost with timolol in patients with open angle glaucoma or ocular hypertension. Acta Ophthalmol Scan 1996;74(2):140-144.

[57] Schultz CL, Mint JM. Drug delivery system for antiglaucomatous medication. US Patent No. 6,410,045, 2000.

[58] Hiratani H, Alvarez-Lorenzo C. The nature of backbone monomers determines the performance of imprinted soft contact lenses as timolol drug delivery systems. Biomaterials 2004;25(6):1105-1113.

[59] Hiratani H, Fujiwara A, Tamiya Y, Mizutani Y, Alvarez-Lorenzo C. Ocular release of timolol from molecularly imprinted soft contact lenses. Biomaterials 2005;26(11):1293-1298.

[60] Ende MTA, Peppas NA. Transport of ionizable drugs and proteins in crosslinked poly(acrylic acid) and poly(acrylic acid-co-2-hydroxyethyl methacrylate) hydrogels .2. Diffusion and release studies. J Control Release 1997;48(1):47-56.

[61] Colombo P, Bettini R, Peppas NA. Observation of swelling process and diffusion front position during swelling in hydroxypropyl methyl cellulose (HPMC) matrices containing a soluble drug. J Control Release 1999;61(1-2):83-91.

[62] Ward JH, Peppas NA. Preparation of controlled release systems by free-radical UV polymerizations in the presence of a drug. J Control Release 2001;71(2):183-192.

[63] Park ES, Chang SY, Hahn M., Chi SC. Enhancing effect of polyoxyethylene alkyl ethers on the skin permeation of ibuprofen. Int J Pharm 2000;209(1-2):109-119.

[64] Aungst BJ, Rogers NJ, Shefter E. Enhancement of naloxane penetration through human skin in vitro using fatty acids, fatty alcohols, surfactans, sulfoxides and amides. Int J Pharm 1986;33(1-3):225-234.

[65] Walters KA, Walker M, Olejnik O. Non-ionic surfactant effects on hairless mouse skin permeability characteristics. J Pharm Pharmacol 1988;40(8):525-529.

[66] Sarpotdar P, Zatz JL. Percutaneous absorption enhancement by non-ionic surfactants. Drug Dev Ind Pharm 1988;12:1625-1647.

[67] Saettone MF, Chetoni P, Cerbai R, Mazzanti G, Braghiroli L. Evaluation of ocular permeation enhancers: in vitro effects on corneal transport of four β-blockers, and in vitro/in vivo toxic activity. Int J Pharm 1996;142(1):103-113.

[68] Furrer P, Mayer JM, Plazonnet B, Gurny R. Ocular tolerance of absorption enhancers in ophthalmic preparations. AAPS PharmSci 2002;4(1):1-5.

[69] Chetoni P, Burgalassi S, Monti D, Saettone MF. Ocular toxicity of some corneal penetration enhancers evaluated by electrophysiology measurements on isolated rabbit cornea. Toxicol In Vitro 2003;17(4):497-504.

[70] Kim Y, Dalhaimer P, Christian DA, Discher DE. Polymeric worm micelles as nano-carriers for drug delivery. Nanotechnology 2005;16:S484-S491.

[71] Jones MC, Leroux JC. Polymeric micelles – a new generation of colloidal drug carriers. Eur J Pharm Biopharm 1999;48(2):101-111.

[72] Hagan SA, Coombes GA, Garnett MC, Dunn SE, Davies MC, Illum L, Davis SS, Harding SE, Purkiss S, Gilbert PR. Polylactide-poly(ethylene glycol) copolymers as drug delivery systems, 1.Characterization of water dispersible micelle-forming systems. Langmuir 1996;12(9):2153-2161.

[73] Torchilin VP. Structure and design of polymeric surfactant-based drug delivery systems. J Control Release 2001;73(2-3):137-172.

[74] Torchilin VP. Micellar nanocarriers: Pharamceutical perspectives. Pharm Res 2007;24(1):1-15.

[75] Vlachou M, Hani N, Efentakis M. Polymers for use in controlled release systems: The effect of surfactants on their swelling properties. J Biomater Appl 2000;15(1):65-77.

[76] Hansson P, Schneider S, Lindman B. Macroscopic phase separation in a polyelectrolyte gel interacting with oppositely charged surfactant: correlation between anomalous deswelling and microstructure. Prog Coll Pol Sci 2000;115:342-346.

[77] Philippova OE, Hourdet D, Audebert R, Khokhlov AR. Interaction of hydrophobically modified poly(acrylic acid) hydrogels with ionic surfactants. Macromolecules 1996;29(8):2822-2830.

[78] Nilsson S, Thuresson K, Hansson P, Lindman Bjorn. Mixed solutions of surfactant and hydrophobically modified polymer – Controlling viscosity and micellar size. J Phys Chem B 1998;102(37):7099-7105.

[79] Barreiro-Iglesias R, Alvarez-Lorenzo C, Concheiro A. Microcalorimetric evidence and rheological consequences of the salt effect on carbopol-surfactant interactions. Prog Coll Pol Sci 2003;122:95-102.

[80] Peppas NA, Bures P, Leobandung W, Ichikawa H. Hydrogels in pharmaceutical formulations. Eur J Pharm and Biopharm 2000;50(1):27-46.

[81] Brannon-Peppas L, Peppas NA. Equilibrium swelling behavior of pH-sensitive hydrogels. Chem Eng Sci 1991;46:715-722.

[82] Beltran S, Baker JP, Hooper HH, Blanch HW, Prausnitz JM. Swelling equilibria for weakly ionizable, temperature sensitive hydrogels. Macromolecules 1991;24:549-551.

[83] Zrinyi M, Szabo D, Kilian HG. Kinetics of the shape change of magnetic field sensitive polymer gels. Polym Gels Netw 1998;6(6):441-454.

[84] Lavon I, Kost J. Mass transport enhancement by ultrasound in non-degradable polymeric controlled release systems. J Control Release 1998;54(1):1-7.

[85] Goldbart R, Kost J. Calcium responsive bioerodible drug delivery system. Pharm Res 1999;16(9):1483-1486.

[86] Paulsson M, Edsman K. Controlled drug release from gels using lipophilic interactions of charged substances with surfactants and polymers. J Colloid Interf Sci 2002;248(1):194-200.

[87] Ritger PL, Peppas NA. A simple equation for description of solute release I. Fickian and non-Fickian release from non-swellable devices in the form of slabs, spheres, cylinders or discs. J Control Release 1987;5(1):23-36.

[88] Amsden B. Solute diffusion within hydrogels-mechanisms and models. Macromolecules 1998;31(23):8382-8395.

[89] Higuchi T. Rate of release of medicaments from ointment bases containing drugs in suspension. J Pharm Res 1961;50(10):874-876.

[90] Paulsson M, Edsman K. Controlled drug release from gels using surfactant aggregates: I. Effect of lipophilic interactions for a series of uncharged substances. J Pharm Sci 2001;90(9):1216-1225.

[91] Paulsson M, Edsman K. Controlled drug release from gels using surfactant aggregates. II. Vesicles formed from mixtures of amphiphilic drugs and oppositely charged surfactants. Pharm Res 2001;18(11):1586-1592.

[92] Bramer T, Bew N, Edsman K. Cationic mixtures involving a drug: a rather general concept that can be utilized for prolonged drug release from the gels. J Pharm Sci 2006;95(4):769-780.

[93] Lin HR, Sung KC. Carbopol/pluronic phase change solutions for ophthalmic drug delivery. J Control Release 2000;69(3):379-388.

[94] Liu JH, Lin L. SDS-aided immobilization and controlled release of camptothecin from agarose hydrogel. Eur J Pharm Sci 2005;25(2-3):237-244.

[95] Liu JH, Lin L, Cai YY. Immobilization of camptothecin with surfactant into hydrogel for controlled drug release. Eur Polym J 2006;42(8):1767-1774.

[96] Liu JH, Lin L. Diffusion of camptothecin immobilized with cationic surfactant into agarose hydrogel containing anionic carrageenan. J Biomed Mater Res A 2007;83(4):1103-1109.

[97] Barreiro-Iglesias R, Alvarez-Lorenzo C, Concheiro A. Incorporation of small quantities of surfactants as a way to improve the rheological and diffusional behavior of carbopol gels. J Control Release 2001;77(1-2):59-75.

[98] Alvarez-Lorenzo C, Concheiro A. Effects of surfactants on gel behavior: Design implications for drug delivery systems. Am J of Drug Deliver 2003;1(2):77-101.

[99] Wu Z, Joo H, Lee TG, Lee K. Controlled release of lidocaine hydrochloride from the surfactant-doped hybrid xerogels. J Control Release 2005;104(3):497-505.

[100] Eeckman F, Moes AJ, Amighi K. Surfactant induced drug delivery based on the use of thermosensitive polymers. Journal of Controlled Release 2003;88(1):105-116.

[101] Gulsen D, Chauhan A. Dispersion of microemulsion drops in HEMA hydrogel: a potential ophthalmic drug delivery vehicle. Int J Pharm 2005;292(1-2):95-117.

[102] Wilhelmus KR. The Draize eye test. Surv Ophthalmol 2001;45(6):493-515.

[103] Weil CS, Scala RA. Study of Intra- and Interlaboratory Variability in the results of rabbit eye and skin irritation tests. Toxicol Appl Pharm 1971;19:276-360.

[104] Vian L, Vincent J, Maurin J, Fabre I, Giroux J, Cano JP. Comparison of three in vitro cytotoxicity assays for estimating surfactant ocular irritation. Toxic in Vitro 1995;9(2):185-190.

[105] Matsukawa K, Masuda K, Kakishima H, Suzuki K, Nakagawa Y, Matsushige C, Imanishi Y, Nakamura T, Mizutani A, Watanabe R, Shingai T, Kaneko T, Hirose A, Onno Y. Interlaboratory Validation of the in vitro eye irritation tests for cosmetic ingredients. (11) EYTEX™. Toxic in Vitro 1999;13:209-217.

[106] Vinardell MP, Mitjans M. Alternative methods for eye and skin irritation tests: An Overview J Pharm Sci 2008;97(1):46-59.

[107] Okamoto Y, Ohkoshi K, Itagaki H, et al. Interlaboratory Validation of the in vitro eye irritation tests for cosmetic ingredients. (3) Evaluation of the Haemolysis Test. Toxic in Vitro 1999;13:115-124.

[108] Okahata Y, Ebato H. Absorption behaviors of surfactant molecules on a lipid-coated quartz-crystal microbalance. An Alternative to Eye-Irritant Tests. Anal Chem 1991;63:203-207.

[109] Cottin M, Zanvit A. Fluorescein leakage lest: a useful tool in ocular safety assessment. Toxic in Vitro 1997;11:399-405.

[110] Curren RD, Harbell JW. In Vitro Alternatives for ocular irritation. Environ Health Persp 1998;106(S2):485-492.

[111] Kato S, Itagaki H, Chiyoda I, et al. Liposomes as an in vitro model for predicting the eye irritancy of chemicals. Toxic in Vitro 1988;2(2):125-130.

[112] Sunamoto J, Iwamoto K, Imokawa G, Tsuchiya S. Possible eye-irritant test using polysaccharide-coated liposomes as a corneal epithelium model. Chem Pharm Bull 1987;35(7):2958-2965.

[113] Saarinen-Savolainen P, Jarvinen T, Suhonen P, Urtti A. Amphiphilic properties of pilocarpine prodrugs. Int J Pharm 1996:133:171-178.

[114] Kim C, Ryuu S, Park K, Lim S, Hwang S. Preparation and physicochemical characterization of phase inverted water/oil microemulsion containing cyclosporin A. Int J Pharm 1997;147(1):131-134.

[115] Ran Y, Zhao L, Xu Q, Yalkowsky SH. Solubilization of Cyclosporin A. AAPS PharmSciTech 2001;2(1):23-26.

[116] Lum E, Perera I, Ho A. Osmolality and buffering agents in soft contact lens packaging solution. CLAE 2004;27(1):21-26.

[117] Warisnoicharoen W, Lansley AB, Lawrence MJ. Nonionic oil-in-water microemulsions: the effect of oil type on phase behaviour. Int J Pharm 2004;198(1):7–27.

[118] Morey TE, Varshney M, Flint JA, Seubert CN, Smith WB, Bjoraker DG, Shah DO, Dennis DM. Activity of microemulsion-based nanoparticles at the human bio-nano interface: concentration-dependant effects on thrombosis and hemolysis in whole blood. J Nanopart Res 2004;6:159-170.

[119] Klammt C, Schwarz D, Fendler K, Haase W, Dotsch V, Bernhard F. Evaluation of detergents for the soluble expression of alpha-helical and beta-barrel-type integral membrane proteins by a preparative scale individual cell-free expression system. Febs J 2005;272(23):6024-6038.

[120] Hait SK, Moulik SP. Determination of critical micelle concentration (CMC) of nonionic surfactants by donor-acceptor interaction with iodine and correlation of CMC with hydrophile-lipophile balance and other parameters of the surfactants. J Surfactants Deterg 2001;4(3):303-309.

[121] Warisnoicharoen W, Lansley AB, Lawrence MJ. Toxicological evaluation of mixtures of nonionic surfactants, alone and in combination with oil. J Pharm Sci 2003;92(4):859-868.

[122] Agatonovic-Kustrin S, Glass BD, Wisch MH, Alany RG. Prediction of a stable microemulsion formulation for the oral delivery of a combination of antitubercular drugs using ANN methodology. Pharm Res 2003;20(11):1760-1765.

[123] Lee Y, Simamor P, Yalkowsky SH. Effect of Brij-78 on systemic delivery of insulin from an ocular device. J Pharm Sci 1997;86(4):430-433.

[124] Hom HH. Use of Cyclosporine 0.05% ophthalmic emulsion for contact lens-intolerant patients. Eye Contact Lens 2006;32(2):109-111.

[125] Kim J, Chauhan A. Dexamethasone transport and ocular delivery from poly(hydroxyethyl methacrylate) gels. Int J Pharm 2008;353(1-2):205-222.

[126] Lord MS, Stenzel MH, Simmons A, Milthrope BK. Lysozyme interaction with poly(HEMA)-based hydrogel. Biomaterials 2006;27(8):1341-1345.

[127] Tonge S, Jones L, Godall S, Tighe B. The ex vivo wettability of soft contact lenses. Curr Eye Res 2001;23(1):51-59.

[128] Ketelson HA, Meadows DL, Stone RP. Dynamic wettability properties of a soft contact lens hydrogel. Colloid Surface B 2005;40(1):1-9.

[129] Szoka F, Papahadjopoulos D. Comparative properties and methods of preparation of lipid vesicles (Liposomes). Ann Rev Biophys Bioeng 1980;9:467-508.

[130] Zuidam NJ, Vrueh R, Crommelin DJA. Characterization of Liposomes. In: Torchilin VP, Weissig V. Liposomes. 2nd Edition New York, Oxford University Press, 2003. p. 31-78.

[131] Kennah HE, Hignet S, Laux PE, Dorko JD, Barrow CS. An objective procedure for quantitating eye irritation based upon changes of corneal thickness. Fundam Appl Toxicol 1989;12(2):258-268.

[132] Tachon P, Cotovio J, Dossou KG, Prunieras M. Assessment of surfactant cytotoxicity: comparison with the Draize eye test. Int J Cosmetic Sci 1989;11(5):233-243.

[133] Jester JV, Li HF, Petroll WM, Parker RD, Cavanagh HD, Carr GJ, Smith B, Maurer JK. Area and depth of surfactant-induced corneal injury correlates with cell death. Invest Ophth Vis Sci 1998;39(6):922-936.

[134] Hall-Manning TJ, Holland GH, Rennie G, REvell R, Hines J, Barratt MD, Basketter DA. Skin Irritation Potential of Mixed Surfactant Systems. Food Chem Toxicol 1998;36(3):233-238.

[135] Howell B, Chauhan A. Amitriptyline overdose treatment by pegylated anionic liposomes. J Colloid Interf Sci 2008;324(1-2):61-70.

[136] Rosen MJ. Surfactants and interfacial phenomena. Hoboken NJ, Wiley-Interscience. 2004. p. 105-177.

[137] Kim JH, Kim MW. Temperature effect on the transport dynamics of a small molecule through a liposome bilayer. Eur Phys J E 2007;23(3):313-317.

[138] Lis LJ, McAlister M, Fuller N, Rand RP, Parsegian VA. Interactions between neutral phospholipid bilayer membranes. Biophys J 1982;37(3):657-666.

[139] New RRC. Liposomes. New York, NY, Oxford University Press. 1990. p. 137.

[140] Balgavy P, Dubnickova M, Kucerka N, Kiselev MA, Yaradaikin SP, Uhrikova D. Bilayer thickness and lipid interface area in unilamellar extruded 1,2-diacylphosphatidylcholine liposomes: a small-angle neutron scattering study. Biochim Biophys Acta 2001;1512(1):40-52.

[141] Maric K, Wiesner B, Lorenz D, Klussmann E, Betz T, Rosenthal W. Cell Volume kinetics of adherent epithelial cells measured by laser scanning reflection microscopy: Determination of water permeability changes of renal principal cells. Biophys J 2001;80(4):1783-1790.

[142] Farinas J, Verkman AS. Cell volume and plasma membrane osmotic water permeability in epithelial cell layers measured by interferometry. Biophys J 1996;71:3511-3522.

[143] Brinkman HC. A calculation of the viscous force exerted by a flowing fluid on a dense swarm of particles. Appl Sci Res 1947;A(1):27-34.

[144] Phillips RJ, Deen WM, Brady JF. Hindered transport of spherical macromolecules in fibrous membranes and gels. AICHE J 1989;35(11):1761-1769.

[145] Solomentsev YE, Anderson JL. Rotation of a sphere in Brinkman fluids. Phys Fluids 1996;8(4):1119-1121.

BIOGRAPHICAL SKETCH

Yash Kapoor was born in1981 in Lucknow, Uttar Pradesh, India. He did his undergraduate work in chemical engineering at the Indian Institute of Technology Kanpur and graduated in May 2004. Thereafter, he joined the Chemical Engineering Department at the University of Florida, Gainesville, Florida as a doctorate candidate. He joined Dr. Anuj Chauhan's group in January 2005 and has been pursuing his research on ophthalmic drug delivery since then.